

STABLE ISOTOPIC INVESTIGATION OF
LATE NEOGENE TERRESTRIAL PALEOECOLOGY AND PALEOCLIMATE
OF THE CIRCUM-MEDITERRANEAN REGION

A DISSERTATION
SUBMITTED TO THE FACULTY OF THE GRADUATE SCHOOL
OF THE UNIVERSITY OF MINNESOTA
BY

SAMUEL DEAN MATSON

IN PARTIAL FULFILLMENT OF THE REQUIREMENTS
FOR THE DEGREE OF
DOCTOR OF PHILOSOPHY

DAVID L. FOX, ADVISOR

AUGUST, 2010

© SAMUEL DEAN MATSON 2010

Acknowledgements

Throughout my experience as a student, I have been surrounded by the insight, guidance, generosity, encouragement, and patience of many amazing people. This dissertation – and the opportunities it afforded me for growth as a student and as a person – would not have been possible without their support. I am very thankful for the positive differences they have made in my life.

I would like to thank my advisor, David Fox, for being an incredible mentor, teacher, and friend. David – I am honored to have been your first graduate student. You have consistently inspired me to maintain high expectations of my own abilities. I have learned a great deal through your guidance, expertise, and passion for knowledge and discovery. I am very appreciative of the freedom you have given me to develop my own research interests and questions, and of the continued encouragement and patience you give me as I try to address them. I am also thankful for the freedom and guidance you have given me as I have explored and developed my passion for teaching. Most importantly, your genuine concern for social justice and your interest in effecting positive change in the world around you continue to inspire me, and I hope to pass this sense of compassion on to my own students.

I would like to thank Emi Ito, Karen Kleinspehn, and Kieran McNulty for serving on my final dissertation defense committee, and for taking the time out of a busy summer full of research travel to critically review the results of my work. Their thoughtful discussions and constructive comments throughout my doctoral program have improved my research every step of the way. I would also like to thank Emi Ito, Karen Kleinspehn,

Bryan Shuman, Justin Revenaugh, and Christian Teyssier for serving on my written and oral examination committees, where their expertise and insight broadened the scope of this research when it was in its early stages.

I am grateful to the many people with whom I have been fortunate to establish collaborative relationships as a part of this research. Through their interest, enthusiasm and support, I have learned a great deal about the importance of interdisciplinary and international partnerships. I would especially like to thank Lluís Gibert and Gary Scott from the Berkeley Geochronological Center for sharing their vast knowledge of the geology of the Baza Basin, and of Spain in general. They have also come to be good friends with whom I look forward to productive collaboration in the future. I am very grateful to Lorenzo Rook at the University of Florence, whose knowledge of the geology of the Baccinello Basin has been extremely helpful, and whose willingness to help me with field work there in the midst of a very busy teaching schedule is greatly appreciated. I thank Laura Celia, Angel Galobart, Meike Köhler, and Salvador Moyà-Sola (Institut Català de Paleontologia, Sabadell, Spain), Jordi Agustí (Universitat Rovira i Virgili, Tarragona, Spain), and Oriol Oms (Universitat Autònoma de Barcelona) for their helpful discussions, access to specimens, and camaraderie.

I would like to thank Maniko Solheid, Amy Myrbo, Kristina Brady, Anders Noren, Mark Griffith, Ellery Frahm, Rick Knurr, and Rebecca Clotts at the University of Minnesota, and Greg Cane and Greg Ludvigson at the University of Kansas, for their analytical assistance. This research would not have been possible without their generous help, and through their expertise I have learned a lot about the logistics of making

research happen. I would also like to thank Sharon Kressler, Kathy Ohler, Greg Gambeski, John Boggs, Joan Vindendahl, and Tonya Warren on the administrative and support staff in the UMN Department of Geology and Geophysics for all their logistical help over the years. The function of the department – including graduate students – is entirely in the hands of these individuals, and I am grateful for their expertise and patience.

The companionship of many close friends has seen me through the many ups and downs of graduate school, and for their collegiality, encouragement, and optimism I am very grateful. I would especially like to thank Seth Kruckenberg, Ryan Kerrigan, Peter Rose, Megan Kelly, Rory MacFadden, Diego Riveros, Amy Myrbo, Lindsay Iredale, Andrew Haveles, Ioan Lascu, Sara Morón, Kristina Brady, Eric Goergen, Brian Bagley, Dylan Blumentritt, Nick Pester, Allison Burnett, Laura Vietti, Anna Henderson, Dan King, Dan Ruscitto, Rebecca Clotts, Graham Baird, Stacia Gordon, Andrew Luhmann, Lars Hansen, Sharon Kressler, Josh Feinberg, Martin Saar, Fred Davis, Robert Dietz, Jessica Till, Chad Wittkop, Anna Courtier, Aydin Aycenk, Adam Nagle, and Stacy Gohman. This list is far from complete, and its extent should be interpreted less as an indicator of the length of my tenure as a graduate student, and more as a representation of the spirit of camaraderie and collegiality upheld by the UMN Department of Geology and Geophysics.

I am deeply indebted to the faculty of the Department of Geology at the University of St. Thomas for the opportunities, support, and friendship they provide me as I continue to pursue my interests in teaching. Tom Hickson, Lisa Lamb, Kevin

Theissen, Rebecca Clotts, Jennifer McGuire, and Erik Smith have all been amazing mentors whose desire to see their students grow and succeed continues to be an inspiration to me. Their enthusiasm and compassion is contagious, and I consider myself extremely fortunate to have spent so much time teaching alongside them – and learning from them – in both the classroom and the field.

I am also very grateful for the insight and guidance of the many teachers and mentors that have been an important part of my life in the years leading up to graduate school. I would especially like to thank Mark Seier, Rod Havel, Mike Voorhies, Rick Otto, and Sandy Mosel. I continue to learn from the important life lessons you have taught me.

Finally, and most importantly, I would like to thank my family for the unconditional love, support, patience, trust, and encouragement they have shown me over the years. I am so thankful you are in my life and I am looking forward to spending more quality time with all of you now that the stress of graduate school is over. Mom – I cannot even begin to express how important you are to me. You are life-giving, literally and figuratively. I will continue to look to your love and giving as a model of how to make the world a better place. Dad – I miss you terribly. I am grateful for the love I learned from you while you were here, and I know that a part of you is with me every day. Erin and McKenna – I am finally done with the “big paper” and my heart feels very happy when I think about getting to spend more time with you. You are the world to me, and I love you so, so, so much!

Dedication

And now these three remain: faith, hope and love. But the greatest of these is love.

Paul of Tarsus, I Corinthians 13:13 (NIV)

This dissertation is dedicated to my family, who taught me love.

Abstract

The late Neogene was an interval of important global change, in which gradual cooling and aridification resulted in terrestrial ecosystems over much of the world that became essentially modern. The geologic record of the circum-Mediterranean region presents an exceptional opportunity to examine the interplay of tectonics, biology, and climate during this important transition, because the paleogeography of this region was influenced heavily by a unique tectonic situation governed by both large-scale convergence between Europe and Africa and smaller-scale extension within the Mediterranean Basin. Effects of this distinct tectonic regime include the establishment of land bridges that allowed migration of animals between Europe, Africa, and Asia, large-scale desiccation of inland seas due to tectonic closure of seaways connecting the Mediterranean Sea and the Atlantic Ocean, and development of intramontane basins that preserve an extensive sedimentary record of past continental environments. In combination with this unique tectonic situation, regional climatic and ecological effects in the circum-Mediterranean region resulted in a late Neogene transition to modern terrestrial ecosystems that was in many ways different than general global patterns. In order to better understand the late Neogene transition both regionally and globally, the research presented here focuses on reconstruction of terrestrial paleoclimate and paleoecology in Spain and Italy through the development of a stable isotopic record from biogenic and authigenic minerals preserved in fossil mammals and continental sediments.

A reconstruction of Late Miocene to Pleistocene paleoclimate and paleoecology in Spain was developed through analysis of the oxygen isotopic composition ($\delta^{18}\text{O}$) of biogenic phosphate in tooth enamel and dentine from fossil mammals. Comparisons of $\delta^{18}\text{O}$ between clades are consistent with morphological interpretations of habitat and physiology, and suggest a semi-aquatic habitat for anthracotheres, hippopotamids, and castorids, and open or mixed habitats for most gracile taxa such as equids and cervids. Comparisons of enamel and dentine $\delta^{18}\text{O}$ indicate slight diagenetic alteration of dentine, but also suggest that such comparisons can be used to reconstruct reasonable values of diagenetic water $\delta^{18}\text{O}$. Since the $\delta^{18}\text{O}$ of modern horses has been demonstrated to be a reasonable proxy for the $\delta^{18}\text{O}$ of local meteoric water, which is in turn strongly dependent on mean annual temperature (MAT) for modern mid- to high-latitudes, the $\delta^{18}\text{O}$ of fossil horses from Spain was used to reconstruct terrestrial paleotemperature. These reconstructions are consistent with global cooling during the late Cenozoic, with MAT for the late Miocene that is warmer than today by $\sim 1\text{--}2^\circ\text{C}$ in NE Spain and by $\sim 4\text{--}5^\circ\text{C}$ in SE Spain. The difference of $\sim 8\text{--}9^\circ\text{C}$ between NE and SE Spain for the Late Miocene is $\sim 60\%$ greater than the MAT difference between these same areas today.

To examine the ways in which a desiccated Mediterranean Basin affected surrounding terrestrial environments during the Messinian Salinity Crisis (MSC), a paleoclimatic record of this event was developed through integrated analyses of sedimentology, $\delta^{18}\text{O}$, and the stable carbon isotopic composition ($\delta^{13}\text{C}$) of latest Miocene authigenic carbonates from the Baza Basin in southern Spain. A transition from dolomite- and calcite-rich palustrine and distal alluvial fan sediments to lacustrine diatomites and

calcite-rich limestones is accompanied by a decrease in both $\delta^{13}\text{C}$ and $\delta^{18}\text{O}$, reflecting increased lake level under a wetter climate. The mean $\delta^{18}\text{O}$ of latest Miocene lacustrine calcite is significantly lower than that of modern closed-basin lakes in the Iberian Peninsula, and likely represents overflow or through-flow conditions with inflow waters derived from the surrounding Betic mountains. This result is consistent with some aspects of climate model reconstructions of the MSC, which suggest strengthened storm tracks from the Atlantic Ocean over southern Europe. Orographic uplift of these air masses along the Betic Cordillera may have resulted in enhanced precipitation and runoff in southern Spain.

To examine the interplay between tectonics, environmental change, and biological evolution, a paleoecological record was developed from the $\delta^{13}\text{C}$ of Late Miocene paleosols from the Baccinello Basin in northern Italy. These paleosols span the extinction of *Oreopithecus bambolii*, which was the only European hominoid to survive an important extinction event ca. 9.6 Ma. *Oreopithecus* is important for understanding the evolutionary history of Late Miocene hominoids, since its peculiar morphology precludes a simple interpretation of its phylogenetic position. The paleosol $\delta^{13}\text{C}$ values show very low temporal and spatial variability (indicating plant ecosystem stability through time) and provide no evidence for ecologically significant changes in floral composition spanning the *Oreopithecus* extinction event. These results validate assumptions about the importance of tectonics and species interaction as an underlying cause for the extinction of *Oreopithecus* and its associated fauna. The paleosol $\delta^{13}\text{C}$ values fall entirely within the

range of isotopic variability for modern plants following the C₃ photosynthetic pathway, indicating that C₄ vegetation was not an important component of biomass.

The research presented in this dissertation underscores the importance of the Mediterranean region for consideration of the interplay of climate, tectonics, and ecology during important global transitions occurring in the Late Miocene. The results of this research validate the utility of stable isotopic approaches to paleoenvironmental reconstruction, and provide a powerful complement to independent means of reconstructing terrestrial systems that are complex and often poorly understood, but nevertheless an extremely important component of the Earth System.

Table of Contents

Acknowledgements.....	i
Dedication.....	v
Abstract.....	vi
Table of Contents.....	x
List of Tables.....	xii
List of Figures.....	xiii
Chapter 1: Introduction and Context.....	1
1. A Context.....	1
1.1. Late Neogene global transitions.....	1
1.2. Late Neogene transitions in the Mediterranean region.....	4
1.3. Tectonic and paleogeographic framework.....	6
2. Objective and Organization of this Dissertation.....	8
References Cited.....	11
Chapter 2: Stable isotopic evidence for terrestrial latitudinal climate gradients in the Late Miocene of the Iberian Peninsula.....	18
1. Introduction.....	19
2. Materials and Methods.....	22
2.1. Geologic Setting.....	22
2.2. Sampling protocol and analytical procedure.....	26
3. Results.....	28
4. Discussion.....	32
4.1. Taxonomic $\delta^{18}\text{O}$ patterns.....	32
4.2. Comparison of enamel and dentine $\delta^{18}\text{O}$	35
4.3. Estimation of paleotemperature from equid $\delta^{18}\text{O}_p$	40
4.4. Implications for terrestrial climate during the Messinian Salinity Crisis.....	45
5. Conclusions.....	49
Acknowledgements.....	51
References Cited.....	52
Figure Captions.....	69
Chapter 3: Wet climate in southeast Spain during the Messinian Salinity Crisis.....	83
1. Introduction.....	84
2. Methods and Results.....	85
3. Interpretation and Discussion.....	88
4. Conclusions and Implications.....	93
Acknowledgements.....	95
References Cited.....	95
Figure Captions.....	107

Chapter 4: Carbon isotopic record of the relative roles of biotic and abiotic factors in the Late Miocene extinction of <i>Oreopithecus bambolii</i> , Baccinello Basin, Tuscany	120
1. Introduction	121
2. Materials and Methods	126
2.1. Geologic Setting	126
2.2. Sampling protocol and analytical procedure	128
3. Results	130
4. Discussion	132
4.1. Paleosol $\delta^{13}\text{C}_{\text{OM}}$ and Late Miocene vegetation at Baccinello	132
4.2. Carbonate $\delta^{13}\text{C}$ and $\delta^{18}\text{O}$	136
4.3. Implications for Late Miocene ecosystem change in Tuscany	139
5. Conclusions	142
Acknowledgements	144
References Cited	145
Figure Captions	162
Chapter 5: Conclusions and directions for future research.....	175
1. Summary and Perspectives.....	175
2. Directions for Future Research	177
References Cited	180
Complete References Cited.....	186
Appendix I	230

List of Tables

Chapter 2: Stable isotopic evidence for terrestrial latitudinal climate gradients in the Late Miocene of the Iberian Peninsula	
Table 2.1. $\delta^{18}\text{O}$ measurements of mammal tooth enamel, dentine, and bone phosphate .	75
Table 2.2. Results of statistical comparisons of bulk enamel $\delta^{18}\text{O}$ between taxonomic groups.....	80
Table 2.3. Results of statistical comparisons of bulk enamel $\delta^{18}\text{O}$ between localities.....	81
Table 2.4. Estimates of precipitation $\delta^{18}\text{O}_w$ and MAT based on equid tooth enamel $\delta^{18}\text{O}_p$	82
Chapter 3: Wet climate in southeast Spain during the Messinian Salinity Crisis	
Table 3.1. $\delta^{13}\text{C}$ and $\delta^{18}\text{O}$ of carbonate samples from Botardo and Las Lumbres.....	113
Table 3.2. Results of MW comparisons of means between BO/LL $\delta^{18}\text{O}_{\text{cal}}$ and modern/Holocene $\delta^{18}\text{O}_{\text{cal}}$ in Iberia.....	115
Chapter 4: Carbon isotopic record of the relative roles of biotic and abiotic factors in the Late Miocene extinction of <i>Oreopithecus bambolii</i> , Baccinello Basin, Tuscany	
Table 4.1. Stable carbon and oxygen isotopic ratios of Baccinello paleosols	170
Table 4.2. Results of MW comparisons of mean $\delta^{13}\text{C}_{\text{OM}}$ between localities and biozones.....	172
Table 4.3. Results of MW comparisons of means between Baccinello $\delta^{13}\text{C}_{\text{OM}}$ (all samples) and $\delta^{13}\text{C}$ of modern members of plant families represented in Baccinello palynoflora	173
Table 4.4. Results of MW comparisons of means between Baccinello $\delta^{13}\text{C}_{\text{OM}}$ (all samples) and $\delta^{13}\text{C}$ of modern plants in various biomes.....	174

List of Figures

Chapter 2: Stable isotopic evidence for terrestrial latitudinal climate gradients in the Late Miocene of the Iberian Peninsula	
Figure 2.1. Geographic position of fossil localities in eastern Spain.....	71
Figure 2.2. Faunal $\delta^{18}\text{O}$ comparisons.	72
Figure 2.3. Comparison of enamel and dentine $\delta^{18}\text{O}$	73
Figure 2.4. Equid $\delta^{18}\text{O}$ results.....	74
Chapter 3: Wet climate in southeast Spain during the Messinian Salinity Crisis	
Figure 3.1. Shaded-relief map of the Guadix-Baza Basin.	110
Figure 3.2. Composite section with $\delta^{13}\text{C}$, $\delta^{18}\text{O}$, XRD, and SEM results for BO and LL.	111
Figure 3.3. Comparison of BO/LL $\delta^{18}\text{O}$ results with modern and Holocene carbonate and water $\delta^{18}\text{O}$ from the Iberian Peninsula.....	112
Chapter 4: Carbon isotopic record of the relative roles of biotic and abiotic factors in the Late Miocene extinction of <i>Oreopithecus bambolii</i> , Baccinello Basin, Tuscany	
Figure 4.1. Simplified geologic map of the Baccinello Basin.	165
Figure 4.2. $\delta^{13}\text{C}_{\text{OM}}$ and $\delta^{13}\text{C}_{\text{CO}_3}$ values of paleosol samples from the Baccinello Basin.	166
Figure 4.3. Comparison of Baccinello paleosol $\delta^{13}\text{C}_{\text{OM}}$ and $\delta^{13}\text{C}_{\text{CO}_3}$ with $\delta^{13}\text{C}$ of modern representatives of Baccinello palynoflora.....	167
Figure 4.4. Comparison of Baccinello paleosol $\delta^{13}\text{C}_{\text{OM}}$ and $\delta^{13}\text{C}_{\text{CO}_3}$ with $\delta^{13}\text{C}$ of plants from modern biomes and ecosystems florally comparable to Baccinello.	168
Figure 4.5. Podere La Locca carbonate $\delta^{18}\text{O}$ and $\delta^{13}\text{C}$	169
Chapter 5: Conclusions and directions for future research	
Figure 5.1. Cyclic sediments exposed along the Júcar River north of Alcalá del Júcar.	185

Chapter 1: Introduction and Context

1. A Context

On a fundamental level, the work comprising this dissertation is motivated by a continuing desire to more fully understand the interactions between the biosphere, lithosphere, hydrosphere, and atmosphere throughout Earth's history. Specifically, my current interests involve understanding the evolution of terrestrial systems, and the degree to which it has been shaped by changes in climate, ecosystems, and paleogeography. Through this dissertation, I explore and engage these interests by reconstructing aspects of paleoclimate and paleoecology in terrestrial systems during the late Neogene in the circum-Mediterranean region. The late Neogene was a time of important global transition, during which the terrestrial flora and fauna in much of the world became essentially modern. Due to its distinct and complex tectonic and paleogeographic history, as well as its extensive late Neogene sedimentary and fossil record, the Mediterranean region offers an excellent opportunity to explore the interaction of life, geology, and climate during this important transition. The purpose of this chapter is to introduce the major global and regional environmental changes of the late Neogene, and offer an overview of the regional tectonics and paleogeography on which they are superimposed, in order to provide a context for the research presented in the remainder of this dissertation.

1.1. Late Neogene global transitions

At a large scale, the environmental changes that occurred in terrestrial environments during the Late Neogene were part of a general, long-term trend of

decreasing temperature throughout most of the Cenozoic. Much of our understanding of Cenozoic changes in global temperature come from stable oxygen isotopic records from benthic foraminifera. These records indicate that following a warming trend through the Paleocene until the Early Eocene, global temperatures began a long-term decrease over the next 50 million years (Zachos et al., 2001a). This general global cooling trend was not steady, however, and was punctuated by several important shorter-term patterns. For example, cooling at the Eocene-Oligocene boundary was associated with the onset of southern hemisphere glaciation in response to tectonic isolation of Antarctica and development of a circum-polar current (Lawver and Gahagan, 2003; Stickley et al., 2004; Liu et al., 2009). A warming trend during the Late Oligocene was followed by a second major expansion of Antarctic ice at the Oligocene-Miocene boundary (Miller et al., 1991; Zachos et al., 2001b; Roberts et al., 2003). Global temperatures increased again through the early Miocene until their Neogene maximum ca. 15 Ma (Zachos et al., 2001a). The general global climate trend since that time has been one of temperature decrease, in which ice sheet growth in East Antarctica during the Late Miocene (Anderson and Shipp, 2001) was followed by the onset of glaciation in the northern hemisphere during the mid-Pliocene (Shackleton et al., 1988; Maslin et al., 1998). This late Neogene cooling phase represents the final transition from the greenhouse world of the Late Cretaceous and early Cenozoic, to the icehouse Earth with bipolar glaciation as we know it today.

Global climate trends during the late Neogene were paralleled by major trends in the evolution of terrestrial ecosystems. These ecological trends indicate that in addition to global cooling, an increase in aridity during the late Neogene resulted in the gradual

replacement of subtropical forests characteristic of many Early and Middle Miocene mid-latitudes by the open grasslands present in these areas today (Potts and Behrensmeyer, 1992; Jacobs et al., 1999). This transition was first identified in fossil mammals and is illustrated especially well by the Equidae (MacFadden, 1998) which became the stereotype for the classic narrative of parallel evolution between grasslands and ungulates (hoofed herbivorous mammals). In this story, “browsing” horses with short-crowned (brachydont) molars specialized for soft vegetation and with anatomical specializations for woodland habitats (e.g., small body size, short limbs, accessory toes) were gradually replaced by “grazing” horses with high-crowned (hypsodont) molars specialized for coarse vegetation and with anatomical specializations for open habitats (e.g., larger size, longer limbs, and single toes). While this traditional “replacement” story is attractive, more recent studies examining entire ungulate faunas in North America reveal that it is probably too simplistic. Instead, these studies indicate that Middle Miocene ungulate faunas were characterized by a high diversity of browsers, grazers, and mixed-feeders over a range of body sizes, inhabiting a mixed woodland-grassland ecosystem with no direct modern analogue (Janis et al., 2000, 2002, 2004). In this case, the late Neogene faunal succession is better described as a decrease in the diversity of browsers relative to grazers, but within an overall decrease in diversity for all three dietary groups.

A more complete – but in some ways more complicated – picture of the global evolution of the grassland biome and its associated fauna is provided by stable carbon isotopic ratios ($\delta^{13}\text{C}$) in mammals and paleosols. Cerling et al. (1993, 1997) documented a sharp increase in $\delta^{13}\text{C}$ of mammal (primarily equid) tooth enamel between 6 and 8 Ma

in SW Asia, East Africa, South America, and southern North America. They interpreted this pattern as a roughly synchronous global increase in the amount of warm-season grasses (C_4 plants) comprising herbivore diets (and hence, landscapes) and attributed this floral transition to an atmospheric pCO_2 decrease that increased plant photorespiration and favored C_4 plants over C_3 plants (trees, shrubs, and cool-season grasses) at mid- to low-latitudes. This interpretation was complicated, however, by subsequent studies. For example, alkenone-based pCO_2 reconstructions (Pagani et al., 1999) showed an increase in pCO_2 between 14 and 9 Ma and stabilization at ca. 280 ppm (~pre-industrial value) between 9 and 5 Ma. Fox and Koch (2003, 2004) used the $\delta^{13}C$ of pedogenic carbonate from the North American Great Plains to demonstrate that C_4 plants comprised up to 34% of biomass throughout the Miocene (before the $\delta^{13}C$ increase in mammals) but did not dominate low-latitude (< 37°N) landscapes until the mid-Pliocene (after the $\delta^{13}C$ increase in mammals). Additionally, the diachroneity of the mammal $\delta^{13}C$ increase between continents and compared to faunal turnover, along with the importance of local or regional influences on C_4 abundance, have increasingly become appreciated (Köhler et al., 1998; Edwards et al., 2010), prompting further consideration of the complexity underlying the evolution of the grassland biome.

1.2. Late Neogene transitions in the Mediterranean region

In parallel with many of the ecological and climatic changes occurring globally, the Mediterranean region also experienced substantial changes in vegetation and faunal structure during the late Neogene. However, this region can be distinguished by several differences from general global trends. For example, one of the most important phases of

faunal turnover in Europe during the Late Miocene was the “Vallesian Crisis” ca. 9.6 Ma (Agustí et al., 1999). This event was similar to global patterns in that it saw the extinction of many forest-adapted taxa (including nearly all European hominoids) that had experienced high diversity in the Middle Miocene. However, it is different in that it preceded comparable extinction events in North America (Tedford et al., 2004) and Asia (Badgley et al., 2008), and palynological records suggest that the Vallesian Crisis was not driven by the replacement of forested habitats with open grasslands (as on other continents), but rather by the replacement of subtropical forests by temperate deciduous forests (Agustí et al., 2003). Further, the C₃-C₄ transition seen in mammals and paleosols from most other continents is not seen in the Mediterranean region; the terrestrial carbon isotope record from Europe provides no evidence for abundant C₄ biomass at any point in its history (Quade et al., 1994; Cerling et al., 1997; Domingo et al., 2009; van Dam and Reichart, 2009). A second notable change in European faunal structure took place during the latest Miocene, ca. 5.5 Ma (Agustí et al., 2006). While contemporaneous with pulses of extinction occurring on other continents (Janis et al., 2002; Tedford et al., 2004), faunal turnover near the Miocene-Pliocene boundary in the Mediterranean region was related to its unique tectonic and paleogeographic situation. In this case, mammal turnover was driven by faunal interchange between Africa and Europe resulting from the desiccation of the Mediterranean Sea and emergence of land bridges between these continents during the Messinian Salinity Crisis (Agustí et al., 2006).

1.3. Tectonic and paleogeographic framework

The evolution of terrestrial systems in the Mediterranean region has been heavily influenced by its unique tectonic setting, in which paleogeography was governed by the interplay between convergent and extensional tectonic systems. At a large scale, the overall tectonic picture of the Mediterranean region during the majority of the Cenozoic has been one of general north-south convergence between the African and European landmasses due to differential seafloor spreading rates between the North and South Atlantic. This convergence led to the closure of the Tethyan seaway that had extended between the Atlantic and Indian Oceans during most of the Mesozoic, and to uplift of much of the western part of the Alpine-Himalayan orogenic belt beginning in the latest Cretaceous and continuing to today (Stampfli et al., 2001). Superimposed on this generally convergent regime, however, are many examples of smaller-scale extensional systems in both oceanic and continental lithosphere. During the early part of the Cenozoic, the western Mediterranean was characterized by SE-dipping oceanic lithosphere that was subducted beneath Africa. During the Late Oligocene, a reversal in the vergence of subduction led to back-arc rifting and development of many of the major marine sub-basins in southwest Europe, such as the Gulf of Lion, the Valencia Trough, and the Liguro-Provençal and Alboran Basins (Rosenbaum et al., 2002).

In the western Mediterranean Basin, continued extension in the Alboran Sea led to westward migration of an east-dipping subduction zone and resulted in a paleogeographic arrangement generally similar to present by ca. 10 Ma (Lonergan and White, 1997; Rosenbaum and Lister, 2004). Tectonic collision of this subduction zone

with the Iberian Massif and with northwest Africa resulted in Late Miocene orogenic uplift of the Betic (southern Iberia) and Rif (northwestern Africa) Cordilleras, which was largely responsible for the closure of seaways connecting the Mediterranean and the Atlantic Ocean during the Messinian Salinity Crisis (Krijgsman et al., 1999; Agustí et al., 2006). Clockwise (Betic) and counterclockwise (Rif) rotation of structural blocks during uplift of these ranges led to the development of a series of intramontane continental basins that accumulated continental sediments throughout the late Neogene and Pleistocene (Garcés et al., 1998; Alfaro et al., 2008).

In the central part of the Mediterranean Basin, the post-Oligocene back-arc rifting that opened the Gulf of Lion and the Ligurian Sea separated Corsica and Sardinia from mainland Europe and caused up to 30° of counterclockwise rotation of these terranes (Montigny et al., 1981), but brought them to their approximate present positions by the late Early Miocene (Rosenbaum et al., 2002). Extension immediately to the east of Corsica and Sardinia opened the northern Tyrrhenian Sea during the Middle and earliest Late Miocene (Brunet et al., 2000). Combined with counterclockwise rotation of the Apennines, this rifting resulted in a fold-and-thrust belt along the east side of the incipient northern Tyrrhenian Sea, connecting what is now northern Sardinia, eastern Liguria, western Tuscany, northwestern Sicily, and northeastern Tunisia (Azzaroli et al., 1986). The interplay of compression and extension along this belt resulted in a tectonically complex series of extensional basins, some of which received continental sediments during the Late Miocene and early Pliocene and contain endemic fossil mammal faunas indicating that the Late Miocene European-African connection in the

central Mediterranean was likely comprised of a series of islands that acted as filter bridges between these continents (Rook et al., 2000).

2. Objective and Organization of this Dissertation

The primary goal of this dissertation is to reconstruct circum-Mediterranean paleoclimate and paleoecology during the late Neogene, in order to better understand the global and regional changes that occurred in terrestrial ecosystems during this time. To address this objective, I use stable carbon and oxygen isotopes preserved in biogenic minerals from fossil mammal skeletons, in authigenic carbonate minerals from pedogenic, palustrine and lacustrine sediments, and in organic residues from paleosols. This work focuses primarily on the western (Spain) and central (northern Italy) areas of the Mediterranean region. Each of these areas includes many Neogene basins that are the focus of continuing comprehensive paleontological, sedimentological, stratigraphic, and geochronological studies. It is my hope that the work presented here will build upon these studies and will contribute to a more detailed understanding of the paleoclimate and paleoecology recorded in these basins.

This introductory chapter is followed by three chapters presented as manuscripts that are either published (Chapter 2) or will be submitted for publication (Chapters 3 and 4) upon successful defense and revision of this dissertation. Each of the chapters addresses slightly different spatial and/or temporal aspects of the objectives for this dissertation, but all of them build upon the theme of late Neogene paleoclimate and paleoecology in the context of Mediterranean tectonics. These chapters are followed by a

brief summary of the primary results and perspectives resulting from this work, along with an introduction to future research plans that are a direct consequence of the investigations described here (Chapter 5).

Chapter 2, “Stable isotopic evidence for terrestrial latitudinal climate gradients in the Late Miocene of the Iberian Peninsula”, explores temporal and spatial patterns of Late Miocene paleotemperature in Spain, and was published in *Palaeogeography, Palaeoclimatology, Palaeoecology* (Matson and Fox, 2010). This research focused on phosphate-bound oxygen isotopes from biogenic apatite in fossil tooth enamel and bone from various mammalian taxa at Neogene (primarily Late Miocene) localities in southeast and northeast Spain. To explore wider spatial and temporal patterns, the isotopic results from these localities were compared with similar data from Mio-Pliocene mammals in Libya, and with Pleistocene mammals from Spain. The data from this study successfully reconstruct expected isotopic patterns between taxa, and provide preliminary evidence for resource partitioning between groups of mammals previously interpreted (based on morphology) to live in similar habitats. Paleotemperature reconstructions in this study focused on the oxygen isotopic composition of fossil horse tooth enamel apatite, and these reconstructions indicate a latitudinal temperature gradient between northern and southern Spain that was likely steeper than today.

Chapter 3, “Wet climate in southeast Spain during the Messinian Salinity Crisis”, examines a narrower interval of time and space than Chapter 2, and focuses on a continental sedimentary sequence in southern Spain that is constrained biostratigraphically and paleomagnetically to the Messinian Salinity Crisis (MSC; ca. 5.9

– 5.3 Ma). Combined isotopic and sedimentological analyses indicate that this sequence records a lake level increase in a continental basin in southern Spain that is coeval with desiccation and a drastic sea level fall in the larger Mediterranean marine basin. While surprising in the context of traditional ideas about high aridity during the MSC, the results presented in Chapter 3 are consistent with some aspects of recent empirical and climate model results indicating wetter climates in parts of the circum-Mediterranean region during this event. The oxygen isotopic composition of lacustrine calcite from this study is consistent with water that was likely derived as runoff or groundwater from higher elevations during the MSC, constraining the paleoelevation and timing of local structural evolution of the Betic Cordillera. The manuscript presented in Chapter 3 will be submitted to *Geology*.

Chapter 4, “Carbon isotopic record of the relative roles of biotic and abiotic factors in the Late Miocene extinction of *Oreopithecus bambolii*, Baccinello Basin, Tuscany”, describes a unique opportunity for not only examining the relationship between tectonics and ecology, but also exploring the relative importance of biotic (i.e., interaction between species within an ecosystem) and abiotic (i.e., external processes such as environmental change) forcings on mammal evolution. In this study, I developed a stable carbon isotopic record from Late Miocene paleosols in northern Italy in order to explore the possibility of environmental change as a contributing factor in the extinction of the hominoid *Oreopithecus bambolii*. This taxon is important for understanding hominoid evolution because it was the last surviving hominoid in Europe, and it evolved many anatomical specializations in an island environment that complicate its

phylogenetic assignment. The results of this research indicate no environmental change associated with the disappearance of *Oreopithecus* from the fossil record, and imply that its extinction was driven largely by competition with mammals arriving from mainland Europe via a land bridge. This result, in turn, emphasizes the interplay between tectonic and biologic evolution. The manuscript presented in Chapter 4 will be submitted to *Journal of Human Evolution*.

References Cited

- Agustí, J., Cabrera, Ll., Garcés, M., and Llenas, M., 1999. Mammal turnover and global climate change in the late Miocene terrestrial record of the Vallès-Penedès Basin (NE Spain). *In*: Agustí, J., Rook, L., and Andrews, P. (Eds.), *The Evolution of Neogene Terrestrial Ecosystems in Europe*. Cambridge University Press, Cambridge, p. 397–412.
- Agustí, J., Sanz de Siria, A., and Garcés, M., 2003. Explaining the end of the hominoid experiment in Europe. *Journal of Human Evolution* 45, 145–53.
- Agustí, J., Garcés, M., and Krijgsman, W., 2006. Evidence for African-Iberian exchanges during the Messinian in the Spanish mammalian record. *Palaeogeography, Palaeoclimatology, Palaeoecology*, v. 238, p. 5–14.
- Alfaro, P., Delgado, J., Sanz de Galdeano, C., Galindo-Zaldívar, J., García-Tortosa, F.J., López-Garrido, A.C., López-Casado, C., Marín-Lechado, C., Gil, A., and Borque, M.J., 2008. The Baza Fault: a major active extensional fault in the central Betic

- Cordillera (south Spain). *International Journal of Earth Sciences (Geologische Rundschau)*, v. 97, p. 1353–1365.
- Anderson, J.B. and Shipp, S.S., 2001. Evolution of the West Antarctic ice-sheet. In: Alley, R.B. and Bindschadler, R.A. (Eds.), *The West Antarctic Ice Sheet: Behavior and Environment*. American Geophysical Union Antarctic Research Series, v. 77, p. 45–58.
- Azzaroli, A., Boccaletti, M., Delson, E., Moratti, G., and Torre, D., 1986. Chronological and paleogeographical background to the study of *Oreopithecus bambolii*. *Journal of Human Evolution*, v. 15, p. 533–540.
- Badgley, C., Barry, J.C., Morgan, M.E., Nelson, S.V., Behrensmeyer, A.K., Cerling, T.E., and Pilbeam, D., 2008. Ecological changes in Miocene mammalian record show impact of prolonged climatic forcing. *Proceedings of the National Academy of Sciences, USA*, v. 105, p. 12145–12149.
- Brunet, C., Monié, P., Jolivet, L., and Cadet, J.-P., 2000. Migration of compression and extension in the Tyrrhenian Sea, insights from $^{40}\text{Ar}/^{39}\text{Ar}$ ages on micas along a transect from Corsica to Tuscany. *Tectonophysics*, v. 321, p. 127–155.
- Cerling, T.E., Wang, Y., and Quade, J., 1993. Expansion of C_4 ecosystems as an indicator of global ecological change in the late Miocene.
- Cerling, T.E., Harris, J.M., MacFadden, B.J., Leakey, M.G., Quade, J., Eisenmann, V., and Ehleringer, J.R., 1997. Global vegetation change through the Miocene/Pliocene boundary. *Nature*, 389, 153–158.

- Domingo, L., Grimes, S.T., Domingo, M.S., and Alberdi, M.T., 2009. Paleoenvironmental conditions in the Spanish Miocene-Pliocene boundary: isotopic analyses of *Hipparion* dental enamel. *Naturwissenschaften*, v. 96, p. 503–511.
- Edwards, E.J., Osborne, C.P., Strömberg, C.A.E., Smith, S.A., and C₄ Grasses Consortium, 2010. The origins of C₄ grasslands: Integrating evolutionary and ecosystem science. *Science*, v. 328, p. 587–591.
- Fox, D.L. and Koch, P.L., 2003. Tertiary history of C₄ biomass in the Great Plains, USA. *Geology*, v. 31, p. 809–812.
- Fox, D.L. and Koch, P.L., 2004. Carbon and oxygen isotopic variability in Neogene paleosol carbonates: constraints on the evolution of the C₄-grasslands of the Great Plains, USA. *Palaeogeography, Palaeoclimatology, Palaeoecology* 207, 305–329.
- Garcés, M., Krijgsman, W., and Agustí, J., 1998. Chronology of the late Turolian deposits of the Fortuna basin (SE Spain): implications for the Messinian evolution of the eastern Betcs. *Earth and Planetary Science Letters*, v. 163, p. 69–81.
- Jacobs, B.F., Kingston, J.D., and Jacobs, L.L., 1999. The origin of grass-dominated ecosystems. *Annals of the Missouri Botanical Gardens*, v. 68, p. 590–643.
- Janis, C.M., Damuth, J., and Theodor, J.M., 2000. Miocene ungulates and terrestrial primary productivity: Where have all the browsers gone? *Proceedings of the National Academy of Sciences, USA*, v. 97, p. 7899–7904.
- Janis, C.M., Damuth, J., and Theodor, J.M., 2002. The origins and evolution of the North American grassland biome: the story from the hoofed mammals. *Palaeogeography, Palaeoclimatology, Palaeoecology*, v. 177, p. 183–198.

- Janis, C.M., Damuth, J., and Theodor, J.M., 2004. The species richness of Miocene browsers, and implications for habitat type and primary productivity in the North American grassland biome. *Palaeogeography, Palaeoclimatology, Palaeoecology*, v. 207, p. 371–398.
- Köhler, M., Moyà-Sola, S., and Agustí, J., 1998. Miocene/Pliocene shift: one step or several? *Nature*, v. 393, p. 126.
- Krijgsman, W., Hilgen, F.J., Raffi, I., Sierro, F.J., and Wilson, D.S., 1999. Chronology, causes and progression of the Messinian Salinity Crisis. *Nature*, v. 400, p. 652–655.
- Lawver, L.A. Gahagan, L.M., 2003. Evolution of Cenozoic seaways in the circum-Antarctic region. *Palaeogeography, Palaeoclimatology, Palaeoecology*, v. 198, p. 11–37.
- Liu, Z., Pagani, M., Zinniker, D., DeConto, R., Huber, M., Brinkhuis, H., Shah, S.R., Leckie, R.M., and Pearson, A., 2009. Global cooling during the Eocene-Oligocene climate transition. *Science*, v. 323, p. 1187–1190.
- Lonergan, L. and White, N., 1997. Origin of the Betic-Rif mountain belt. *Tectonics*, v. 16, p. 504–522.
- MacFadden, B.J., 1998. Equidae. *In*: Janis, C.M., Scott, K.M., and Jacobs, L.L. (Eds.), *Evolution of Tertiary Mammals of North America*. Cambridge University Press, Cambridge, p. 537–559.
- Maslin, M.A., Li, X.S., Loutre, M.-F., and Berger, A., 1998. The contribution of orbital forcing to the progressive intensification of northern hemisphere glaciation. *Quaternary Science Reviews*, v. 17, p. 411–426.

- Matson, S.D. and Fox, D.L., 2010. Stable isotopic evidence for terrestrial latitudinal climate gradients in the Late Miocene of the Iberian Peninsula. *Palaeogeography, Palaeoclimatology, Palaeoecology*, v. 287, p. 28–44.
- Montigny, R., Edel, J.B., and Thuizat, R., 1981. Oligo-Miocene rotation of Sardinia: K-Ar ages and paleomagnetic data of Tertiary volcanics. *Earth and Planetary Science Letters*, v. 54, p. 261–271.
- Pagani, M., Freeman, K.H., and Arthur, M.A., 1999. Late Miocene atmospheric CO₂ concentrations and the expansion of C₄ grasses. *Science*, v. 285, p. 876–879.
- Potts, R. and Behrensmeyer, A.K., 1992. Late Cenozoic terrestrial ecosystems. *In*: Behrensmeyer, A.K., Damuth, J., DiMichele, W., Potts, R., Sues, H.D., and Wing, S. (Eds.), *Terrestrial Ecosystems Through Time*. University of Chicago Press, Chicago, p. 419–519.
- Quade, J., Solounias, N., and Cerling, T.E., 1994. Stable isotopic evidence from paleosol carbonates and fossil teeth in Greece for forest or woodlands over the past 11 Ma. *Palaeogeography, Palaeoclimatology, Palaeoecology*, v. 108, p. 41–53.
- Rook, L., Gallai, G., and Torre, D., 2000. Lands and endemic mammals in the Late Miocene of Italy: Constraints for paleogeographic outlines of Tyrrhenian area. *Palaeogeography, Palaeoclimatology, Palaeoecology*, v. 238, p. 263–269.
- Rosenbaum, G. and Lister, G.S., 2004. Formation of arcuate orogenic belts in the western Mediterranean region. *Special Paper – Geological Society of America*, v. 393, p. 41–56.

- Rosenbaum, G., Lister, G.S., and Duboz, C., 2002. Reconstruction of the tectonic evolution of the western Mediterranean since the Oligocene. *Journal of the Virtual Explorer*, v. 8, p. 107–126.
- Shackleton, N.J., Imbrie, J., Pisias, N.G., and Rose, J., 1988. The evolution of oceanic oxygen-isotope variability in the North Atlantic over the past three million years. *Philosophical Transactions of the Royal Society of London, Series B*, v. 318, p. 679–688.
- Stampfli, G.M., Borel, G.D., Cavazza, W., Mosar, J., and Ziegler, P.A., 2001. Palaeotectonic and palaeogeographic evolution of the western Tethys and PeriTethyan domain (IGCP Project 369). *Episodes*, v. 24, p. 222–228.
- Stickley, C.E., Brinkhuis, H., Schellenberg, S.A., Sluijs, A., Röhl, U., Fuller, M., Grauert, M., Huber, M., Warnaar, J., and Williams, G.L., 2004. Timing and nature of the deepening of the Tasmanian Gateway. *Paleoceanography*, v. 19, p. 1–18.
- Tedford, R.H., Albright, L.B., III, Barnosky, A.D., Ferrusquia-Villafranca, I., Hunt, R.M., Jr., Storer, J.E., Swisher, C.C., III, Voorhies, M.R., Webb, S.D., and Whistler, D.P., 2004. Mammalian biochronology of the Arikarean through Hemphillian interval (Late Oligocene through early Pliocene epochs). *In*: Woodburne, M.O. (Ed.), *Late Cretaceous and Cenozoic Mammals of North America: Biostratigraphy and Geochronology*. Columbia University Press, New York, p. 169–231.
- van Dam, J.A. and Reichart, G.J., 2009. Oxygen and carbon isotope signatures in late Neogene horse teeth from Spain and application as temperature and seasonality proxies. *Palaeogeography, Palaeoclimatology, Palaeoecology*, v. 274, p. 64–81.

Zachos, J., Pagani, M., Sloan, L., Thomas, E., and Billups, K., 2001a. Trends, rhythms, and aberrations in global climate 65 Ma to present. *Science*, v. 292, p. 686–693.

Zachos, J.C., Shackleton, N.J., Revenaugh, J.S., Pälike, H., and Flower, B.P., 2001b. Climate response to orbital forcing across the Oligocene-Miocene boundary. *Science*, v. 292, p. 274–278.

Chapter 2: Stable isotopic evidence for terrestrial latitudinal climate gradients in the Late Miocene of the Iberian Peninsula

Samuel D. Matson and David L. Fox

Department of Geology and Geophysics, University of Minnesota, 108 Pillsbury Hall, 310 Pillsbury Drive SE, Minneapolis, Minnesota 55455

Published in *Palaeogeography, Palaeoclimatology, Palaeoecology*,
v. 287, no. 1–4, p. 28–44

Used with permission of Elsevier

The late Neogene of the Mediterranean region is marked by significant faunal and floral turnover in terrestrial ecosystems, paleogeographic and paleoceanographic changes associated with the Messinian Salinity Crisis (MSC), and regional climate transition associated with the onset of northern hemisphere glaciation. In this paper we report stable oxygen isotope compositions ($\delta^{18}\text{O}$) of terrestrial mammal faunas from the Late Miocene, Pliocene and Pleistocene of Spain, and compare these data with Late Miocene mammal $\delta^{18}\text{O}$ values from northern Libya. Since tooth enamel $\delta^{18}\text{O}$ from modern horses has been demonstrated to be a reasonable proxy for the $\delta^{18}\text{O}$ of local meteoric water, which is in turn strongly dependent on mean annual temperature (MAT), we use the $\delta^{18}\text{O}$ of fossil horse tooth enamel to estimate MAT. Our paleotemperature reconstructions are consistent with global cooling during the late Cenozoic, with MAT for the Late Miocene that is warmer than today by $\sim 1\text{--}2^\circ\text{C}$ in NE Spain and by $\sim 4\text{--}5^\circ\text{C}$ in SE Spain. The difference of $\sim 8\text{--}9^\circ\text{C}$ between NE and SE Spain for the Late Miocene is $\sim 60\%$ greater than the MAT difference between these same areas today. The $\delta^{18}\text{O}$ values from Libya are lower than those for southern Spain, and may suggest cooler and/or wetter climates in

northeastern Africa during the latest Miocene and early Pliocene. We examined intrafaunal $\delta^{18}\text{O}$ patterns to make interpretations about paleoecology and to qualitatively assess paleoaridity. Comparisons of $\delta^{18}\text{O}$ values between clades are consistent with a semi-aquatic lifestyle for anthracotheres, hippopotamids, and castorids. We also compare intra-tooth samples of enamel and dentine to examine possible diagenetic alteration of these materials. Comparisons of enamel and dentine $\delta^{18}\text{O}$ suggest slight diagenetic alteration of dentine, but we demonstrate that these $\delta^{18}\text{O}$ values can be used to reconstruct reasonable values of diagenetic water $\delta^{18}\text{O}$. Overall, our data do not support large climatic changes in the Iberian Peninsula during the MSC, but are consistent with long-term global cooling and sharper latitudinal climate gradients in Spain during the Neogene.

Keywords: Spain; oxygen isotopes; mammals; Neogene; paleoclimate; Messinian Salinity Crisis

1. Introduction

Some of the most important Cenozoic changes in global climate and terrestrial ecosystems occurred during the Neogene. Global cooling throughout the Neogene led to the Late Miocene expansion of Antarctic continental ice sheets (Anderson and Shipp, 2001; Zachos et al., 2001) that initially formed at the Eocene-Oligocene boundary (Liu et al., 2009), and to glaciation in the northern hemisphere during the Pliocene (Shackleton et al., 1988; Maslin et al., 1998; Zachos et al., 2001). Aridification during this period is reflected by terrestrial ecosystems that had been characterized by forested environments

throughout the early Cenozoic but became dominated by more open mixed woodland and C₃ grasslands during the Miocene, and later by C₄ grasslands at mid- to low latitudes in the latest Miocene and Pliocene (Potts and Behrensmeyer, 1992; Quade and Cerling, 1995; Cerling et al., 1997; Jacobs et al., 1999; Fox and Koch, 2003; Strömberg, 2005). Associated with this change in vegetation was a global turnover in ungulate faunas, in which brachyodont browsing taxa were gradually replaced by gracile, hypsodont grazing taxa throughout the Late Miocene (Janis et al., 2000, 2004). This gradual faunal turnover culminated in the widespread extinction of non-hypsodont ungulates during the latest Miocene and early Pliocene (Janis et al., 2002; Tedford et al., 2004).

The Mediterranean region experienced broadly similar patterns during the Neogene, but this area is also distinguished by several important differences from general global trends. For example, while terrestrial ecosystems in the Mediterranean region also experienced the Miocene transition to more open mixed woodland and grassland environments (Agustí et al., 1999; Solounias et al., 1999), they have remained dominated by C₃ vegetation to the present (Quade et al., 1994; Cerling et al., 1997). In addition to global changes in climate, regional changes in circum-Mediterranean paleogeography helped to drive important changes in the composition of mammal faunas. The Messinian Salinity Crisis (MSC) is the most intensively studied of these paleogeographic changes, and it had important ecological implications for both marine and terrestrial ecosystems. During the MSC, combined tectonic and glacio-eustatic isolation of the Mediterranean Basin from the Atlantic Ocean between 5.59 and 5.33 Ma (Krijgsman et al., 1999) led to widespread desiccation of the Mediterranean Sea, a base-level drop of up to 1,500 m,

deep incision of river valleys emptying into the Mediterranean Basin, and deposition of up to 2-3 km-thick evaporite sequences (Hsü et al, 1973, 1977; Krijgsman, 2002). The MSC event also affected terrestrial ecosystems through faunal interchanges between Africa and Europe (Agustí et al., 2006; van der Made et al., 2006). Paleoclimatic reconstructions for the MSC interval have largely focused on the timing and climatic causes for this event (Hodell et al., 1994; Clauzon et al., 1996; Krijgsman et al., 1999), but more recent studies have begun to explore its potential effects on regional climate (Fluteau et al., 2003; Blanc, 2006; Fauquette et al., 2006; Costeur et al., 2007).

To investigate changes in terrestrial climate during the Late Neogene of the Mediterranean region, we developed a stable oxygen isotope record from Late Miocene and Pliocene fossil mammals from Spain. For temporal and geographic comparison, we also report similar data from the Pleistocene of southern Spain and the latest Miocene of northern Libya. A primary connection between climate and oxygen isotopes in continental systems is the strong positive correlation between mean annual temperature (MAT) and the oxygen isotopic composition ($\delta^{18}\text{O}$ value) of meteoric water ($\delta^{18}\text{O}_w$) for modern temperate latitudes, which is related to preferential rainout of the heavy oxygen isotope (^{18}O) during poleward transport of air masses (Dansgaard, 1964; Rozanski et al., 1993; Fricke and O'Neil, 1999). Though the slope and intercept of the global MAT- $\delta^{18}\text{O}$ relationship can change depending on temporal changes in latitudinal temperature gradients and the $\delta^{18}\text{O}$ of precipitation source water (Boyle, 1997; Fricke and O'Neil, 1999), if the modern MAT- $\delta^{18}\text{O}$ relationship was generally similar in the past then records of the $\delta^{18}\text{O}$ of past meteoric waters can be used as proxies for paleotemperature.

Stable oxygen isotopes in fossil mammal skeletons have been widely used as a proxy for paleo-precipitation $\delta^{18}\text{O}$ (Koch, 1998; Kohn and Cerling, 2002). Mammals offer a unique advantage for isotopic studies compared to other animals because they internally regulate their body temperature, thereby eliminating variable fractionation due to temperature variation during skeletal tissue growth (Longinelli, 1984; Luz and Kolodny, 1985). The $\delta^{18}\text{O}$ of mammalian skeletal hydroxylapatite (i.e., tooth enamel and dentine, and bone) is directly controlled by the $\delta^{18}\text{O}$ of body water, which is in turn a function of several oxygen influxes (e.g., breath O_2 and H_2O , drinking water, H_2O and free or chemically bound oxygen in diet) and effluxes (e.g., breath CO_2 and H_2O , water in urine and feces, transcutaneous water loss). For large-bodied mammal species that rely on drinking water, hydroxylapatite $\delta^{18}\text{O}$ is controlled primarily by the $\delta^{18}\text{O}$ of local meteoric water and by relative humidity (Luz et al., 1984; Kohn, 1996; Kohn et al., 1996).

2. Materials and Methods

2.1. Geologic Setting

The majority of the data reported in this paper come from the Mio-Pliocene Neogene Fortuna and Teruel Basins, and the Plio-Pleistocene Baza Basin. We also report data from the late Miocene localities of Venta del Moro (VM) and Almenara-M (AM) in eastern Spain, and from the latest Miocene Sahabi locality (SH) in northern Libya. Venta del Moro is located in the Cabriel Basin, approximately 80 km west of the city of Valencia (Figure 2.1). The sedimentary infill of the Cabriel Basin is dominated by lacustrine limestones and marls, and fluvial sandstones, conglomerates and mudstones.

An age of approximately 5.9 Ma for Venta del Moro has been proposed based on biostratigraphic and magnetostratigraphic studies (Agustí et al., 2006; Montoya et al., 2006; Opdyke et al., 1990, 1997). The Almenara-M locality is an isolated karst fissure-fill located in a carbonate massif near the Mediterranean coast between Castellón and Valencia (Figure 2.1). The rodent fauna at Almenara-M suggests an age between approximately 6.1 and 5.3 Ma, and the karst development there has traditionally been associated with base-level drawdown and erosion during the MSC (Agustí et al., 2006; Köhler et al., 2000; Krijgsman et al., 1999). The Qasr as-Sahabi locality is located in northern Libya, approximately 120 km southeast of the Gulf of Sirt between Ajdabiyah and the Jalu oasis. The fossils used in this study come from the Sahabi Formation (members T, U, and V of de Heinzelin and El-Arnauti, 1987), which is composed of interbedded transgressive marine sands, lenticular sand and gravel channel deposits, incipient paleosols, and dolomite beds. The Sahabi fauna includes both terrestrial (e.g., mammals, crocodiles, birds, turtles) and marine (e.g., sharks, sirenians, cetaceans) taxa, and unconformably overlies highly gypsified middle and Late Miocene marine facies (Boaz et al., 1987). This locality has been interpreted to represent fluvial incision and subsequent estuarine deposition associated with the onset and recovery phases of the MSC near the Miocene-Pliocene boundary (de Heinzelin and El-Arnauti, 1987).

Biostratigraphic correlations suggest an age of approximately 5.2 or slightly older for the Sahabi fauna (de Heinzelin and El-Arnauti, 1987; Bernor and Scott, 2003; Beyer, 2008)

The fossil localities Librilla (LB), Molina de Segura (MS), and La Alberca (LA) are located in the Fortuna Basin in southeastern Spain, approximately 20 km west of the

city of Murcia (Figure 2.1). The basin lies at the contact between the Internal and External Zones of the Betic Cordillera, and is bounded in the north by the ENE-WSW-trending Crevillente Fault and in the south by the NE-SW-trending Alhama de Murcia Fault. Basin subsidence associated with transtension along these sinistral faults is recorded by a late Tortonian transgressive marine sequence consisting of turbidites, pelagic marls, deltaic deposits and reef complexes (Garcés et al., 2001). These sediments are overlain by a late Tortonian regressive marine unit consisting of marls, diatomites, and gypsum representing a period of localized basin restriction (Garcés et al., 1998, 2001; Krijgsman, et al., 2000). The fossils used in this study come from interbedded Messinian lacustrine carbonates and alluvial conglomerates and sandstones that conformably overlie the evaporite sequence and were derived from massifs of Meso-Cenozoic carbonates (External Zone) and Paleozoic-Cenozoic metamorphic complexes (Internal Zone) that were uplifted during a period of latest Miocene transpression. Biochronologic (Mein et al., 1973; Steininger et al., 1996; Agustí et al., 2006), radiometric (Kuiper et al., 2006), magnetostratigraphic (Garcés et al., 1998, 2001), and astrochronologic (Kruvier, et al., 2002) studies of these terrestrial sediments suggest ages of approximately 5.9 – 6.3 Ma for Librilla, 6.6 – 6.0 Ma for Molina de Segura, and 5.6 Ma for La Alberca.

The fossil localities Venta Micena (VA), Puerto Lobo (PL), Barranco del Paso (BP), and Barranco León (BL) are located in the Baza Basin in southeastern Spain, approximately 100 km east of the city of Granada (Figure 2.1). The Baza Basin forms the eastern part of the largest of the intramontane basins of the Betic Cordillera, and like the Fortuna Basin, it is located at the boundary between the Internal and External Betic

Zones. Subsidence during the Late Miocene isolated the Baza Basin from the Mediterranean Sea and from surrounding basins, and led to the deposition of 2,000 – 3,000 m (Alfaro et al., 2008) of lacustrine and palustrine carbonates and mudstones and alluvial sandstones under endorheic conditions from the Late Miocene until the Middle Pleistocene (Garcés et al., 1997a; Gibert et al., 2006; Scott et al., 2007). After this time, neotectonic uplift combined with stream piracy from a tributary of the Guadalquivir River to the north led to external drainage and the incision of Neogene strata that characterizes this area today (Scott et al., 2007). Detailed basin analysis combined with biostratigraphic and magnetostratigraphic studies (Gibert et al., 2007; Scott et al., 2007) suggest ages of approximately 1.3 Ma for Venta Micena and Barranco del Paso, 1.25 Ma for Barranco León, and 0.8 Ma for Puerto Lobo.

The fossil localities Los Mansuetos (LM), Concud (CC), El Arquillo (AQ), and La Calera (LC) are located in the Teruel Basin in northeastern Spain, near the town of Teruel (Figure 2.1). The Teruel Basin extends more than 100 km in a NNE-SSW direction, roughly perpendicular to the NW-SE-trending Iberian Chain in which it is located. The basin is a half-graben, bounded on its southeastern margin by Mesozoic carbonates and evaporites in the footwall blocks of a series of NNE-SSW-trending normal faults (Anadón and Moissenet, 1996). Basin subsidence took place through tectonic extension along these faults during the Miocene. Early Miocene deposits are located along the eastern margin of the graben, but the majority of the basin infill is represented by a ~500 m-thick record of Late Miocene to Pliocene alluvial sandstones and gravels, and lacustrine and palustrine limestones and marls (Alonso-Zarza and Calvo,

2000; Anadón and Moissenet, 1996) from which the fossils used in this study were recovered. Biostratigraphic (Alcalá, 1994; van Dam et al., 2001), astrochronologic (van Dam et al., 2006), and magnetostratigraphic (Garcés et al., 1997b) studies of the Teruel Basin suggest ages of approximately 7.2 – 7.1 Ma for Concud and Los Mansuetos, 6.4 – 6.1 Ma for El Arquillo, and 4.3 Ma for La Calera.

2.2. Sampling protocol and analytical procedure

Samples used in this study were collected from fossil materials housed at the Institut Català de Paleontologia in Sabadell, Spain, and the Museo Josep Gibert in Orce, Spain. Powdered enamel, dentine, and bone samples were collected using a diamond bur bit mounted into a variable-speed, handheld rotary drill. For the enamel samples, cementum and the outermost ~0.5 mm of enamel were removed from a ~2 mm wide longitudinal band along the lingual or buccal margins of the fossil teeth. This outer material was isolated from the samples collected for isotopic analysis to avoid inclusion of surface contaminants. Bulk samples were then collected along a longitudinal transect from the underlying enamel. For eight horse teeth and a single gomphothere molar, serial samples were collected at ~1 cm intervals measured from the root of the tooth. Care was taken during sample collection to not disturb diagnostic morphology on the occlusal surface of the teeth, and all samples were drilled at low speed to minimize heating and potential isotopic fractionation.

The hydroxylapatite powder samples were converted to Ag_3PO_4 using the method described by Bassett et al. (2007), which is a modified version of the method described by O’Neil et al. (1994). Approximately 1.5 mg aliquots of enamel powder were dissolved

over 24 hours in 100 μl of 0.5M nitric acid in 1.5 ml polypropylene microcentrifuge tubes. The solution was then neutralized with 75 μl of 0.5M potassium hydroxide. Calcium salts were precipitated using 200 μl of 0.36M potassium fluoride and were separated through centrifugation and transfer of the supernatant to a second 1.5 ml microcentrifuge tube. Silver phosphate was then precipitated by adding 0.25 ml of silver amine solution (0.2M AgNO_3 , 0.35M NH_4NO_3 , 0.74M NH_4OH) and letting ammonia exsolve slowly from the tubes over 24 hours at 50°C in a drying oven.

The resulting yellow Ag_3PO_4 crystals were rinsed five times with 1 ml of distilled, deionized water, dried for 24 hours at 50°C in a drying oven, and transferred into 3.5 x 5 mm Ag capsules that were folded tightly. The prepared samples were then reduced to CO through high-temperature pyrolysis in a Finnigan high temperature conversion-elemental analyzer (TC-EA) at the University of Kansas (KU) Stable Isotope Laboratory, and at the University of Saskatchewan (USK) Isotope Laboratory. The CO was introduced via a continuous helium flow into a Thermo Electron Finnigan MAT 253 (KU) or Delta-Plus (USK) isotope ratio mass spectrometer, and its isotopic composition was measured. The sample $^{18}\text{O}/^{16}\text{O}$ ratios were calibrated to the Vienna Standard Mean Ocean Water (VSMOW) scale using a four-point calibration curve ($R^2 > 0.9994$) based on Acros Ag_3PO_4 , NIST ANU Sucrose, IAEA-601 benzoic acid, and Sigma Aldrich Cellulose standards. Analytical precision for the TC/EA analyses was maintained 0.34‰ or better based on compiled $\delta^{18}\text{O}$ analyses of phosphorite (NIST 120c) subjected to the same preparation procedure as the apatite samples. Stable oxygen isotopic ratios reported in this paper follow the conventional δ -notation: $\delta^{18}\text{O} = [(\text{R}_{\text{sample}})/(\text{R}_{\text{standard}}) - 1] \times 1000$,

where $R = {}^{18}\text{O}/{}^{16}\text{O}$ and standard is Vienna Standard Mean Ocean Water (VSMOW). The δ values are reported in parts per thousand (‰). Statistical comparisons reported in this paper were made using SPSS PASW Statistics 17, Microsoft Excel, and RMA (Bohanek, 2002) software. Uncertainties reported for calculated variables follow the error propagation formulas described by Ku (1966).

3. Results

The results of the isotopic analyses are presented in Table 2.1 and in Figure 2.2. The $\delta^{18}\text{O}$ values from bulk enamel samples range from 14.5‰ to 27.2‰ ($\bar{x} = 20.1\text{‰}$, $s.d. = 2.3\text{‰}$, $n = 87$). The lowest enamel $\delta^{18}\text{O}$ values in the dataset come from two samples of the anthracothere *Libycosaurus petrocchii* (14.5‰ and 16.0‰, Sahabi), the hippopotamids *Hexaprotodon* (16.0‰, El Arquillo) and *Hippopotamus* (14.6‰, Barranco León), and from a single sample of the castorid *Dipoides* (14.7‰, Los Mansuetos). Rhinocerotids yield slightly higher values, ranging from 17.3‰ to 18.9‰ ($\bar{x} = 18.1\text{‰}$, $s.d. = 0.8\text{‰}$, $n = 4$). The four samples from suids yield both a slightly higher mean value (18.7‰) and range ($s.d. = 1.3\text{‰}$) than the rhinocerotids. A single sample from the ursid *Agriotherium* from Venta del Moro at 19.4‰ falls within the range of suid values, but is approximately 1‰ higher than the mean value for suids. The largest number of bulk enamel samples ($n = 42$) in this study come from equids, represented by the genera *Hipparion* (Sahabi; Teruel, Fortuna, and Cabriel Basins) and *Equus* (Baza Basin). The $\delta^{18}\text{O}$ values for equids range from 16.3‰ at El Arquillo to 24.1‰ at Molina de Segura ($\bar{x} = 20.3\text{‰}$, $s.d. = 1.8\text{‰}$). The $\delta^{18}\text{O}$ values of bovids ($\bar{x} = 20.7\text{‰}$, $s.d. = 1.2\text{‰}$, $n = 10$)

range from 18.9‰ at La Calera to 22.7‰ at El Arquillo and have a slightly higher mean value than that of equids, though they fall within the range of equid values. A single sample from the gomphothere *Tetralophodon* from El Arquillo has a value of 21.7‰, and falls within the upper end of the range of bovid values. The highest $\delta^{18}\text{O}$ mean value and range are seen in cervids ($\bar{x} = 21.7\text{‰}$, $s.d. = 2.9\text{‰}$, $n = 12$), which range from 17.6‰ at Los Mansuetos to 27.2‰ at Librilla. Five samples of isolated cervid or bovid teeth (labeled “Artiodactyla indet.” in Table 2.1) that could not be identified with higher taxonomic resolution have $\delta^{18}\text{O}$ values ($\bar{x} = 20.5\text{‰}$, $s.d. = 1.1\text{‰}$) that fall within the range of cervid $\delta^{18}\text{O}$ and have a mean value similar to that of bovinds.

Statistical comparisons between taxonomic groups based on Student’s *t*-tests and non-parametric Mann-Whitney *U* tests (since not all samples were normally distributed) for sample means are summarized in Table 2.2. These comparisons reveal that the mean $\delta^{18}\text{O}$ value for hippopotamids is significantly different than that of bovinds, cervids, and equids at a 95% confidence level. Also, the mean $\delta^{18}\text{O}$ value for rhinocerotids was significantly different than that of bovinds, cervids, equids, and the group of unidentifiable bovinds or cervids. Finally, suids have a significantly different mean $\delta^{18}\text{O}$ value than that of bovinds. It is important to note that while significant differences were found for hippopotamids, rhinocerotids, and suids, the sample sizes for these groups are small and statistical comparisons between taxa should thus be interpreted with caution.

The highest faunal $\delta^{18}\text{O}$ means for the bulk enamel samples are seen at the Late Miocene localities of Librilla ($\bar{x} = 23.0\text{‰}$, $s.d. = 3.3\text{‰}$, $n = 6$) and Molina de Segura ($\bar{x} = 22.3\text{‰}$, $s.d. = 1.5\text{‰}$, $n = 9$) in the Fortuna Basin. The faunal mean $\delta^{18}\text{O}$ for La Alberca

($\bar{x} = 20.8\text{‰}$, $s.d. = 1.1\text{‰}$, $n = 3$) is slightly lower than that of Librilla and Molina de Segura. Compared to the Fortuna Basin, the faunal $\delta^{18}\text{O}$ means for the Miocene localities in the Teruel Basin are much lower and are similar to one another, ranging from 19.3‰ at Conclud ($s.d. = 1.2\text{‰}$, $n = 10$) to 19.6‰ at El Arquillo ($s.d. = 2.0\text{‰}$, $n = 21$). The faunal $\delta^{18}\text{O}$ means from the Pleistocene Baza Basin are comparable to the Teruel Basin for the 1.3 – 1.25 Ma localities ($\bar{x} = 19.5\text{‰}$, $s.d. = 2.6\text{‰}$, $n = 7$), while the mean of the two samples from the 0.9 Ma locality of Puerto Lobo (18.3‰) is lower. The lowest faunal mean $\delta^{18}\text{O}$ comes from the Late Miocene locality of Sahabi ($\bar{x} = 17.7\text{‰}$, $s.d. = 2.3\text{‰}$, $n = 5$) in northern Libya. Student's t -tests and Mann-Whitney U tests comparing locality means are presented in Table 2.3. These comparisons reveal that the differences between the Late Miocene localities in the Fortuna and Teruel Basins are significant at a 95% confidence level. The combined mean of the three Fortuna Basin localities is also significantly higher than the combined means for the Teruel Basin ($p < 0.001$) and Baza Basin ($p = 0.003$).

The $\delta^{18}\text{O}$ values of 48 teeth for which both enamel and dentine were sampled are reported in Table 2.1 and shown in Figures 2.2A and 2.3B. The enamel values for these samples range from 14.5‰ to 24.1‰ ($\bar{x} = 19.9\text{‰}$, $s.d. = 2.1\text{‰}$), while the corresponding dentine values have a slightly smaller range (13.1‰ to 22.1‰) and lower mean value ($\bar{x} = 18.7\text{‰}$, $s.d. = 1.7\text{‰}$). The majority of the dentine values are depleted in ^{18}O relative to corresponding enamel values, but nine of the 48 dentine samples are ^{18}O -enriched relative to enamel. The differences in $\delta^{18}\text{O}$ between enamel and corresponding dentine are not consistent, and range from -3.4‰ to 4.2‰ ($\bar{x} = 1.2\text{‰}$, $s.d. = 1.4\text{‰}$). Ordinary

least-squares (OLS) regression of dentine $\delta^{18}\text{O}$ onto enamel $\delta^{18}\text{O}$ for the 48 samples results in a significant positive relationship ($r = 0.73$, $p < 0.001$), but the slope of the regression line (0.59) is less than unity. OLS regression of dentine $\delta^{18}\text{O}$ onto enamel $\delta^{18}\text{O}$ for each of the Neogene localities (Concud, $n = 6$; Los Mansuetos, $n = 10$; El Arquillo, $n = 9$; Molina de Segura, $n = 5$; Sahabi, $n = 4$) reveals significant relationships between these variables at Concud ($p = 0.042$) and Molina de Segura ($p = 0.003$) only. A significant relationship ($p = 0.036$) is also found through OLS regression of the same variables for a group of five Pleistocene samples from three coeval localities (Venta Micena, $n = 3$, Barranco del Paso, $n = 1$, Barranco León, $n = 1$) from the Baza Basin. The equations of the regression lines for each locality are presented in Figure 2.3B.

The $\delta^{18}\text{O}$ values for serial samples collected from eight equid (*Hipparion*) teeth from Concud, El Arquillo, Los Mansuetos, La Alberca, and Venta del Moro, and from a single gomphothere (*Tetralophodon*) molar from El Arquillo, are reported in Table 2.1 and shown in Figure 2.4C. The $\delta^{18}\text{O}$ ranges for individual teeth are only weakly correlated with the number of samples collected per tooth ($r = 0.58$, $p = 0.102$). The highest mean value and range (4.3‰) in $\delta^{18}\text{O}$ for the serially sampled teeth are seen in an equid tooth from Los Mansuetos ($\bar{x} = 22.4\text{‰}$, $s.d. = 1.8\text{‰}$, $n = 5$). A second tooth from this locality also displays a high variability (3.0‰), but has the lowest mean value ($\bar{x} = 17.5\text{‰}$, $s.d. = 1.1\text{‰}$, $n = 4$). The smallest ranges (1.8‰) are seen in an equid tooth ($\bar{x} = 19.5\text{‰}$, $s.d. = 1.0\text{‰}$, $n = 3$) and a gomphothere tooth ($\bar{x} = 21.0\text{‰}$, $s.d. = 0.8\text{‰}$, $n = 4$) that are both from El Arquillo. The two other serially sampled equids from El Arquillo have ranges of 1.9 and 2.6‰ and mean values of 20.0 and 18.1‰, respectively. Pairwise

comparisons of variance between all serially-sampled teeth reveal no significant differences (F -test, $p > 0.116$), but Student's t -test comparisons reveal differences in means that are significant at a 95% confidence level both between and within localities.

If bulk samples from equid teeth are capturing the full range of intra-tooth isotopic variability, then the $\delta^{18}\text{O}$ of bulk samples should correlate strongly with the mean $\delta^{18}\text{O}$ of serial samples for corresponding teeth. OLS regression of serial mean $\delta^{18}\text{O}$ onto corresponding bulk sample $\delta^{18}\text{O}$ for the nine serially sampled teeth (Figure 2.4B) reveals a significant relationship ($r = 0.86$, $p = 0.003$) between these variables. The equid tooth from Concud has a serial mean value that is 1.5% higher than the corresponding bulk sample value. If this outlier is excluded, the relationship between bulk and serial mean values for the remaining eight teeth is much stronger ($r = 0.95$, $p < 0.001$), with an OLS slope (1.1) near unity and an error for the regression intercept that includes zero.

4. Discussion

4.1. Taxonomic $\delta^{18}\text{O}$ patterns

The bulk enamel $\delta^{18}\text{O}$ values reported here exhibit patterns that are consistent with results from published isotopic studies of closely related taxa in modern and fossil faunas. For example, anthracotheres, hippopotamids and castorids from this study are consistently the most ^{18}O -depleted taxa in the faunas in which they are found (Figure 2.2). We interpret the low $\delta^{18}\text{O}$ values for these taxa as representing a semi-aquatic lifestyle. Bocherens et al. (1996) observed a similar pattern in extant *Hippopotamus* from Amboseli National Park in Kenya, where this taxon is depleted in ^{18}O by 2.5–3‰ relative

to browsing taxa such as elephants and rhinoceroses, and by more than 5‰ relative to grazing taxa such as zebras, wildebeests, and buffalo. These authors attributed the low $\delta^{18}\text{O}$ values for *Hippopotamus* either to nocturnal grazing or incorporation of aquatic C_3 vegetation into the diet (based on low $\delta^{13}\text{C}$ values), or to a semi-aquatic lifestyle that reduces evaporative water loss and isotopic fractionation of body water. A more recent study of extant *Hippopotamus* from Tsavo National Park by Cerling et al. (2008) demonstrated that this taxon is depleted in ^{18}O by a similar amount relative to other taxa, even when its diet consists of terrestrial C_4 vegetation. Physiological modeling results reported by Clementz et al. (2008) suggest that hippopotamid $\delta^{18}\text{O}$ values that are consistently low relative to associated faunas can be explained in large part by a high water turnover rate associated with a semi-aquatic lifestyle. The low $\delta^{18}\text{O}$ for the single castorid sample is also consistent with a semi-aquatic lifestyle. Though a terrestrial burrowing castorid (*Rhizospalax*) is known from the Oligocene in France, European castorids exhibit morphological specializations for semi-aquatic behavior since the early Miocene (Hugué and Escuillie, 1996; van Dam and Weltje, 1999; García-Alix et al., 2007). While the extinction of anthracotheres near the Miocene-Pliocene boundary precludes their comparison with modern analogues, these taxa have also been interpreted as semi-aquatic based on morphological and stable isotopic evidence (Clementz et al., 2008). Interestingly, Sahabi is the only locality in this study that includes anthracotheres (*Libycosaurus*), and the hippopotamid *Hexaprotodon* from Sahabi is not as ^{18}O -depleted relative to its associated fauna when compared to hippopotamids from other localities. Recent phylogenetic analyses of Hippopotamidae nest this clade within

Anthracotheriidae (Boisserie et al., 2005), and the diversification of hippopotamids has been spatially and temporally associated with the extinction of anthracotheres (Gaziry, 1987). Our isotopic data from Sahabi are consistent with possible ecological niche partitioning in terms of habitat between *Libycosaurus* and *Hexaprotodon*.

The $\delta^{18}\text{O}$ values for other taxa in this study are also consistent with expected patterns based on extant faunas. Levin et al (2006) categorized extant African taxa as evaporation insensitive (EI) and evaporation sensitive (ES) based on the dependence of their enamel $\delta^{18}\text{O}$ on the difference between potential evapotranspiration and mean annual precipitation for several climatically distinct areas in eastern Africa. ES taxa generally have higher $\delta^{18}\text{O}$ values than co-occurring EI taxa, with larger differences under greater aridity. The difference between ES and EI taxa is likely due to the relative contributions of drinking water and leaf water to body water, since the leaf water $\delta^{18}\text{O}$ is more sensitive to evaporation than surface water $\delta^{18}\text{O}$ (Farris and Strain, 1978; Luz and Kolodny, 1985, 1989). The relatively low $\delta^{18}\text{O}$ values for fossil rhinocerotids, suids, and equids in this study are consistent with the EI distinction for their close modern relatives. Furthermore, the high $\delta^{18}\text{O}$ values for most cervids in this study are consistent with a high contribution of leaf water to total body water characteristic of ES taxa. The study by Levin et al. (2006) did not include cervids, but earlier studies of modern deer (*Odocoileus*) from North America demonstrate that cervid $\delta^{18}\text{O}$ can be strongly influenced by aridity (Land et al., 1980; Luz et al., 1990; Cormie et al., 1994). Cervid $\delta^{18}\text{O}$ from some localities (e.g., Molina de Segura, Los Mansuetos, Concud) is low relative to the coeval fauna, suggesting physiological or behavioral variation among

cervid species that precludes designation of the entire family as ES. Levin et al. (2006) found a similarly variable dependence of $\delta^{18}\text{O}$ on aridity for bovids.

Though the ES-EI distinction is difficult to assign to extinct fossil taxa, variance in $\delta^{18}\text{O}$ values within faunas should be positively correlated to aridity and should allow at least a qualitative assessment of changes in aridity. In this case, the ^{18}O -enrichment of ES taxa within a fauna relative to EI taxa in the same fauna should be greater under more arid conditions, increasing the variance in $\delta^{18}\text{O}$ values. The means and standard deviations for each fauna are shown in Figure 2.2B. The patterns in faunal variance do not change substantially when only the taxa represented at every locality (Equidae and Ruminanta) are considered (Figure 2.2B). Librilla exhibits the highest faunal $\delta^{18}\text{O}$ variance (suggesting greatest aridity), but the variance of other localities in the Fortuna Basin is lower. Faunal $\delta^{18}\text{O}$ variance in the Teruel Basin is also variable, with some localities suggesting relatively high aridity (El Arquillo, Los Mansuetos) and others lower (Concud, La Calera).

4.2. Comparison of enamel and dentine $\delta^{18}\text{O}$

Isotopic fidelity during diagenesis is of primary importance to any isotopic study of fossil materials. This study focused on the PO_4 fraction of enamel hydroxylapatite ($\delta^{18}\text{O}_p$), since enamel has relatively large, densely packed crystallites and is therefore considered to be much more resistant to diagenetic alteration than dentine or bone (Newesely, 1989; Weiner et al., 1989; Hedges et al., 2002; Zazzo et al., 2004). Phosphate is unlikely to undergo inorganic ^{18}O exchange at surface temperatures (Tudge, 1960; Kohn et al., 1999), though microbially mediated precipitation of diagenetic phosphate can

occur within days of burial (Zazzo et al., 2004). We collected bulk dentine samples from 48 teeth from which enamel was also sampled, since comparison of the $\delta^{18}\text{O}$ of these materials provides a preliminary assessment of isotopic fidelity.

Complete preservation of original isotopic signatures in both enamel and dentine should result in a strong 1:1 correlation between their $\delta^{18}\text{O}$ values (Figures 2.3A and 2.3B). The dentine and enamel values from this study do not have a perfect 1:1 relationship (Figure 2.3B), suggesting some isotopic exchange in one or both of these materials. The extent of alteration is likely small, since OLS regression of enamel onto dentine results in a strong, significant, positive relationship ($r = 0.73, p < 0.001$) and the taxonomic $\delta^{18}\text{O}$ patterns discussed above are consistent with observations for modern taxa.

Isotopic exchange between apatite and surrounding pore waters should drive primary apatite values toward a diagenetic endmember. While enamel-dentine $\delta^{18}\text{O}$ comparisons cannot conclusively determine the extent of diagenetic alteration in each material, the smaller crystallites and greater porosity of dentine make it much more likely than enamel to have experienced alteration. In this case, if the endmember is enriched or depleted in ^{18}O relative to the range of primary values, alteration should result in values that consistently fall above or below the 1:1 line, respectively. If the endmember lies within the range of primary values, then diagenesis should result in decreased variance and values that lie both above and below the 1:1 line. If enamel is relatively pristine while dentine has undergone complete isotopic exchange with surrounding pore waters, then all of the dentine $\delta^{18}\text{O}$ values should match that of the diagenetic endmember,

resulting in a horizontal regression line in a bivariate plot of enamel and dentine $\delta^{18}\text{O}$ (shown schematically for a hypothetical diagenetic endmember of 18‰ in Figure 2.3A). Incomplete and variable ^{18}O exchange between dentine and water should result in values having variable offset from the 1:1 line in the same plot, and a regression slope between 0 and 1. In this case, the $\delta^{18}\text{O}$ of the diagenetic PO_4 endmember should be indicated by the dentine $\delta^{18}\text{O}$ value corresponding to the point of intersection between the 1:1 line and a regression line through the data (Figure 2.3A).

A bivariate plot of corresponding enamel and dentine $\delta^{18}\text{O}$ values is shown in Figure 2.3B. The values fall both above and below the 1:1 line, consistent with a diagenetic endmember within the range of primary values. The lower variance for dentine $\delta^{18}\text{O}$ (*s.d.* = 1.7‰) compared to enamel (*s.d.* = 2.1‰) is consistent with more extensive alteration of the former, though this difference is not statistically significant (F-test 1-tail $p = 0.065$). OLS regression lines for the six localities that have three or more enamel/dentine pairs are also shown in Figure 2.3B, along with the dentine $\delta^{18}\text{O}$ value corresponding to the point of intersection between each regression line and the 1:1 line. The predicted diagenetic endmember $\delta^{18}\text{O}$ values for Molina de Segura, Concud, El Arquillo, and Los Mansuetos range from 17.2‰ to 18.7‰, while the predicted value for Sahabi is slightly higher, at 19.2‰. The predicted value for the three roughly coeval (1.25 – 1.3 Ma) localities in the Baza Basin (9.9‰) is much lower.

If diagenetic PO_4 is in isotopic equilibrium with soil pore waters and if PO_4 diagenesis takes place on geologically short timescales as suggested by Zazzo et al. (2004), then the $\delta^{18}\text{O}$ of pore waters in isotopic equilibrium with diagenetic phosphate

should be comparable to that of soil water $\delta^{18}\text{O}$ during the lifetime of the animals. In this case, reconstruction of past soil water $\delta^{18}\text{O}$ should be possible by using estimates of diagenetic phosphate $\delta^{18}\text{O}$ over a range of temperatures (T , in $^{\circ}\text{C}$) in the phosphate-water-temperature equation of Longinelli and Nuti (1973), rearranged to solve for $\delta^{18}\text{O}_w$:

$$\delta^{18}\text{O}_w = 0.23T + \delta^{18}\text{O}_p - 25.9 \quad (1)$$

Though this approach requires several assumptions and is somewhat hampered by lack of temperature constraint, it nonetheless represents a new, independent, and potentially useful means of estimating past surface water $\delta^{18}\text{O}$. As a preliminary test of this hypothesis, we calculated diagenetic water $\delta^{18}\text{O}$ over the temperature range 0–30 $^{\circ}\text{C}$ for each locality and compared our estimates with modern precipitation $\delta^{18}\text{O}$ for the same areas. The predicted Miocene and Pleistocene pore water $\delta^{18}\text{O}$ values are shown in Figure 2.3C, along with modern temperature and precipitation $\delta^{18}\text{O}$ data for four Global Isotopes in Precipitation (GNIP) stations in northern Libya (Rafah) and northeastern (Tortosa and Zaragoza) and southeastern (Murcia) Spain (IAEA, 2009). Over the range of modern MAT for the three climate stations, the predicted pore water $\delta^{18}\text{O}$ values are comparable to mean annual $\delta^{18}\text{O}$ for modern precipitation, but are approximately 0-3‰ higher. This difference is consistent with either higher $\delta^{18}\text{O}$ for Miocene precipitation or Miocene precipitation that is similar to today, but with slight evaporative ^{18}O enrichment of pore waters relative to precipitation. The latter explanation is likely, since soil water is generally enriched in ^{18}O relative to meteoric water (Cerling and Quade, 1993), but higher precipitation $\delta^{18}\text{O}$ associated with warmer Miocene temperatures (see discussion in section 4.3) cannot be ruled out. Future study of materials that can be used as proxies

for the degree of ^{18}O -enrichment of soil water relative to meteoric water (e.g., thin-section-scale subsampling of vadose and meteoric phreatic cements in pedogenic carbonate) may help to discriminate between these explanations. The predicted pore water $\delta^{18}\text{O}$ for the Pleistocene samples ranges from -11 to -12‰ over the same temperature range as for the calculations for the older samples. This estimate is approximately 6 to 7‰ lower than modern mean annual precipitation $\delta^{18}\text{O}$ near the Baza Basin. This difference is consistent with Pleistocene temperatures that are much lower than today and/or a source for Pleistocene pore waters that is depleted in ^{18}O relative to precipitation. The latter can be explained by Pleistocene uplift of the nearby Sierra Nevada, which contribute ^{18}O -depleted snowmelt to groundwater in the Baza Basin today.

Interestingly, the pore water $\delta^{18}\text{O}$ values predicted through this approach are consistent with estimates of Neogene-Pleistocene precipitation $\delta^{18}\text{O}$ for the Iberian Peninsula based on independent approaches. For example, estimates of Miocene precipitation for the Teruel Basin based on serial samples of the carbonate fraction of equid tooth enamel reported by van Dam and Reichart (2009) range from -10.6 to -3.6‰ ($\bar{x} = -7.0\text{‰}$) for Los Mansuetos, -7.4 to -3.8‰ ($\bar{x} = -5.4\text{‰}$) for El Arquillo, and -9.0 to -1.8‰ ($\bar{x} = -5.8\text{‰}$) for Conclud. Our estimates of low pore water $\delta^{18}\text{O}$ for the Baza Basin are also consistent with previous studies of this basin. For example, estimates of Pleistocene precipitation $\delta^{18}\text{O}$ for the Guadix-Baza Basin based on equid phosphate $\delta^{18}\text{O}$ are approximately -10 to -7‰ at 1.3 Ma (Sánchez-Chillon et al., 1994; Van Dam and Reichart, 2009). Ortiz et al. (2006) report similarly low $\delta^{18}\text{O}$ of -9 to -5‰ for modern

precipitation and reservoir water in the Guadix-Baza Basin, but demonstrate that Pleistocene endorheic lake waters may have been evaporatively enriched in ^{18}O by 4 to 9‰ relative to ground water based on the $\delta^{18}\text{O}$ of ostracode shells. In summary, comparison of enamel and dentine $\delta^{18}\text{O}$ from diagenetically altered hydroxylapatite results in reasonable reconstructions of past soil water $\delta^{18}\text{O}$, but this new approach warrants further testing.

4.3. Estimation of paleotemperature from equid $\delta^{18}\text{O}_p$

One of the clearest patterns in the data presented here is that the Late Miocene localities from the Fortuna Basin (Librilla and Molina de Segura) are isotopically distinct both from Late Miocene localities in the Teruel Basin and from Pleistocene localities in the Baza Basin (Figure 2.2; Table 2.3). This pattern is especially apparent when comparisons are made using species of a single taxon (Equidae) present at nearly every locality (Figure 2.4A). To explore the paleoclimatic implications of these differences, we use equid $\delta^{18}\text{O}$ as a proxy for precipitation $\delta^{18}\text{O}$, which is in turn a proxy for mean annual temperature (MAT). For modern mid- to high-latitudes, the $\delta^{18}\text{O}_w$ of precipitation is strongly correlated to MAT, with a regression slope of approximately 0.55‰/°C (Rozanski et al., 1993). Van Dam and Reichart (2009) report a slightly lower slope of 0.45‰/°C based on data from 11 climate stations on the Iberian Peninsula. Using the same isotopic data (IAEA, 2009) as van Dam and Reichart (2009) and an independent but similar set of temperature data (NCDC, 2009), we also find a significant (OLS regression $p < 0.001$) dependence of mean annual precipitation $\delta^{18}\text{O}_w$ ($\text{MA}\delta^{18}\text{O}_w$) on MAT with a slope for the Iberian Peninsula that is lower than the global slope:

$$\text{MA}\delta^{18}\text{O}_w = (0.419 \pm 0.080)*\text{MAT} - (11.6 \pm 1.25) \quad (R^2 = 0.75) \quad (2)$$

OLS regression with $\text{MA}\delta^{18}\text{O}_w$ as the independent variable and MAT as the dependent variable results in the following equation:

$$\text{MAT} = (1.79 \pm 0.344)*\text{MA}\delta^{18}\text{O}_w + (24.6 \pm 1.80) \quad (R^2 = 0.75) \quad (3)$$

We include our OLS result because this regression method is commonly used and will be familiar to most readers. Whereas OLS assumes the independent variable is measured without error, reduced major axis (RMA) regression does not. RMA is thus a more appropriate regression model for data such as these (as noted also by van Dam and Reichart (2009)). RMA regression results in higher slopes than OLS (Sokal and Rohlf, 1995), which has implications for our climatic reconstructions below. RMA regression of $\text{MA}\delta^{18}\text{O}_w$ onto MAT for the same 11 climate stations results in the following significant (slope 99% confidence interval excludes zero) relationship:

$$\text{MA}\delta^{18}\text{O}_w = (0.483 \pm 0.080)*\text{MAT} - (12.5 \pm 1.25) \quad (R^2 = 0.75) \quad (4)$$

RMA regression with $\text{MA}\delta^{18}\text{O}_w$ as the independent variable and MAT as the dependent variable results in the following relationship:

$$\text{MAT} = (2.07 \pm 0.344)*\text{MA}\delta^{18}\text{O}_w + (26.0 \pm 1.80) \quad (R^2 = 0.75) \quad (5)$$

As described above, using this approach to estimate MAT from proxies for $\delta^{18}\text{O}_w$ assumes that the modern spatial relationship between these variables was not substantially different in the past.

Fossil horses have been the focus of intense sampling for isotopic studies, partly because their teeth are well-represented in the fossil record globally and are relatively easy to sample. Thus, a large dataset exists with which to compare our equid data. In a

recent study of equid $\delta^{18}\text{O}$ primarily from the Teruel Basin, van Dam and Reichart (2009) found that Late Miocene MAT in this area was approximately 5°C warmer than present. Their measurements of $\delta^{18}\text{O}$ were based on the carbonate fraction of enamel hydroxylapatite ($\delta^{18}\text{O}_c$), which covaries strongly with phosphate $\delta^{18}\text{O}_p$ for modern mammals. The relationship between $\delta^{18}\text{O}_p$ and $\delta^{18}\text{O}_c$ can be described by OLS regression for the combined datasets from Bryant et al. (1996) and Iacumin et al. (1996):

$$\delta^{18}\text{O}_p = 0.97 * \delta^{18}\text{O}_c - 7.93 \quad (R^2 = 0.98) \quad (6)$$

Figure 2.4A shows the equid $\delta^{18}\text{O}$ data from this study along with the means of serial $\delta^{18}\text{O}_c$ samples from van Dam and Reichart (2009; converted to $\delta^{18}\text{O}_p$ equivalent using equation 6). Our measured equid $\delta^{18}\text{O}_p$ values for the Teruel Basin ($\bar{x} = 19.5\text{‰}$, *s.d.* = 1.3‰, *n* = 25) are indistinguishable from the predicted $\delta^{18}\text{O}_p$ values of van Dam and Reichart (2009) for the same basin, at both the locality and basin level (*t*-test, 2-tail *p* > 0.06). Equid enamel $\delta^{18}\text{O}_p$ from the Fortuna Basin ($\bar{x} = 22.5\text{‰}$, *s.d.* = 1.3‰, *n* = 11) is significantly higher than that of the Teruel Basin both for our dataset (*t*-test, 2-tail *p* < 0.001) and for that of van Dam and Reichart (2009) (*t*-test, 2-tail *p* < 0.001).

Horses are large-bodied, obligate-drinking, hindgut fermenters with a relatively high rate of water turnover (Kohn et al., 1996; McNab, 2002). As such, they are an evaporation insensitive (EI) taxon (Levin et al., 2006) whose body water $\delta^{18}\text{O}$ should reasonably track the $\delta^{18}\text{O}$ of their drinking water. Though drinking water $\delta^{18}\text{O}_w$ can be variable and ^{18}O -enriched relative to precipitation $\delta^{18}\text{O}_w$ (Hoppe et al., 2004a), OLS regression for the combined datasets of Bryant et al. (1994), Sanchez-Chillón (1994),

Delgado-Huertas et al. (1995), and Hoppe et al. (2004a) nonetheless shows a significant ($p < 0.001$) dependence of modern equid $\delta^{18}\text{O}_p$ on precipitation $\delta^{18}\text{O}_w$:

$$\delta^{18}\text{O}_p = (0.606 \pm 0.063) * \delta^{18}\text{O}_w + (22.5 \pm 0.571) \quad (R^2 = 0.70) \quad (7)$$

OLS regression with $\delta^{18}\text{O}_w$ as the dependent variable and $\delta^{18}\text{O}_p$ as the independent variable results in the following expression:

$$\delta^{18}\text{O}_w = (1.15 \pm 0.119) * \delta^{18}\text{O}_p - (28.3 \pm 2.13) \quad (R^2 = 0.70) \quad (8)$$

RMA regression also results in a significant (slope 99% confidence interval excludes zero) dependence of equid $\delta^{18}\text{O}_p$ on precipitation $\delta^{18}\text{O}_w$:

$$\delta^{18}\text{O}_p = (0.727 \pm 0.063) * \delta^{18}\text{O}_w + (23.5 \pm 0.571) \quad (R^2 = 0.70) \quad (9)$$

RMA regression with $\delta^{18}\text{O}_p$ as the independent variable and $\delta^{18}\text{O}_w$ as the dependent variable results in the following expression:

$$\delta^{18}\text{O}_w = (1.38 \pm 0.119) * \delta^{18}\text{O}_p - (32.4 \pm 2.13) \quad (R^2 = 0.70) \quad (10)$$

Applying Equation 10 to our equid data results in the $\delta^{18}\text{O}_w$ estimates summarized in Table 2.4. The $\delta^{18}\text{O}_w$ estimates from the Baza (-8.1‰ to -5.8‰; $\bar{x} = -6.4$ ‰) and Teruel (-6.3‰ to -4.8‰; $\bar{x} = -5.5$ ‰) Basins are within the range of $\delta^{18}\text{O}_w$ estimates reported by Sanchez-Chillón et al. (1994) and van Dam and Reichart (2009) for these same basins. The highest estimates are from the Fortuna Basin (-5.1‰ to -0.5‰; $\bar{x} = -1.4$ ‰), especially for Molina de Segura (-1.1‰) and Librilla (-0.5‰).

Applying Equation 5 to the $\delta^{18}\text{O}_w$ values calculated from our equid data results in the MAT estimates summarized in Table 2.4. Our MAT estimate for the latest Miocene of the Fortuna Basin ($23.2 \pm 7.4^\circ\text{C}$) is $\sim 4.7^\circ\text{C}$ warmer than present at the nearest climate station of Murcia (MAT = 18.5°C), while our reconstruction for the Teruel Basin ($14.6 \pm$

7.1°C) is more comparable to modern temperatures (Teruel, MAT = 13.4°C). Higher Late Miocene temperatures are consistent with cooling of the Iberian Peninsula during the late Neogene and Pleistocene, which parallels the global cooling and aridification during this time. The latest Miocene temperature gradient between the Teruel and Fortuna Basins ($8.6 \pm 10.3^\circ\text{C}$) is $\sim 3.5^\circ\text{C}$ greater than the MAT difference between Murcia and Teruel today. We base our MAT estimates on RMA regression since it is a statistically appropriate model for these data, but the temperature gradient between the Teruel and Fortuna Basins using OLS regression ($6.7 \pm 9.0^\circ\text{C}$; calculated using Equations 3 and 8) is also higher than the modern gradient, although lower than that of RMA due to differences in these regression models (Sokal and Rohlf, 1995). Equid $\delta^{18}\text{O}$ values from the Pleistocene Baza Basin suggest a MAT of $12.9 \pm 7.2^\circ\text{C}$, which is approximately 3°C cooler than present at the nearest climate station of Granada (15.8°C).

Though the exact timing relationship between intra-annual climatic variation and mammal tooth enamel formation is complex and has been the focus of much recent study (Fricke et al., 1998; Passey and Cerling, 2002; Hoppe et al., 2004b; Nelson, 2005; van Dam and Reichart, 2009), serial samples of equid teeth should provide at least a qualitative approximation of the seasonality of temperature. The serial samples of horse teeth sampled in this study are shown in Figure 2.4C, and are compared with serial samples reported by van Dam and Reichart (2009). Though these authors collected more samples per tooth, the weak relationship between $\delta^{18}\text{O}$ range and number of samples per tooth for our dataset suggests only a minimal sampling bias. The range in $\delta^{18}\text{O}$ for serial samples from most of the Teruel Basin localities is comparable to that from the Fortuna

Basin (La Alberca), suggesting similar levels of intra-annual climate variability. Los Mansuetos is a notable exception with much higher variability. Van Dam and Reichart (2009) also report high variability in serial samples from Los Mansuetos and for Conclud, which they interpret to represent high seasonal climate variability.

Fricke et al. (1998) report that the relationship between seasonal difference (June-July-August mean minus December-January-February mean) in temperature (ΔT) and precipitation $\delta^{18}\text{O}_w$ ($\Delta\delta^{18}\text{O}_w$) for modern mid- to high-latitude climate stations can be summarized by the following expression (rearranged to solve for ΔT):

$$\Delta T = 2.66 * \Delta\delta^{18}\text{O}_w + 5.62 \quad (R^2 = 0.78) \quad (11)$$

As a first approximation for seasonal temperature range, we used Equation 10 to estimate the $\delta^{18}\text{O}_w$ range implied by our serial $\delta^{18}\text{O}_p$ samples, and then applied Equation 11 to the maximum and minimum $\delta^{18}\text{O}_w$ values in order to approximate ΔT . Calculated Late Miocene ΔT for the Teruel Basin is variable (from 12.2°C at El Arquillo to 21.4°C at Los Mansuetos), with an average ΔT for the 7 teeth (15.0°C) that is lower than the modern seasonal temperature range at Teruel (17.8°C) but within the range of previous Miocene ΔT estimates for the Teruel Basin (11.1°C to 23.8°C) reported by van Dam and Reichart (2009). The ΔT calculated from a single equid molar from the Fortuna Basin (14.1°C) is closer to the modern ΔT at the nearby climate station of Murcia (14.9°C).

4.4. Implications for terrestrial climate during the Messinian Salinity Crisis

The high $\delta^{18}\text{O}$ values for the Fortuna Basin faunas relative to those of the Teruel and Baza Basins can be interpreted as either a temporal or a spatial gradient in

paleoclimate. The Fortuna Basin localities are terminal Miocene in age and immediately precede, or potentially include, the initiation of the main desiccation phase of the MSC (Garcés et al., 1998; Kruvier et al., 2002). If the high $\delta^{18}\text{O}$ values from these localities represent a temporal change related to the MSC, then our data are consistent with a substantial increase in temperature and/or aridity in southern Spain immediately prior to or during the main desiccation phase. This interpretation stands in contrast to a number of previous studies of independent paleoclimate proxies. For example, pollen records show no significant climate shift associated with the MSC (Bertini et al., 1998; Bertini, 2006; Fauquette et al., 2006). This was especially true for southern Spain, where these records suggest warm and arid conditions throughout the MSC interval. The pollen records are in agreement with results from hydrologic budget and atmospheric general circulation models, which suggest little change associated with the MSC in southwestern Europe (Fluteau, et al., 2003; Blanc, 2006). Based on rank order mammalian body sizes within faunas (cenogram analysis), Costeur et al. (2007) also report comparable temperatures before and after the MSC in southern Spain (Guadix-Baza Basin), but these authors report a strong increase in temperatures across the same interval northern Spain (Calatayud-Daroca-Teruel Basin).

Since our samples from the Teruel and Fortuna Basins differ in both their ages and in their geographic locations, an alternative explanation for the high $\delta^{18}\text{O}$ values in the Fortuna Basin is that they reflect a spatial, rather than a temporal, climate gradient. Several observations support this interpretation. First, reconstructed MAT for the Late Miocene locality of Venta del Moro is intermediate between that of the Fortuna and

Teruel Basins, consistent with its intermediate geographic position between these areas. Second, $\delta^{18}\text{O}$ values of mammals from the intra-MSL locality of Almenara-M do not exhibit any strong patterns relative to $\delta^{18}\text{O}$ values of pre-MSL mammals. Finally, interpretation of our results as a spatial climate gradient is consistent with previous studies indicating strong latitudinal climate gradients throughout the Late Miocene. For example, while pollen-based climate reconstructions do not suggest any temporal change associated with the MSL, they do show strong Late Miocene N-S temperature and moisture gradients indicated by a southward increase in herbs relative to trees for the Mediterranean region in general, and for the Iberian Peninsula in particular (Bertini, 2006; Fauquette et al., 1999, 2006). Similarly, reconstructions of temperature and moisture gradients based on rodent faunas suggest N-S gradients for the Iberian Peninsula that were especially strong during the latest Miocene and early Pliocene (van Dam and Weltje, 1999; van Dam, 2006). In light of these observations, we interpret the difference in Late Miocene mammal $\delta^{18}\text{O}$ between northern and southern Spain as reflecting a latitudinal, rather than temporal, climate gradient. In this case, our results are consistent with a latest Miocene temperature gradient between NE and SE Spain that is ~60% greater than today.

Our results and those of earlier studies (Bertini et al., 1998; Bertini, 2006; Blanc, 2006; Fauquette et al., 2006; van Dam, 2006; Costeur et al., 2007) indicate a Late Miocene latitudinal climate structure for the Mediterranean region that is different than today, but not necessarily a result of the MSL. These results are perhaps somewhat surprising, since previous studies have found significant regional climate effects in

response to desiccation events that were much smaller in scale than the MSC. For example, Small et al. (2001a, 2001b) report a $\sim 9^{\circ}\text{C}$ increase in seasonal temperature range, a $2\text{-}3^{\circ}\text{C}$ increase in diurnal temperature range, and a MAT increase of up to 6°C in response to the desiccation of the Aral Sea between 1960 and 1997. In this case, the dry floor of the Aral Sea further enhanced the rate of evaporation, forming a positive feedback to desiccation. Hostetler et al. (1994) modeled lake-atmosphere feedbacks for Pleistocene Lake Bonneville in Utah that also had a substantial effect on moderating climate, contributing up to 38% of regional precipitation and up to 59% of local precipitation. The fact that southwestern Europe shows little or no climatic response to the MSC suggests that the Mediterranean Sea was not a significant precipitation vapor source for this area during the Late Miocene. Today, the Atlantic Ocean is the primary source for most modern Iberian precipitation, which falls primarily in the cool season. Intra-annual rainfall variability is driven by seasonal migration of the subtropical high pressure zone, and inter-annual variability is driven by the North Atlantic Oscillation. The lack of a response to the MSC in southwestern Europe and the persistence of C_3 vegetation in this area throughout the Neogene suggest that the synoptic-scale climate structure and “Mediterranean climate” characterizing this area today was in place by the Late Miocene.

In contrast to southwestern Europe, northeastern Africa may have experienced a much greater response to the MSC desiccation. Based on the incision rates of fluvial systems across northern Africa, Griffin (2002) argued that the MSC increased precipitation in northeast Africa by creating a strong low pressure zone over the

Mediterranean Basin, thereby increasing the intensity of the Asian monsoon and drawing moisture from the Indian Ocean into the Mediterranean region. This hypothesis is in agreement with palynological data recording an increase in grasses, sedges, and megathermic taxa in the Nile Delta region during this time (Fauquette, 2006), and with late Messinian evaporites having low $^{87}\text{Sr}/^{86}\text{Sr}$ ratios potentially related to increased Nile outflow (Keogh and Butler, 1999). Griffin (2006) suggested that increased moisture combined with the MSC drawdown of base level was responsible for creating the paleo-river channels in northern Libya in which the Sahabi fossil fauna accumulated. Our samples from Sahabi, while limited, generally have low $\delta^{18}\text{O}$ values relative to Late Miocene localities in Spain and suggest cooler or wetter climates in Libya during this time. Clearly, the contrast in climatic response to the MSC between the eastern and western Mediterranean warrants further investigation.

5. Conclusions

The Late Neogene represents an interval of important global climatic and ecological transition, including the onset of northern hemisphere glaciation and the replacement of forested ecosystems by open shrublands and grasslands. The Mediterranean region experienced important regional events during this time period, including the desiccation of the Mediterranean Sea during the Messinian Salinity Crisis. In this study we used stable oxygen isotopic data from Late Neogene and Pleistocene mammal faunas from Spain and northern Libya to estimate paleotemperature and paleoaridity in order to evaluate the effect of these global and regional changes on

terrestrial ecosystems. Based on the data presented here, our primary results and conclusions are:

1) Anthracotheres, hippopotamids, and castorids from localities in Spain have low $\delta^{18}\text{O}$ values relative to those of co-occurring taxa, providing independent evidence for semi-aquatic lifestyle for these taxa inferred from morphology. Hippopotamids from the latest Miocene locality of Sahabi in northern Libya are enriched in ^{18}O relative to co-occurring anthracotheres and are not strongly ^{18}O -depleted relative to the remainder of the associated fauna. This pattern is consistent with ecological niche partitioning between hippopotamids and anthracotheres during a time of important faunal turnover for these taxa.

2) Comparisons of intra-tooth enamel and dentine $\delta^{18}\text{O}$ values suggest slight diagenetic alteration of dentine PO_4 . Using these values to estimate diagenetic endmember PO_4 in equilibrium with surrounding pore waters suggests water $\delta^{18}\text{O}_w$ that is consistent with independent estimates. One exception to this pattern is the low $\delta^{18}\text{O}_w$ estimated for the Baza Basin (Plio-Pleistocene), which may be partly explained by tectonic uplift of the Betic Cordillera during the Pleistocene.

3) Mammal faunas from the latest Miocene of southern Spain (Fortuna Basin) are ^{18}O -enriched relative to those of the Late Miocene of northern Spain (Teruel Basin), the Late Miocene of northern Libya (Sahabi) and the Pleistocene of southern Spain (Baza Basin). One possible explanation for these patterns is temporal change in temperature and/or aridity, potentially associated with the Messinian Salinity Crisis. In this case, MAT increased sharply between 7.2 and 6.0 Ma, and then decreased between 6.0 and 1 Ma.

High faunal $\delta^{18}\text{O}$ variance in some localities from the Fortuna Basin suggests the higher temperatures were accompanied by higher aridity, but this pattern is not consistent throughout the basin. However, we favor an alternative explanation for the higher $\delta^{18}\text{O}$ values from the Fortuna Basin in which they reflect latitudinal, rather than temporal, climate gradients. In this case, temperature gradients between northeastern and southeastern Spain during the latest Miocene were approximately 3.5°C steeper than today. Our Late Miocene MAT estimates for both the Teruel and Fortuna Basins are warmer than present, consistent with cooling of the Iberian Peninsula during the Late Neogene.

5) Our results are consistent with earlier studies suggesting that the Iberian Peninsula experienced strong latitudinal climate gradients throughout the Late Miocene, without drastic changes associated with the Messinian Salinity Crisis itself. Latest Miocene mammal $\delta^{18}\text{O}$ from northern Libya is lower than that of southern Spain, consistent with earlier studies indicating cooler and/or wetter climates in northeastern Africa during the Messinian Salinity Crisis.

Acknowledgements

This research would not have been possible without the generous assistance, thoughtful discussion, and access to specimens provided by Ll. Gibert and G. Scott (Berkeley Geochronological Center, Berkeley, CA, and Museo Josep Gibert, Orce, Spain), and L. Celià, A. Galobart, and J. Agustí (Institut Català de Paleontologia, Sabadell, Spain). We thank L. Domingo Martinez, M. Furió, I. Casanovas Vilar, M.

Köhler, S. Moyà-Solà, P. Koch, M. Clementz, P. Wheatley, and J. Yeakel for their thoughtful discussions, and two anonymous reviewers for their critical assessment and valuable comments. While their suggestions improved this project and the resulting manuscript, any remaining errors are the responsibility of the authors alone. We thank G. Cane (University of Kansas), T. Prokopiuk (University of Saskatchewan), K. Macleod (University of Missouri) and D. Andreasen (University of California – Santa Cruz) for their invaluable analytical assistance. This research was supported by a Geological Society of America Graduate Student Research Grant, a University of Minnesota International Thesis Research Grant, and three summer research grants from the Department of Geology and Geophysics at the University of Minnesota.

References Cited

- Agustí, J., Cabrera, L., Garcés, M., and Llenas, M., 1999. Mammal turnover and global climate change in the late Miocene terrestrial record of the Vallès-Penedès Basin (NE Spain). *In*: Agustí, J., Rook, L., and Andrews, P. (Eds.), *The Evolution of Neogene Terrestrial Ecosystems in Europe*. Cambridge University Press, Cambridge, UK, p. 397–412.
- Agustí, J., Garcés, M., and Krijgsman, W., 2006. Evidence for African-Iberian exchanges during the Messinian in the Spanish mammalian record. *Palaeogeography, Palaeoclimatology, Palaeoecology*, 238, 5–14.
- Alcalá, L., 1994. *Macromamíferos neógenos de la fosa de Alfambra-Teruel*. Instituto de Estudios Turolenses-Museo Nacional de Ciencias Naturales, Teruel.

- Alfaro, P., Delgado, J., Sanz de Galdeano, C., Galindo-Zaldívar, J., García-Tortosa, F.J., López-Casado, C., Marín-Lechado, C., Gil, A., and Borque, M.J., 2008. The Baza Fault: a major active extensional fault in the central Betic Cordillera (south Spain). *International Journal of Earth Sciences*, 97, 1353–1365.
- Alonso-Zarza, A.M. and Calvo, J.P., 2000. Palustrine sedimentation in an episodically subsiding basin: the Miocene of the northern Teruel Graben (Spain). *Palaeogeography, Palaeoclimatology, Palaeoecology*, 160, 1–21.
- Anadón, P. and Moissenet, E., 1996. Neogene basins in the Eastern Iberian Range. *In*: Friend, P.F. and Dabrio, C.J. (Eds.), *Tertiary Basins of Spain: The Stratigraphic Record of Crustal Kinematics*. Cambridge University Press, Cambridge, 68–76.
- Anderson, J.B. and Shipp, S.S., 2001. Evolution of the West Antarctic ice-sheet. *In*: Alley, R.B. and Bindschadler, R.A. (Eds.), *The West Antarctic Ice Sheet: Behavior and Environment*. American Geophysical Union Antarctic Research Series, 77, 45–58.
- Bassett, D., MacLeod, K.G., Miller, J.F., Ethington, R.L., 2007. Oxygen isotopic composition of biogenic phosphate and the temperature of Early Ordovician seawater. *Palaios*, 22, 98–103.
- Bernor, R.L. and Scott, R.S., 2003. New interpretations of the systematics, biogeography and paleoecology of the Sahabi hipparions (latest Miocene) (Libya). *Geodiversitas*, 25, 297–319.
- Bertini, A., Londeix, L., Maniscalco, R., di Stefano, A., Suc, J.-P., Clauzon, G., Gautier, F., and Grasso, M., 1998. Paleobiological evidence of depositional conditions in the

- Salt Member, Gessoso-Solfifera Formation (Messinian, Upper Miocene) of Sicily. *Micropaleontology*, 44, 413–433.
- Bertini, A., 2006. The Northern Apennines palynological record as a contribute for the reconstruction of the Messinian palaeoenvironments. *Sedimentary Geology*, 188–189, 235–259.
- Beyer, C., 2008. Establishment of a chronostratigraphical framework for the As Sahabi sequence in northeast Libya. *In* N.T. Boaz, A. El-Arnauti, P. Pavlakis, and M.J. Salem (eds.) *Circum-Mediterranean Geology and Biotic Evolution During the Neogene Period: The Perspective from Libya*. Garyounis Scientific Bulletin Special Issue 5, University of Garyounis, Benghazi, Libya, p. 59–69.
- Blanc, P.-L., 2006. Improved modeling of the Messinian Salinity Crisis and conceptual implications. *Palaeogeography, Palaeoclimatology, Palaeoecology*, 238, 349–372.
- Boaz, N.T., El-Arnauti, A., Gaziry, A.W., de Heinzelin, J., and Boaz., D.D., 1987. *Neogene Paleontology and Geology of Sahabi.*, Alan R. Liss, Inc., New York.
- Bocherens, H., Koch, P.L., Mariotti, A., Geraads, D., and Jaeger, J.-J., 1996. Isotopic biogeochemistry (^{13}C , ^{18}O) of mammalian enamel from African Pleistocene hominid sites. *Palaios*, 11, 306–318.
- Bohanek, A.J., 2002. Software for reduced major axis regression.
<http://www.bio.sdsu.edu/andy/rma.html>. 2009.
- Boisserie, J.-R., Lihoreau, F., and Brunet, M., 2005. The position of Hippopotamidae within Cetartiodactyla. *Proceedings of the National Academy of Sciences – USA*, 102, 1537–1541.

- Boyle, E.A., 1997. Cool tropical temperatures shift the global $\delta^{18}\text{O}$ -T relationship: An explanation for the ice core $\delta^{18}\text{O}$ – borehole thermometry conflict? *Geophysical Research Letters*, 24, 273–276.
- Bryant, J.D., Luz, B., and Froelich, P.N., 1994. Oxygen isotopic composition of fossil horse tooth phosphate as a record of continental paleoclimate. *Palaeogeography, Palaeoclimatology, Palaeoecology*, 107, 303–316.
- Bryant, J.D., Koch, P.L., Froelich, P.N., Showers, W.J., and Genna, B.J., 1996. Oxygen isotope partitioning between phosphate and carbonate in mammalian apatite. *Geochimica et Cosmochimica Acta*, 60, 5145–5148.
- Cerling, T.E. and Quade J., 1993, Stable carbon and oxygen isotopes in soil carbonates. *In* P.K. Swart, K.C. Lohmann, J.A. McKenzie, and S.M. Savin (eds.) *Climate Change in Continental Isotopic Records*. *Geophysical Monograph 78*, American Geophysical Union, Washington, D.C., p. 217–231.
- Cerling, T.E., Harris, J.M., MacFadden, B.J., Leakey, M.G., Quade, J., Eisenmann, V., and Ehleringer, J.R., 1997. Global vegetation change through the Miocene/Pliocene boundary. *Nature*, 389, 153–158.
- Cerling, T.E., Harris, J.M., Hart, J.A., Kaleme, P., Klingel, H., Leakey, M.G., Levin, N.E., Lewison, R.L., and Passey, B.H., 2008. Stable isotope ecology of the common hippopotamus. *Journal of Zoology*, 276, 204–212.
- Clauzon, G., Suc, J.-P., Gautier, F., Berger, A., and Loutre, M.-F., 1996. Alternate interpretation of the Messinian salinity crisis: Controversy resolved? *Geology*, 24, 363–366.

- Clementz, M.T., Holroyd, P.A., and Koch, P.L., 2008. Identifying aquatic habits of herbivorous mammals through stable isotope analysis. *Palaios*, 23, 574–585.
- Cormie, A.B., Luz, B., and Schwarz, H.P., 1994. Relationship between the hydrogen and oxygen isotopes of deer bone and their use in the estimation of relative humidity. *Geochimica et Cosmochimica Acta*, 58, 3439–3449.
- Costeur, L., Montuire, S., Legendre, S., and Maridet, O., 2007. The Messinian event: What happened to the peri-Mediterranean mammalian communities and local climate? *Geobios*, 40, 423–431.
- Dansgaard, W., 1964. Stable isotopes in precipitation. *Tellus*, 16, 436–438.
- de Heinzelin, J. and El-Arnauti, A., 1987. The Sahabi Formation and related deposits. *In* N.T. Boaz, A. El-Arnauti, A.W. Gaziry, J. de Heinzelin, and D.D. Boaz., 1987. *Neogene Paleontology and Geology of Sahabi.*, Alan R. Liss, Inc., New York., p. 1–21.
- Delgado-Huertas, A., Iacumin, P., Stenni, B., Sánchez-Chillón, B., and Longinelli, A., 1995. Oxygen isotope variations of phosphate in mammalian bone and tooth enamel. *Geochimica et Cosmochimica Acta*, 59, 4299–4305.
- Farris, F. and Strain B.R., 1978. The effects of water-stress on leaf H₂¹⁸O enrichment. *Radiation and Environmental Biophysics*, 15, 167–202.
- Fauquette, S., Suc, J.-P., Guiot, J., Diniz, F., Feddi, N., Zheng, Z., Bessais, E., and Drivaliari, A., 1999. Climate and biomes in the West Mediterranean area during the Pliocene. *Palaeogeography, Palaeoclimatology, Palaeoecology*, 152, 15–36.

- Fauquette, S., Suc, J.-P., Bertini, A., Popescu, S.-M., Warny, S., Taoufiq, N.B., Perez Villa, M.-J., Chikhi, H., Feddi, N., Subally, D., Clauzon, G., and Ferrier, J., 2006. How much did climate force the Messinian salinity crisis? Quantified climatic conditions from pollen records in the Mediterranean region. *Palaeogeography, Palaeoclimatology, Palaeoecology*, 238, 281–301.
- Fluteau, F., Suc, J.P., and Fauquette, S., 2003. Modelling the climatic consequences of the Messinian Salinity Crisis. *Geophysical Research Abstracts*, 5, 11387.
- Fox, D.L. and Koch, P.L., 2003. Tertiary history of C₄ biomass in the Great Plains, USA. *Geology*, 31, 809–812.
- Fricke, H.C., Clyde, W.C., and O'Neil, J.R., 1998. Intra-tooth variations in $\delta^{18}\text{O}$ (PO₄) of mammalian tooth enamel as a record of seasonal variations in continental climate variables. *Geochimica et Cosmochimica Acta*, 62, 1839–1850.
- Fricke, H.C. and O'Neil, J.R., 1999. The correlation between ¹⁸O/¹⁶O ratios of meteoric water and surface temperature: Its use in investigating terrestrial climate change over geologic time. *Earth and Planetary Science Letters*, 170, 181–196.
- Garcés, M., Agustí, J., and Parés, J.M., 1997a. Late Pliocene continental magnetochronology in the Guadix-Baza Basin (Betic Ranges, Spain). *Earth and Planetary Science Letters*, 146, 677–687.
- Garcés, M., Krijgsman, W., van Dam, J., Calvo, J.P., Alcalá, L., and Alonso-Zarza, A.M., 1997b. Late Miocene alluvial sediments from the Teruel area: Magnetostratigraphy, magnetic susceptibility, and facies organization. *Acta Geologica Hispanica*, 32, 171–184.

- Garcés, M., Krijgsman, W., and Agustí, J., 1998. Chronology of the late Turolian deposits of the Fortuna basin (SE Spain): implications for the Messinian evolution of the eastern Betics. *Earth and Planetary Science Letters*, 163, 69–81.
- Garcés, M., Krijgsman, W., and Agustí, J., 2001. Chronostratigraphic framework and evolution of the Fortuna basin (Eastern Betics) since the Late Miocene. *Basin Research*, 13, 199–216.
- García-Alix, A., Minwer-Barakat, R., Martín-Suárez, E., and Freudenthal, M., 2007. The southernmost record of fossil Castoridae (Mammalia, Rodentia) in Europe. *Geodiversitas*, 29, 435–440.
- Gaziry, A.W., 1987. *Merycopotamus petrocchii* (Artiodactyla, Mammalia) from Sahabi, Libya. In N.T. Boaz, A. El-Arnauti, A.W. Gaziry, J. de Heinzelin, and D.D. Boaz., 1987. *Neogene Paleontology and Geology of Sahabi.*, Alan R. Liss, Inc., New York., p. 287–302.
- Gibert, L., Scott, G., and Ferràndez-Cañadel, C., 2006. Evaluation of the Olduvai subchron in the Orce ravine (SE Spain). Implications for Plio-Pleistocene mammal biostratigraphy and the age of the Orce archaeological sites. *Quaternary Science Reviews*, 25, 507–525.
- Gibert, L., Scott, G., Martin, R., Gibert, J., 2007. The Early to Middle Pleistocene boundary in the Baza Basin (Spain). *Quaternary Science Reviews*, 26, 2067–2089.
- Griffin, D.L., 2002. Aridity and humidity: two aspects of late Miocene climate of North Africa and the Mediterranean. *Palaeogeography, Palaeoclimatology, Palaeoecology*, 182, 65–91.

- Griffin, D.L., 2006. The late Neogene Sahabi rivers of the Sahara and their climatic and environmental implications for the Chad Basin. *Journal of the Geological Society*, London, 163, 905–921.
- Hedges, R.E.M., 2002. Bone diagenesis: An overview of processes. *Archaeometry*, 44, 319–328.
- Hodell, D.A., Benson, R.H., Kent, D.V., Boersma, A., and Rakic-El Bied, K., 1994. Magnetostratigraphic, biostratigraphic, and stable isotope stratigraphy of an upper Miocene drill core from the Sale Briqueterie (northwestern Morocco): A high-resolution chronology for the Messinian stage. *Paleoceanography*, 9, 835–856.
- Hoppe, K.A., Amundson, R., Vavra, M., McClaran, P., and Anderson, D.L., 2004a. Isotopic analysis of tooth enamel carbonate from modern North American feral horses: implications for paleoenvironmental reconstructions. *Palaeogeography, Palaeoclimatology, Palaeoecology*, 203, 299–311.
- Hoppe, K.A., Stover, S.M., Pascoe, J.R., and Amundson, R., 2004b. Tooth enamel biomineralization in extant horses: implications for isotopic microsampling. *Palaeogeography, Palaeoclimatology, Palaeoecology*, 206, 355–365.
- Hostetler, S.W., Giorgi, F., Bates, G.T., and Bartlein, P.J., 1994. Lake-atmosphere feedbacks associated with Paleolakes Bonneville and Lahontan. *Science*, 263, 665–668.
- Hsü, K.J., Ryan, W.B.F., and Cita, M.B., 1973. Late Miocene desiccation of the Mediterranean. *Nature*, 242, 240–244.

- Hsü, K.J., Montadert, L., Beroulli, D., Cita, M.B., Erickson, A., Garrison, R.E., Kidd, R.B., Mèlierés, F., Müller, C., and Wright, R., 1977. History of the Mediterranean salinity crisis. *Nature*, 267, 399–403.
- Huguene, M. and Esuillie, F., 1996. Fossil evidence for the origin of behavioral strategies in Early Miocene Castoridae, and their role in the evolution of the family. *Paleobiology*, 22, 507–513.
- Iacumin, P., Bocherens, H., Mariotti, A., and Longinelli, A., 1996. Oxygen isotope analyses of co-existing carbonate and phosphate in biogenic apatite: a way to monitor diagenetic alteration of bone phosphate? *Earth and Planetary Science Letters*, 142, 1–6.
- IAEA, 2009. Global Network of Isotopes in Precipitation (GNIP) data: 2000–2004. <http://isohis.iaea.org>. 2009.
- Jacobs, B.F., Kingston, J.D., and Jacobs, L.L., 1999. The origin of grass-dominated ecosystems. *Annals of the Missouri Botanical Gardens*, 68, 590–643.
- Janis, C.M., Damuth, J., and Theodor, J.M., 2000. Miocene ungulates and terrestrial primary productivity: Where have all the browsers gone? *Proceedings of the National Academy of Sciences, USA*, 97, 7899–7904.
- Janis, C.M., Damuth, J., and Theodor, J.M., 2002. The origins and evolution of the North American grassland biome: the story from the hoofed mammals. *Palaeogeography, Palaeoclimatology, Palaeoecology*, 177, 183–198.
- Janis, C.M., Damuth, J., and Theodor, J.M., 2004. The species richness of Miocene browsers, and implications for habitat type and primary productivity in the North

- American grassland biome. *Palaeogeography, Palaeoclimatology, Palaeoecology*, 207, 371–398.
- Keogh, S.M. and Butler, R.W.H., 1999. The Mediterranean water body in the late Messinian: interpreting the record from marginal basins on Sicily. *Journal of the Geological Society, London*, 156, 837–846.
- Koch, P.L., 1998. Isotopic reconstruction of past continental environments. *Annual Review of Earth and Planetary Sciences*, 27, 573–613.
- Köhler, M., Moyà-Solà, S., and Alba, D.M., 2000. *Macaca* (Primates, Cercopithecoidea) from the Late Miocene of Spain. *Journal of Human Evolution*, 38, 447–452.
- Kohn, M.J., 1996. Predicting animal $\delta^{18}\text{O}$: Accounting for diet and physiological adaptation. *Geochimica et Cosmochimica Acta*, 60, 4811–4829.
- Kohn, M.J., Schoeninger, M.J., and Barker, William W., 1999. Altered states: Effects of diagenesis on fossil tooth chemistry. *Geochimica et Cosmochimica Acta*, 63, 2737–2747.
- Kohn, M.J. and Cerling, T.E., 2002. Stable isotope compositions of biological apatite. In: Kohn, M.J., Rakovan, J., and Hughes, J.M. (Eds.), *Phosphates: Geochemical, Geobiological, and Materials Importance*. *Reviews in Mineralogy and Geochemistry*, 48, 455–488.
- Kohn, M.J., Schoeninger, M.J., and Valley, J.W., 1996. Herbivore tooth oxygen isotope compositions: Effects of diet and physiology. *Geochimica et Cosmochimica Acta*, 60, 3889–3896.

- Krijgsman, W., Hilgen, F.J., Raffi, I., Sierro, F.J., and Wilson, D.S., 1999. Chronology, causes and progression of the Messinian Salinity Crisis. *Nature*, 400, 652–655.
- Krijgsman, W., Garcés, M., Agustí, J., Raffi, I., Taberner, C., and Zachariasse, W.J., 2000. The ‘Tortonian salinity crisis’ of the eastern Betics (Spain). *Earth and Planetary Science Letters*, 181, 497–511.
- Krijgsman, W., 2002. The Mediterranean: *Mare Nostrum* of Earth sciences. *Earth and Planetary Science Letters*, 205, 1–12.
- Kruvier, P.P., Krijgsman, W., Langereis, C.G., and Dekkers, M.J., 2002. Cyclostratigraphy and rock-magnetic investigation of the NRM signal in late Miocene palustrine-alluvial deposits of the Librilla section (SE Spain). *Journal of Geophysical Research*, 107, 1–18.
- Ku, H., 1966. Notes on the use of propagation of error formulas. *Journal of Research of the National Bureau of Standards*, 70C, 263–273.
- Kuiper, K.F., Krijgsman, W., Garcés, M., and Wijbrans, J.R., 2006. Revised isotopic ($^{40}\text{Ar}/^{39}\text{Ar}$) age for the lamproite volcano of Cabezos Negros, Fortuna Basin (Eastern Betics, SE Spain). *Palaeogeography, Palaeoclimatology, Palaeoecology*, 238, 53–63.
- Land, L.S., Lundelius, E.L., and Valastro, S., 1980. Isotopic ecology of deer bones. *Palaeogeography, Palaeoclimatology, Palaeoecology*, 32, 143–151.
- Levin, N.E., Cerling, T.E., Passey, B.H., Harris, J.M., and Ehleringer, J.R., 2006. A stable isotope aridity index for terrestrial environments. *Proceedings of the National Academy of Sciences – USA*, 103, 11201–11205.

- Liu, Z., Pagani, M., Zinniker, D., DeConto, R., Huber, M., Brinkhuis, H., Shah, S.R., Leckie, R.M., and Pearson, A., 2009. Global cooling during the Eocene-Oligocene climate transition. *Science*, 323, 1187–1190.
- Longinelli, A., 1984. Oxygen isotopes in mammal bone phosphate: A new tool for paleohydrological and paleoclimatological research. *Geochimica et Cosmochimica Acta*, 48, 385–390.
- Longinelli, A. and Nuti, S., 1973. Revised phosphate-water isotopic temperature scale. *Earth and Planetary Science Letters*, 19, 373–376.
- Luz, B. and Kolodny, Y., 1985. Oxygen isotope variations in phosphate of biogenic apatites, IV. Mammal teeth and bones. *Earth and Planetary Science Letters*, 75, 29–36.
- Luz, B. and Koldny, Y., 1989. Oxygen isotope variation in bone phosphate. *Applied Geochemistry*, 4, 317–323.
- Luz, B., Kolodny, Y., and Horowitz, M., 1984. Fractionation of oxygen isotopes between mammalian bone-phosphate and environmental drinking water. *Geochimica et Cosmochimica Acta*, 48, 1689–1693.
- Luz, B., Cormie, A.B., and Schwarz, H.P., 1990. Oxygen isotope variations in phosphate of deer bones. *Geochimica et Cosmochimica Acta*, 54, 1723–1728.
- Maslin, M.A., Li, X.S., Loutre, M.-F., and Berger, A., 1998. The contribution of orbital forcing to the progressive intensification of northern hemisphere glaciation. *Quaternary Science Reviews*, 17, 411–426.

- McNab, B.K., 2002. *The Physiological Ecology of Vertebrates: A View from Energetics*. Cornell University Press, Ithaca, New York, 624 p.
- Mein, P., Bizon, G., Bizon, J.J., and Montenat, C., 1973. Le gisement de Mammifères de La Alberca (Murcia, Espagne méridionale). Corrélation avec les formations marines du Miocène terminal. *Comptes Rendus de l'Académie des Sciences de Paris, Série D*, 276, 3077–3080.
- Montoya, P., Morales, J., Robles, F., Abella, J., Benavent, J.V., Marín, M.D., and Ruiz Sánchez, F.J., 2006. Las nuevas excavaciones (1995-2006) en el yacimiento del Mioceno final de Venta del Moro, Valencia. *Estudios Geológicos*, 62, 313–326.
- NCDC, 2009. Surface Data – Global Summary of the Day: 1957–2009. <http://www.ncdc.noaa.gov/>. 2009.
- Nelson, S.V., 2005. Paleoseasonality inferred from equid teeth and intra-tooth isotopic variability. *Palaeogeography, Palaeoclimatology, Palaeoecology*, 222, 122–144.
- Newesely, H., 1989. Fossil bone apatite. *Applied Geochemistry*, 4, 233–245.
- O'Neil, J.R., Roe, L.J., Reinhard, E., and Blake, R.E., 1994. A rapid and precise method of oxygen isotope analysis of biogenic phosphate. *Israel Journal of Earth Sciences*, 43, 203–212.
- Opdyke, N., Mein, P., Moissenet, E., Pérez-González, A., Lindsay, E., and Petko, M., 1990. The magnetic stratigraphy of the Late Miocene sediments of the Cabriel Basin, Spain. *In*: Lindsay, E.H., Fahlbusch, V., and Mein, P. (Eds.), *European Neogene Mammal Chronology*. Plenum Press, New York, pp. 507–514.

- Opdyke, N., Mein, P., Lindsay, E., Perez-Gonzales, A., Moissenet, E., and Norton, V.L., 1997. Continental deposits, magnetostratigraphy and vertebrate paleontology, late Neogene of Eastern Spain. *Palaeogeography, Palaeoclimatology, Palaeoecology*, 133, 129–148.
- Ortiz, J.E., Torres, T., Delgado, A., Reyes, E., Llamas, J.F., Soler, V., and Raya, J., 2006. Pleistocene paleoenvironmental evolution at continental middle latitude inferred from carbon and oxygen stable isotope analysis of ostracodes from the Guadix-Baza Basin (Granada, SE Spain). *Palaeogeography, Palaeoclimatology, Palaeoecology*, 240, 536–561.
- Passey, B.H. and Cerling, T.E., 2002. Tooth enamel mineralization in ungulates: Implications for recovering a primary isotopic time-series. *Geochimica et Cosmochimica Acta*, 66, 3225–3234.
- Potts, R. and Behrensmeyer, A.K., 1992. Late Cenozoic terrestrial ecosystems. In: Behrensmeyer, A.K., Damuth, J., DiMichele, W., Potts, R., Sues, H.D., and Wing, S. (Eds.), *Terrestrial Ecosystems Through Time*. University of Chicago Press, Chicago, p. 419–519.
- Quade, J. and Cerling, T.E., 1995. Expansion of C4 grasses in the Late Miocene of northern Pakistan: evidence from stable isotopes in paleosols. *Palaeogeography, Palaeoclimatology, Palaeoecology*, 115, 91–116.
- Quade, J., Solounias, N., and Cerling, T.E., 1994. Stable isotopic evidence from paleosol carbonates and fossil teeth in Greece for woodlands over the past 11 Ma. *Palaeogeography, Palaeoclimatology, Palaeoecology*, 108, 41–53.

- Rozanski, K., Araguás-Araguás, L., and Gonfiantini, R., 1993. Isotopic patterns in modern global precipitation. *In* P.K. Swart, K.C. Lohmann, J.A. McKenzie, and S.M. Savin (eds.) *Climate Change in Continental Isotopic Records*. Geophysical Monograph 78, American Geophysical Union, Washington, D.C., p. 1–36.
- Sánchez-Chillón, B., Alberdi, M.T., Leone, G., Bonadonna, F.P., Stenni, B., and Longinelli, A., 1994. Oxygen isotopic composition of fossil equid tooth and bone phosphate: an archive of difficult interpretation. *Palaeogeography, Palaeoclimatology, Palaeoecology*, 107, 317–328.
- Scott, G.R., Gibert, L., and Gibert, J., 2007. Magnetostratigraphy of the Orce region (Baza Basin), SE Spain: New chronologies for Early Pleistocene faunas and hominid occupation sites. *Quaternary Science Reviews*, 26, 415–435.
- Shackleton, N.J., Imbrie, J., Pisias, N.G., and Rose, J., 1988. The evolution of oceanic oxygen-isotope variability in the North Atlantic over the past three million years. *Philosophical Transactions of the Royal Society of London, Series B*, 318, 679–688.
- Small, E.E., Giorgi, F., Sloan, L.C., and Hostetler, S., 2001a. The effects of desiccation and climatic change on the hydrology of the Aral Sea. *Journal of Climate*, 14, 300–322.
- Small, E.E., Sloan, L.C., and Nychka, D., 2001b. Changes in surface air temperature caused by desiccation of the Aral Sea. *Journal of Climate*, 14, 284–299.
- Sokal, R.R. and Rohlf, F.J., 1995. *Biometry: The Principles and Practice of Statistics in Biological Research*. W.H. Freeman and Co., New York, 887 pp.

- Solounias, N., Plavcan, J.M., Quade, J., and Witmer, L., 1999. The paleoecology of the Pkermian Biome and the savanna myth. *In*: Agustí, J., Rook, L., and Andrews, P. (Eds.), *The Evolution of Neogene Terrestrial Ecosystems in Europe*. Cambridge University Press, Cambridge, UK, p. 436–453.
- Steininger, F.F., Berggren, W.A., Kent, D.V., Bernor, R.L., Sen, S., and Agustí, J., 1996. Circum-Mediterranean Neogene (Miocene and Pliocene) marine-continental chronologic correlations of European mammal units. *In*: Bernor, R.L., Fahlbusch, V., and Mittmann, H.-W. (Eds.), *The Evolution of Western Eurasian Neogene Mammal Faunas*. Columbia University Press, New York, pp. 7–46.
- Strömberg, C., 2005. Decoupled taxonomic radiation and ecological expansion of open-habitat grasses in the Cenozoic of North America. *Proceedings of the National Academy of Sciences, USA*, 102, 11980–11984.
- Tedford, R.H., Albright, L.B., III, Barnosky, A.D., Ferrusquia-Villafranca, I., Hunt, R.M., Jr., Storer, J.E., Swisher, C.C., III, Voorhies, M.R., Webb, S.D., and Whistler, D.P., 2004. Mammalian biochronology of the Arikarean through Hemphillian interval (Late Oligocene through early Pliocene epochs). *In*: Woodburne, M.O. (Ed.), *Late Cretaceous and Cenozoic Mammals of North America: Biostratigraphy and Geochronology*. Columbia University Press, New York, p. 169–231.
- Tudge, A.P., 1960. A method of analysis of oxygen isotopes in orthophosphate – its use in the measurement of paleotemperatures. *Geochimica et Cosmochimica Acta*, 18, 81–93.

- van Dam, J.A., 2006. Geographic and temporal patterns in the late Neogene (12–3 Ma) aridification of Europe: The use of small mammals as paleoprecipitation proxies. *Palaeogeography, Palaeoclimatology, Palaeoecology*, 238, 190–218.
- van Dam, J.A. and Weltje, G.J., 1999. Reconstruction of Late Miocene climate of Spain using rodent palaeocommunity successions: an application of end-member modeling. *Palaeogeography, Palaeoclimatology, Palaeoecology*, 151, 267–305.
- van Dam, J.A. and Reichart, G.J., 2009. Oxygen and carbon isotope signatures in late Neogene horse teeth from Spain and application as temperature and seasonality proxies. *Palaeogeography, Palaeoclimatology, Palaeoecology*, 274, 64–81.
- van Dam, J.A., Alcalá, L., Alonso-Zarza, A., Calvo, J.P., Garcés, M., and Krijgsman, W., 2001. The Upper Miocene mammal record from the Teruel-Alfambra region (Spain): the MN system and continental stage/age concepts discussed. *Journal of Vertebrate Paleontology*, 21, 367–385.
- Van Dam, J.A., Abdul Aziz, H., Álvarez Sierra, M.A., Hilgen, F.J., van den Hoek Ostende, L.W., Lourens, L., Mein, P., van der Meulen, A.J., and Pelaez-Campomanes, P., 2006. Long-period astronomical forcing of mammal turnover. *Nature*, 443, 687–691.
- Van der Made, J., Morales, J., and Montoya, P., 2006. Late Miocene turnover in the Spanish mammal record in relation to palaeoclimate and the Messinian Salinity Crisis. *Palaeogeography, Palaeoclimatology, Palaeoecology*, 238, 228–246.
- Weiner, S., Traub, W., Elster, H., and DeNiro, M.J., 1989. The molecular structure of bone and its relation to diagenesis. *Applied Geochemistry*, 4, 231–232.

Zachos, J., Pagani, M., Sloan, L., Thomas, E., and Billups, K., 2001. Trends, rhythms, and aberrations in global climate 65 Ma to present. *Science*, 292, 686–693.

Zazzo, A., Lecuyer, C., Mariotti, A., 2004. Experimentally-controlled carbon and oxygen isotope exchange between bioapatites and water under inorganic and microbially-mediated conditions. *Geochimica et Cosmochimica Acta*, 68, 1–12.

Figure Captions

Figure 2.1. Geographic position of fossil localities in eastern Spain. A) Geographic map showing the locations of the Teruel, Baza, and Fortuna Basins, and the fossil localities Almenara-M (AM) and Venta del Moro (VM). B) Generalized geologic map of the Baza Basin, showing the positions of the fossil localities Puerto Lobo (PL), Barranco León (BL), Venta Micena (VA), and Barranco del Paso (BP). C) Generalized geologic map of the Fortuna Basin, showing the positions of the fossil localities Librilla (LB), Molina de Segura (MS), and La Alberca (LA). D) Generalized geologic map of the Teruel Basin, showing the positions of the fossil localities Conclud (CC), El Arquillo (AQ), Los Mansuetos (LM), and La Calera (LC).

Figure 2.2. Faunal $\delta^{18}\text{O}$ comparisons. A) Whole fauna results. Bulk enamel values are indicated by large symbols with black outlines. Bulk dentine and bone $\delta^{18}\text{O}$ values are indicated by small symbols with gray outlines. Locality abbreviations as in text and in Figure 2.1. B) Mean $\delta^{18}\text{O} \pm 1$ standard deviation for whole faunas (black-outlined symbols and black lines) and for equids and ruminants only (gray-outlined symbols and gray lines).

Figure 2.3. Comparisons of enamel and dentine $\delta^{18}\text{O}$. A) Schematic diagram showing expected $\delta^{18}\text{O}$ shifts toward diagenetic endmember for altered dentine phosphate. B) Enamel and dentine $\delta^{18}\text{O}$ for intra-tooth samples from this study, with OLS regression lines for each locality. Predicted $\delta^{18}\text{O}$ of diagenetic endmember phosphate is based on the point of intersection between each regression line and a 1:1 line. C) Estimated $\delta^{18}\text{O}$ of water in equilibrium with predicted diagenetic endmember phosphate over the temperature range 0-30°C (indicated by lines as in B). Means and standard deviations for MAT and mean annual precipitation $\delta^{18}\text{O}$ for modern climate stations over the period 2000-2004 (indicated by large symbols) and full range of observed values over the same period (indicated by small gray symbols).

Figure 2.4. Equid $\delta^{18}\text{O}$ results. A) Comparisons of equid bulk enamel $\delta^{18}\text{O}$ from this study and from van Dam and Reichart (2009). B) Comparison of bulk enamel $\delta^{18}\text{O}$ from this study with mean $\delta^{18}\text{O}$ of serial samples from the same specimens. C) Enamel $\delta^{18}\text{O}$ from serial samples of equid and gomphothere molars from this study and from van Dam and Reichart (2009). Individual serial measurements are indicated by small black symbols, means of serial samples are indicated by large symbols as in A, and $\delta^{18}\text{O}$ of bulk samples indicated by “X”.

Figure 2.1. Geographic position of fossil localities in eastern Spain.

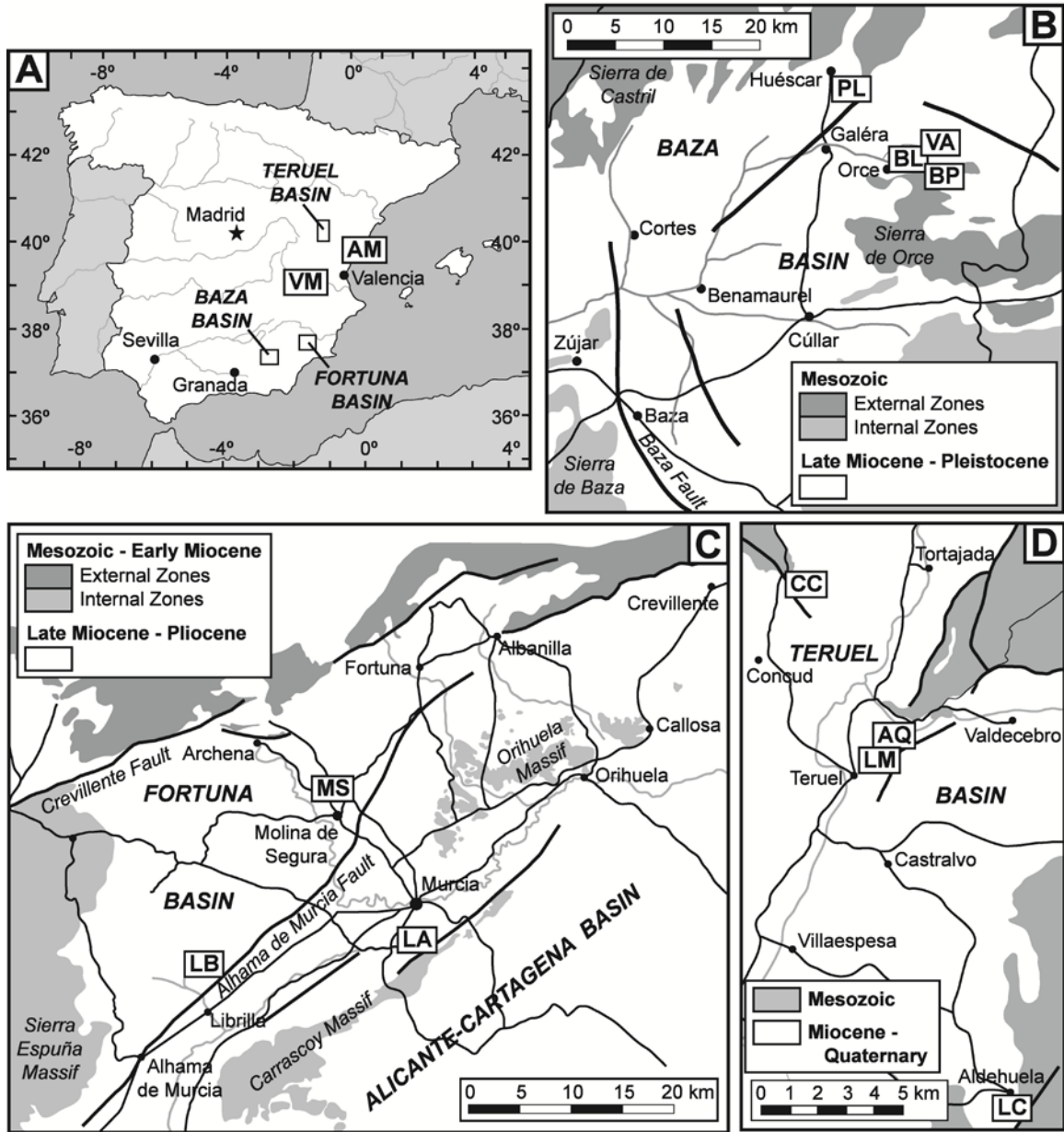


Figure 2.2. Faunal $\delta^{18}\text{O}$ comparisons.

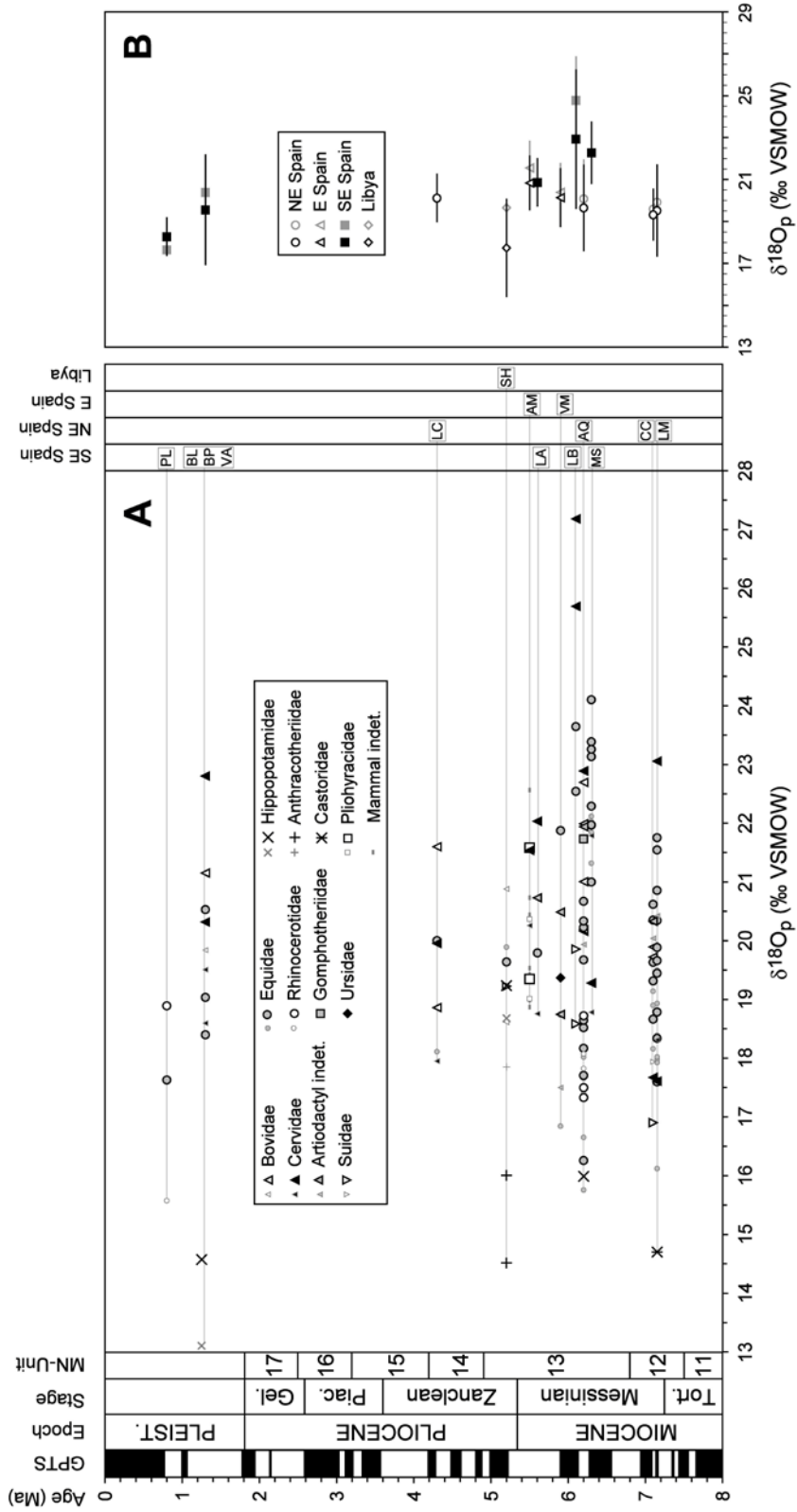


Figure 2.3. Comparison of enamel and dentine $\delta^{18}\text{O}$.

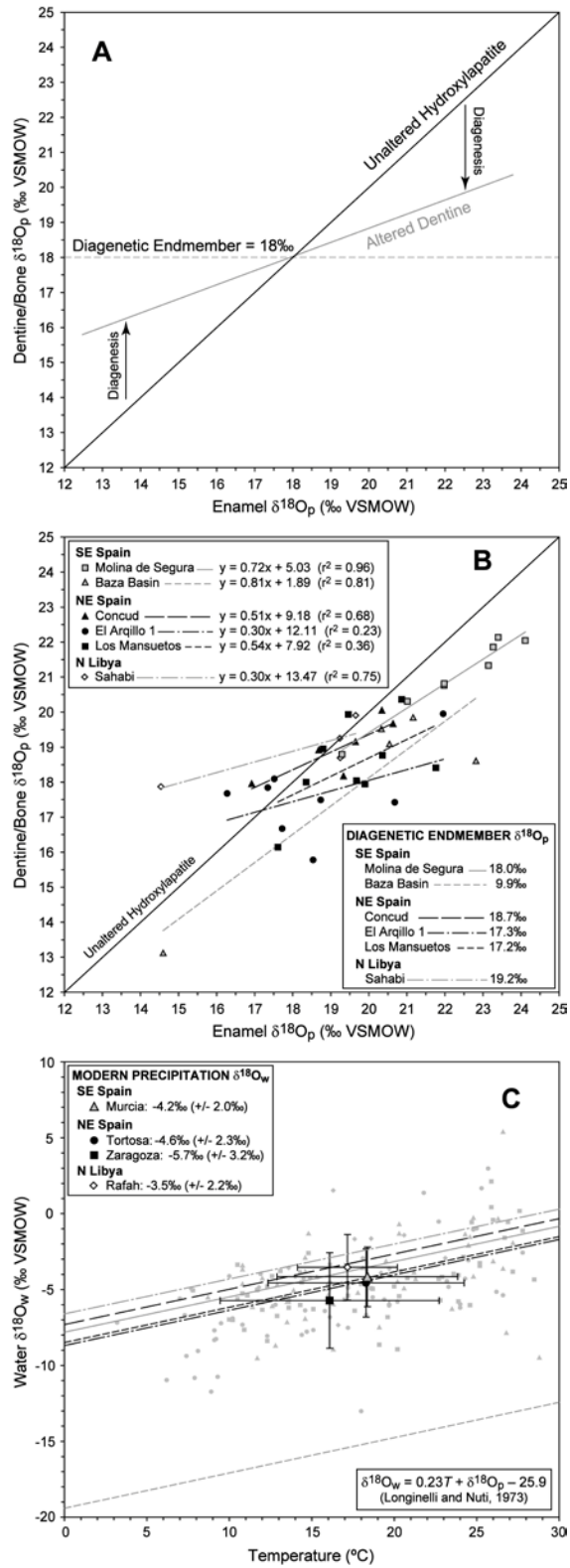


Figure 2.4. Equid $\delta^{18}\text{O}$ results.

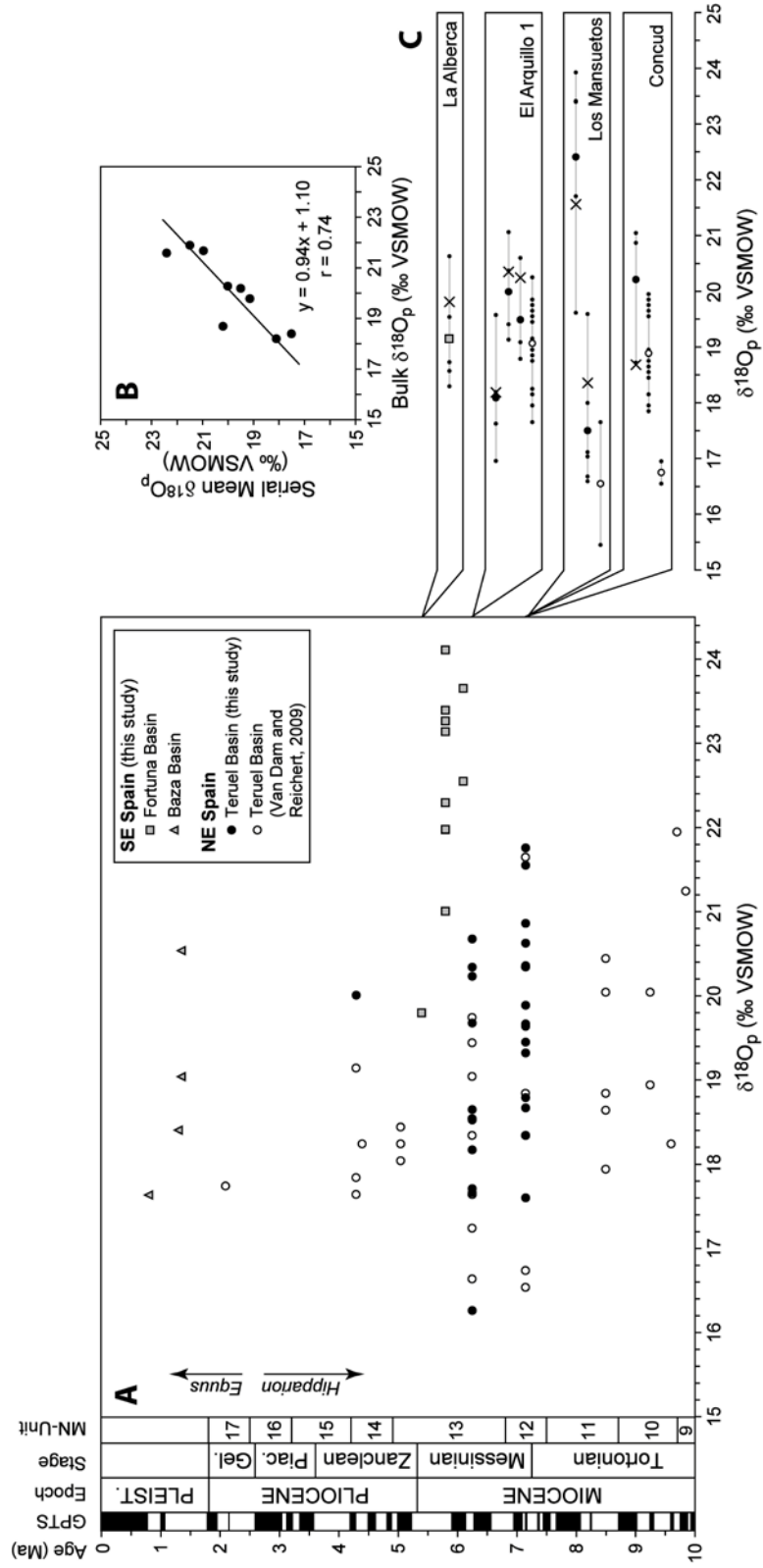


Table 2.1. $\delta^{18}\text{O}$ measurements of mammal tooth enamel, dentine, and bone phosphate.

Specimen	Basin	Locality	Age (Ma)	Taxon	Material	Sample type*	$\delta^{18}\text{O}_p$	Lab
IPS-20519-2	Teruel	CC	7.2–7.1	Bovidae	enamel	bulk	19.9	KU
IPS-20519-3	Teruel	CC	7.2–7.1	Bovidae	enamel	bulk	19.7	KU
IPS-1971	Teruel	CC	7.2–7.1	Cervidae	enamel	bulk	17.7	KU
IPS-41056	Teruel	CC	7.2–7.1	Equidae	enamel	bulk	19.6	KU
IPS-41054	Teruel	CC	7.2–7.1	Equidae	enamel	bulk	20.6	KU
IPS-41053	Teruel	CC	7.2–7.1	Equidae	enamel	bulk	20.4	KU
IPS-41055	Teruel	CC	7.2–7.1	Equidae	enamel	bulk	19.3	KU
IPS-41056	Teruel	CC	7.2–7.1	Equidae	dentine	bulk	19.2	KU
IPS-41054	Teruel	CC	7.2–7.1	Equidae	dentine	bulk	19.7	KU
IPS-41055	Teruel	CC	7.2–7.1	Equidae	dentine	bulk	18.2	KU
IPS-41045	Teruel	CC	7.2–7.1	Equidae	enamel	bulk	18.7	KU
IPS-41045	Teruel	CC	7.2–7.1	Equidae	dentine	bulk	18.9	KU
IPS-41045	Teruel	CC	7.2–7.1	Equidae	enamel	serial (06)	20.9	KU
IPS-41045	Teruel	CC	7.2–7.1	Equidae	enamel	serial (10)	21	KU
IPS-41045	Teruel	CC	7.2–7.1	Equidae	enamel	serial (14)	18.7	KU
IPS-1090	Teruel	CC	7.2–7.1	Suidae	enamel	bulk	16.9	KU
IPS-1090	Teruel	CC	7.2–7.1	Suidae	dentine	bulk	18	KU
IPS-33202	Teruel	CC	7.2–7.1	Artiodactyla indet.	enamel	bulk	20.3	KU
IPS-33202	Teruel	CC	7.2–7.1	Artiodactyla indet.	dentine	bulk	20.1	KU
IPS-32843	Teruel	LM	7.2–7.1	Castoridae	enamel	bulk	14.7	KU
IPS-1883	Teruel	LM	7.2–7.1	Cervidae	enamel	bulk	17.6	KU
IPS-32836-1	Teruel	LM	7.2–7.1	Cervidae	enamel	bulk	23.1	KU
IPS-1881	Teruel	LM	7.2–7.1	Cervidae	bone	bulk	18.3	KU
IPS-37931-1	Teruel	LM	7.2–7.1	Equidae	enamel	bulk	18.4	KU
IPS-37931-1	Teruel	LM	7.2–7.1	Equidae	dentine	bulk	18	KU
IPS-37931-1	Teruel	LM	7.2–7.1	Equidae	enamel	serial (08)	19.6	KU
IPS-37931-1	Teruel	LM	7.2–7.1	Equidae	enamel	serial (14)	18	KU
IPS-37931-1	Teruel	LM	7.2–7.1	Equidae	enamel	serial (21)	16.6	KU
IPS-37931-1	Teruel	LM	7.2–7.1	Equidae	enamel	serial (26)	17.1	KU
IPS-37931-1	Teruel	LM	7.2–7.1	Equidae	enamel	serial (32)	17	KU
IPS-37931-1	Teruel	LM	7.2–7.1	Equidae	enamel	serial (38)	16.7	KU
IPS-37931-10	Teruel	LM	7.2–7.1	Equidae	enamel	bulk	18.8	KU
IPS-37931-10	Teruel	LM	7.2–7.1	Equidae	dentine	bulk	18.9	KU
IPS-37931-2	Teruel	LM	7.2–7.1	Equidae	enamel	bulk	21.6	KU
IPS-37931-2	Teruel	LM	7.2–7.1	Equidae	dentine	bulk	19.5	KU
IPS-37931-2	Teruel	LM	7.2–7.1	Equidae	enamel	serial (06)	19.6	KU
IPS-37931-2	Teruel	LM	7.2–7.1	Equidae	enamel	serial (12)	21.7	KU
IPS-37931-2	Teruel	LM	7.2–7.1	Equidae	enamel	serial (18)	23.4	KU
IPS-37931-2	Teruel	LM	7.2–7.1	Equidae	enamel	serial (23)	23.4	KU

Table 2.1 (continued)

Specimen	Basin	Locality	Age (Ma)	Taxon	Material	Sample type	$\delta^{18}\text{O}_p$	Lab
IPS-37931-2	Teruel	LM	7.2–7.1	Equidae	enamel	serial (30)	23.9	KU
IPS-37931-3	Teruel	LM	7.2–7.1	Equidae	enamel	bulk	20.4	KU
IPS-37931-3	Teruel	LM	7.2–7.1	Equidae	dentine	bulk	18.8	KU
IPS-37931-4	Teruel	LM	7.2–7.1	Equidae	enamel	bulk	19.9	KU
IPS-37931-4	Teruel	LM	7.2–7.1	Equidae	dentine	bulk	17.9	KU
IPS-37931-5	Teruel	LM	7.2–7.1	Equidae	enamel	bulk	17.6	KU
IPS-37931-5	Teruel	LM	7.2–7.1	Equidae	dentine	bulk	16.1	KU
IPS-37931-6	Teruel	LM	7.2–7.1	Equidae	enamel	bulk	19.5	KU
IPS-37931-6	Teruel	LM	7.2–7.1	Equidae	dentine	bulk	19.9	KU
IPS-37931-7	Teruel	LM	7.2–7.1	Equidae	enamel	bulk	21.8	KU
IPS-37931-7	Teruel	LM	7.2–7.1	Equidae	dentine	bulk	18.4	KU
IPS-37931-8	Teruel	LM	7.2–7.1	Equidae	enamel	bulk	20.9	KU
IPS-37931-8	Teruel	LM	7.2–7.1	Equidae	dentine	bulk	20.4	KU
IPS-37931-9	Teruel	LM	7.2–7.1	Equidae	enamel	bulk	19.7	KU
IPS-37931-9	Teruel	LM	7.2–7.1	Equidae	dentine	bulk	18	KU
IPS-32836-2	Teruel	LM	7.2–7.1	Artiodactyla indet.	bone	bulk	20.4	KU
IPS-37061	Fortuna	MS	6.6–6.0	Cervidae	enamel	bulk	19.3	KU
IPS-37061	Fortuna	MS	6.6–6.0	Cervidae	dentine	bulk	18.8	KU
IPS-37061	Fortuna	MS	6.6–6.0	Cervidae	bone	bulk	21.8	KU
IPS-14709	Fortuna	MS	6.6–6.0	Equidae	enamel	bulk	21	KU
IPS-37059-1	Fortuna	MS	6.6–6.0	Equidae	enamel	bulk	22.3	KU
IPS-37059-2	Fortuna	MS	6.6–6.0	Equidae	enamel	bulk	22	KU
IPS-37059-3	Fortuna	MS	6.6–6.0	Equidae	enamel	bulk	22	KU
IPS-37059-4	Fortuna	MS	6.6–6.0	Equidae	enamel	bulk	23.1	KU
IPS-37059-4	Fortuna	MS	6.6–6.0	Equidae	dentine	bulk	21.3	KU
IPS-37059-5	Fortuna	MS	6.6–6.0	Equidae	enamel	bulk	23.3	KU
IPS-37059-5	Fortuna	MS	6.6–6.0	Equidae	dentine	bulk	21.9	KU
IPS-37065-1	Fortuna	MS	6.6–6.0	Equidae	enamel	bulk	23.4	KU
IPS-37065-1	Fortuna	MS	6.6–6.0	Equidae	dentine	bulk	22.1	KU
IPS-37065-2	Fortuna	MS	6.6–6.0	Equidae	enamel	bulk	24.1	KU
IPS-37065-2	Fortuna	MS	6.6–6.0	Equidae	dentine	bulk	22	KU
IPS-37063-1	Fortuna	MS	6.6–6.0	Mammalia indet.	bone	bulk	21.6	KU
IPS-37063-2	Fortuna	MS	6.6–6.0	Mammalia indet.	bone	bulk	20.3	KU
IPS-29022-1	Teruel	AQ	6.4–6.1	Bovidae	enamel	bulk	22.7	KU
IPS-29022-2	Teruel	AQ	6.4–6.1	Bovidae	enamel	bulk	22	KU
IPS-29021	Teruel	AQ	6.4–6.1	Bovidae	enamel	bulk	20.2	KU
IPS-29078	Teruel	AQ	6.4–6.1	Bovidae	enamel	bulk	20.2	KU
IPS-28992	Teruel	AQ	6.4–6.1	Bovidae	enamel	bulk	21	KU
IPS-37922	Teruel	AQ	6.4–6.1	Cervidae	enamel	bulk	22.9	KU
IPS-28980-1	Teruel	AQ	6.4–6.1	Equidae	enamel	bulk	20.2	USK

Table 2.1 (continued)

Specimen	Basin	Locality	Age (Ma)	Taxon	Material	Sample type	$\delta^{18}\text{O}_p$	Lab
IPS-28980-1	Teruel	AQ	6.4–6.1	Equidae	enamel	serial (03)	18.8	USK
IPS-28980-1	Teruel	AQ	6.4–6.1	Equidae	enamel	serial (15)	19.1	USK
IPS-28980-1	Teruel	AQ	6.4–6.1	Equidae	enamel	serial (21)	20.6	USK
IPS-28980-2	Teruel	AQ	6.4–6.1	Equidae	enamel	bulk	20.3	USK
IPS-28980-2	Teruel	AQ	6.4–6.1	Equidae	enamel	serial (10)	19.1	USK
IPS-28980-2	Teruel	AQ	6.4–6.1	Equidae	enamel	serial (17)	21.1	USK
IPS-28980-2	Teruel	AQ	6.4–6.1	Equidae	enamel	serial (30)	20.4	USK
IPS-28980-2	Teruel	AQ	6.4–6.1	Equidae	enamel	serial (40)	19.4	USK
IPS-28980-3	Teruel	AQ	6.4–6.1	Equidae	enamel	bulk	18.5	KU
IPS-28980-3	Teruel	AQ	6.4–6.1	Equidae	dentine	bulk	15.8	KU
IPS-28980-4	Teruel	AQ	6.4–6.1	Equidae	enamel	bulk	18.7	KU
IPS-28980-5	Teruel	AQ	6.4–6.1	Equidae	enamel	bulk	18.2	KU
IPS-28980-5	Teruel	AQ	6.4–6.1	Equidae	enamel	serial (10)	19.6	KU
IPS-28980-5	Teruel	AQ	6.4–6.1	Equidae	enamel	serial (20)	18.2	KU
IPS-28980-5	Teruel	AQ	6.4–6.1	Equidae	enamel	serial (27)	17	KU
IPS-28980-5	Teruel	AQ	6.4–6.1	Equidae	enamel	serial (35)	17.6	KU
IPS-37923-1	Teruel	AQ	6.4–6.1	Equidae	enamel	bulk	16.3	KU
IPS-37923-1	Teruel	AQ	6.4–6.1	Equidae	dentine	bulk	17.7	KU
IPS-37923-2	Teruel	AQ	6.4–6.1	Equidae	enamel	bulk	19.7	KU
IPS-37923-2	Teruel	AQ	6.4–6.1	Equidae	dentine	bulk	18	KU
IPS-37923-3	Teruel	AQ	6.4–6.1	Equidae	enamel	bulk	17.7	KU
IPS-37923-3	Teruel	AQ	6.4–6.1	Equidae	dentine	bulk	16.7	KU
IPS-37923-4	Teruel	AQ	6.4–6.1	Equidae	enamel	bulk	20.7	KU
IPS-37923-4	Teruel	AQ	6.4–6.1	Equidae	dentine	bulk	17.4	KU
IPS-12834	Teruel	AQ	6.4–6.1	Gomphotheriidae	enamel	bulk	21.7	KU
IPS-12834	Teruel	AQ	6.4–6.1	Gomphotheriidae	enamel	serial (10)	19.8	KU
IPS-12834	Teruel	AQ	6.4–6.1	Gomphotheriidae	enamel	serial (18)	21	KU
IPS-12834	Teruel	AQ	6.4–6.1	Gomphotheriidae	enamel	serial (28)	21.6	KU
IPS-12834	Teruel	AQ	6.4–6.1	Gomphotheriidae	enamel	serial (36)	21.4	KU
IPS-36190	Teruel	AQ	6.4–6.1	Hippopotimadae	enamel	bulk	16	KU
IPS-38817	Teruel	AQ	6.4–6.1	Rhinocerotidae	enamel	bulk	17.5	KU
IPS-38819	Teruel	AQ	6.4–6.1	Rhinocerotidae	enamel	bulk	18.7	KU
IPS-38818	Teruel	AQ	6.4–6.1	Rhinocerotidae	enamel	bulk	17.3	KU
IPS-38817	Teruel	AQ	6.4–6.1	Rhinocerotidae	dentine	bulk	18.1	KU
IPS-38819	Teruel	AQ	6.4–6.1	Rhinocerotidae	dentine	bulk	17.5	KU
IPS-38818	Teruel	AQ	6.4–6.1	Rhinocerotidae	dentine	bulk	17.8	KU
IPS-37926	Teruel	AQ	6.4–6.1	Artiodactyla indet.	enamel	bulk	22	KU
IPS-37926	Teruel	AQ	6.4–6.1	Artiodactyla indet.	dentine	bulk	19.9	KU
IPS-22547	Fortuna	LB	6.3–5.9	Cervidae	enamel	bulk	25.7	USK
IPS-33716	Fortuna	LB	6.3–5.9	Cervidae	enamel	bulk	27.2	USK

Table 2.1 (continued)

Specimen	Basin	Locality	Age (Ma)	Taxon	Material	Sample type	$\delta^{18}\text{O}_p$	Lab
IPS-34714	Fortuna	LB	6.3–5.9	Equidae	enamel	bulk	22.6	USK
IPS-34717	Fortuna	LB	6.3–5.9	Equidae	enamel	bulk	23.7	USK
IPS-33712	Fortuna	LB	6.3–5.9	Suidae	enamel	bulk	19.9	USK
IPS-33713	Fortuna	LB	6.3–5.9	Suidae	enamel	bulk	18.6	USK
IPS-33063-1	Cabriel	VM	5.9	Equidae	enamel	bulk	21.9	KU
IPS-33063-1	Cabriel	VM	5.9	Equidae	dentine	bulk	18.8	KU
IPS-33063-1	Cabriel	VM	5.9	Equidae	enamel	serial (10)	22.3	KU
IPS-33063-1	Cabriel	VM	5.9	Equidae	enamel	serial (18)	22.3	KU
IPS-33063-1	Cabriel	VM	5.9	Equidae	enamel	serial (25)	21.3	KU
IPS-33063-1	Cabriel	VM	5.9	Equidae	enamel	serial (42)	20.1	KU
IPS-33079-1	Cabriel	VM	5.9	Equidae	dentine	bulk	18.8	KU
IPS-33079-2	Cabriel	VM	5.9	Equidae	dentine	bulk	16.9	KU
IPS-33063-2	Cabriel	VM	5.9	Ursidae	enamel	bulk	19.4	KU
IPS-33078	Cabriel	VM	5.9	Artiodactyla indet.	enamel	bulk	18.8	KU
IPS-33075	Cabriel	VM	5.9	Artiodactyla indet.	enamel	bulk	20.5	KU
IPS-33075	Cabriel	VM	5.9	Artiodactyla indet.	dentine	bulk	17.5	KU
IPS-33718	Fortuna	LA	5.6	Cervidae	enamel	bulk	22	KU
IPS-33718	Fortuna	LA	5.6	Cervidae	dentine	bulk	18.8	KU
IPS-34726	Fortuna	LA	5.6	Equidae	enamel	bulk	19.8	KU
IPS-34726	Fortuna	LA	5.6	Equidae	enamel	serial (12)	20.6	KU
IPS-34726	Fortuna	LA	5.6	Equidae	enamel	serial (22)	19.5	KU
IPS-34726	Fortuna	LA	5.6	Equidae	enamel	serial (31)	18.3	KU
IPS-34726	Fortuna	LA	5.6	Equidae	enamel	serial (41)	18.7	KU
IPS-34726	Fortuna	LA	5.6	Equidae	enamel	serial (51)	18.6	KU
IPS-35331	Fortuna	LA	5.6	Artiodactyla indet.	enamel	bulk	20.7	KU
IPS-37073		AM	6.1–5.3	Cervidae	enamel	bulk	21.5	USK
IPS-37073		AM	6.1–5.3	Cervidae	dentine	bulk	20.3	USK
IPS-37071		AM	6.1–5.3	Pliohyracidae	enamel	bulk	19.4	USK
IPS-37070		AM	6.1–5.3	Pliohyracidae	enamel	bulk	21.6	USK
IPS-37071		AM	6.1–5.3	Pliohyracidae	dentine	bulk	19	USK
IPS-37070		AM	6.1–5.3	Pliohyracidae	dentine	bulk	20.4	USK
IPS-37077		AM	6.1–5.3	Carnivora indet.	bone	bulk	19.5	USK
IPS-37078		AM	6.1–5.3	Carnivora indet.	bone	bulk	19.4	USK
IPS-37068		AM	6.1–5.3	Mammalia indet.	bone	bulk	20.7	USK
IPS-37072		AM	6.1–5.3	Mammalia indet.	bone	bulk	19.5	USK
IPS-37075		AM	6.1–5.3	Mammalia indet.	bone	bulk	18.8	USK
IPS-37082		AM	6.1–5.3	Mammalia indet.	bone	bulk	22.5	USK
IPS-37081		AM	6.1–5.3	Mammalia indet.	bone	bulk	20.4	USK
IPS-37079		AM	6.1–5.3	Mammalia indet.	bone	bulk	19	USK
IPS-37080		AM	6.1–5.3	Testudines indet.	bone	bulk	21.5	USK

Table 2.1 (continued)

Specimen	Basin	Locality	Age (Ma)	Taxon	Material	Sample type*	$\delta^{18}\text{O}_p$	Lab
IPS-37511		SH	5.2	Anthracotheridae	enamel	bulk	14.5	USK
IPS-37515		SH	5.2	Anthracotheridae	enamel	bulk	16	USK
IPS-37511		SH	5.2	Anthracotheridae	dentine	bulk	17.9	USK
IPS-37520		SH	5.2	Bovidae	bone	bulk	20.9	USK
IPS-37519		SH	5.2	Bovidae	bone	bulk	18.6	USK
IPS-37517		SH	5.2	Equidae	enamel	bulk	19.7	USK
IPS-37517		SH	5.2	Equidae	dentine	bulk	19.9	USK
IPS-37514		SH	5.2	Hippopotamidae	enamel	bulk	19.2	USK
IPS-37514		SH	5.2	Hippopotamidae	dentine	bulk	18.7	USK
IPS-37518		SH	5.2	Suidae	enamel	bulk	19.2	USK
IPS-37518		SH	5.2	Suidae	dentine	bulk	19.3	USK
IPS-37816	Teruel	LC	4.3	Bovidae	enamel	bulk	21.6	KU
IPS-37813	Teruel	LC	4.3	Bovidae	enamel	bulk	18.9	KU
IPS-37817	Teruel	LC	4.3	Cervidae	enamel	bulk	20	KU
IPS-37817	Teruel	LC	4.3	Cervidae	dentine	bulk	18	KU
IPS-37809	Teruel	LC	4.3	Equidae	enamel	bulk	20	KU
IPS-37809	Teruel	LC	4.3	Equidae	dentine	bulk	18.1	KU
BB.BZ.01	Baza	BP	1.3	Equidae	enamel	bulk	20.5	KU
BB.BZ.01	Baza	BP	1.3	Equidae	dentine	bulk	19.1	KU
BB.BP.01	Baza	BP	1.3	Equidae	enamel	bulk	19	KU
BB.VM.03	Baza	VA	1.3	Bovidae	enamel	bulk	21.2	KU
BB.VM.03	Baza	VA	1.3	Bovidae	dentine	bulk	19.9	KU
BB.VM.01	Baza	VA	1.3	Cervidae	enamel	bulk	20.3	KU
BB.VM.01	Baza	VA	1.3	Cervidae	dentine	bulk	19.5	KU
BB.VM.02	Baza	VA	1.3	Cervidae	enamel	bulk	22.8	KU
BB.VM.02	Baza	VA	1.3	Cervidae	dentine	bulk	18.6	KU
BB.VM.04	Baza	VA	1.3	Equidae	enamel	bulk	18.4	KU
BB.BL.01	Baza	BL	1.25	Hippopotamidae	enamel	bulk	14.6	KU
BB.BL.01	Baza	BL	1.25	Hippopotamidae	dentine	bulk	13.1	KU
BB.CSC.01	Baza	PL	0.8	Proboscidean	dentine	bulk	16.6	KU
BB.PL.01	Baza	PL	0.8	Equidae	enamel	bulk	17.6	KU
BB.PL.02	Baza	PL	0.8	Rhinocerotidae	enamel	bulk	18.9	KU
BB.PL.02	Baza	PL	0.8	Rhinocerotidae	dentine	bulk	15.6	KU

*Number in parentheses for serial samples represents distance in mm from base of tooth.

Table 2.2. Results of statistical comparisons of bulk enamel $\delta^{18}\text{O}$ between taxonomic groups *

	Anthracotheridae	Artiodactyla indet.	Bovidae	Cervidae	Equidae	Hippopotamidae	Pliohyracidae	Rhinocerotidae	Suidae
Anthracotheridae	1	-	-	-	-	-	-	-	-
Artiodactyla indet.	0.095 <i>-1.936</i>	1	0.666 <i>-0.442</i>	0.39 <i>-0.886</i>	0.836 <i>0.208</i>	0.019 <i>3.204</i>	-	0.01 <i>3.466</i>	0.06 <i>2.242</i>
Bovidae	0.03 <i>-2.152</i>	0.859 <i>-0.184</i>	1	0.327 <i>-1.014</i>	0.461 <i>0.743</i>	0.001 <i>4.319</i>	-	0.001 <i>4.102</i>	0.012 <i>2.956</i>
Cervidae	0.022 <i>-2.191</i>	0.506 <i>-0.739</i>	0.346 <i>-0.957</i>	1	0.051 <i>2.002</i>	0.016 <i>2.76</i>	-	0.033 <i>2.36</i>	0.069 <i>1.967</i>
Equidae	0.002 <i>-2.367</i>	0.627 <i>-0.518</i>	0.341 <i>-0.952</i>	0.154 <i>-1.426</i>	1	0.002 <i>3.286</i>	-	0.025 <i>2.321</i>	0.093 <i>1.719</i>
Hippopotamidae	0.4 <i>-0.889</i>	0.071 <i>-1.938</i>	0.014 <i>-2.37</i>	0.018 <i>-2.309</i>	0.014 <i>-2.321</i>	1	-	0.28 <i>-1.212</i>	0.194 <i>-1.498</i>
Pliohyracidae	0.333 <i>-1.549</i>	1 <i>0</i>	0.758 <i>-0.323</i>	0.659 <i>-0.548</i>	0.932 <i>-0.085</i>	0.2 <i>-1.732</i>	1	-	-
Rhinocerotidae	0.133 <i>-1.852</i>	0.032 <i>-2.205</i>	0.002 <i>-2.764</i>	0.013 <i>-2.425</i>	0.012 <i>-2.418</i>	0.629 <i>-0.707</i>	0.133 <i>-1.852</i>	1	0.496 <i>-0.724</i>
Suidae	0.133 <i>-1.852</i>	0.063 <i>-1.96</i>	0.014 <i>-2.339</i>	0.042 <i>-2.062</i>	0.091 <i>-1.696</i>	0.229 <i>-1.249</i>	0.267 <i>-1.389</i>	0.686 <i>-0.577</i>	1

*Results from Student's t-test are shown in the shaded upper right part of the table; results of non-parametric Mann-Whitney U tests are shown in lower left. Two-tail p -values are shown as upper number in each cell (with differences in means that are significant at a 95% confidence level highlighted in bold). Lower, italicized number in each cell represents t -statistic (for Student's t -test) or Z -statistic (for Mann-Whitney U test).

Table 2.3. Results of statistical comparisons of bulk enamel $\delta^{18}\text{O}$ between localities*

	CC	LM	AQ	LC	LB	MS	LA	VA/BL/BP	PL	VM	AM	SH
CC	1	0.77 -0.296	0.575 -0.567	0.268 -1.161	0.042 -2.597	<0.001 -4.851	0.078 -1.941	0.807 -0.249	–	0.298 -1.087	0.088 -1.872	0.209 1.436
LM	0.738 -0.341	1	0.863 -0.174	0.613 -0.517	0.015 -2.698	0.003 -3.31	0.325 -1.02	0.974 -0.033	–	0.608 -0.525	0.338 -0.993	0.144 1.535
AQ	0.633 -0.507	0.944 -0.089	1	0.664 -0.44	0.006 -3.02	0.002 -3.491	0.329 -0.999	0.923 0.097	–	0.656 -0.452	0.341 -0.973	0.078 1.844
LC	0.374 -0.99	0.549 -0.68	0.858 -0.222	1	0.146 -1.612	0.024 -2.61	0.424 -0.871	0.699 0.399	–	0.985 -0.02	0.463 -0.793	0.09 2.016
LB	0.056 -1.952	0.046 -2.018	0.036 -2.1	0.352 -1.066	1	0.666 0.453	0.341 1.022	0.064 2.055	–	0.153 1.577	0.338 1.028	0.016 2.949
MS	0.001 -3.104	0.002 -2.973	0.001 -3.1	0.034 -2.163	0.607 -0.59	1	0.161 1.514	0.019 2.65	–	0.031 2.481	0.161 1.514	0.001 4.542
LA	0.077 -1.859	0.296 -1.144	0.31 -1.091	0.629 -0.707	0.381 -1.033	0.209 -1.389	1	0.44 0.812	–	0.488 0.748	0.98 0.027	0.076 2.142
VA/ BL/ BP	0.601 -0.586	0.877 -0.198	0.836 -0.239	1 0	0.138 -1.571	0.016 -2.383	0.517 -0.798	1	–	0.696 -0.403	0.453 -0.789	0.242 1.244
PL	0.273 -1.289	0.476 -0.85	0.443 -0.873	0.267 -1.389	0.143 -1.667	0.036 -2.126	0.2 -1.732	0.333 -1.171	1	–	–	–
VM	0.454 -0.849	0.703 -0.453	0.642 -0.519	1 0	0.257 -1.279	0.034 -2.163	0.4 -1.061	0.927 -0.189	0.267 -1.389	1	0.521 -0.689	0.113 1.814
AM	0.161 -1.521	0.439 -0.875	0.452 -0.829	0.857 -0.354	0.381 -1.033	0.145 -1.574	1 -0.218	0.383 -1.026	0.2 -1.732	0.857 -0.354	1	0.082 2.091
SH	0.075 -1.777	0.143 -1.529	0.121 -1.594	0.111 -1.715	0.607 -0.59	0.002 -2.87	0.036 -2.236	0.268 -1.218	0.857 -0.387	0.19 -1.47	0.071 -1.938	1

*Presentation as in Table 2.2.

Table 2.4. Estimates of precipitation $\delta^{18}\text{O}_w$ and MAT based on equid tooth enamel $\delta^{18}\text{O}_p$ *

Locality	Age (Ma)	N	$\delta^{18}\text{O}_p$	s.e.	$\delta^{18}\text{O}_w$	s.e	MAT	s.e
TERUEL BASIN	7.15-4.3	25	19.5	0.3	-5.5	3.2	14.6	7.1
Los Mansuetos	7.2-7.1	10	19.0	0.4	-5.0	3.2	15.7	7.1
Concud	7.2-7.1	5	19.7	0.4	-5.2	3.2	15.3	7.1
El Arquillo	6.4-6.1	9	18.9	0.5	-6.3	3.2	13.0	7.1
La Calera	4.3	1	20.0		-4.8	3.2	16.1	7.0
Venta del Moro	5.9	1	21.9		-2.2	3.4	21.5	7.2
FORTUNA BASIN	6.1-5.6	11	22.8	0.4	-1.4	3.5	23.2	7.4
Librilla	6.3-5.9	2	23.2	0.6	-0.5	3.6	25.1	7.6
Molina de Segura	6.6-6.0	8	22.7	0.4	-1.1	3.5	23.6	7.4
La Alberca	5.6	1	19.8		-5.1	3.2	15.5	7.0
BAZA BASIN	1.3-0.8	4	18.9	0.6	-6.4	3.2	12.9	7.2
VA, BP, BL	1.25-1.3	3	19.3	0.6	-5.8	3.2	14.1	7.2
Puerto Lobo	0.8	1	17.6		-8.1	3.0	9.2	7.0

*These values were calculated using RMA regression (Equations 5 and 10). The equivalent values for OLS regression can be calculated with Equations 3 and 8.

Chapter 3: Wet climate in southeast Spain during the Messinian Salinity Crisis

Samuel D. Matson^{1*}, Lluís Gibert², Gary R. Scott² and David L. Fox¹

¹*Department of Geology and Geophysics, University of Minnesota, 108 Pillsbury Hall, 310 Pillsbury Drive SE, Minneapolis, MN 55455-0231, USA*

²*Berkeley Geochronology Center, 2455 Ridge Road, Berkeley, CA 94709-1211, USA*

**present address: Department of Geosciences, Boise State University, 1910 University Drive, Boise, Idaho 83725-1535, USA*

Prepared for submission to *Geology*

We use the stable carbon ($\delta^{13}\text{C}$) and oxygen ($\delta^{18}\text{O}$) isotope composition of lacustrine, palustrine, and pedogenic carbonates to reconstruct continental paleoenvironment during the Messinian Salinity Crisis (latest Miocene, 5.9 – 5.3 Ma) in the intramontane Baza Basin (Betic Cordillera, southeast Spain). A transition from dolomite- and calcite-rich palustrine and distal alluvial fan sediments to lacustrine diatomites and calcite-rich limestones is accompanied by a decrease in both $\delta^{13}\text{C}$ and $\delta^{18}\text{O}$, reflecting increased lake level under a wetter climate. The mean $\delta^{18}\text{O}$ of latest Miocene lacustrine calcite is distinct from that of modern closed-basin lakes in the Iberian Peninsula, and likely represents overflow or through-flow lake conditions with inflow waters derived from the surrounding Betic mountains. We propose that strengthened storm tracks from the Atlantic Ocean over southern Europe combined with orographic uplift of air masses along the Betic Cordillera resulted in enhanced precipitation and runoff in southeast Spain during the Messinian Salinity Crisis.

1. Introduction

The extreme desiccation of the Mediterranean Basin during the Messinian Salinity Crisis (MSC) in the latest Miocene was one of the most rapid and dramatic episodes of oceanic change during the Neogene. During this event, combined tectonic and glacioeustatic (Hodell et al., 1996; Krijgsman et al., 1999) isolation of the Mediterranean from the Atlantic coupled with a regionally negative hydrologic budget led to a Mediterranean sea level fall of 1500 m or more (Meijer and Krijgsman, 2005; Cita, 2006), deposition of up to 10^6 km³ of evaporites (Hsü et al., 1973, 1977), deep incision of river canyons (Barber, 1981; Lofi et al., 2005), widespread extinction of benthic and planktonic foraminifera (Cita, 1976; Kouwenhoven et al., 1999), and interchange of African and Eurasian mammal faunas, presumably across emergent land bridges (Agustí et al., 2006; van der Made et al., 2006; Minwer-Barakat et al., 2009). The marine record of the MSC indicates this event had severe environmental and ecological consequences (Andersen et al., 2001; Pierre et al., 2002; Pierre and Rouchy, 2004; Rouchy and Caruso, 2006), but our understanding of the consequences of the MSC for terrestrial ecosystems in the Mediterranean region remains poorly understood. While some records imply warm and arid circum-Mediterranean terrestrial climate throughout the MSC (Bertini et al., 1998; Bertini, 2006; Fauquette et al., 2006; Costeur et al., 2007), other studies suggest the desiccated Mediterranean Basin may have actually led to enhanced precipitation in some parts of this region (Griffin, 2002; Willett et al., 2006; Murphy et al., 2009).

We use the stable carbon and oxygen isotopic composition ($\delta^{13}\text{C}$ and $\delta^{18}\text{O}$) of pedogenic, palustrine, and lacustrine carbonates to reconstruct continental environments

during the MSC in the Baza Basin (southeast Spain), which forms the eastern part of the largest of the intramontane basins of the Betic Cordillera (Figure 3.1). The Baza Basin (>3000 km²) was tectonically isolated from the Mediterranean Sea during the Late Miocene and received non-marine sediments under primarily endorheic conditions until the Middle Pleistocene, when neotectonic uplift combined with stream piracy led to the current regime of fluvial incision and exposed a fossiliferous record of Miocene-Pleistocene lacustrine, palustrine, fluvial, and deltaic sediments (Calvache and Viseras, 1997).

2. Methods and Results

We measured stratigraphic sections and collected carbonate-rich hand samples at 1–5 m intervals from two localities – Botardo (BO) and Barranco de las Lumbres (LL) – at the northeast margin of the Baza Basin (Figure 3.1). The BO and LL sections are geographically separated by <10 km and can be correlated lithostratigraphically based on an upward transition from interbedded cross-stratified sandstone, siltstone, and micritic carbonate mudstone with root traces, which we interpret as alternating distal alluvial fan and palustrine facies, to interbedded diatomite and massive carbonate with fossil gastropods, which we interpret as lacustrine facies. The top of our measured section at BO includes the micromammal fossil localities Botardo-1 and Botardo-2 (Figure 3.2), which correspond to the Turolian-Ruscinian biostratigraphic boundary (MN-13, Intrazone 13/14) and indicate a minimum age of ca. 5.3 Ma for our composite section (Martín Suárez, 1988; Ruiz-Bustos, 1999, 2007). A paleomagnetic reversal from normal

to reverse polarity in the lower part of the LL section, which we interpret as the boundary between chrons C3An.1n and C3r (5.894 Ma; Cande and Kent, 1995), constrains the maximum age of our composite section to ca. 5.9 Ma. Our composite section overlaps in time with the MSC, which has been dated to 5.96 – 5.33 Ma through high-resolution magneto-, bio-, and cyclostratigraphic analyses (Krijgsman et al., 1999).

We determined the mineralogical composition of the samples through powder X-ray diffraction (XRD) on a Rigaku Miniflex diffractometer at the University of Minnesota (UMN), using CuK_α radiation from 5° to $65^\circ 2\theta$ with a 0.02° step and 0.6 s count time. The XRD results were verified through scanning electron microscopy (SEM) and energy-dispersive X-ray spectroscopy (EDS) for selected samples using a Hitachi TM-1000 tabletop microscope at the Limnological Research Center at UMN. While samples from lacustrine facies at BO and the upper part of LL are dominated by calcite and amorphous silica (diatomite), samples from the alluvial/palustrine facies in the lower part of LL contain calcite, dolomite, quartz and minor halite (Figure 3.2E). We created 17 mixtures of standard calcite, dolomite, and quartz powders with calcite-dolomite molar ratios between 0 and 1, used Jade 6 software to measure the area of the three highest calcite and dolomite peaks for the mixtures and for the BO and LL samples, and then used reduced major axis regression (RMA) to establish a predictive relationship between XRD peak area and percent calcite vs. dolomite. Estimated error for percent calcite based on repeated XRD of the standard powders is approximately $\pm 3\%$. Percent calcite increases upsection from approximately 34% in the alluvial/palustrine interval at LL to greater than 99% in the lacustrine facies at both LL and BO (Figure 3.2A).

We analyzed carbonate $\delta^{13}\text{C}$ and $\delta^{18}\text{O}$ for the BO/LL samples at the UMN Stable Isotope Laboratory. Powder microsamples of hand samples were collected using a 0.5 mm bit in a rotary drill, roasted *in vacuo* at 400 °C for 1 h, and the $\delta^{13}\text{C}$ and $\delta^{18}\text{O}$ of CO_2 produced by reaction with 100% H_3PO_4 at 70°C for 5 min in a Kiel II automatic carbonate preparation device was measured with a Finnigan MAT 252 isotope ratio mass spectrometer. Results were normalized to Vienna Pee Dee Belemnite (VPDB) and analytical precision ($<0.1\text{‰}$ for both $\delta^{13}\text{C}$ and $\delta^{18}\text{O}$) was determined based on replicate analyses of multiple aliquots of international standards (NBS-18, NBS-19) during all sample sequences. We assume dolomite powders reacted completely as all samples showed no visible reaction after 5 min, and repeated analysis ($n = 10$) of pure, stoichiometric dolomite standard powders under reaction times varying from 5 to 240 min showed low variability ($s.d. = 0.03\text{‰}$ for $\delta^{13}\text{C}$; $s.d. = 0.12\text{‰}$ for $\delta^{18}\text{O}$) and no relationship between reaction time and isotopic composition (ordinary least-squares regression or OLS, $p = 0.38$ for $\delta^{13}\text{C}$, $p = 0.27$ for $\delta^{18}\text{O}$). For mixed calcite-dolomite samples, we analyzed $\delta^{13}\text{C}$ and $\delta^{18}\text{O}$ for bulk carbonate and also for separate powder aliquots that were treated with 0.1M ethylenediaminetetraacetic acid (EDTA) solution for 30 min to remove calcite (verified by XRD). We then used the $\delta^{13}\text{C}$ and $\delta^{18}\text{O}$ of the mixed and dolomite-only samples along with percent calcite (determined through XRD) in a linear mixing model to calculate the $\delta^{13}\text{C}$ and $\delta^{18}\text{O}$ of the calcite endmember. The isotopic and stratigraphic data for the BO and LL samples are presented in Table 3.1. The samples show a statistically significant stepwise decrease upsection in $\delta^{13}\text{C}$ (Figure 3.2B) from the alluvial/palustrine beds at LL ($\bar{x} = -5.0\text{‰}$, $s.d. = 0.55\text{‰}$, $n = 18$ for bulk

carbonate; $\bar{x} = -5.3\text{‰}$, $s.d. = 0.51\text{‰}$, $n = 5$ for calcite) to the lacustrine beds at LL and BO ($\bar{x} = -8.5\text{‰}$, $s.d. = 1.07\text{‰}$, $n = 26$ for bulk carbonate; $\bar{x} = -8.6\text{‰}$, $s.d. = 0.98\text{‰}$, $n = 24$ for calcite) for both bulk carbonate (Mann-Whitney U or MW $p < 0.001$) and calcite (MW $p = 0.001$). The samples also show a significant decrease in $\delta^{18}\text{O}$ upward through the BO/LL composite section (Figure 3.2C) for both bulk carbonate (-0.07‰/m ; OLS $p < 0.001$) and for calcite (-0.04‰/m ; OLS $p = 0.004$). Mean $\delta^{18}\text{O}$ of the lacustrine facies at BO and LL ($\bar{x} = -7.0\text{‰}$, $s.d. = 0.68\text{‰}$, $n = 26$ for bulk carbonate; $\bar{x} = -7.1\text{‰}$, $s.d. = 0.65\text{‰}$, $n = 24$ for calcite) is less variable and significantly lower (MW $p < 0.001$ for bulk carbonate; MW $p = 0.028$ for calcite) than that of the alluvial/palustrine facies at LL ($\bar{x} = -5.4\text{‰}$, $s.d. = 0.96\text{‰}$, $n = 18$ for bulk carbonate; $\bar{x} = -6.2\text{‰}$, $s.d. = 0.77\text{‰}$, $n = 5$ for calcite), while mean $\delta^{18}\text{O}$ of the lacustrine facies at LL is indistinct from that of BO (MW $p = 0.061$ for bulk carbonate; MW $p = 0.209$, Student's t -test $p = 0.120$ for calcite).

3. Interpretation and Discussion

Several observations of the data presented here indicate a transition to a wet climate in SE Spain during the terminal Miocene. First, the change from alluvial and palustrine facies in the lower part of the BO/LL composite section, to lacustrine facies (massive calcite and diatomites) in the upper part of the section, is consistent with an increase in lake level due to either basin subsidence or increased precipitation. Second, the micritic dolomite and minor halite in the alluvial/palustrine facies is consistent with an arid or semi-arid climate, while the nearly pure calcite in the lacustrine facies indicates more humid conditions. Third, SEM and EDS analysis of sediments from three

stratigraphic levels in the lacustrine sequence at BO and LL (Figures 3.2B, 3.2C, 3.2D) with much higher $\delta^{13}\text{C}$ and $\delta^{18}\text{O}$ than stratigraphically adjacent beds reveals clasts containing sponge spicules, bryozoans, recrystallized coccolithophores, and minor barite. We interpret these isotopic and sedimentological data as reflecting increased detrital input from Mesozoic marine carbonates in the surrounding mountains resulting from periods of higher precipitation and enhanced runoff.

A fourth observation consistent with a transition to wetter climate is the shift to more negative $\delta^{13}\text{C}$ in the lacustrine carbonate, which can be explained by increased runoff and/or more open lake conditions. The $\delta^{13}\text{C}$ of primary lacustrine carbonate is determined by the $\delta^{13}\text{C}$ of dissolved inorganic carbon (DIC) in lake water, which is related to the $\delta^{13}\text{C}$ of lake source waters, primary productivity, and isotopic exchange with atmospheric CO_2 (which is a function of water residence time). More humid conditions can cause low $\delta^{13}\text{C}$ in lacustrine DIC (and hence, primary calcite) by delivering more ^{13}C -depleted DIC from terrestrial vegetation via enhanced runoff and/or decreasing water residence time (Talbot, 1990). Low $\delta^{13}\text{C}$ values may also be related to decreased primary productivity in lake surface waters, though in many eutrophic lakes microbially mediated decomposition of organic matter can serve as a ^{13}C -depleted source to the DIC reservoir (Hollander and Smith, 2001). Our data are not sufficient to rule out changes in primary productivity and/or decomposition. Finally, the decrease in calcite $\delta^{18}\text{O}$ ($\delta^{18}\text{O}_{\text{cal}}$) upsection at BO/LL can also be explained by a transition to wetter climate. The $\delta^{18}\text{O}$ of freshwater calcite is determined by the temperature of mineral precipitation (negative correlation) and the $\delta^{18}\text{O}$ of the water from which it precipitates (positive

correlation). While the decrease in $\delta^{18}\text{O}_{\text{cal}}$ upsection at BO/LL can be interpreted as a temperature increase, a more likely explanation in light of the sedimentological and mineralogical evidence is that it reflects decreasing evaporative enrichment in ^{18}O of surface waters under increasingly wet conditions.

To better understand the hydroclimatic implications of the $\delta^{18}\text{O}$ values for lacustrine calcite in the BO/LL section, we compare them to published data for Holocene lacustrine $\delta^{18}\text{O}_{\text{cal}}$ in Spain, and with predicted $\delta^{18}\text{O}_{\text{cal}}$ in equilibrium with $\delta^{18}\text{O}$ and temperature reported for modern waters across the Iberian Peninsula (Table 3.2), calculated using the equilibrium calcite-water-temperature equation of Kim and O'Neil (1997):

$$10^3 \ln[(\delta^{18}\text{O}_{\text{cal}} + 10^3)/(\delta^{18}\text{O}_{\text{water}} + 10^3)] = 18.03(10^3/T) - 32.42 \quad (1)$$

where T is temperature (Kelvin) and $\delta^{18}\text{O}_{\text{cal}}$ and $\delta^{18}\text{O}_{\text{water}}$ are relative to Vienna Standard Mean Ocean Water (VSMOW) (Figure 3.3A). A summary of the published Holocene data is presented in Table 3.2. Mean $\delta^{18}\text{O}_{\text{cal}}$ (-7.1‰ VPDB) from BO/LL is significantly lower than all observed and predicted $\delta^{18}\text{O}_{\text{cal}}$ for modern closed lakes (MW $p < 0.038$), and is also significantly lower (based on pairwise MW comparisons with $\alpha = 0.05$) than mean observed and predicted $\delta^{18}\text{O}_{\text{cal}}$ for modern open lakes, precipitation, runoff, and groundwater at most (17 of 18) low-elevation sites (≤ 300 masl). The mean $\delta^{18}\text{O}_{\text{cal}}$ from BO/LL is in the upper end of the range of predicted $\delta^{18}\text{O}_{\text{cal}}$ from modern groundwater in the Baza Basin and surrounding Sierra Nevada, Cazorla, and Segura mountains (-12.8 to -6.2‰; Cruz-San Julian et al., 1992; Kohfahl et al., 2008b), and is indistinct from predicted $\delta^{18}\text{O}_{\text{cal}}$ for modern winter precipitation in the Baza Basin (MW $p = 0.678$;

Cruz-San Julian et al., 1992) and for runoff in the Sierra Nevada (MW $p = 0.862$; Kohfahl et al., 2008b) at a mean elevation (994 masl) comparable to that of the present elevation of BO/LL (1030 masl).

The similarity between $\delta^{18}\text{O}_{\text{cal}}$ at BO/LL and that for environmental waters at modern elevations near the Baza Basin is surprising since latest Tortonian marine deposits and late Pleistocene fluvial incision in the Guadix-Baza Basin imply that its Late Miocene elevation was probably much lower than today (Fernández et al., 1996; Calvache and Viseras, 1997; Soria et al., 1998; García Aguilar and Martín, 2000). Indeed, mean $\delta^{18}\text{O}_{\text{cal}}$ for the nearby, lower-elevation sites of Murcia (62 masl, predicted $\delta^{18}\text{O}_{\text{cal}}$ for precipitation = -6.3‰ VPDB; IAEA, 2010) and Laguna Zoñar (300 masl, observed $\delta^{18}\text{O}_{\text{cal}} = +1.3\text{‰}$ VPDB, predicted $\delta^{18}\text{O}_{\text{cal}}$ for lake water = $+2.2\text{‰}$ VPDB; Valero-Garcés et al., 2003; Martín-Puertas et al., 2009) is significantly higher than that of BO/LL (MW $p < 0.001$). However, uplift of the surrounding Sierra Nevada and Sierra de los Filabres had likely already begun by the mid-late Tortonian (Johnson et al., 1997; Sanz de Galdeano and López-Garrido, 1999; Braga et al., 2003; Sanz de Galdeano and Alfaro, 2004). Today, mean annual precipitation in the Sierra Nevada (~ 975 mm; Simón et al., 2000; Casas et al., 2006) is 2 – 3 times that of the Guadix-Baza and Granada Basins below (300 – 500 mm; Anadón et al., 1986; NCDC, 2010). The $\delta^{18}\text{O}$ values from BO/LL suggest that the surrounding Betic ranges were already at relatively high elevations and were an important source of input to lake water in the Baza Basin during the latest Miocene.

Most studies suggest that the Baza Basin was endorheic from the Late Miocene until the mid-Pleistocene (Sanz de Galdeano and Vera, 1992; Calvache and Viseras, 1997; Soria et al., 1998). The isotopic data from lacustrine carbonate at BO/LL are not consistent with fully endorheic conditions; rather, they indicate an overflow or through-flow lake. Modern closed-basin lakes typically display covariance between $\delta^{13}\text{C}$ and $\delta^{18}\text{O}$, with a correlation coefficient > 0.8 (Talbot, 1990). While $\delta^{13}\text{C}$ and $\delta^{18}\text{O}$ for the alluvial/palustrine facies at BO/LL covary strongly ($R^2 = 0.98$), the $\delta^{13}\text{C}$ - $\delta^{18}\text{O}$ covariance in the lacustrine facies is much weaker ($R^2 = 0.55$). Further, while the $\delta^{18}\text{O}_{\text{cal}}$ from BO/LL is ca. 3 – 12‰ lower than that for modern Spanish closed-basin lakes, it is much more similar to modern open lakes, precipitation, runoff, and groundwater, especially at higher elevations (Figure 3.3A). If the $\delta^{18}\text{O}$ of Late Miocene precipitation and runoff was generally similar to today, then the isotopic data from BO/LL are consistent with little to no evaporative ^{18}O -enrichment (suggesting short residence time) of lake water.

The lacustrine $\delta^{18}\text{O}_{\text{cal}}$ at BO/LL can be used to predict the $\delta^{18}\text{O}$ of equilibrium lake water ($\delta^{18}\text{O}_{\text{lw}}$) over a range of temperature (using Equation 1), which can in turn be used to predict the $\delta^{18}\text{O}$ of lake input water ($\delta^{18}\text{O}_i$) over a range of temperature, relative humidity (h), and ratio of outflow (Q_o) to inflow (Q_i) fluxes (Figures 3.3B and 3.3C) by rearranging the steady-state equation for lake water derived by Gat (1995):

$$\delta^{18}\text{O}_i = \delta^{18}\text{O}_{\text{lw}} - [(1 - h)(\varepsilon_{\text{eq}} + \varepsilon_{\text{kin}})]/[h + (1 - h)(1 - Q_o/Q_i)^{-1}] \quad (2)$$

where ε_{eq} is the equilibrium fractionation enrichment factor and can be calculated as a function of temperature (Majoube, 1971; Li et al., 2008):

$$\varepsilon_{\text{eq}} = 10^3[\exp(1137T^2 - 0.4156T^1 - 0.00207) - 1] \quad (3)$$

and ϵ_{kin} is the kinetic fractionation enrichment factor, which can be calculated as a function of h and the ratio of isotopic diffusivities ($\alpha_{\text{kin}} = 0.994$ for $^{18}\text{O}/^{16}\text{O}$; Merlivat and Jouzel, 1979; Li et al., 2008):

$$\epsilon_{\text{kin}} = 10^3(1 - h)(1/\alpha_{\text{kin}} - 1) \quad (4)$$

The most ^{18}O -depleted surface waters reported for modern Spain come from high elevations (>1100 masl) in the Betic Cordillera and have $\delta^{18}\text{O}$ values of -9.5 to -10‰ VSMOW (Kohfahl et al., 2008b; Vandenschrick et al., 2002). Since large ice sheets did not develop in the northern hemisphere until the mid-Pliocene (Ravelo et al., 2004), ocean water (hence, precipitation and runoff) during the Late Miocene was likely ~1‰ lighter than today (Lear et al., 2000; Zachos et al., 2001). If we consider -11‰ VSMOW as a cutoff for the most ^{18}O -depleted surface waters in southern Spain during the Late Miocene, then BO/LL lake water should be ≥ -11 ‰ (shaded areas in Figures 3.3B and 3.3C). Mean annual temperature on the Iberian Peninsula during the Late Miocene was likely higher than today (van Dam and Reichart, 2009), and potentially as high as ~23 °C in southern Spain (Matson and Fox, 2010). However, even for very high temperature (30°C, Figure 3.3C), applying Equation 2 to mean lacustrine $\delta^{18}\text{O}_{\text{cal}}$ at BO/LL predicts either unreasonably low $\delta^{18}\text{O}_i$ (< -18‰ VSMOW) or relatively high h (> 44%) for fully closed-basin conditions ($Q_o/Q_i \sim 0$).

4. Conclusions and Implications

Our reconstruction of continental environments in the Baza Basin during the MSC indicates highstand for an overflow or throughflow lake whose input waters were derived

from relatively high elevations, consistent with a wet climate in SE Spain during this time. Previous studies have suggested that enhanced vertical movement of air masses over the desiccated Mediterranean Basin during the MSC resulted in local positive precipitation anomalies, especially for high elevations and for eastern parts of the Mediterranean region (Griffin, 2002; Willett et al., 2006; Murphy et al., 2009). Today the majority of precipitation in southern Spain is derived from the Atlantic Ocean, and decadal-scale wet periods coincide with a negative phase of the North Atlantic Oscillation, in which a stronger Azores High and weaker Icelandic Low steer moisture over southern Europe from the Atlantic Ocean. While climate models predict increased air subsidence and higher evaporation:precipitation over SE Spain during the MSC, they also predict strengthened winter storm tracks over southern Europe due to a southward shift in the latitude of westerly zonal winds arriving from the Atlantic (Murphy et al., 2009). We propose that orographic uplift of these air masses along the Betic Cordillera during the MSC was sufficient to induce local condensation and precipitation, despite the greater air subsidence predicted by climate models for SE Iberia in general. This hypothesis can be tested by comparing our $\delta^{18}\text{O}$ results with similar data from contemporaneous lacustrine deposits in other nearby intramontane basins (e.g., Granada Basin; Martín-Suárez et al., 1998; García-Alix et al., 2008, 2008b) and from other latest Miocene Spanish basins outside of the Betic Cordillera (e.g., Teruel Basin; Alonso-Zarza and Calvo, 2000; van Dam et al., 2001). Further, since the deuterium-excess (d) of modern precipitation derived from the Atlantic Ocean is much lower than that derived from the Mediterranean (Cruz-San Julian et al., 1992) any proxy for d in past meteoric

water (e.g., parallel analyses of lacustrine carbonate $\delta^{18}\text{O}$ and compound-specific stable hydrogen isotopes in occluded organic matter; Henderson and Shuman, 2009) can be used to verify an Atlantic origin for the precipitation and surface water flowing into the BO/LL lake.

Acknowledgements

This research was supported by a GSA Graduate Student Research Grant and two UMN Dept. of Geology and Geophysics summer research grants to Matson. We thank A. Myrbo, K. Brady, A. Noren, E. Ito, K. Kleinspehn, K. McNulty, S. Morón, and R. Knurr (UMN), T. Hickson, L. Lamb, and K. Theissen (University of St. Thomas) and N. Murphy (Lawrence Berkeley National Laboratory) for analytical assistance and/or thoughtful discussions. Though their suggestions improved the quality of this manuscript, any errors remaining in its final form are the responsibility of the authors alone. We dedicate this paper to the memory of Dr. Josep Gibert Clols, whose legacy of work on Iberian paleontology remains an inspiration for continued research.

References Cited

Agustí, J., Garcés, M., and Krijgsman, W., 2006, Evidence for African-Iberian exchanges during the Messinian in the Spanish mammalian record: *Palaeogeography, Palaeoclimatology, Palaeoceanography*, v. 238, p. 5–14.

- Alonso-Zarza, A.M. and Calvo, J.P., 2000, Palustrine sedimentation in an episodically subsiding basin: the Miocene of the northern Teruel Graben (Spain): *Palaeogeography, Palaeoclimatology, Palaeoceanography*, v. 160, p. 1–21.
- Anadón, P., De Deckker, P., and Julià, R., 1986, The Pleistocene lake deposits of the NE Baza Basin (Spain): salinity variations and ostracod succession: *Hydrobiologia*, v. 143, p. 199–208.
- Andersen, N., Paul, H.A., Bernasconi, S.M., McKenzie, J.A., Behrens, A., Schaeffer, P., and Albrecht, P., 2001, Large and rapid climate variability during the Messinian salinity crisis: Evidence from deuterium concentrations of individual biomarkers: *Geology*, v. 29, p. 799–802.
- Andrews, J.E., Pedley, M., and Dennis, P.F., 2000, Palaeoenvironmental records in Holocene Spanish tufas: a stable isotope approach in search of reliable climatic archives: *Sedimentology*, v. 47, p. 961–978.
- Barber, P.M., 1981, Messinian subaerial erosion of the Proto-Nile delta: *Marine Geology*, v. 44, p. 253–272.
- Bertini, A., 2006, The northern Apennines palynological record as a contribute for the reconstruction of the Messinian palaeoenvironments: *Sedimentary Geology*, v. 188–189, p. 235–258.
- Bertini, A., Londeix, L., Maniscalco, R., Di Stefano, A., Suc, J.-P., Clauzon, G., Gautier, F., and Grasso, M., 1998, Paleobiological evidence of depositional conditions in the Salt Member, Gessoso-Solfifera Formation (Messinian, Upper Miocene) of Sicily, *Micropaleontology*, v. 44, p. 413–433.

- Braga, J.C., Martín, J.M., and Quesada, C., 2003, Patterns and average rates of late Neogene-Recent uplift of the Betic Cordillera, SE Spain: *Geomorphology*, v. 50, p. 3–26.
- Calvache, M.L. and Viseras, C., 1997, Long-term control mechanisms of stream piracy processes in southeast Spain: *Earth Surface Processes and Landforms*, v. 22, p. 93–105.
- Cande, S.C. and Kent, D.V., 1995, Revised calibration of the geomagnetic polarity timescale for the late Cretaceous and Cenozoic: *Journal of Geophysical Research*, v. 100, p. 6093–6095.
- Casas, J.J., Gessner, M.O., Langton, P.H., Calle, D., Descals, E., and Salinas, M.J., 2006, Diversity of patterns and processes in rivers of eastern Andalusia: *Limnetica*, v. 25, p. 155–170.
- Cerling, T.E., Harris, J.M., MacFadden, B.J., Leakey, M.G., Quade, J., Eisenmann, V., and Ehleringer, J.R., 1997, Global vegetation change through the Miocene/Pliocene boundary: *Nature*, v. 389, p. 153–158.
- Cita, M.B., 1976, Biodynamic effects of the Messinian salinity crisis on the evolution of planktonic foraminifera in the Mediterranean: *Palaeogeography, Palaeoclimatology, Palaeoceanography*, v. 20, p. 23–42.
- Cita, M.B., 2006, Exhumation of Messinian evaporites in the deep-sea and creation of deep anoxic brine-filled collapsed basins: *Sedimentary Geology*, v. 188–189, p. 357–378.

- Costeur, L., Montuire, S., Legendre, S., and Maridet, O., 2007, The Messinian event: What happened to the peri-Mediterranean mammalian communities and local climate?: *Geobios*, v. 40, p. 423–431.
- Cruz-San Julian, J., Araguas, L., Rozanski, K., Cardenal, J., Hidalgo, M.C., García-Lopez, S., Martínez-Garrido, J.C., Moral, F., and Olias, M., 1992, Sources of precipitation over South-Eastern Spain and groundwater recharge. An isotopic study: *Tellus*, v. 44B, p. 226–236.
- Fauquette, S., Suc, J.-P., Bertini, A., Popescu, S.-M., Warny, S., Taoufiq, N.B., Perez Villa, M.-J., Chikhi, H., Feddi, N., Subally, D., Clauzon, G., and Ferrier, J., 2006, How much did climate force the Messinian salinity crisis? Quantified climatic conditions from pollen records in the Mediterranean region: *Palaeogeography, Palaeoclimatology, Palaeoceanography*, v. 238, p. 281–301.
- Fernández, J., Soria, J., and Viseras, C., 1996, Stratigraphic architecture of the Neogene basins in the central sector of the Betic Cordillera (Spain): tectonic control and base-level changes, *in* Friend, P.F. and Dabrio, C., eds., *Tertiary Basins of Spain: The stratigraphic record of crustal kinematics*: Cambridge, Cambridge University Press, p. 353–365.
- García, C.M. and Niell, F.X., 1993, Seasonal change in a saline temporary lake (Fuente de Piedra, southern Spain): *Hydrobiologia*, v. 267, p. 211–223.
- García Aguilar, J.M. and Martín, J.M., 2000, Late Neogene to recent continental history and evolution of the Guadix-Baza Basin (SE Spain): *Revista de la Sociedad Geologica de España*, v. 13, p. 65–77.

- García-Alix, A., Minwer-Barakat, R., Martín Suárez, E., Freudenthal, M., and Martín, J.M., 2008, Late Miocene-Early Pliocene climatic evolution of the Granada Basin (southern Spain) deduced from the paleoecology of the micromammal associations: *Palaeogeography, Palaeoclimatology, Palaeoceanography*, v. 265, p. 214–225.
- García-Alix, A., Minwer-Barakat, R., Martín, J.M., Martín Suárez, E., and Freudenthal, M., 2008b, Biostratigraphy and sedimentary evolution of Late Miocene and Pliocene continental deposits of the Granada Basin: *Lethaia*, v. 41, p. 431–446.
- Gat, J.R., 1995, Stable isotopes of fresh and saline lakes, *in* Lerman, A., Imboden, D., and Gat, J., eds., *Physics and chemistry of lakes*: New York, Springer-Verlag, p. 139–165.
- González-Sampériz, P., Valero-Garcées, B.L., Moreno, A., Morellon, M., Navas, A., Machín, J., and Delgado-Huertas, A., 2008, Vegetation changes and hydrological fluctuations in the Central Ebro Basin (NE Spain) since the Late Glacial period: Saline lake records: *Palaeogeography, Palaeoclimatology, Palaeoecology*, v. 259, p. 157–181.
- Griffin, D.L., 2002, Aridity and humidity: two aspects of the late Miocene climate of North Africa and the Mediterranean: *Palaeogeography, Palaeoclimatology, Palaeoecology*, v. 182, p. 65–91.
- Henderson, A.K. and Shuman, B.N., 2009, Hydrogen and oxygen isotopic compositions of lake water in the western United States: *Geological Society of America Bulletin*, v. 121, p. 1179–1189.

- Hodell, D.A., Benson, R.H., Kent, D.V., Boersma, A., and Rakic-El Bied, K., 1996, Magnetostratigraphic, biostratigraphic, and stable isotope stratigraphy of an Upper Miocene drill core from the Salé Briqueterie (northwestern Morocco): A high-resolution chronology for the Messinian stage: *Paleoceanography*, v. 9, p. 835–855.
- Hollander, D.J. and Smith, M.A., 2001, Microbially mediated carbon cycling as a control on the $\delta^{13}\text{C}$ of sedimentary carbon in eutrophic Lake Mendota (USA): New models for interpreting isotopic excursions in the sedimentary record: *Geochimica et Cosmochimica Acta*, v. 65, p. 4321–4337.
- Hsü, K.J., Ryan, W.B.F., and Cita, M.B., 1973, Late Miocene desiccation of the Mediterranean: *Nature*, v. 242, p. 240–244.
- Hsü, K.J., Montadert, L., Beroulli, D., Cita, M.B., Erickson, A., Garrison, R.E., Kidd, R.B., Mèlières, F., Müller, C., and Wright, R., 1977, History of the Mediterranean salinity crisis: *Nature*, v. 267, p. 399–403.
- IAEA, 2010, Global Network of Isotopes in Precipitation (GNIP) data: 1961–2004: <http://isohis.iaea.org> (May 2010).
- Johnson, C., Harbury, N., and Hurford, A.J., 1997, The role of extension in the Miocene denudation of the Nevado-Filábride Complex, Betic Cordillera (SE Spain): *Tectonics*, v. 16, p. 189–204.
- Kim, S.-T and O’Neil, J.R., 1997, Equilibrium and nonequilibrium oxygen isotope effects in synthetic carbonates: *Geochimica et Cosmochimica Acta*, v. 61, p. 3461–3475.
- Kohfahl, C., Rodriguez, M., Fenk, C., Menz, C., Benavente, J., Hubberten, H., Meyer, H., Paul, L., Knappe, A., López-Geta, J.A., and Pekdeger, A., 2008a, Characterising flow

- regime and interrelation between surface-water and ground-water in the Fuente de Piedra salt lake basin by means of stable isotopes, hydrogeochemical and hydraulic data: *Journal of Hydrology*, v. 351, p. 170–187.
- Kohfahl, C., Sprenger, C., Benavente Herrera, J., Meyer, H., Fernández Chacón, F., and Pekdeger, A., 2008b, Recharge sources and hydrogeochemical evolution of groundwater in semiarid and karstic environments: A field study in the Granada Basin (Southern Spain): *Applied Geochemistry*, v. 23, p. 846–862.
- Kouwenhoven, T.J., Seidenkrantz, M.-S., and van der Zwaan, G.J., 1999, Deep-water changes: the near-synchronous disappearance of a group of benthic foraminifera from the Late Miocene Mediterranean: *Palaeogeography, Palaeoclimatology, Palaeoecology*, v. 152, p. 259–281.
- Krijgsman, W., Hilgen, F.J., Raffi, I., Sierro, F.J., and Wilson, D.S., 1999, Chronology, causes and progression of the Messinian Salinity Crisis: *Nature*, v. 400, p. 652–655.
- Lear, C.H., Elderfield, H., and Wilson, P.A., 2000, Cenozoic deep-sea temperatures and global ice volumes from Mg/Ca in benthic foraminiferal calcite: *Science*, v. 287, p. 269–272.
- Li, Hong-Chun, Xiao-Mei Xu, Teh-Lung Ku, Chen-Feng You, Buchenheim, H.P., and Peters, R., 2008, Isotopic and geochemical evidence of palaeoclimate changes in Salton Basin, California, during the past 20 kyr: 1. $\delta^{18}\text{O}$ and $\delta^{13}\text{C}$ records in lake tufa deposits: *Palaeogeography, Palaeoclimatology, Palaeoecology*, v. 259, p. 182–197.
- Lofi, J., Gorini, C., Berné, S., Clauzon, G., Dos Reis, A.T., Ryan, W.B.F., and Steckler, M., 2005, Erosional processes and paleo-environmental changes in the western Gulf

- of Lions (SW France) during the Messinian Salinity Crisis: *Marine Geology*, v. 217, p. 1–30.
- Luzón, A., Mayayo, M.J., and Pérez, A., 2009, Stable isotope characterization of co-existing carbonates from the Holocene Gallocanta lake (NE Spain): Palaeolimnological implications: *International Journal of Earth Sciences (Geologische Rundschau)*, v. 98, p. 1129–1150.
- Majoube, M., 1971, Fractionnement en oxygen-18 et en deuterium entre l'eau et sa vapor: *Journal de Chemie et de Physique*, v. 68, p. 1423–1426.
- Martín-Puertas, C., Valero-Garcés, B.L., Mata, M.P., González-Sampériz, P., Bao, R., Moreno, A., and Stefanova, V., 2008, Arid and humid phases in southern Spain during the last 4000 years: the Zoñar Lake record, *Córdoba: The Holocene*, v. 18, p. 907–921.
- Martín-Puertas, C., Valero-Garcés, B.L., Brauer, A., Mata, M.P., Delgado-Huertas, A., and Dulski, P., 2009, The Iberian-Roman Humid Period (2600–1600 cal yr BP) in the Zoñar Lake varve record (Andalucía, southern Spain): *Quaternary Research*, v. 71, p. 108–120.
- Martín-Suárez, E., 1988, Sucesiones de micromamíferos en la depresión de Guadix-Baza (España) [Ph.D. thesis]: Universidad de Granada, 241 p.
- Martín-Suárez, E., Oms, O., Freudenthal, M., Agustí, J., and Parés, J.M., 1998, Continental Mio-Pliocene transition in the Granada Basin: *Lethaia*, v. 31, p. 161–166.

- Matson, S.D. and Fox, D.L., 2010, Stable isotopic evidence for terrestrial latitudinal climate gradients in the Late Miocene of the Iberian Peninsula: *Palaeogeography, Palaeoclimatology, Palaeoecology*, v. 287, p. 28–44.
- Meijer, P.Th. and Krijgsman, W., 2005, A quantitative analysis of the desiccation and re-filling of the Mediterranean during the Messinian Salinity Crisis: *Earth and Planetary Science Letters*, v. 240, p. 510–520.
- Merlivat, L. and Jouzel, J., 1979, Global climatic interpretation of the deuterium-oxygen 18 relationship for precipitation: *Journal of Geophysical Research*, v. 84, p. 5029–5033.
- Minwer-Barakat, R., García-Alix, A., Agustí, J., Martín Suarez, E., and Freudenthal, M., 2009, The micromammal fauna from Negratín-1 (Guadix Basin, southern Spain): New evidence of African-Iberian mammal exchanges during the Late Miocene: *Journal of Paleontology*, v. 83, p. 854–879.
- Moral, F., Cruz-Sanjulián, J.J., and Olías, M., 2008, Geochemical evolution of groundwater in the carbonate aquifers of Sierra de Segura (Betic Cordillera, southern Spain): *Journal of Hydrology*, v. 360, p. 281–296.
- Murphy, L.N., Kirk-Davidoff, D.B., Mahowald, N., and Otto-Bliesner, B.L., 2009, A numerical study of the climate response to lowered Mediterranean Sea level during the Messinian Salinity Crisis: *Palaeogeography, Palaeoclimatology, Palaeoecology*, v. 279, p. 41–59.
- NCDC, 2010, Surface Data – Global Summary of the Day: 1974–2010: <http://www.ncdc.noaa.gov> (May 2010).

- Pierre, C. and Rouchy, J.-M., 2004, Isotopic compositions of diagenetic dolomites in the Tortonian marls of the western Mediterranean margins: evidence of past gas hydrate formation and dissociation: *Chemical Geology*, v. 205, p. 469–484.
- Pierre, C., Rouchy, J.-M., and Blanc-Valleron, M.-M., 2002, Gas hydrate dissociation in the Lorca Basin (SE Spain) during the Mediterranean Messinian salinity crisis: *Sedimentary Geology*, v. 147, p. 247–252.
- Ravelo, A.C., Andreasen, D.H., Lyle, M., Lyle, A.O., and Wara, M.W., 2004, Regional climate shifts caused by gradual global cooling in the Pliocene epoch: *Nature*, v. 429, p. 263–267.
- Rouchy, J.M. and Caruso, A., 2006, The Messinian salinity crisis in the Mediterranean basin: A reassessment of the data and an integrated scenario: *Sedimentary Geology*, v. 188–189, p. 35–67.
- Ruiz-Bustos, A., 1999, Biostratigraphy of the continental deposits in the Granada, Guadix, and Baza Basins (Betic Cordillera), *in* Proceedings, Congreso Internacional de Paleontología Humana, Orce, Spain, 1995: Museo de Prehistoria y Paleontología “J. Gibert”, p. 153–174.
- Ruiz Bustos, A., 2007, Aportaciones de las faunas de mamíferos a la bioestratigrafía y paleoecología de la Cuenca de Guadix y Baza, *in* Sanz de Galdeano, C. and Peláez, J.A., eds., Estructura, tectónica activa, sismicidad, geomorfología y dataciones existentes: Granada, Universidad de Granada, p. 11–27.

- Sacks, L.A., Herman, J.S., Konikow, L.F., and Vela, A.L., 1992, Seasonal dynamics of groundwater-lake interactions at Doñana National Park, Spain: *Journal of Hydrology*, v. 136, p. 123–154.
- Sanz de Galdeano, C. and Alfaro, P., 2004, Tectonic significance of the present relief of the Betic Cordillera: *Geomorphology*, v. 63, p. 175–190.
- Sanz de Galdeano, C. and López-Garrido, A.C., 1999, Nature and impact of the Neotectonic deformation in the western Sierra Nevada (Spain): *Geomorphology*, v. 30, p. 259–272.
- Sanz de Galdeano, C. and Vera, J.A., 1992, Stratigraphic record and palaeogeographical context of the Neogene basins in the Betic Cordillera, Spain: *Basin Research*, v. 4, p. 21–36.
- Simón, M., Sánchez, S., and García, I., 2000, Soil-landscape evolution on a Mediterranean high mountain: *Catena*, v. 39, p. 211–231.
- Soria, J.M., Viseras, C., and Fernández, J., 1998, Late Miocene-Pleistocene tectono-sedimentary evolution and subsidence history of the central Betic Cordillera (Spain): a case study in the Guadix intramontane basin: *Geological Magazine*, v. 135, p. 565–574.
- Talbot, M.R., 1990, A review of the palaeohydrological interpretation of carbon and oxygen isotopic ratios in primary lacustrine carbonates: *Chemical Geology*, v. 80, p. 261–279.

- Valero-Garcés, B.L., Delgado-Huertas, A., Navas, A., Machín, J., González-Sampériz, P., and Kelts, K., 2000, Quaternary palaeohydrological evolution of a playa lake: Salada Mediana, central Ebro Basin, Spain: *Sedimentology*, v. 47, p. 1135–1156.
- Valero-Garcés, B.L., Navas, A., Mata, P., Delgado-Huertas, A., Machín, J., González-Sampériz, P., Moreno Caballud, A., Schwalb, A., Ariztegui, D., Schnellmann, M., Bao, R., and González-Barrios, A., 2003, Sedimentary facies analyses in lacustrine cores: From initial core descriptions to detailed paleoenvironmental reconstructions. A case study from Zoñar Lake (Córdoba province, Spain), *in* Valero-Garcés, B.L., ed., *Limnogeology in Spain: A tribute to Kerry Kelts*: Madrid, Consejo Superior de Investigaciones Científicas, p. 385–414.
- Valero-Garcés, B.L., Moreno, A., Navas, A., Mata, P., Machín, J., Delgado Huertas, A., González Sampériz, P., Schwalb, A., Morellón, M., Hai Cheng, and Edwards, R.L., 2008, The Taravilla lake and tufa deposits (Central Iberian Range, Spain) as palaeohydrological and palaeoclimatic indicators: *Palaeogeography, Palaeoclimatology, Palaeoecology*, v. 259, p. 136–156.
- van Dam, J.A., Alcalá, L., Alonso Zarza, A., Calvo, J.P., Garcés, M., and Krijgsman, W., 2001, The Upper Miocene mammal record from the Teruel-Alfambra region (Spain). The MN system and continental stage/age concepts discussed: *Journal of Vertebrate Paleontology*, v. 21, p. 367–385.
- van Dam, J.A. and Reichart, G.J., 2009, Oxygen and carbon isotope signatures in late Neogene horse teeth from Spain and application as temperature and seasonality proxies: *Palaeogeography, Palaeoclimatology, Palaeoecology*, v. 274, p. 64–81.

van der Made, J., Morales, J., and Montoya, P., Late Miocene turnover in the Spanish mammal record in relation to palaeoclimate and the Messinian Salinity Crisis:

Palaeogeography, Palaeoclimatology, Palaeoecology, v. 238, p. 228–246.

Vandenschrick, G., van Wesemael, B., Frot, E., Pulido-Bosch, A., Molina, L., Stiévenard,

M., and Souchez, R., 2002, Using stable isotope analysis (δD – $\delta^{18}O$) to characterize

the regional hydrology of the Sierra de Gador, south east Spain: *Journal of*

Hydrology, v. 265, p. 43–55.

Willett, S.D., Schlunegger, F., and Picotti, V., 2006, Messinian climate change and

erosional destruction of the central European Alps: *Geology*, v. 34, p. 613–616.

Zachos, J., Pagani, M., Sloan, L., Thomas, E., and Billups, K., 2001, Trends, rhythms,

and aberrations in global climate 65 Ma to present: *Science*, v. 292, p. 686–693.

Figure Captions

Figure 3.1. Shaded-relief map of the Guadix-Baza Basin, showing the locations of the

Botardo (BO) and Las Lumbres (LL) sections and the surrounding mountain ranges.

The Baza Basin is located at the boundary between the Internal (I) and External (E)

Zones of the Betic Cordillera. Locations of modern precipitation and surface water

stations are indicated by the black circles in the map inset.

Figure 3.2. Composite section for Botardo (BO; circles) and Las Lumbres (LL; squares),

based on lithostratigraphic correlation of lowest appearance of lacustrine diatomites.

Stratigraphic positions of the C3An.1n–C3r magnetic reversal and the terminal

Miocene/basal Pliocene fossil localities Botardo-1 (B1) and Botardo-2 (B2) (Martín

Suárez, 1988; Ruiz-Bustos, 1999, 2007) are indicated. A) Calcite (vs. dolomite) content of bulk samples determined through XRD. B and C) $\delta^{13}\text{C}$ and $\delta^{18}\text{O}$ of calcite (white symbols), dolomite (black symbols), and mixed calcite-dolomite samples (gray symbols). “X” symbols in B and C indicate samples that contain clasts of marine carbonate and, except where noted, are not included in the results and discussion. D) SEM photomicrographs of detrital marine carbonate including coccolithophores (cc), sponge spicules (sp), and bryozoan fragments (bz). E) XRD diffractograms of representative samples from the alluvial/palustrine facies (lower) and lacustrine facies (upper). Dashed gray lines indicate stratigraphic positions of samples shown in D and E.

Figure 3.3. A. Comparison of mean $\delta^{18}\text{O}$ for lacustrine calcite from BO and LL with mean $\delta^{18}\text{O}$ for Holocene lacustrine carbonate (black squares; Andrews et al., 2000; Valero-Garcés et al., 2000, 2008; González-Sampériz et al., 2008; Luzón et al., 2009; Martín-Puertas et al., 2009) and with mean $\delta^{18}\text{O}$ for calcite (calculated using Equation 1) in equilibrium with modern lake water (gray squares; Sacks et al., 1992; García and Niell, 1993; Valero-Garcés et al., 2000, 2003, 2008; Kohfahl et al., 2008; Martín-Puertas et al., 2009; Luzón et al., 2009), groundwater (gray triangles; Cruz-San Julian et al., 1992; Sacks et al., 1992; García and Niell, 1993; Valero-Garcés et al., 2000; 2003, 2008; Vandenschrack et al., 2002; Kohfahl et al., 2008, 2008b; Moral et al., 2008; Martín-Puertas et al., 2009; Luzón et al., 2009), runoff (gray diamonds; García and Niell, 1993; Valero-Garcés et al., 2000, 2008; Vandenschrack et al., 2002; Kohfahl et al., 2008, 2008b; Luzón et al., 2009), and amount-weighted precipitation

(Cruz-San Julian et al., 1992; Valero-Garcés et al., 2000; IAEA, 2010) for sites across the Iberian Peninsula, plotted as a function of elevation. For published data from sites that were sampled over a range of elevations (Cruz-San Julian et al., 1992; Vandenschrick et al., 2002; Kohfahl et al., 2008b), the mean elevation is shown. B and C. $\delta^{18}\text{O}$ (vs. VSMOW) for lake inflow waters (contours; calculated using Equation 4) as a function of Q_o/Q_i , relative humidity, and the $\delta^{18}\text{O}_{\text{lw}}$ in equilibrium with mean lacustrine $\delta^{18}\text{O}_{\text{cal}}$ from BO/LL (calculated using Equation 1) at 20 °C (B) and 30 °C (C). Shaded areas represent inflow water $\delta^{18}\text{O} > -11\text{‰}$ VSMOW, which we consider to be a reasonable minimum for runoff in SE Spain during the Late Miocene.

Figure 3.1. Shaded-relief map of the Guadix-Baza Basin.

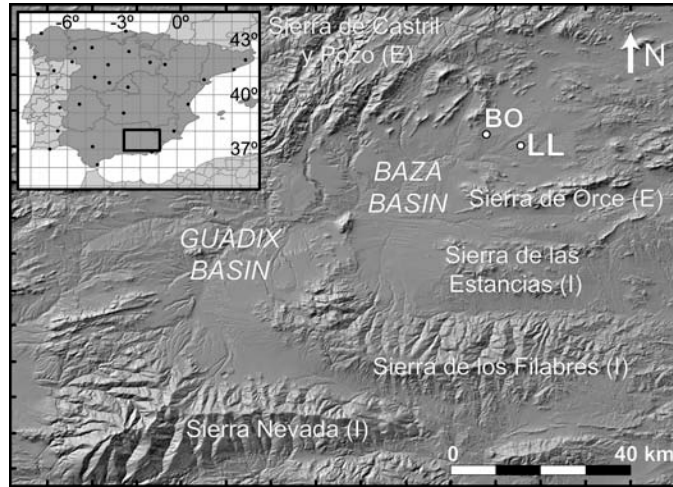


Figure 3.2. Composite section with $\delta^{13}\text{C}$, $\delta^{18}\text{O}$, XRD, and SEM results for BO and LL.

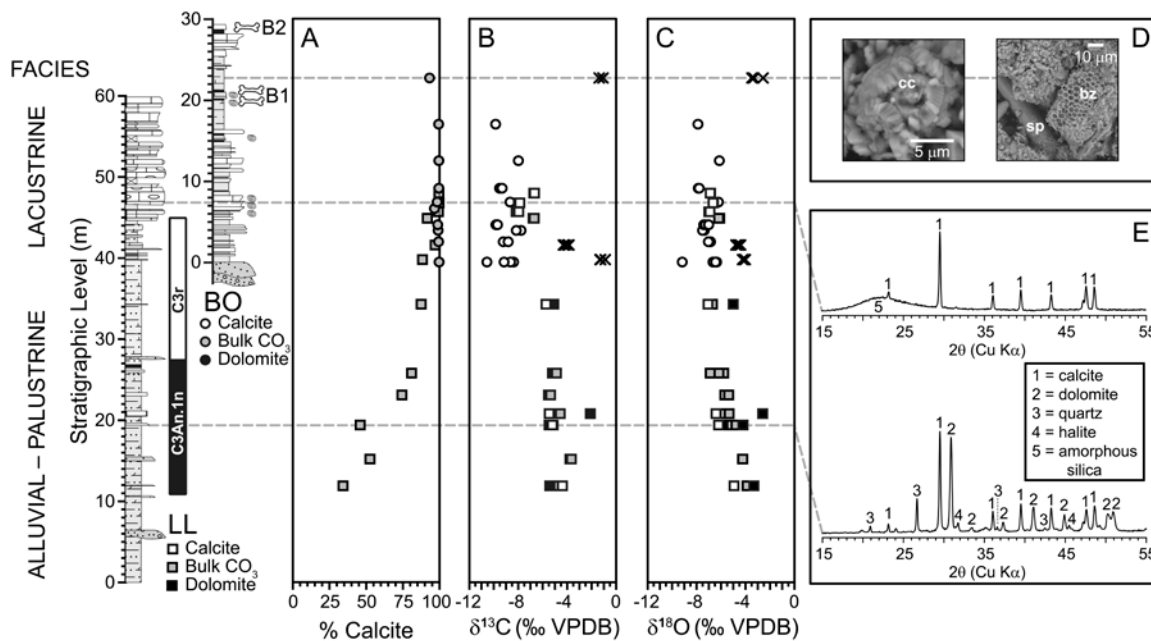


Figure 3.3. Comparison of BO/LL $\delta^{18}\text{O}$ results with modern and Holocene carbonate and water $\delta^{18}\text{O}$ from the Iberian Peninsula.

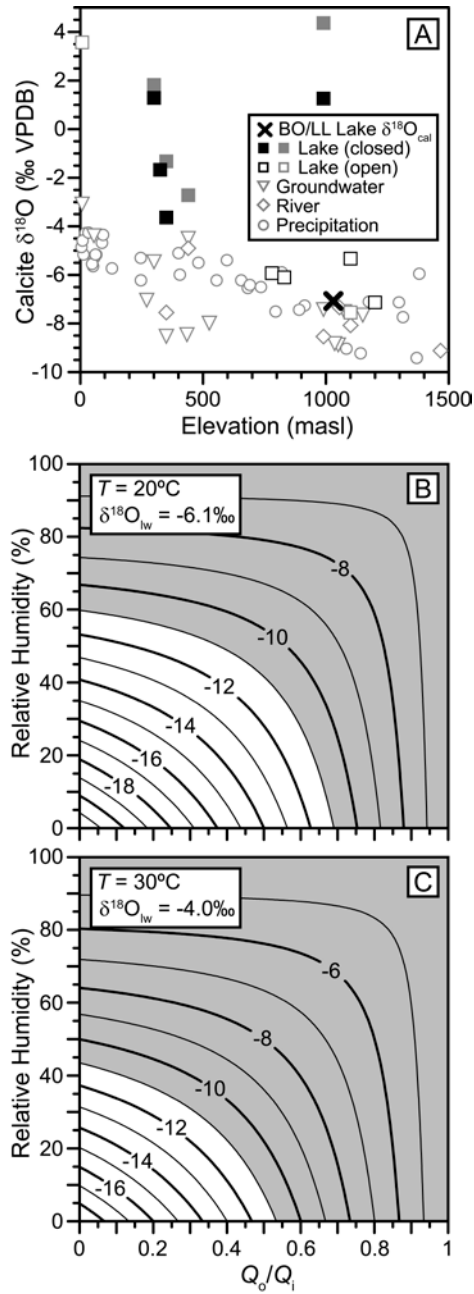


Table 3.1. $\delta^{13}\text{C}$ and $\delta^{18}\text{O}$ of carbonate samples from Botardo and Las Lumbres[†]

Locality	Composite			Facies	Material	$\delta^{13}\text{C}$ (‰VPDB)	$\delta^{18}\text{O}$ (‰VPDB)
	Strat. Level (m)	Strat. Level (m)	Percent calcite				
LL	11.9	11.9	34.3	AP	bulk carbonate	-5.07	-3.88
LL	11.9	11.9	34.3	AP	calcite*	-4.40	-4.94
LL	11.9	11.9	34.3	AP	dolomite	-5.42	-3.32
LL	15.2	15.2	52.6	AP	bulk carbonate	-3.72	-4.24
LL	19.4	19.4	46.0	AP	bulk carbonate	-5.28	-5.12
LL	19.4	19.4	46.0	AP	calcite*	-5.22	-6.20
LL	19.4	19.4	46.0	AP	dolomite	-5.32	-4.21
LL	20.8	20.8	77.5	AP	bulk carbonate	-4.72	-5.55
LL	20.8	20.8	77.5	AP	calcite*	-5.47	-6.41
LL	20.8	20.8	77.5	AP	dolomite	-2.11	-2.60
LL	23.1	23.1	74.3	AP	bulk carbonate	-5.45	-5.54
LL	23.1	23.1	74.3	AP	calcite*	-5.47	-6.23
LL	23.1	23.1	74.3	AP	dolomite	-5.39	-3.51
LL	25.8	25.8	81.0	AP	bulk carbonate	-5.02	-6.25
LL	34.3	34.3	87.5	AP	bulk carbonate	-5.66	-6.82
LL	34.3	34.3	87.5	AP	calcite*	-5.73	-7.07
LL	34.3	34.3	87.5	AP	dolomite	-5.10	-5.01
LL	39.8	39.8	88.4	DM	bulk carbonate	-1.18	-4.10
LL	39.8	39.8	88.4	DM	calcite*	-1.27	-4.22
LL	39.8	39.8	88.4	DM	dolomite	-0.53	-3.19
LL	41.6	41.6	97.0	DM	bulk carbonate	-4.08	-4.59
LL	44.9	44.9	91.7	LC	bulk carbonate	-6.75	-6.16
LL	45.7	45.7	99.3	LC	calcite	-7.96	-6.91
LL	45.7	45.7	99.3	LC	calcite	-8.17	-6.95
LL	45.7	45.7	99.3	LC	calcite	-8.15	-6.98
LL	45.7	45.7	99.3	LC	calcite	-8.15	-7.00
LL	46.8	46.8	99.6	LC	calcite	-7.99	-6.62
LL	46.8	46.8	99.6	LC	calcite	-7.88	-6.66
LL	48	48	99.6	LC	calcite	-6.73	-6.85
LL	48	48	99.6	LC	calcite	-6.68	-6.89
BO	3.6	39.5	99.7	LC	calcite	-8.39	-6.66
BO	3.6	39.5	99.7	LC	calcite	-10.56	-9.17
BO	3.6	39.5	99.7	LC	calcite	-8.63	-6.36
BO	3.6	39.5	99.7	LC	calcite	-9.16	-6.45
BO	6.1	42	99.4	LC	calcite	-9.22	-6.86

Table 3.1 (continued)

Locality	Composite			Facies	Material	$\delta^{13}\text{C}$ (‰VPDB)	$\delta^{18}\text{O}$ (‰VPDB)
	Strat. Level (m)	Strat. Level (m)	Percent calcite				
BO	6.1	42	99.4	LC	calcite	-8.82	-7.03
BO	7.5	43.4	99.0	LC	calcite	-7.77	-7.37
BO	7.5	43.4	99.0	LC	calcite	-8.16	-7.51
BO	8.2	44.1	98.8	LC	calcite	-9.82	-7.41
BO	8.2	44.1	98.8	LC	calcite	-9.76	-7.27
BO	8.2	44.1	98.8	LC	calcite	-9.70	-7.01
BO	11	46.9	98.4	LC	calcite	-8.67	-6.22
BO	12.7	48.6	99.6	LC	calcite	-9.52	-7.86
BO	12.7	48.6	99.6	LC	calcite	-9.32	-7.79
BO	16.1	52	99.6	LC	calcite	-7.99	-6.14
BO	20.6	56.5	99.4	LC	calcite	-9.85	-7.89
BO	26.3	62.2	93.2	DM	bulk carbonate	-1.38	-3.48
BO	26.3	62.2	93.2	DM	bulk carbonate	-1.07	-3.33
BO	26.3	62.2	93.2	DM	bulk carbonate	-1.08	-2.57

[†] $\delta^{13}\text{C}$ and $\delta^{18}\text{O}$ values (italicized) for samples with stars in "Material" column were calculated using percent calcite and isotopic values for bulk carbonate and for dolomite (see text). AP = alluvial/palustrine facies, LC = lacustrine facies, DM = detrital marine carbonate.

Table 3.2. Results of MW comparisons of means between BO/LL $\delta^{18}\text{O}_{\text{cal}}$ and modern/Holocene $\delta^{18}\text{O}_{\text{cal}}$ in Iberia*

Location	Latitude	Longitude	Elevation (m)	N	Mean $\delta^{18}\text{O}_{\text{water}}$ (‰VSMOW)	Mean Calculated $\delta^{18}\text{O}_{\text{cal}}$ (‰VPDB)	Mean Measured $\delta^{18}\text{O}_{\text{cal}}$ (‰VPDB)	$\delta^{18}\text{O}_{\text{cal}}$ s.d. (‰VPDB)	Sample Type	MW Z	MW p
La Salineta ⁴	41.5	0.2	325	19	–	–	-1.7	1.1	C (CL)	-1.057	0.290
Gallocanta ⁸	41.0	1.5	990	21	–	–	1.3	3.0	C (CL)	-4.764	< 0.001
Zoñar ⁹	37.5	4.7	300	70	–	–	1.3	1.7	C (CL)	-4.833	< 0.001
Salada Mediana ¹²	41.5	0.7	350	12	–	–	-3.6	1.8	C (CL)	-5.198	< 0.001
Alcaraz ¹	38.7	2.5	1200	12	–	–	-7.1	0.3	C (OL)	-5.577	< 0.001
del Rey ¹	39.0	2.9	780	18	–	–	-5.9	0.3	C (OL)	-5.630	< 0.001
Redondilla ¹	38.9	2.8	830	32	–	–	-6.1	0.3	C (OL)	-5.733	< 0.001
Taravilla ¹⁴	40.7	-2.0	1100	85	–	–	-5.3	1.8	C (OL)	-7.284	< 0.001
Fuente de Piedra ^{3,6}	37.1	-4.7	439	1	-3.0	-2.7	–	–	LW (CL)	–	–
Gallocanta Lake ⁸	41.0	1.5	990	3	5.5	4.4	–	4.3	LW (CL)	-2.778	0.005
Salada Mediana ¹²	41.5	0.7	350	5	2.1	1.8	–	5.2	LW (CL)	-2.079	0.038
Laguna Zoñar ^{13,10}	37.5	4.7	300	17	2.4	-1.3	–	1.5	LW (CL)	-5.399	< 0.001
Doñana N.P. ¹¹	37.0	-6.5	7	4	5.9	3.6	–	3.2	LW (OL)	-3.152	0.002
Taravilla ¹⁴	40.7	-2.0	1100	5	-8.1	-7.6	–	0.3	LW (OL)	-2.021	0.043
Fuente de Piedra ^{3,6}	37.1	-4.7	439	1	-5.2	-4.9	–	–	RW	–	–

Table 3.2 (continued)

Location	Latitude	Longitude	Elevation (m)	N	Mean $\delta^{18}\text{O}_{\text{water}}$ (‰VSMOW)	Mean Calculated $\delta^{18}\text{O}_{\text{cal}}$ (‰VPDB)	Mean Measured $\delta^{18}\text{O}_{\text{cal}}$ (‰VPDB)	$\delta^{18}\text{O}_{\text{cal}} \text{ s.d.}$ (‰VPDB)	Sample Type	MW Z	MW <i>p</i>
Granada Basin ⁷	37.2	-3.6	1055	8	-8.2	-7.3	–	1.4	RW	-1.088	0.277
Gallocanta Lake ⁸	41.0	1.5	990	1	-8.6	-8.5	–	–	RW	–	–
Salada Mediana ¹²	41.5	0.7	350	7	-7.3	-7.6	–	1.7	RW	-1.370	0.171
Taravilla ¹⁴	40.7	-2.0	1100	3	-8.6	-8.1	–	0.1	RW	-2.547	0.011
Sierra de Gador ¹⁵	36.9	-2.8	1466	17	-8.9	-9.1	–	0.9	RW	-4.976	< 0.001
Baza ²	37.5	-2.8	1050	21	-8.9	-8.9	–	–	GW	–	–
Cazorla ²	37.9	-3.0	1075	65	-8.3	-7.5	–	–	GW	–	–
Doñana ²	36.9	-6.4	55	25	-5.1	-4.4	–	–	GW	–	–
Gádor ²	37.0	-2.5	525	23	-8.2	-8.0	–	–	GW	–	–
Lújar ²	36.8	-3.4	270	17	-7.3	-7.0	–	–	GW	–	–
Segura ²	37.7	-2.9	1150	38	-8.5	-7.7	–	–	GW	–	–
Fuente de Piedra ^{3,6}	37.1	-4.7	439	22	-3.3	-4.5	–	2.6	GW	-3.167	0.002
Granada Basin ⁷	37.2	-3.6	1035	32	-8.6	-8.8	–	1.3	GW	-5.762	< 0.001
Gallocanta Lake ⁸	41.0	1.5	990	6	-7.0	-7.4	–	1.5	GW	-1.556	0.120
Doñana N.P. ¹¹	37.0	-6.5	7	11	-1.3	-3.1	–	3.5	GW	-4.264	< 0.001

Table 3.2 (continued)

Location	Latitude	Longitude	Elevation (m)	N	Mean $\delta^{18}\text{O}_{\text{water}}$ (‰VSMOW)	Mean Calculated $\delta^{18}\text{O}_{\text{cal}}$ (‰VPDB)	Mean Measured $\delta^{18}\text{O}_{\text{cal}}$ (‰VPDB)	$\delta^{18}\text{O}_{\text{cal}} \text{ s.d.}$ (‰VPDB)	Sample Type	MW Z	MW <i>p</i>
Salada Mediana ¹²	41.5	0.7	350	2	-8.3	-8.5	–	0.1	GW	-2.117	0.034
Laguna Zoñar ^{10, 13}	37.5	4.7	300	13	-4.9	-5.5	–	0.4	GW	-4.963	< 0.001
Taravilla ¹⁴	40.7	-2.0	1100	2	-8.2	-7.7	–	0.4	GW	-1.540	0.124
Sierra de Gador ¹⁵	36.9	-2.8	434	22	-8.2	-8.5	–	1.0	GW	-4.443	< 0.001
Baza ²	37.5	-2.8	1174	6	-6.6	-7.1	–	1.3	GW	-0.104	0.917
Cazorla ²	37.9	-3.0	1369	13	-9.7	-9.4	–	2.0	GW	-3.786	< 0.001
Doñana ²	36.9	-6.4	33	6	-4.5	-4.3	–	2.5	GW	-2.645	0.008
Gádor ²	37.0	-2.5	1297	10	-7.3	-7.1	–	3.2	GW	-1.096	0.273
Lújar ²	36.8	-3.4	820	8	-5.7	-5.9	–	2.2	GW	-1.262	0.207
Segura ²	37.7	-2.9	1313	10	-8.1	-7.7	–	2.7	GW	-1.210	0.226
Almeria Aeropuerto ⁵	36.9	-2.4	21	39	-4.9	-4.3	–	2.3	PW	-5.124	< 0.001
Avila ⁵	40.7	-4.7	1141	3	-10.6	-9.2	–	2.4	PW	-2.083	0.037
Barcelona ⁵	41.4	2.1	65	86	-5.5	-5.2	–	2.1	PW	-4.871	< 0.001
Beja ⁵	38.0	-7.5	246	22	-5.6	-5.3	–	1.4	PW	-4.640	< 0.001
Braganca ⁵	41.8	-6.7	690	30	-7.6	-6.4	–	1.8	PW	-1.741	0.082
Burgos/ Villafría ⁵	42.4	-3.6	891	12	-9.0	-7.4	–	2.1	PW	-0.973	0.330

Table 3.2 (continued)

Location	Latitude	Longitude	Elevation (m)	N	Mean $\delta^{18}\text{O}_{\text{water}}$ (‰VSMOW)	Mean Calculated $\delta^{18}\text{O}_{\text{cal}}$ (‰VPDB)	Mean Measured $\delta^{18}\text{O}_{\text{cal}}$ (‰VPDB)	$\delta^{18}\text{O}_{\text{cal}} \text{ s.d.}$ (‰VPDB)	Sample Type	MW Z	MW <i>p</i>
Caceres Trujillo ⁵	39.5	-6.3	405	51	-6.5	-6.0	–	2.4	PW	-2.771	0.006
Ciudad Real ⁵	39.0	-3.9	682	53	-7.7	-6.5	–	2.8	PW	-1.089	0.276
Faro ⁵	37.0	-8.0	9	105	-4.7	-4.6	–	1.5	PW	-6.779	< 0.001
Gerona Aeropuerto ⁵	41.9	2.8	129	41	-5.6	-5.7	–	1.8	PW	-3.793	< 0.001
Gibraltar ⁵	36.2	-5.4	5	225	-4.7	-4.9	–	1.5	PW	-6.723	< 0.001
La Coruna ⁵	43.4	-8.4	57	58	-5.7	-5.3	–	1.6	PW	-4.984	< 0.001
Leon/ Virgen del Camino ⁵	42.6	-5.7	913	56	-9.0	-7.3	–	2.4	PW	-0.556	0.578
Madrid- Retiro ⁵	40.4	-3.7	655	72	-7.0	-6.2	–	2.5	PW	-2.107	0.035
Moron Base Sevilla ⁵	37.2	-5.6	88	41	-4.8	-4.7	–	2.2	PW	-5.165	< 0.001
Murcia ⁵	38.0	-1.2	62	51	-5.7	-5.2	–	2.7	PW	-4.395	< 0.001
Penhas Douradas ⁵	40.4	-7.6	1380	152	-7.7	-6.0	–	1.7	PW	-4.190	< 0.001
Ponferrada ⁵	42.5	-6.6	555	3	-7.3	-6.2	–	1.4	PW	-1.235	0.217
Portalegre ⁵	39.3	-7.4	597	158	-5.9	-5.4	–	1.8	PW	-4.944	< 0.001
Porto ⁵	41.1	-8.6	93	144	-4.5	-4.4	–	1.8	PW	-6.958	< 0.001

Table 3.2 (continued)

Location	Latitude	Longitude	Elevation (m)	N	Mean $\delta^{18}\text{O}_{\text{water}}$ (‰VSMOW)	Mean Calculated $\delta^{18}\text{O}_{\text{cal}}$ (‰VPDB)	Mean Measured $\delta^{18}\text{O}_{\text{cal}}$ (‰VPDB)	$\delta^{18}\text{O}_{\text{cal}} s.d.$ (‰VPDB)	Sample Type	MW Z	MW <i>p</i>
Salamanca/M atacan ⁵	41.0	-5.5	795	8	-8.2	-7.5	–	1.6	PW	-1.001	0.317
Santander ⁵	43.5	-3.8	52	59	-5.8	-5.6	–	1.5	PW	-4.259	< 0.001
Soria ⁵	41.8	-2.5	1083	3	-10.3	-9.0	–	1.0	PW	-2.701	0.007
Tortosa ⁵	40.8	0.5	48	58	-5.0	-5.6	–	1.8	PW	-4.586	< 0.001
Valencia ⁵	39.5	-0.4	13	52	-4.7	-5.2	–	2.2	PW	-4.168	< 0.001
Valladolid ⁵	41.6	-4.8	735	56	-8.0	-6.5	–	2.8	PW	-0.388	0.698
Vila Real ⁵	41.3	-7.7	481	29	-6.4	-5.5	–	1.8	PW	-3.645	< 0.001
Zaragoza Aeropuerto ⁵	41.7	-1.7	247	56	-6.3	-6.2	–	2.5	PW	-1.711	0.087
Los Monegros ¹²	41.6	0.2	400	6	-5.3	-5.1	–	4.0	PW	-1.296	0.195

*Result of Mann-Whitney U (MW) comparison of means with lacustrine calcite from BO/LL (mean = -7.08‰ VPDB, *s.d.* = 0.65‰, *n* = 24). Differences that are significant at a 95% confidence level are indicated by bold text in "MW *p*" column. C = calcite, CL = closed lake, OL = open lake, LW = lake water, RW = runoff water, GW = groundwater, PW = precipitation water

References:

¹Andrews et al. (2000), ²Cruz-San Julian et al. (1992), ³Garcia and Niell (1993), ⁴González-Sampérez et al. (2008), ⁵IAEA (2010), ⁶Kohfahl et al. (2008), ⁷Kohfahl et al. (2008b), ⁸Luzon et al. (2009), ⁹Martín-Puertas et al. (2008), ¹⁰Martín-Puertas et al. (2009), ¹¹Sacks et al. (1992), ¹²Valero-Garces et al. (2000), ¹³Valero-Garces et al. (2003), ¹⁴Valero-Garces et al. (2008), ¹⁵Vandenschrick (2002)

Chapter 4: Carbon isotopic record of the relative roles of biotic and abiotic factors in the Late Miocene extinction of *Oreopithecus bambolii*, Baccinello Basin, Tuscany

Samuel D. Matson^{a*}, Lorenzo Rook^b, Oriol Oms^c, and David L. Fox^a

^a*Department of Geology and Geophysics, University of Minnesota, Minneapolis, Minnesota 55455*

^b*Dipartimento di Scienze della Terra, Università di Firenze, via G. la Pira 4, 50121, Firenze, Italy*

^c*Departamento de Geologia, Facultad de Ciències, Universitat Autònoma de Barcelona, 08193, Bellaterra, Barcelona, Spain*

^{*}*present address: Department of Geosciences, Boise State University, 1910 University Drive, Boise, Idaho 83725-1535*

Prepared for submission to *Journal of Human Evolution*

Oreopithecus bambolii is a Late Miocene hominoid with an extensive fossil record in the Baccinello Basin (Tuscany, Italy), and was the only European hominoid to survive a major extinction event ca. 9.6 Ma. *Oreopithecus* lived in the insular Tusco-Sardinian paleobioprovince, where it evolved many unique anatomical specializations that make it important for understanding the mechanisms and history of Late Miocene hominoid evolution. The eventual extinction of *Oreopithecus* and its associated fauna ca. 6.5 Ma has generally been attributed to interaction with species that arrived from continental Europe following tectonic collision of the Tusco-Sardinian province with mainland Italy, but palynological, paleontological, and sedimentological records indicate an environmental shift toward more arid and variable climates across the extinction event.

To explore the possibility of environmental change as a contributing factor in the extinction of *Oreopithecus*, we developed a stable carbon and oxygen isotope record

from organic matter and authigenic carbonate in paleosols from the Baccinello Basin. These data show very low temporal and spatial variability (indicating plant ecosystem stability through time and space) and provide no evidence for ecologically significant changes in floral composition spanning the extinction event. These results confirm the importance of species interaction as an underlying cause for the extinction of *Oreopithecus* and its associated fauna. The carbon isotope values fall entirely within the range of isotopic variability for modern plants following the C₃ photosynthetic pathway (trees, shrubs, cool-season grasses), indicating that C₄ vegetation (warm-season grasses) was not an important component of biomass. When corrected for temporal variation in the carbon isotopic composition of atmospheric carbon dioxide, the paleosol carbon isotope values are consistent with predicted values based on modern plants and the Baccinello palynoflora, confirming the reliability of paleosol isotopic records as paleoecological proxies.

Keywords: *Oreopithecus*; carbon isotopes; paleosols; Italy; Baccinello Basin; Neogene

1. Introduction

The evolution and extinction of Late Miocene hominoids and their associated fauna in the circum-Mediterranean region occurred within the context of important global and regional environmental changes that profoundly influenced the present distribution of terrestrial ecosystems. Detailed temperature records from planktonic and benthic foraminifera indicate global cooling throughout the Neogene that led to the expansion of

existing Antarctic continental ice sheets during the Late Miocene (Anderson and Shipp, 2001; Zachos et al., 2001; Liu et al., 2009), and eventually to widespread glaciation in the northern hemisphere during the Plio-Pleistocene (Shackleton et al., 1988; Maslin et al., 1998; Zachos et al., 2001). The global decrease in temperature was accompanied by an increase in aridity throughout the Neogene, which led to the gradual replacement of closed forest ecosystems by more open, mixed woodland and C₃ grassland during the Miocene, and by C₄ grasslands at mid- to low latitudes in the latest Miocene and Pliocene (Potts and Behrensmeyer, 1992; Quade and Cerling, 1995; Cerling et al., 1997; Jacobs et al., 1999; Fox and Koch, 2003; Strömberg, 2005). Patterns in Late Miocene hominoid diversity were also influenced by important regional tectonic, paleogeographic, and climatic factors. For example, tectonic extension in the Mediterranean region within the broader context of convergence between Africa and Europe facilitated faunal interchange between these continents through the establishment of land bridges and the creation of inland seas which were periodically desiccated under a regionally dry climate (Krijgsman et al., 1999; Agustí et al., 2006).

These climatic and vegetation changes are reflected in fossil mammal faunas by the gradual replacement of diverse forest-adapted taxa (e.g., brachydont browsing ungulates) by gracile, hypsodont grazing taxa globally throughout the Late Miocene, and the eventual extinction of most non-hypsodont ungulates during the latest Miocene and early Pliocene (Janis et al., 2000, 2002, 2004; Tedford et al., 2004). One important phase of this gradual faunal transition in the circum-Mediterranean region was the “Vallesian Crisis” (ca. 9.6 Ma), during which a sharp decline in the diversity of humid-adapted taxa

characteristic of Middle Miocene Europe (e.g., rhinoceroses, tapirs, cervoids, some suids) was accompanied by the sudden disappearance of nearly all European hominoids, including *Ankarapithecus*, *Dryopithecus*, and *Graecopithecus* (Agustí et al., 2003; Agustí, 2007). Paleobotanical records indicating a transition from subtropical to deciduous forests suggest that the extinction of these browsing and (in the case of the hominoids) frugivorous taxa was related to an increase in seasonality (Agustí et al., 2003).

Oreopithecus bambolii from the Late Miocene of the Tusco-Sardinian paleobioprovince (Italy) was the only European hominoid to survive the Vallesian Crisis (Bernor et al., 2001; Agustí et al. 2003; Agustí, 2007), and its relatively extensive fossil record has been the focus of intense study for more than a century (Gervais, 1872; Delson, 1986). *Oreopithecus* was part of an endemic group of mammals (the “Maremma fauna”, ca. 9.5 – 6.5 Ma) displaying specializations for insularity (e.g., hypsodonty and large body size in rodents, absence of non-lutrine carnivores; Azzaroli et al., 1986; Rook et al., 1996) and inhabiting an archipelago that extended between Europe and northern Africa. The insular environment of *Oreopithecus* resulted in its peculiar morphology, which precludes a simple interpretation of its phylogenetic position and is a focus for much of the continued interest and controversy surrounding this taxon (Straus and Schon, 1960; Berzi, 1973; Szalay and Berzi, 1973; Azzaroli et al., 1986; Delson, 1986; Harrison, 1986; Szalay and Langdon, 1986; Jungers, 1988; Rook et al., 1996, 1999b, 2004; Köhler and Moyà-Sola, 1997; Moyà-Sola et al., 1999, 2005; Sarmiento and Marcus, 2000; Susman, 2004, 2005; Marzke and Shrewsbury, 2006; Begun, 2007; Harrison, 2010).

Despite the importance of *Oreopithecus* for understanding hominoid evolution, the mechanism driving the eventual extinction of this last Late Miocene European hominoid ca. 6.5 Ma has not been clearly demonstrated. The disappearance of the specialized, endemic Maremma fauna is often attributed to species interaction (Agustí, 2007), since the last appearance of this fauna is followed very closely by the tectonic collision of the Tusco-Sardinian province with mainland Italy and the arrival of mammals from continental Europe (e.g., *Hipparion*, *Stephanorhinus*, *Machairodus*; Benvenuti et al., 2001; Rook et al., 1999). However, palynological records from the Tusco-Sardinian province indicate that the extinction of the Maremma fauna also coincides with a transition to a more arid and variable climate (Benvenuti et al., 1994; Agustí, 2007), suggesting environmental change may have played a role. In this case, the extinction of *Oreopithecus* may be more similar to that of *Sivapithecus* (a hominoid from southwest Asia that also survived the Vallesian Crisis), in which forest fragmentation under an increasingly arid climate has been implicated (Nelson, 2007).

To explore the relative roles of biotic (i.e., species interaction) and abiotic (i.e., environmental change) factors in the extinction of *Oreopithecus bambolii* and its associated fauna, we developed stable carbon and oxygen isotopic records from organic matter (OM) and authigenic carbonate in paleosols spanning the *Oreopithecus* extinction event in the Baccinello Basin in southern Tuscany, Italy. The stable carbon isotopic composition ($\delta^{13}\text{C}$)¹ of paleosols is well-established as a proxy for the type of vegetation

¹ All carbon and oxygen isotopic ratios in this paper are reported using the conventional δ -notation:

$$\delta \text{ value} = [(R_{\text{sample}}/R_{\text{standard}}) - 1] \times 1000$$

where $R = {}^{13}\text{C}/{}^{12}\text{C}$ or ${}^{18}\text{O}/{}^{16}\text{O}$ and standard is Vienna Pee Dee Belemnite (VPDB). The δ values are given in parts per thousand (‰).

covering past landscapes (see review by Koch, 1998). Plants following the C₃ photosynthetic pathway (Calvin Cycle; trees, shrubs, and cool-season grasses) have a mean $\delta^{13}\text{C}$ value of -27‰ (range = -35‰ to -22‰) while plants using the C₄ pathway (Hatch-Slack cycle; warm-season grasses and some sedges) have a mean $\delta^{13}\text{C}$ value of -13‰ (range = -14‰ to -10‰). While the distinct $\delta^{13}\text{C}$ values of these plant groups make isotopic approaches especially useful for determining the relative proportions of past C₃ and C₄ biomass, the effects of abiotic factors (e.g., temperature, P_{CO_2} , light level, aridity, salt stress, CO₂ recycling in closed-canopy forests) on isotopic fractionation during carbon fixation also allow reconstruction of microhabitats within purely C₃ ecosystems (Ehleringer and Cooper, 1988; Van der Merwe and Medina, 1989; Cerling et al., 2004). The $\delta^{13}\text{C}$ of soil organic matter ($\delta^{13}\text{C}_{\text{OM}}$) reflects the $\delta^{13}\text{C}$ of the overlying vegetation, though organic residues can be enriched in ¹³C relative to vegetation by variable amounts depending on which plant structures (i.e., foliage or roots) are incorporated into the soil (Hobbie et al., 2004) and on the level of OM decomposition (Balesdent et al., 1993; Garten et al., 2000; Chen et al., 2005). Through radiocarbon dating of soil profiles, Chen et al. (2005) demonstrated that the $\delta^{13}\text{C}_{\text{OM}}$ of soils in advanced stages of OM decomposition (> 1500-1800 yr old) is stable and is ¹³C-enriched relative to vegetation by less than 1-2‰.

Authigenic carbonate in soils forms in carbon isotopic equilibrium with root- and microbially-respired CO₂ dissolved in soil water, and in oxygen isotopic equilibrium with soil water itself. The $\delta^{13}\text{C}$ of pedogenic carbonate ($\delta^{13}\text{C}_{\text{CO}_3}$) is thus also related to the $\delta^{13}\text{C}$ of past vegetation, but is enriched in ¹³C by relative to biomass due to CO₂ diffusion

from the soil (+4–5‰) and to temperature-dependent isotopic fractionation during carbonate precipitation (+10–12‰), resulting in an offset between $\delta^{13}\text{C}_{\text{CO}_3}$ and $\delta^{13}\text{C}_{\text{OM}}$ ($\Delta^{13}\text{C}_{\text{CO}_3\text{-OM}}$) of +14–17‰ (Cerling et al., 1991). Hence, soil $\delta^{13}\text{C}_{\text{CO}_3}$ values for typical endmember C_3 and C_4 ecosystems should be approximately -12.5 and +1.5, respectively. While atmospheric CO_2 (which is isotopically heavier than soil-respired CO_2) can influence $\delta^{13}\text{C}_{\text{CO}_3}$ in shallow and arid-climate soils, the $\delta^{13}\text{C}$ of carbonate formed below ca. 30 cm in a soil should reflect only biogenic CO_2 for typical soil respiration rates and modern atmospheric composition (Cerling et al., 1991). The oxygen isotopic composition ($\delta^{18}\text{O}$) of pedogenic carbonate is a function of the $\delta^{18}\text{O}$ of soil water, and is related to climate via a strong positive correlation between meteoric water $\delta^{18}\text{O}$ ($\delta^{18}\text{O}_{\text{MW}}$) and mean annual temperature (MAT) for modern mid- to high-latitudes (+0.55‰ per °C; Rozanski et al., 1993). The use of pedogenic carbonate $\delta^{18}\text{O}$ as a paleothermometer is not straightforward, however, since temperature-dependent fractionation during carbonate precipitation (-0.23‰ per °C) acts in the opposite direction to the $\delta^{18}\text{O}_{\text{MW}}$ -MAT relationship, and environmental factors other than temperature (e.g., aridity) can enrich both meteoric and soil water in ^{18}O .

2. Materials and Methods

2.1. Geologic Setting

Oreopithecus bambolii is known from several localities in Tuscany (Baccinello, Casteani, Montemassi, Montebamboli, Ribolla) and Sardinia (Fiume Santo) in Italy (Rook et al., 1999), but its most extensive fossil record and clearest stratigraphic context

are in the Baccinello Basin in southern Tuscany (Grosseto Province). The Baccinello Basin comprises the southern part of the Baccinello-Cinigiano Basin, which is approximately 8 km wide and 25 km long and is oriented N-S between Amiata Mountain to the east and the Ombrone River valley to the west (Figure 4.1). The Baccinello Basin sediments consist of palustrine and lacustrine mustones, lignites, sandstones and carbonates interspersed with alluvial siltstones, sandstones, and conglomerates, comprising a 500 m-thick sequence lying above Oligocene sandstones (in the west) and Late Cretaceous to Eocene marine shales and limestones (in the east). Two unconformity-bounded stratigraphic units are present in the basin; the lower unit is Late Miocene in age (Tortonian-Messinian) while the upper unit is latest Miocene in age and consists predominantly of clast-supported conglomerates and sandstones (Benvenuti et al., 2001). These sediments accumulated in a low-elevation, tectonically active continental basin along the Late Miocene Mid-Tuscan Ridge, which formed a series of periodically connected islands between what is now northwestern Tuscany and northern Tunisia (Martini and Sagri, 1993; Benvenuti et al., 2001).

While the endemic nature and low taxonomic diversity of the Maremma fauna has hampered high-resolution biostratigraphic correlation with faunas from mainland Europe, the Baccinello sedimentary sequence has been divided into four local vertebrate biozones (from oldest to youngest: V-0, V-1, V-2, and V-3; Lorenz, 1968; Engesser, 1989). *Oreopithecus* is known from zones V-0, V-1, and V-2, each of which include the endemic Maremma fauna but have slight differences in faunal composition between them (Benvenuti et al., 2001; Bernor et al., 2001). Interval V-2 represents the last appearance

datum (LAD) of the Maremma fauna; the V-3 fauna has an entirely different composition and includes several pan-European genera. The V-0 fauna includes the murid rodent *Hurzelerimys vireti* (Rook et al., 1999a), which allows biostratigraphic correlation to the MN-11 European biozone (Late Miocene, 8.7–7.5 Ma; Agustí et al., 2001). The V-3 fauna includes several mammals (e.g., *Hipparion*, *Mesopithecus*, *Procapreolus*, *Stephanorhinus*; Rook et al., 1999a) that allow robust biostratigraphic correlation with the MN-13 European biozone (latest Miocene/early Pliocene, 6.8–4.9 Ma; Agustí et al., 2001). $^{40}\text{Ar}/^{39}\text{Ar}$ radiometric dating of a volcanic ash located between the V-1 and V-2 biozones in the eastern part of the basin revealed an age of 7.55 ± 0.03 Ma (Rook et al., 2000).

2.2. Sampling protocol and analytical procedure

We collected sediment hand samples from stratigraphic sections at four localities in the Baccinello Basin (Figure 4.1). The Fosso della Fittaia (FF) locality is located at the mouth of a small creek emptying into the Trasubbie River, and is comprised predominantly of lignites and mudstones (some with isolated siderite nodules) containing fossils representing the V-0 and V-1 biozones. Vegetative cover at Fosso della Fittaia makes detailed stratigraphic measurement and description difficult, but we were able to collect samples with a stratigraphic resolution of approximately 1–5 m. The Trasubbie (TB) locality is located along the north bank of the Trasubbie River, approximately 1 km northeast of Fosso della Fittaia. Trasubbie consists of a ca. 15 m outcrop of alternating brown and gray mudstone, siltstone, and sandstone and contains a vertebrate fauna representative of the V-2 biozone. Better exposure allowed measurement and description

of longer measured sections from the other two localities, Podere La Locca (PLL; ca. 25 m section) and Ribardella (RB; >100 m section). Both contain mammal fossils representative of the V-3 biozone and are comprised of gray to brown, poorly developed paleosols interspersed locally with lenticular, cross-bedded sandstones. Podere La Locca is also located in the southern part of the basin near the Trasubbie River, less than 1.5 km north of Fosso della Fittaia, while Ribardella is located in the northern part of the basin along the Melacce River, approximately 5 km northwest of the other localities (Figure 4.1). A single stratigraphic horizon at Podere La Locca contained small (< 5 mm diameter) carbonate nodules, which we sampled laterally across the outcrop at 2-m intervals. Sampling sites were selected to remain clear of modern vegetation and were excavated ca. 0.3–0.5 below the present outcrop surface to expose a fresh surface for sample collection.

For carbon isotopic analysis of bulk organic matter in paleosols, we collected 200 mg of powder from individual hand samples using a 2 mm diamond bur bit mounted into a variable-speed, handheld rotary drill. The powder samples were transferred to 15 mL polypropylene centrifuge tubes, reacted to completion at room temperature in 0.5M HCl, rinsed five times with an excess of distilled, deionized water, dried for 72 h at 50 °C in a drying oven, and then crushed and homogenized using a mortar and pestle.

Approximately 7 mg from each of the treated samples was transferred into 5 × 9 mm tin capsules that were folded tightly to minimize trapped air. The prepared samples were combusted in a Costech ECS 4010 Elemental Combustion System and the $^{13}\text{C}/^{12}\text{C}$ of the resulting CO_2 was measured using a Thermo-Finnigan Delta-V isotope ratio mass

spectrometer (IRMS) at the University of Minnesota Stable Isotope Laboratory. The raw sample $\delta^{13}\text{C}$ values were normalized to the mean $\delta^{13}\text{C}$ value of multiple samples ($N = 23$) of an in-house standard (Montana II Soil; NIST SRM 2711) analyzed with the samples. The analytical precision for these samples is better than $\pm 0.16\text{‰}$.

For carbon and oxygen isotopic analysis of pedogenic carbonate, individual carbonate nodules were cut using a lapidary saw, rinsed in water, and dried. Approximately 5 mg of powder sample was collected from a clean internal surface on each of the nodules using a 0.5 mm diamond bur bit mounted into a variable-speed, handheld rotary drill. The powder samples were roasted *in vacuo* at 400 °C for 1 h to remove water and any organic contaminants. The samples were reacted with 100% H_3PO_4 at 70 °C in a Kiel III automatic preparation device and the $\delta^{13}\text{C}$ and $\delta^{18}\text{O}$ of the resulting CO_2 was measured using a Thermo-Finnigan MAT 253 IRMS at the W.M. Keck Paleoenvironmental and Environmental Stable Isotope Laboratory at the University of Kansas. Analytical precision was maintained at better than 0.1‰ for both $\delta^{13}\text{C}$ and $\delta^{18}\text{O}$ through replicate analyses of international standards (NBS-18 and NBS-19).

3. Results

The $\delta^{13}\text{C}_{\text{OM}}$ values for soil samples from the Baccinello Basin are reported in Table 4.1 and presented in relative stratigraphic order in Figure 4.2. The mean $\delta^{13}\text{C}$ for the entire set of OM samples ($N = 55$) is -24.9‰ (range = -22 to -26.5‰), and variability around the mean is low ($s.d. = 0.63\text{‰}$). While most of the variability comes from the Fosso della Fittaia ($N = 10$, $\bar{x} = -24.8\text{‰}$, $s.d. = 1.26$, range = 4.5‰), the difference

between the mean $\delta^{13}\text{C}_{\text{OM}}$ value at Fosso della Fittaia and that of the entire sample set is within analytical error. The mean $\delta^{13}\text{C}_{\text{OM}}$ of Podere La Locca ($N = 38$, $\bar{x} = -24.8\text{‰}$, $s.d. = 0.30$, range = 1.9‰) is identical to that of Fosso della Fittaia, while the mean $\delta^{13}\text{C}_{\text{OM}}$ values at Trasubbie ($N = 3$, $\bar{x} = -25.6\text{‰}$, $s.d. = 0.15$, range = 0.3‰) and Ribardella ($N = 4$, $\bar{x} = -25.5\text{‰}$, $s.d. = 0.31$, range = 0.7‰) are slightly lower. The results of non-parametric Mann-Whitney U (MW) comparisons of means between localities and between biostratigraphic intervals are reported in Table 4.2. Although statistically significant at a 95% confidence level (MW $p = 0.012$), the difference between the pooled mean $\delta^{13}\text{C}_{\text{OM}}$ of samples from intervals V-0/1 and V-2 ($\bar{x} = -25.0\text{‰}$) and the pooled mean $\delta^{13}\text{C}_{\text{OM}}$ of samples from interval V-3 ($\bar{x} = -24.8\text{‰}$) is small and is close to the analytical error (0.16‰). The statistical significance of the difference in means between levels V-0/1/2 and V-3 is likely driven by the low $\delta^{13}\text{C}_{\text{OM}}$ variability within and between localities.

The $\delta^{13}\text{C}_{\text{CO}_3}$ values for 11 pedogenic carbonate samples from a single stratigraphic horizon at Podere La Locca are reported in Table 4.1 and presented in Figure 4.2 (assuming $\Delta^{13}\text{C}_{\text{CO}_3\text{-OM}} = 14.9\text{‰}$; see figure caption). The mean $\delta^{13}\text{C}_{\text{CO}_3}$ for these samples is -11.2‰, and the variability ($s.d. = 0.32$, range = 1.14‰) is comparable to the variability in $\delta^{13}\text{C}_{\text{OM}}$ for the entire Podere La Locca section. The difference between mean $\delta^{13}\text{C}_{\text{CO}_3}$ from the carbonate horizon and mean $\delta^{13}\text{C}_{\text{OM}}$ from 1 m above and below it (-25.0‰) is 13.8‰, which is slightly larger than difference between mean $\delta^{13}\text{C}_{\text{CO}_3}$ from the carbonate horizon and mean $\delta^{13}\text{C}_{\text{OM}}$ for the entire Podere La Locca section (13.6‰).

The $\delta^{18}\text{O}$ values for same 11 pedogenic carbonate samples are reported in Table 4.1. The carbonate $\delta^{18}\text{O}$ values ($\bar{x} = -3.6\text{‰}$, $s.d. = 0.15$, range = 0.5‰) have a smaller range than

$\delta^{13}\text{C}_{\text{CO}_3}$ from the same samples. Ordinary least-squares regression of $\delta^{13}\text{C}_{\text{CO}_3}$ onto $\delta^{18}\text{O}$ reveals a statistically significant ($p < 0.00001$) negative relationship ($\delta^{13}\text{C}_{\text{CO}_3} = -1.59*\delta^{18}\text{O} - 16.9$).

4. Discussion

4.1. Paleosol $\delta^{13}\text{C}_{\text{OM}}$ and Late Miocene vegetation at Baccinello

To evaluate the implications of the Baccinello paleosol $\delta^{13}\text{C}_{\text{OM}}$ data for paleofloral reconstruction, we compiled a list of 1,302 published $\delta^{13}\text{C}$ values for modern vegetation (representing 4,152 individual plants) for comparison with the $\delta^{13}\text{C}_{\text{OM}}$ values reported here. This list expands upon the data compiled by Diefendorf et al. (2010) and is presented in Appendix I. The Baccinello paleosol $\delta^{13}\text{C}_{\text{OM}}$ values fall entirely within the range of $\delta^{13}\text{C}$ values from modern plants following the C_3 photosynthetic pathway, but are at the positive end of the range for modern C_3 plants (Figure 4.2).

Since the $\delta^{13}\text{C}$ of atmospheric CO_2 ($\delta^{13}\text{C}_{\text{CO}_2}$) has not been constant through geologic time, a more direct comparison between modern and Late Miocene plant $\delta^{13}\text{C}$ can be made by adjusting the Baccinello $\delta^{13}\text{C}$ values to account for past variation in atmospheric $\delta^{13}\text{C}_{\text{CO}_2}$. We follow the approach of Passey et al. (2002), who used time series of $\delta^{13}\text{C}$ from planktonic foraminifera ($\delta^{13}\text{C}_{\text{PF}}$) as a proxy for past atmospheric $\delta^{13}\text{C}_{\text{CO}_2}$, assuming the isotopic fractionation of $-7.9 \pm 1.1\%$ observed between modern atmospheric CO_2 and planktonic foraminiferal calcite. Since limited biostratigraphic control of the Baccinello Basin sediments reduces the temporal precision with which we can constrain past

atmospheric $\delta^{13}\text{C}_{\text{CO}_2}$, we use the mean $\delta^{13}\text{C}_{\text{PF}}$ between 9.5 and 7.6 Ma (+2.5‰; Pagani et al., 1999) for interval V-0/1 and between 7.6 and 4.9 Ma (+2.2‰; Whitman and Berger, 1993; Pagani et al., 1999) for intervals V-2 and V-3, resulting in past atmospheric $\delta^{13}\text{C}_{\text{CO}_2}$ values of -5.4‰ and -5.7‰, respectively. To correct the Baccinello $\delta^{13}\text{C}$ data we assume a modern atmospheric $\delta^{13}\text{C}_{\text{CO}_2}$ of -8.0‰, which results in a shift of -2.6‰ for the V-0/1 samples and a shift of -2.3‰ for the V-2 and V-3 samples and places them much closer to the mean $\delta^{13}\text{C}$ for modern C_3 vegetation.

The paleosol $\delta^{13}\text{C}_{\text{OM}}$ values presented here are consistent with previous estimates of the vegetation comprising the Baccinello ecosystem. Harrison and Harrison (1989) conducted a detailed palynological study of 7 samples from an *Oreopithecus*-bearing lignite in the V-1 biostratigraphic interval. Using the plant taxa reported in that study, we restricted our compilation of published $\delta^{13}\text{C}$ values for modern plants to the 21 families dominating the palynoflora at Baccinello (Figure 4.3) and used their mean $\delta^{13}\text{C}$ values (weighted by palynomorph abundance; Harrison and Harrison, 1989) to predict the mean $\delta^{13}\text{C}$ of Late Miocene vegetation in this area. The mean $\delta^{13}\text{C}_{\text{OM}}$ for paleosols is 4.0‰ more positive than the predicted mean $\delta^{13}\text{C}$ for Baccinello vegetation (-28.9‰), but correcting the paleosol data to account for past atmospheric $\delta^{13}\text{C}_{\text{CO}_2}$ reduces this difference to 1.7‰. While pairwise Mann-Whitney U comparisons of means between the Baccinello $\delta^{13}\text{C}_{\text{OM}}$ values and $\delta^{13}\text{C}$ values for each of plant families (Table 4.3) reveal that the paleosol data are statistically distinct from the majority (16 of 20) of the modern plant families with 95% confidence, correcting the paleosol data to account for past atmospheric $\delta^{13}\text{C}_{\text{CO}_2}$ results in much greater similarity; the corrected $\delta^{13}\text{C}_{\text{OM}}$ values are

indistinguishable from more than half (12 of 20) of the modern plant families.

Additionally, the low variability of the paleosol data likely amplifies the statistical significance of some of the differences revealed by these comparisons.

Since variability in plant $\delta^{13}\text{C}$ is driven by environmental as well as taxonomic influences, we also restricted our compilation of published $\delta^{13}\text{C}$ values for modern plants to the biomes and ecosystems most comparable to that predicted for the Late Miocene of the Baccinello Basin in order to compare with the paleosol $\delta^{13}\text{C}_{\text{OM}}$ data (Figure 4.4). Previous palynological, paleontological, and sedimentological studies (Harrison and Harrison, 1989; Benvenuti et al., 1994, 2001; Carnieri and Mallegni, 2003) indicate that the Baccinello ecosystem was likely a subtropical to warm-temperate environment in relative proximity to the ocean, with freshwater lakes and swamps in closed forests located far from upland areas. Based on the palynoflora of the V-1 lignites, Harrison and Harrison (1989) suggested that the closest modern analogue to Baccinello ecosystem is the mixed mesophytic forest bordering the Yangtze River in eastern Asia. We are not aware of an isotopic record of modern vegetation from the Yangtze mixed mesophytic forest that can be compared with the Baccinello data. However, the mean of corrected Baccinello $\delta^{13}\text{C}_{\text{OM}}$ values (-27.2‰) lies between the mean plant $\delta^{13}\text{C}$ for a subtropical monsoon forest (-25.4‰; Ding Hu Shan Biosphere Preserve, eastern China; Ehleringer et al., 1987; Chen et al., 2005) that is nearby and in some ways comparable to the Yangtze mixed mesophytic forest, and the mean plant $\delta^{13}\text{C}$ for a true mixed mesophytic forest in east-central North America (-29.4‰; Walker Branch Watershed, Tennessee; Garten and Taylor, 1992; Garten et al., 2000). The Baccinello $\delta^{13}\text{C}_{\text{OM}}$ values are statistically distinct

from plant $\delta^{13}\text{C}$ values from each of these ecosystems (Table 4.4), although the statistical significance is, again, likely driven in part by the low variability in Baccinello $\delta^{13}\text{C}_{\text{OM}}$.

In addition to the taxonomic and environmental factors governing the $\delta^{13}\text{C}$ of overlying vegetation, the $\delta^{13}\text{C}$ of organic residues preserved in paleosols is also sensitive to carbon isotope fractionation during both early and late stages of soil development, such as preferential incorporation of different plant tissues into soil (Hobbie et al., 2004) or preferential decay of ^{13}C -depleted labile organic compounds (e.g., tannins) relative to ^{13}C -enriched compounds (e.g., lignin) (Melillo et al., 1989; Wedin et al., 1995). While the precise carbon isotope dynamics during soil development are complex and are also sensitive to climate (Garten et al., 2000; Chen et al., 2005), soil organic matter in advanced stages of decomposition is typically stable and is enriched in ^{13}C by only 1–2‰ relative to overlying vegetation. For example, the mean $\delta^{13}\text{C}_{\text{OM}}$ values for topsoil and old (>1800 yr) soil at the subtropical monsoon forest in eastern China are 0.7‰ and 1.2‰ more positive, respectively, than mean plant $\delta^{13}\text{C}$ (Ehleringer et al., 1987; Chen et al., 2005), and mean topsoil $\delta^{13}\text{C}_{\text{OM}}$ in the mixed mesophytic forest in Tennessee is 1.1‰ more positive than mean plant $\delta^{13}\text{C}$ (Garten and Taylor, 1992; Garten et al., 2000). Assuming a 2‰ difference between soil and plant $\delta^{13}\text{C}$ results in a mean $\delta^{13}\text{C}_{\text{OM}}$ for the Baccinello samples that is within 0.3‰ of both the mean plant $\delta^{13}\text{C}$ for the modern mixed mesophytic forest (Figure 4.4, Table 4.4) and the palynomorph abundance-weighted mean plant $\delta^{13}\text{C}$ predicted for Baccinello (Figure 4.3).

4.2. Carbonate $\delta^{13}\text{C}$ and $\delta^{18}\text{O}$

Though pedogenic carbonate in this study was restricted to a single paleosol horizon at Podere La Locca, the $\delta^{13}\text{C}$ and $\delta^{18}\text{O}$ of this carbonate offers at least a qualitative glimpse of climate during a short temporal interval within the V-3 biozone. The difference between $\delta^{13}\text{C}_{\text{CO}_3}$ for the carbonate horizon and $\delta^{13}\text{C}_{\text{OM}}$ ($\Delta^{13}\text{C}_{\text{CO}_3\text{-OM}}$) is 13.6‰ (for the entire Podere La Locca section) to 13.8‰ (for OM samples within 1 m of the carbonate horizon). This difference is very close to the typical range of 14–17‰ for $\Delta^{13}\text{C}_{\text{CO}_3\text{-OM}}$ in modern soils (Cerling et al., 1989), but is slightly lower. The slight discrepancy between $\Delta^{13}\text{C}_{\text{CO}_3\text{-OM}}$ for the Baccinello samples and that for typical modern soils cannot be explained by incorporation of atmospheric CO_2 into the soil CO_2 reservoir (which can occur in shallow, low-productivity and/or arid-climate soils or under high atmospheric $p\text{CO}_2$) at Baccinello, since atmospheric $\delta^{13}\text{C}_{\text{CO}_2}$ is more positive than soil $\delta^{13}\text{C}_{\text{CO}_2}$ and incorporation of atmospheric CO_2 should thus increase $\Delta^{13}\text{C}_{\text{CO}_3\text{-OM}}$. Since the timescale of formation for pedogenic carbonate can be on the order of several tens of kyr (Fox and Koch, 2004; Kohn and Law, 2006), heterogeneity in soil CO_2 between the time of OM accumulation and carbonate precipitation is an alternative explanation. However, the small size of the pedogenic nodules (< 5 mm diameter, indicating a relatively short timescale for soil carbonate development; Fox and Koch, 2004) and the relative temporal invariance of $\delta^{13}\text{C}_{\text{OM}}$ for the combined Baccinello section in general and the Podere La Locca section in particular suggest that this explanation is not likely. Since differences in molecular diffusion rate between ^{13}C and ^{12}C can cause $\delta^{13}\text{C}_{\text{CO}_3}$ values to be ca. 4–5‰ more positive than $\delta^{13}\text{C}_{\text{OM}}$ for the same soil (Cerling, 1984; Cerling et al., 1989), another

explanation for the relatively low $\Delta^{13}\text{C}_{\text{CO}_3\text{-OM}}$ at Baccinello is that diffusion of CO_2 from the soil was slightly lower than that of typical modern soils, implying lower soil respiration rates. This explanation is consistent with the preservation of relatively high amounts of organic matter in many of the Baccinello Basin sediments (e.g., lignites), but is constrained by the fact that very low soil respiration should allow diffusion of atmospheric CO_2 into the soil CO_2 reservoir. A final explanation is that the temperature of carbonate precipitation at Podere La Locca was substantially higher than the temperatures typical of Italy today. This explanation rests on the fact that $\Delta^{13}\text{C}_{\text{CO}_3\text{-OM}}$ is inversely related to temperature due to the temperature-dependent carbon isotope fractionation between soil CO_2 and carbonate, which can be described by the following relationship from Deines et al. (1974):

$$10^3 \ln[(\delta^{13}\text{C}_{\text{CaCO}_3} + 10^3)/(\delta^{13}\text{C}_{\text{CO}_2} + 10^3)] = 1.194*(10^6/T^2) - 3.63 \quad (1)$$

where T is temperature (Kelvin). For the typical carbon isotope fractionation associated with CO_2 diffusion from modern soils (ca. 4.4‰; Cerling et al., 1989), Equation 1 predicts temperatures of carbonate formation that are on the order of 28–30°C, which is nearly twice the MAT at low-elevation (< 200 m) sites in Italy today (NCDC, 2010).

Since $\delta^{18}\text{O}_{\text{MW}}$ is strongly related to MAT for modern mid- to high-latitudes (Rozanski et al., 1993), the $\delta^{18}\text{O}$ of sedimentary carbonate ($\delta^{18}\text{O}_{\text{CO}_3}$) is often used as a proxy for past temperatures (Koch, 1998). However, a direct link between carbonate $\delta^{18}\text{O}$ and paleoclimate is complicated by the fact that $\delta^{18}\text{O}_{\text{CO}_3}$ is inversely related to the temperature of carbonate precipitation. This relationship can be described by the calcite-water-temperature equation of Kim and O'Neil (1997):

$$10^3 \ln[(\delta^{18}\text{O}_{\text{CaCO}_3} + 10^3)/(\delta^{18}\text{O}_{\text{W}} + 10^3)] = 18.03*(10^3/T) - 32.42 \quad (2)$$

where T is temperature (Kelvin) and $\delta^{18}\text{O}_{\text{CaCO}_3}$ and $\delta^{18}\text{O}_{\text{W}}$ are the $\delta^{18}\text{O}$ values of calcite and the water from which it precipitates (respectively), relative to the Vienna Standard Mean Ocean Water (VSMOW) international isotopic standard. To explore the paleoclimatic implications of the Baccinello $\delta^{18}\text{O}_{\text{CO}_3}$ data, we compare them with $\delta^{18}\text{O}_{\text{CaCO}_3}$ predicted (using Equation 2) for modern amount-weighted mean annual $\delta^{18}\text{O}_{\text{MW}}$ (IAEA, 2010) and MAT (NCDC, 2010) at 12 low-elevation climate stations (Appendix II) on the Italian Peninsula (Figure 4.5A). The mean $\delta^{18}\text{O}_{\text{CO}_3}$ for the 11 carbonate samples from Podere La Locca (-3.8‰) is 2.4‰ higher than the mean predicted $\delta^{18}\text{O}_{\text{CO}_3}$ for the modern climate stations. This difference should actually be slightly greater, considering that large ice sheets did not develop in the northern hemisphere until the mid-Pliocene (Ravelo et al., 2004) and ocean water (hence, precipitation) during the Late Miocene was thus likely ~1‰ lighter than today (Lear et al., 2000; Zachos et al., 2001). The difference between Late Miocene $\delta^{18}\text{O}_{\text{CO}_3}$ and that predicted for modern Italy is consistent with the expected higher temperatures during the Late Miocene (since the positive $\delta^{18}\text{O}_{\text{MW}}$ -MAT relationship is nearly twice the negative temperature-dependent isotopic fractionation during calcite precipitation), though an equally viable explanation is evaporative ^{18}O -enrichment of soil water relative to precipitation. Indeed, modern pedogenic carbonate typically forms in arid to semi-arid environments where mean annual precipitation is less than 75 cm/year (Cerling, 1984). While the total variability in both $\delta^{13}\text{C}$ and $\delta^{18}\text{O}$ for the 11 carbonate samples is low, the statistically significant (ordinary least-squares regression $p < 0.00001$) negative

relationship between $\delta^{13}\text{C}_{\text{CO}_3}$ and $\delta^{18}\text{O}_{\text{CO}_3}$ (Figure 4.5B) is interesting and cannot be easily explained. The pedogenic carbonate samples from Podere La Locca come from a single stratigraphic horizon, sampled laterally across 15–20 m. While local environmental variability in canopy cover, temperature, soil evaporation, or other factors can be expected to influence both the $\delta^{13}\text{C}$ of vegetation and the $\delta^{18}\text{O}$ of soil water, these factors should generally lead to a positive relationship between $\delta^{13}\text{C}$ and $\delta^{18}\text{O}$ in pedogenic carbonate. The observed negative relationship between $\delta^{13}\text{C}_{\text{CO}_3}$ and $\delta^{18}\text{O}_{\text{CO}_3}$ may reflect slight variation in vegetative cover across the paleo-landscape, in which higher rates of soil respiration (causing greater CO_2 diffusion from the soil and ^{13}C -enrichment of soil CO_2) were associated with areas of greater vegetative cover that reduced the amount of evaporative ^{18}O -enrichment of soil water.

4.3. Implications for Late Miocene ecosystem change in Tuscany

When both the $\delta^{13}\text{C}$ of Late Miocene atmospheric CO_2 and the 1–2‰ ^{13}C -enrichment of modern soils relative to their overlying flora are taken into account, the $\delta^{13}\text{C}_{\text{OM}}$ values from Baccinello paleosols are very consistent with paleofloral reconstructions based on palynological analysis of the Baccinello lignites (Harrison and Harrison, 1989), suggesting the $\delta^{13}\text{C}_{\text{OM}}$ data are reliable as paleoecological indicators. The variability in paleosol $\delta^{13}\text{C}_{\text{OM}}$ values is low relative to the range in $\delta^{13}\text{C}$ for modern plants (even when only individual taxa, ecosystems, or photosynthetic pathways are considered), on both short (i.e., within localities) and long (i.e., between localities) temporal scales, implying plant ecosystem stability through time. Most importantly for the objectives of this study, the $\delta^{13}\text{C}_{\text{OM}}$ of the *Oreopithecus*-bearing beds (intervals V-0/1

and V-2) show no ecologically significant difference from the $\delta^{13}\text{C}_{\text{OM}}$ of sediments lying just above the LAD of the Maremma fauna (interval V-3). We interpret these observations to mean that vegetation change was not an important factor in the extinction of *Oreopithecus bambolii* and the rest of the Maremma fauna.

While the palynological study of Harrison and Harrison (1989) focused on a lignite seam in the V-1 biozone from which a nearly complete skeleton of *Oreopithecus bambolii* was recovered (Hürzeler, 1958), Benvenuti et al. (1994) included a longer time series of fossil pollen as part of their larger study of the paleontology and sedimentology in the Baccinello Basin. In that study, Benvenuti et al. (1994) describe a trend toward greater aridity and more variable climate continuing from the V-2 biozone through the V-3 biozone, based on several observations including an increase in size and hypsodonty of artiodactyls, murids, and glirids, an increase in the abundance of pollen from xerophilous herbaceous plants accompanied by a decrease in the abundance of pollen from humid subtropical and warm-temperate plants, an increase in oxidation and carbonate content of palustrine sediments, and the presence of the green alga *Botryococcus* in lacustrine sediments. Interestingly, this trend toward more arid and variable conditions is not recorded in paleosol $\delta^{13}\text{C}_{\text{OM}}$ from the same area and time interval. While the presence of lignite and siderite in V-0/1 sediments from Fosso della Fittaia and the presence of an isolated pedogenic carbonate horizon from Podere La Locca may indicate an increase in aridity between these time horizons, the $\delta^{13}\text{C}_{\text{OM}}$ record throughout the Baccinello composite section is remarkably constant, especially for the large sample size and higher stratigraphic resolution of the Podere La Locca samples.

While still small relative to the range in $\delta^{13}\text{C}$ seen in modern plants, the higher $\delta^{13}\text{C}_{\text{OM}}$ variability at Fosso della Fittaia relative to Podere La Locca suggests that environmental variability (as recorded by temporal changes in plant ecosystems) was lower – rather than higher – in the V-3 interval compared to the V-0/1 interval.

The time interval for the data presented here (9.5 – 4.9 Ma) spans the period during which the diets of many tropical, subtropical, and low-latitude temperate herbivores became dominated by C_4 vegetation in Africa, Asia, and North and South America (ca. 8–6 Ma; Cerling et al., 1993, 1997). The $\delta^{13}\text{C}_{\text{OM}}$ and $\delta^{13}\text{C}_{\text{CO}_3}$ values from Late Miocene paleosols in the Baccinello Basin fall entirely within the range of modern C_3 plants (especially when corrected for past atmospheric $\delta^{13}\text{C}_{\text{CO}_2}$), indicating that C_4 vegetation was not a substantial part of the ecosystem at any time during the Baccinello record. This result is consistent with nearly all other continental carbon isotopic records from the Mediterranean region from Middle Miocene to present (Quade et al., 1994; Cerling et al., 1997; Domingo et al., 2009a, 2009b; van Dam and Reichart, 2009), which also show no evidence for substantial European C_4 biomass throughout this interval. Today C_4 plants are present in Europe but comprise less than 5% of species (Collins and Jones, 1986), and are likely an even lower percentage of biomass. Although the climate and ecosystems in much of the Mediterranean region have characteristics that should increase photorespiration and therefore favor C_4 vegetation (e.g., high temperature, low precipitation, light stress in open environments) and at least some parts of this region likely had these characteristics during the Late Miocene (Matson and Fox, 2010), the higher amount of cool-season relative to warm-season precipitation favors C_3 plants

today and has presumably done so throughout the Neogene (Cerling et al., 1997). However, pollen records indicate that the “Mediterranean climate” (cool, wet winters and hot, dry summers) characterizing this region today was not established until the mid-Pliocene (Suc et al., 1995; Suc and Popescu, 2005), ca. 2–5 Myr after C₄ plants began to dominate many herbivore diets on most other continents. Clearly, the reasons why southern Europe did not experience a similar increase in C₄ biomass warrant further exploration.

5. Conclusions

Oreopithecus bambolii is a Late Miocene fossil hominoid with an extensive fossil record from southern Tuscany, Italy. *Oreopithecus* inhabited an insular environment in the Tusco-Sardinian paleobioprovince and evolved many unique anatomical adaptations, making it an important taxon for understanding the mechanisms and history of hominoid evolution. *Oreopithecus* was the only hominoid in Europe known to have survived a major extinction event ca. 9.6 Ma, and is present in sediments in the Baccinello Basin (Grosseto Province, Italy) that are 3–4 Myr younger than this event. While the eventual extinction of *Oreopithecus* and its associated fauna ca. 6.5 Ma has generally been attributed to an influx of mammals from mainland Europe following the tectonic collision of the Tusco-Sardinian islands with the Italian peninsula, previous paleoenvironmental studies of the Baccinello Basin have revealed evidence for an increase in aridity and climate variability that may have contributed to the extinction of *Oreopithecus*.

To explore the possibility of environmental change as a contributing factor in the extinction of *Oreopithecus*, we developed a stable carbon and oxygen isotopic record from organic matter and pedogenic carbonate in paleosols spanning the extinction event in the Baccinello Basin. Based on this isotopic record we can draw the following results and conclusions:

- 1) The $\delta^{13}\text{C}_{\text{OM}}$ values throughout the Baccinello composite section have very low variability relative to the range for modern plants, implying plant ecosystem stability through time. The isotopic data provide no evidence for an ecologically significant difference in vegetation between the ecosystems inhabited by *Oreopithecus* and those from after its extinction. This result suggests that the extinction of *Oreopithecus* and its associated fauna was driven largely by interaction with species from mainland Europe, confirming the assumptions of previous workers.
- 2) When past variation in atmospheric $\delta^{13}\text{C}_{\text{CO}_2}$, along with the isotopic fractionation between modern plants and soil organic matter, are accounted for, the paleosol $\delta^{13}\text{C}_{\text{OM}}$ values from Baccinello are consistent with estimates of past plant $\delta^{13}\text{C}$ based on the $\delta^{13}\text{C}$ of modern plants and ecosystems comparable to those of Baccinello. The offset between $\delta^{13}\text{C}_{\text{OM}}$ and $\delta^{13}\text{C}_{\text{CO}_3}$ for a single stratigraphic horizon at one locality is very close to the expected offset between $\delta^{13}\text{C}_{\text{OM}}$ and $\delta^{13}\text{C}_{\text{CO}_3}$ based on modern soils. These results lend credence to the reliability of the isotopic record.
- 3) The low variability of $\delta^{13}\text{C}_{\text{OM}}$ throughout the Baccinello record stands in contrast to previous palynological, paleontological and sedimentological studies indicating an increase in aridity and climate variability during the latest Miocene in Tuscany. This

result implies that if environmental changes did indeed take place during this time, they were not drastic enough to substantially alter the floral composition of the landscape, at least in terms of what can be distinguished isotopically.

4) The $\delta^{13}\text{C}_{\text{OM}}$ of Late Miocene paleosols in the Baccinello Basin fall entirely within the range of $\delta^{13}\text{C}$ for modern plants following the C_3 photosynthetic pathway, suggesting that C_4 vegetation was not an important part of the landscape at any time represented by the Baccinello sedimentary record. This result is consistent with all western European continental isotopic records from the Middle Miocene to present, and with modern vegetation in this area.

Acknowledgements

This research was supported by a University of Minnesota International Thesis research grant and a summer research grant from the Department of Geology and Geophysics at the University of Minnesota to Matson. This research would not have been possible without the access to outcrops and enthusiastic support provided by landowners and citizens of the village of Baccinello. We thank Greg Cane (University of Kansas) and Maniko Solheid (University of Minnesota) for their invaluable analytical assistance, and Lluís Gibert (Berkeley Geochronological Center), and Kieran McNulty, Emi Ito, Karen Kleinspehn, Andrew Haveles, Sara Morón, Peter Rose, and Niki Garrett (University of Minnesota) for thoughtful discussion and comments. While their suggestions improved the quality of this manuscript, they should not be held accountable for any errors remaining in its final form. We dedicate this paper to Mr. Frank Amodeo (San Jose, CA),

whose enthusiasm, cultural expertise, and generous gift of several delicious Tuscan meals made for a successful and enjoyable field campaign.

References Cited

- Agustí, J., 2007. The biotic environments of the Late Miocene hominids. In: Henke, W. and Tattersall, I. (Eds.), *Handbook of Paleoanthropology*. Springer, Berlin, pp. 979–1010.
- Agustí, J., Cabrera, L., Garcés, M., Krijgsman, W., Oms, O., and Parés, J.M., 2001. A calibrated mammal scale for the Neogene of Western Europe. State of the art. *Earth-Science Reviews* 52, 247–260.
- Agustí, J., Sanz de Siria, A., and Garcés, M., 2003. Explaining the end of the hominoid experiment in Europe. *Journal of Human Evolution* 45, 145–53.
- Agustí, J., Garcés, M., and Krijgsman, W., 2006. Evidence for African-Iberian exchanges during the Messinian in the Spanish mammalian record. *Palaeogeography, Palaeoclimatology, Palaeoecology* 238, 5–14.
- Anderson, J.B. and Shipp, S.S., 2001. Evolution of the West Antarctic ice-sheet. In: Alley, R.B. and Bindshadler, R.A. (Eds.), *The West Antarctic Ice Sheet: Behavior and Environment*. American Geophysical Union Antarctic Research Series 77, 45–58.
- Azzaroli, A., Boccaletti, M., Delson, E., Moratti, G., and Torre, D., 1986. Chronological and paleogeographical background to the study of *Oreopithecus bambolii*. *Journal of Human Evolution* 15, 533–540.

- Bai, E., Boutton, T.W., Liu, F., Wu, X.B., Archer, S.R., and Hallmark, C.T., 2008. Spatial variation of the stable nitrogen isotope ratio of woody plants along a topographic gradient in a subtropical. *Oecologia* 159, 493–503.
- Baldocchi, D.D. and Bowling, D.R., 1999. Modelling the discrimination of ^{13}C above and within a temperate broad-leaved forest canopy on hourly to seasonal time scales. *Plant, Cell, and Environment* 26, 231–244.
- Balesdent, J., Girardin, C., and Mariotti, A., 1993. Site-related $\delta^{13}\text{C}$ of tree leaves and soil organic matter in a temperate forest. *Ecology*, 74, 1713–1721.
- Begun, D.R., 2007. Fossil record of Miocene Hominoids. In: Henke, W. and Tattersall, I. (Eds.), *Handbook of Paleoanthropology*. Springer, Berlin, pp. 921–977.
- Bender, M.M., 1971. Variations in the $^{13}\text{C}/^{12}\text{C}$ ratios of plants in relation to the pathway of photosynthetic carbon dioxide fixation. *Phytochemistry* 10, 1239–1244.
- Benvenuti, M., Bertini, A., and Rook, L., 1994. Facies analysis, vertebrate paleontology and palynology in the Late Miocene Baccinello-Cinigiano Basin (southern Tuscany). *Memorie della Società Geologica Italiana* 48, 415–423.
- Benvenuti, M., Papini, M., and Rook, L., 2001. Mammal biochronology, UBSU and paleoenvironment evolution in a post-collisional basin: evidence from the Late Miocene Baccinello-Cinigiano basin in southern Tuscany, Italy. *Bollettino della Società Paleontologica Italiana* 120, 97–118.
- Berzi, A., 1973. The *Oreopithecus bambolii*. *Journal of Human Evolution* 2, 25–27.

- Bonal, D., Sabatier, D., Motpied, P., Tremeaux, D., and Guehl, J.M., 2000. Interspecific variability of $\delta^{13}\text{C}$ among trees in rainforests of French Guiana: functional groups and canopy integration. *Oecologia* 124, 454–468.
- Brooks, J.R., Flanagan, L.B., Buchmann, N., and Ehleringer, J.R., 1997. Carbon isotope composition of boreal plants: Functional grouping of life forms. *Oecologia*, 110, 301–311.
- Buchmann, N., Guehl, J.-M., Barigah, T.S., and Ehleringer, J.R., 1997. Interseasonal comparison of CO_2 concentrations, isotopic composition, and carbon dynamics in an Amazonian rainforest (French Guiana). *Oecologia* 110, 120–131.
- Carnieri, E. and Mallegni, F., 2003. A new specimen and dental microwear in *Oreopithecus bambolii*. *HOMO* 54, 29–35.
- Cerling, T.E., 1984. The stable isotopic composition of modern soil carbonate and its relationship to climate. *Earth and Planetary Science Letters* 71, 229–240.
- Cerling, T.E., Quade, J., Wang, Y., and Bowman, J.R., 1989. Carbon isotopes in soils and palaeosols as ecology and palaeoecology indicators. *Nature* 341, 138–139.
- Cerling, T.E., Solomon, D.K., Quade, J., and Bowman, J.R., 1991. On the isotopic composition of carbon in soil carbon dioxide. *Geochimica et Cosmochimica Acta* 55, 3403–3405.
- Cerling, T.E., Wang, Y., and Quade, J., 1993. Expansion of C_4 ecosystems as an indicator of global ecological change in the late Miocene. *Nature* 361, 344–345.

- Cerling, T.E., Harris, J.M., MacFadden, B.J., Leakey, M.G., Quade, J., Eisenmann, V., and Ehleringer, J.R., 1997. Global vegetation change through the Miocene/Pliocene boundary. *Nature* 389, 153–158.
- Cerling, T.E., Hart, J.A., Hart, T.B., 2004. Stable isotope ecology in the Ituri Forest. *Oecologia* 138, 5–12.
- Chen, Q., Shen, C., Sun, Y., Peng, S., Yi, W., Li, Z., and Jiang, M., 2005. Spatial and temporal distribution of carbon isotopes in soil organic matter at the Dinghushan Biosphere Reserve, South China. *Plant and Soil* 273, 115–128.
- Chevillat, V.S., Siegwolf, R.T.W., Pepin, S., and Körner, C., 2005. Tissue-specific variation of $\delta^{13}\text{C}$ in mature canopy trees in a temperate forest in central Europe. *Basic and Applied Ecology* 6, 519–534.
- Collins, R.P. and Jones, M.B., 1986. The influence of climatic factors on the distribution of C4 species in Europe. *Plant Ecology* 64, 121–129.
- Collister, J.W., Rieley, G., Stern, B., Eglinton, G., and Fry, B., 1994. Compound-specific $\delta^{13}\text{C}$ analyses of leaf lipids from plants with differing carbon dioxide metabolisms. *Organic Geochemistry* 21, 619–627.
- Deines, P., Langmuir, D., and Harmon, R.S., 1974. Stable carbon isotope ratios and the existence of a gas phase in the evolution of carbonate ground waters. *Geochimica et Cosmochimica Acta* 38, 1147–1164.
- Delson, E., 1986. An anthropoid enigma: Historical introduction the study of *Oreopithecus bambolii*. *Journal of Human Evolution* 15, 523–531.

- DeLucia, E.H. and Schlesinger, W.H., 1991. Resource-use efficiency and drought tolerance in adjacent Great Basin and Sierran plants. *Ecology* 72, 51–58.
- Diefendorf, A.F., Mueller, K.E., Wing, S.L., Koch, P.L., and Freeman, K.H., 2010. Global patterns in leaf ^{13}C discrimination and implications for studies of past and future climate. *Proceedings of the National Academy of Sciences USA* 107, 5738–5743.
- Dodd, M.B., Lauenroth, W.K., and Welker, J.M., 1998. Differential water resource use by herbaceous and woody plant life-forms in a shortgrass steppe community. *Oecologia* 117, 504–512.
- Domingo, L., Cuevas-González, J., Grimes, S.T., Hernández Fernández, M., and López-Martínez, N., 2009a. Multiproxy reconstruction of the palaeoclimate and palaeoenvironment of the Middle Miocene Somosaguas site (Madrid, Spain) using herbivore dental enamel. *Palaeogeography, Palaeoclimatology, Palaeoecology*, 272, 53–68.
- Domingo, L., Grimes, S.T., Domingo, M.S., and Alberdi, M.T., 2009b. Paleoenvironmental conditions in the Spanish Miocene-Pliocene boundary: isotopic analyses of Hipparion dental enamel. *Naturwissenschaften* 96, 503–511.
- Dungait, J.A.J., Docherty, G., Straker, V., and Evershed, R.P., 2008. Interspecific variation in bulk tissue, fatty acid and monosaccharide $\delta^{13}\text{C}$ values of leaves from a mesotrophic grassland plant community. *Phytochemistry* 69, 2041–2051.
- Ehleringer, J.R. and Cooper, T.A., 1988. Correlations between carbon isotope ratio and microhabitat in desert plants. *Oecologia* 76, 562–566.

- Ehleringer, J.R., Lin, Z.F., Field, C.B., Sun, G.C., and Kuo, C.Y., 1987. Leaf carbon isotope ratios of plants from a subtropical monsoon forest. *Oecologia* 72, 109–114.
- Engesser, B., 1989. The Late Tertiary small mammals of the Maremma region (Tuscany, Italy). II Part: Muridae and Cricetidae (Rodentia, Mammalia). *Bollettino della Società Paleontologica Italiana* 29, 227–252.
- Escuerdo, A., Mediavilla, S., and Heilmeyer, H., 2008. Leaf longevity and drought: avoidance of the costs and risks of early leaf abscission as inferred from the leaf carbon isotopic composition. *Functional Plant Biology* 35, 705–713.
- Fox, D.L. and Koch, P.L., 2003. Tertiary history of C₄ biomass in the Great Plains, USA. *Geology* 31, 809–812.
- Fox, D.L. and Koch, P.L., 2004. Carbon and oxygen isotopic variability in Neogene paleosol carbonates: constraints on the evolution of the C₄-grasslands of the Great Plains, USA. *Palaeogeography, Palaeoclimatology, Palaeoecology* 207, 305–329.
- Garten, C.T. and Taylor, G.E., Jr., 1992. Foliar $\delta^{13}\text{C}$ within a temperate deciduous forest: spatial, temporal, and species sources of variation. *Oecologia* 90, 1–7.
- Garten, C.T., Jr., Cooper, L.W., Post, W.M., III, and Hanson, P.J., 2000. Climate controls on forest soil C isotope ratios in the southern Appalachian Mountains. *Ecology* 81, 1108–1119.
- Gerdol, R., Iacumin, P., Marchesini, R., and Bragazza, L., 2000. Water- and nutrient-use efficiency of a deciduous species, *Vaccinium myrtillus*, and an evergreen species, *V. vitis-idaea*, in a subalpine dwarf shrub heath in the Southern Alps, Italy. *Oikos* 88, 19–32.

- Gervais, P., 1972. Sur un singe fossile, d'espèce non encore décrite, qui a été découvert au Monte-Bamboli (Italie). Comptes Rendus de l'Académie des Sciences de Paris 74, 1217–1223.
- Hanba, Y.T., Mori, S., Lei, T.T., Koike, T., and Wada, E., 1997. Variations in leaf $\delta^{13}\text{C}$ along a vertical profile of irradiance in a temperate Japanese forest. *Oecologia* 110, 253–261.
- Harrison, T., 1986. A reassessment of the phylogenetic relationships of *Oreopithecus bambolii* Gervais. *Journal of Human Evolution* 15, 541–583.
- Harrison, T., 2010. Apes among the tangled branches of human origins. *Science* 327, 532–534.
- Harrison, T.S. and Harrison, T., 1989. Palynology of the late Miocene *Oreopithecus*-bearing lignite from Baccinello, Italy. *Palaeogeography, Palaeoclimatology, Palaeoecology* 76, 45–65.
- He, C.-X., Li, J.-Y., Zhou, P., Guo, M., and Zheng, Q.-S., 2008. Changes of leaf morphological, anatomical structure and carbon isotope ratio with the height of the Wangtian Tree (*Parashorea chinensis*) in Xishuangbanna, China.
- Hemming, D., Yakir, D., Ambus, P., Aurela, M., Bessons, C., Black, K., Buchmann, N., Burlett, R., Cescatti, A., Clement, R., Gross, P., Granier, A., Grünwald, T., Havrankova, K., Janous, D., Janssens, I.A., Knohl, A., Östner, B., Kowalski, A., Laurila, T., Mata, C., Marcolla, B., Matteucci, G., Moncrieff, J., Moors, E.J., Osborne, B., Santos Pereira, J., Pihlatie, M., Pilegaard, K., Ponti, F., Rosova, Z.,

- Rossi, F., Scartazza, A., and Vesala, T., 2005. Pan-European $\delta^{13}\text{C}$ values of air and organic matter from forest ecosystems. *Global Change Biology* 11, 1065–1093.
- Hobbie, E.A., Johnson, M.G., Rygielwicz, P.T., Tingey, D.T., and Olszyk, D.M., 2004. Isotopic estimates of new carbon inputs into litter and soils in a four-year climate change experiment with Douglas-fir. *Plant and Soil* 259, 331–343.
- Holtum, J.A.M. and Winter, K., 2005. Carbon isotope composition of canopy leaves in a tropical forest in Panama throughout a seasonal cycle. *Trees* 19, 545–551.
- Hultine, K.R. and Marshall, J.D., 2000. Altitude trends in conifer leaf morphology and stable carbon isotope composition. *Oecologia* 123, 32–40.
- Hürzeler, J., 1958. *Oreopithecus bambolii* Gervais. A preliminary report. *Verhandlungen der Naturforschenden Gesellschaft in Basel* 69, 1–48.
- IAEA, 2010. Global Network of Isotopes in Precipitation (GNIP) data: 1961–2004. <http://isohis.iaea.org>. 2010.
- Inagaki, Y., Miura, S., and Kohzu, A., 2004. Effects of forest type and stand age on litterfall quality and soil N dynamics in Shikoku district, southern Japan. *Forest Ecology and Management* 202, 107–117.
- Jacobs, B.F., Kingston, J.D., and Jacobs, L.L., 1999. The origin of grass-dominated ecosystems. *Annals of the Missouri Botanical Gardens* 68, 590–643.
- Janis, C.M., Damuth, J., and Theodor, J.M., 2000. Miocene ungulates and terrestrial primary productivity: Where have all the browsers gone? *Proceedings of the National Academy of Sciences USA* 97, 7899–7904.

- Janis, C.M., Damuth, J., and Theodor, J.M., 2002. The origins and evolution of the North American grassland biome: the story from the hoofed mammals. *Palaeogeography, Palaeoclimatology, Palaeoecology* 177, 183–198.
- Janis, C.M., Damuth, J., and Theodor, J.M., 2004. The species richness of Miocene browsers, and implications for habitat type and primary productivity in the North American grassland biome. *Palaeogeography, Palaeoclimatology, Palaeoecology* 207, 371–398.
- Jessup, K.E., Barnes, P.W., and Boutton, T.W., 2003. Vegetation dynamics in a *Quercus-Juniperus* savanna: An isotopic assessment. *Journal of Vegetation Science* 14, 841–852.
- Jones, T.J., Luton, C.D., Santiago, L.S., and Goldstein, G., 2010. Hydraulic constraints on photosynthesis in subtropical evergreen broad leaf forest and pine woodland trees of the Florida Everglades. *Trees* 24, 471–478.
- Jungers, W.L., 1988. Body size and morphometric affinities of the appendicular skeleton in *Oreopithecus bambolii* (IGF 11778). *Journal of Human Evolution* 16, 445–456.
- Keough, J.R., Sierszen, M.E., and Hagley, C.A., 1996. Analysis of a Lake Superior coastal food web with stable isotope techniques. *Limnogeology and Oceanography* 41, 136–146.
- Kim, S.-T and O'Neil, J.R., 1997, Equilibrium and nonequilibrium oxygen isotope effects in synthetic carbonates: *Geochimica et Cosmochimica Acta*, v. 61, p. 3461–3475.

- Kloeppel, B.D., Gower, S.T., Treichel, I.W., and Kharuk, S., 1998. Foliar carbon isotope discrimination in *Larix* species and sympatric evergreen conifers: a global comparison. *Oecologia* 114, 153–159.
- Koch, P.L., 1998. Isotopic reconstruction of past continental environments. *Annual Review of Earth and Planetary Sciences* 26, 573–613.
- Köhler, M. and Moyà-Sola, S., 1997. Ape-like or hominid-like? The positional behavior of *Oreopithecus bambolii* reconsidered. *Proceedings of the National Academy of Sciences USA* 94, 11747–11750.
- Kohn, M.J. and Law, J.M., 2006. Stable isotope chemistry of fossil bone as a new paleoclimate indicator. *Geochimica et Cosmochimica Acta* 70, 931–946.
- Kohorn, L.U., Goldstein, G., and Rundel, P.W., 1994. Morphological and isotopic indicators of growth environment: variability in $\delta^{13}\text{C}$ in *Simmondsia chinensis*, a dioecious desert shrub. *Journal of Experimental Botany* 45, 1817–1822.
- Krijgsman, W., Hilgen, F.J., Raffi, I., Sierro, F.J., and Wilson, D.S., 1999. Chronology, causes and progression of the Messinian salinity crisis. *Nature* 400, 652–655.
- Le Roux, X., Bariac, T., Sinoquet, H., Genty, B., Piel, C., Mariotti, A., Girardin, C., and Richard, P., 2001. Spatial distribution of leaf water-use efficiency and carbon isotope discrimination within an isolated tree crown. *Plant, Cell and Environment* 24, 1021–1032.
- Lear, C.H., Elderfield, H., and Wilson, P.A., 2000. Cenozoic deep-sea temperatures and global ice volumes from Mg/Ca in benthic foraminiferal calcite. *Science* 287, 269–272.

- Leffler, A.J. and Enquist, B.J., 2002. Carbon isotope composition of tree leaves from Guanacaste, Costa Rica: comparison across tropical forests and tree life history. *Journal of Tropical Ecology* 18, 151–159.
- Li, Z.-H., Leavitt, S.W., Mora, C.I., and Liu, R.-M., 2005. Influence of earlywood-latewood size and isotope differences on long-term tree-ring $\delta^{13}\text{C}$ trends. *Chemical Geology* 216, 191–201.
- Liu, Z., Pagani, M., Zinniker, D., DeConto, R., Huber, M., Brinkhuis, H., Shah, S.R., Leckie, R.M., and Pearson, A., 2009. Global cooling during the Eocene-Oligocene climate transition. *Science* 323, 1187–1190.
- Lockheart, M.J., Van Bergen, P.F., and Evershed, R.P., 1997. Variations in the stable carbon isotope compositions of individual lipids from the leaves of modern angiosperms: implications for the study of higher land plant-derived sedimentary organic matter. *Organic Geochemistry* 26, 137–153.
- Lorenz, H.G., 1968. Stratigraphisches und micropaläontologisches Untersuchungen des Braunkohlengbietes von Baccinello (Grosseto, Italien). *Rivista Italiana di Paleontologia e Stratigrafia* 74, 147–270.
- Martini, I.P. and Sagri, M., 1993. Tectono-sedimentary characteristics of the late Miocene-Quaternary extensional basins of northern Appenines, Italy. *Earth-Sciences Review* 34, 197–233.
- Marzke, M.W. and Shrewsbury, M.M., 2006. The *Oreopithecus* thumb: Pitfalls in reconstructing muscle and ligament attachments from fossil bones. *Journal of Human Evolution* 51, 213–215.
- Matson, S.D. and Fox, D.L., 2010. Stable isotopic evidence

- for terrestrial latitudinal climate gradients in the Late Miocene of the Iberian Peninsula. *Palaeogeography, Palaeoclimatology, Palaeoecology* 287, 28–44.
- Maslin, M.A., Li, X.S., Loutre, M.-F., and Berger, A., 1998. The contribution of orbital forcing to the progressive intensification of northern hemisphere glaciation. *Quaternary Science Reviews* 17, 411–426.
- McArthur, J.V. and Moorhead, K.K., 1996. Characterization of riparian species and stream detritus using multiple stable isotopes. *Oecologia* 107, 232–238.
- Melillo, J.M., Aber, J.D., Linkins, A.E., Ricca, A., Fry, B., and Nadelhoffer, K.J., 1989. Carbon and nitrogen dynamics along the decay continuum: Plant litter to soil organic matter. *Plant and Soil* 115, 189–198.
- Mooney, H.A., Bullock, S.H., and Ehleringer, J.R., 1989. Carbon isotope ratios of plants of a tropical dry forest in Mexico. *Functional Ecology* 3, 137–142.
- Moyà-Sola, S., Köhler, M., and Rook, L., 1999. Evidence of hominid-like precision grip capability in the hand of the Miocene ape *Oreopithecus*. *Proceedings of the National Academy of Sciences USA* 96, 313–317.
- Moyà-Sola, S., Köhler, M., and Rook, L., 2005. The *Oreopithecus* thumb: a strange case in hominoid evolution. *Journal of Human Evolution* 49, 395–404.
- Nagy, L. and Proctor, J., 2000. Leaf $\delta^{13}\text{C}$ signatures in heath and lowland evergreen rain forest species from Borneo. *Journal of Tropical Ecology* 16, 757–761.
- NCDC, 2010. Surface Data – Global Summary of the Day: 1961–2004.
<http://www.ncdc.noaa.gov>. 2010.

- Nelson, S.V., 2007. Isotopic reconstructions of habitat change surrounding the extinction of *Sivapithecus*, a Miocene hominoid, in the Siwalik Group of Pakistan. *Palaeogeography, Palaeoclimatology, Palaeoecology* 243, 204–222.
- Passey, B.H., Cerling, T.E., Perkins, M.E., Voorhies, M.R., Harris, J.M., and Tucker, S.T., 2002. Environmental change in the Great Plains: An isotopic record from fossil horses. *The Journal of Geology* 110, 123–140.
- Peñuelas and Azcón-Bieto, 1992. Changes in leaf $\Delta^{13}\text{C}$ of herbarium plant species during the past 3 centuries of CO_2 increase. *Plant, Cell and Environment* 15 485–489.
- Potts, R. and Behrensmeyer, A.K., 1992. Late Cenozoic terrestrial ecosystems. In: Behrensmeyer, A.K., Damuth, J., DiMichele, W., Potts, R., Sues, H.D., and Wing, S. (Eds.), *Terrestrial Ecosystems Through Time*. University of Chicago Press, Chicago, pp. 419–519.
- Quade, J. and Cerling, T.E., 1995. Expansion of C_4 grasses in the Late Miocene of northern Pakistan: evidence from stable isotopes in paleosols. *Palaeogeography, Palaeoclimatology, Palaeoecology*, 115 91–116.
- Quade, J., Solounias, N., and Cerling, T.E., 1994. Stable isotopic evidence from paleosol carbonates and fossil teeth in Greece for forest or woodlands over the past 11 Ma. *Palaeogeography, Palaeoclimatology, Palaeoecology* 108, 41–53.
- Rook, L., Harrison, T., and Engesser, B., 1996. The taxonomic status and biochronological implications of new finds of *Oreopithecus* from Baccinello (Tuscany, Italy). *Journal of Human Evolution* 30, 3–27.

- Rook, L., Abbazzi, L., and Engesser, B., 1999a. An overview on the Italian Miocene land mammal faunas. In: Agustí, J., Rook, L., Andrews, P. (Eds.), *The Evolution of Neogene Terrestrial Ecosystems in Europe*. Cambridge University Press, Cambridge, pp. 191–204.
- Rook, L., Bondioli, L., Köhler, M., Moyà-Sola, S., and Macchiarelli, R., 1999b. *Oreopithecus* was a bipedal ape after all: Evidence from the iliac cancellous architecture. *Proceedings of the National Academy of Sciences USA* 96, 8795–8799.
- Rook, L., Renne, P., Benvenuti, M., and Papini, M., 2000. Geochronology of *Oreopithecus*-bearing succession at Baccinello (Italy) and the extinction pattern of European Miocene hominoids. *Journal of Human Evolution* 39, 577–582.
- Rook, L., Bondioli, L., Casali, F., Rossi, M., Köhler, M., Moyà-Sola, S., and Macchiarelli, R., 2004. The bony labyrinth of *Oreopithecus bambolii*. *Journal of Human Evolution* 46, 349–356.
- Rozanski, K., Araguás-Araguás, L., and Gonfiantini, R., 1993. Isotopic patterns in modern global precipitation. In: Swart, P.K., Lohmann, K.C., McKenzie, J.A., Savin, S.M. (Eds.), *Climate Change in Continental Isotopic Records: Geophysical Monograph 78*. American Geophysical Union, Washington, D.C., pp. 1–36.
- Sandquist, D.R. and Cordell, S., 2007. Functional diversity of carbon-gain, water-use, and leaf-allocation traits in trees of a threatened lowland dry forest in Hawaii. *American Journal of Botany* 94, 1459–1469.

- Sarmiento, E.E. and Marcus, L.F., 2000. The Os navicular of humans, great apes, OH 8, Hadar, and *Oreopithecus*: Function, phylogeny, and multivariate analyses. *American Museum Novitates* 3288, 1–38.
- Shackleton, N.J., Imbrie, J., Pisias, N.G., and Rose, J., 1988. The evolution of oceanic oxygen-isotope variability in the North Atlantic over the past three million years. *Philosophical Transactions of the Royal Society of London Series B* 318, 679–688.
- Straus, W.L., Jr., and Schon, M.A., 1960. Cranial capacity of *Oreopithecus bambolii*. *Science* 132, 670–672.
- Strömberg, C., 2005. Decoupled taxonomic radiation and ecological expansion of open-habitat grasses in the Cenozoic of North America. *Proceedings of the National Academy of Sciences USA* 102, 11980–11984.
- Suc, J.-P. and Popescu, S.-M., 2005. Pollen records and climatic cycles in the North Mediterranean region since 2.7 Ma. In: Head, M.J. and Gibbard, P.L. (Eds.), *Early-Middle Pleistocene Transitions: The Land-Ocean Evidence*. Geological Society Special Publication, London, pp. 147–158.
- Suc, J.-P., Diniz, F., Leroy, S., Poumont, C., Bertini, A., Dupont, L., Clet, M., Bessais, E., Zheng, Z., Fauquette, S., and Ferrier, J., 1995. Zanclean (Brunssumian) to early Piacenzian (early-middle Reuverian) climate from 4° to 54° north latitude (West Africa, West Europe and West Mediterranean areas). *Mededelingen Rijks Geologische Dienst* 52, 43–56.
- Susman, R.L., 2004. *Oreopithecus bambolii*: and unlikely case of hominidlike grip capability in a Miocene ape. *Journal of Human Evolution* 46, 105–117.

- Susman, R.L., 2005. *Oreopithecus*: still apelike after all these years. *Journal of Human Evolution* 49, 405–411.
- Szalay, F.S. and Berzi, A., 1973. Cranial anatomy of *Oreopithecus*. *Science* 180, 183–185.
- Szalay, F.S. and Langdon, J.H., 1986. The foot of *Oreopithecus*: an evolutionary assessment. *Journal of Human Evolution* 15, 585–621.
- Tedford, R.H., Albright, L.B., III, Barnosky, A.D., Ferrusquia-Villafranca, I., Hunt, R.M., Jr., Storer, J.E., Swisher, C.C., III, Voorhies, M.R., Webb, S.D., and Whistler, D.P., 2004. Mammalian biochronology of the Arikareean through Hemphillian interval (Late Oligocene through early Pliocene epochs). In: Woodburne, M.O. (Ed.), *Late Cretaceous and Cenozoic Mammals of North America: Biostratigraphy and Geochronology*. Columbia University Press, New York, pp. 169–231.
- Terwilliger, V.J., Changes in the $\delta^{13}\text{C}$ values of trees during a tropical rainy season: some effects in addition to diffusion and carboxylation by Rubisco. *American Journal of Botany* 84, 1693–1700.
- Toft, N.L., Anderson, J.E., and Nowak, R.S., 1989. Water use efficiency and carbon isotope composition of plants in a cold desert environment. *Oecologia* 80, 11–18.
- Uemura, A., Harayama, H., Koike, N., and Ishida, A., 2006. Coordination of crown structure, leaf plasticity and carbon gain within the crowns of three winter-deciduous mature trees. *Tree Physiology* 26, 633–641.

- Valentini, R., Scarascia Mugnozz, G.E., and Ehleringer, J.R., 1992. Hydrogen and carbon isotope ratios of selected species of a Mediterranean macchia ecosystem. *Functional Ecology* 6, 627–631.
- Valentini, R., Anfodillo, T., and Ehleringer, J.R., 1994. Water sources and carbon isotope composition ($\delta^{13}\text{C}$) of selected tree species of the Italian Alps. *Canadian Journal of Forest Research* 24, 1575–1578.
- van Dam, J.A. and Reichart, G.J., 2009. Oxygen and carbon isotope signatures in late Neogene horse teeth from Spain and application as temperature and seasonality proxies. *Palaeogeography, Palaeoclimatology, Palaeoecology*, 274, 64–81.
- Van de Water, P.K., Leavitt, S.W., and Betancourt, J.L., 2002. Leaf $\delta^{13}\text{C}$ variability with elevation, slope aspect, and precipitation in the southwest United States. *Oecologia* 132, 332–343.
- Van der Merwe, N.J. and Medina, E., 1989. Photosynthesis and $^{13}\text{C}/^{12}\text{C}$ ratios in Amazonian rain forests. *Geochimica et Cosmochimica Acta* 53, 1091–1094.
- Wedin, D.A., Tieszen, L.L., Dewey, B., and Pastor, J., 1995. Carbon isotope dynamics during grass decomposition and soil organic matter formation. *Ecology* 76, 1383–1392.
- Whitman, J.M. and Berger, W.H., 1993. Pliocene-Pleistocene carbon isotope record, site 586, Ontong Java Plateau. In: Maddox, E.M. (Ed.), *Proceedings of the Ocean Drilling Program, Scientific Results* 130, 333–348.

Williams, D.G. and Ehleringer, J.R., 1996. Carbon isotope discrimination in three semi-arid woodland species along a monsoon gradient. *Oecologia* 106, 455–460.

Zachos, J., Pagani, M., Sloan, L., Thomas, E., and Billups, K., 2001. Trends, rhythms, and aberrations in global climate 65 Ma to present. *Science* 292, 686–693.

Figure Captions

Figure 4.1. Geologic Map of the Baccinello Basin (after Benvenuti et al, 2001 and Rook et al., 1996), showing the position of localities described in this study. A and B = Fosso della Fittaia (FF; V-0/1), D = Trassubie (TB; V-2), F = Podere La Locca (PLL; V-3), G = Ribardella (RB; V-3).

Figure 4.2. $\delta^{13}\text{C}_{\text{OM}}$ (gray circles) and $\delta^{13}\text{C}_{\text{CO}_3}$ (white diamonds) values of paleosol samples from the Baccinello Basin, in relative stratigraphic order. Note difference in vertical scale between Ribardella and Podere La Locca. Trassubie and Fosso Fittaia samples are shown in relative stratigraphic order only; the stratigraphic distance between samples within each locality is on the order of 1-5 meters. Black vertical lines represent mean $\delta^{13}\text{C}_{\text{OM}}$ for all samples (dashed) and for each locality (solid). Gray vertical lines represent mean $\delta^{13}\text{C}_{\text{OM}}$ for the Baccinello samples adjusted for past atmospheric $\delta^{13}\text{C}_{\text{CO}_2}$ (see text) for all samples (dashed) and for each locality (solid). $\delta^{13}\text{C}_{\text{CO}_3}$ values have been adjusted by -14.9‰ to represent their equivalent $\delta^{13}\text{C}_{\text{OM}}$ values assuming 1) an isotopic fractionation of $+4.4\text{‰}$ (Cerling et al., 1989) due to CO_2 diffusion from the soil, 2) the temperature-dependent relationship between $\delta^{13}\text{C}$ of CO_2 and CaCO_3 reported by Deines et al. (1974), and 3) the MAT (16.2°) for

12 modern low-elevation (< 205 m) climate stations in Italy (Appendix II; NCDC, 2010). Histogram at bottom of figure represents the distribution of published $\delta^{13}\text{C}$ values for modern C_3 and C_4 vegetation (Appendix I). Plants using the Crassulacean Acid Metabolism (CAM) photosynthetic pathway are not included in the histogram, but have $\delta^{13}\text{C}$ values lying between the C_3 and C_4 endmembers.

Figure 4.3 Comparison of Baccinello paleosol $\delta^{13}\text{C}_{\text{OM}}$ and $\delta^{13}\text{C}_{\text{CO}_3}$ with $\delta^{13}\text{C}$ of modern representatives of Baccinello palynoflora. Mean (black diamonds) ± 1 *s.d.* (gray bars) and range (thin white bars) are shown. Plant families are listed in relative palynomorph abundance based on Harrison and Harrison (1989). Relative pollen fraction from each spermatophyte family is shown as thick white bars on right side of figure; note that pteridophytes comprise ca. 74% of total palynomorphs (Harrison and Harrison, 1989). Modern plant $\delta^{13}\text{C}$ values are listed in Appendix I. Vertical dashed line represents predicted mean $\delta^{13}\text{C}$ for Baccinello vegetation, calculated by weighting the modern mean $\delta^{13}\text{C}$ for each family by palynomorph abundance at Baccinello. $\delta^{13}\text{C}_{\text{OM}}$ and $\delta^{13}\text{C}_{\text{CO}_3}$ values have been corrected for past atmospheric $\delta^{13}\text{C}_{\text{CO}_2}$ (see text) and $\delta^{13}\text{C}_{\text{CO}_3}$ values have been adjusted to equivalent soil $\delta^{13}\text{C}_{\text{CO}_2}$ values as in Figure 4.2. Histogram for modern C_3 and C_4 plants (bottom of figure) as in Figure 4.2.

Figure 4.4. Comparison of Baccinello paleosol $\delta^{13}\text{C}_{\text{OM}}$ and $\delta^{13}\text{C}_{\text{CO}_3}$ with $\delta^{13}\text{C}$ of plants from modern biomes and ecosystems florally comparable to Baccinello. Mean (black diamonds) ± 1 *s.d.* (gray bars) and range (thin white bars) are shown. Modern plant $\delta^{13}\text{C}$ values are listed in Appendix I. CMBF = Closed Moist Broadleaf Forest

(subcanopy), OMBF = Open Moist Broadleaf Forest (canopy and gap), DBF = Dry Broadleaf Forest, GSS = Grassland, Savanna and Shrubland, BMF = Broadleaf and Mixed Forest, CF = Coniferous Forest, DXS = Desert and Xeric Shrubland, MFWS = Mediterranean Forest, Woodland, and Scrub. Modern ecosystems likely to be most comparable to that of Baccinello are represented by bold, italicized text: MMF = Mixed Mesophytic Forest (Garten and Taylor, 1992; Garten et al., 2000), SMF = Subtropical Monsoon Forest (Ehleringer et al., 1987; Chen et al., 2005), CM = Coastal Macchia (Valentini et al., 1992). Solid vertical gray line represents the mean $\delta^{13}\text{C}_{\text{OM}}$ for all samples. $\delta^{13}\text{C}_{\text{OM}}$ and $\delta^{13}\text{C}_{\text{CO}_3}$ values have been corrected for past atmospheric $\delta^{13}\text{C}_{\text{CO}_2}$ (see text) and $\delta^{13}\text{C}_{\text{CO}_3}$ have been adjusted to equivalent soil $\delta^{13}\text{C}_{\text{CO}_2}$ values as in Figures 4.2 and 4.3. Histogram for modern C_3 and C_4 plants (bottom of figure) as in Figures 4.2 and 4.3.

Figure 4.5. Podere La Locca carbonate $\delta^{18}\text{O}$ and $\delta^{13}\text{C}$. A) Comparison of measured paleosol $\delta^{18}\text{O}_{\text{CO}_3}$ (gray circles) with predicted $\delta^{18}\text{O}_{\text{CO}_3}$ (black circles) of calcite in equilibrium with modern amount-weighted mean annual precipitation $\delta^{18}\text{O}$ and MAT for 12 climate stations in Italy (Appendix II), calculated using Equation 2. Mean $\delta^{18}\text{O}_{\text{CO}_3}$ values are indicated by horizontal dashed lines. B) Linear regression of $\delta^{13}\text{C}$ onto $\delta^{18}\text{O}$ for 11 pedogenic carbonate samples from Podere La Locca.

Figure 4.1. Simplified geologic map of the Baccinello Basin.

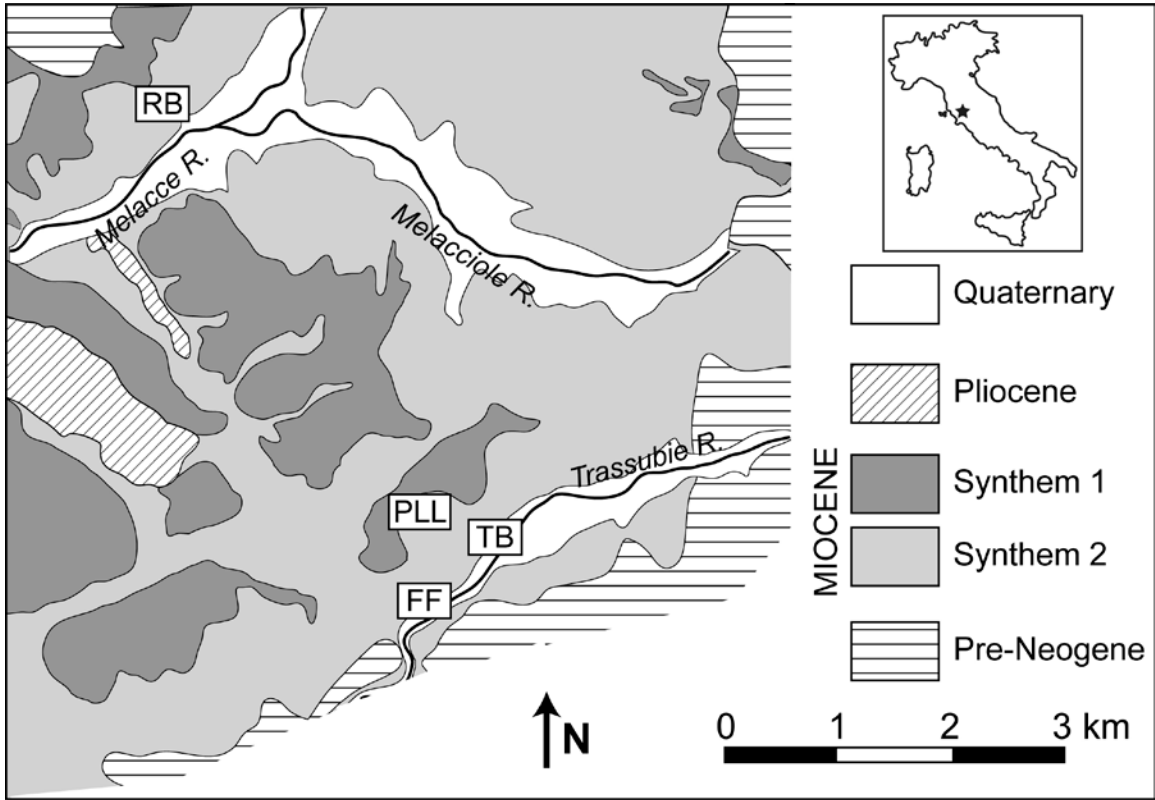


Figure 4.2. $\delta^{13}\text{C}_{\text{OM}}$ and $\delta^{13}\text{C}_{\text{CO}_3}$ values of paleosol samples from the Baccinello Basin.

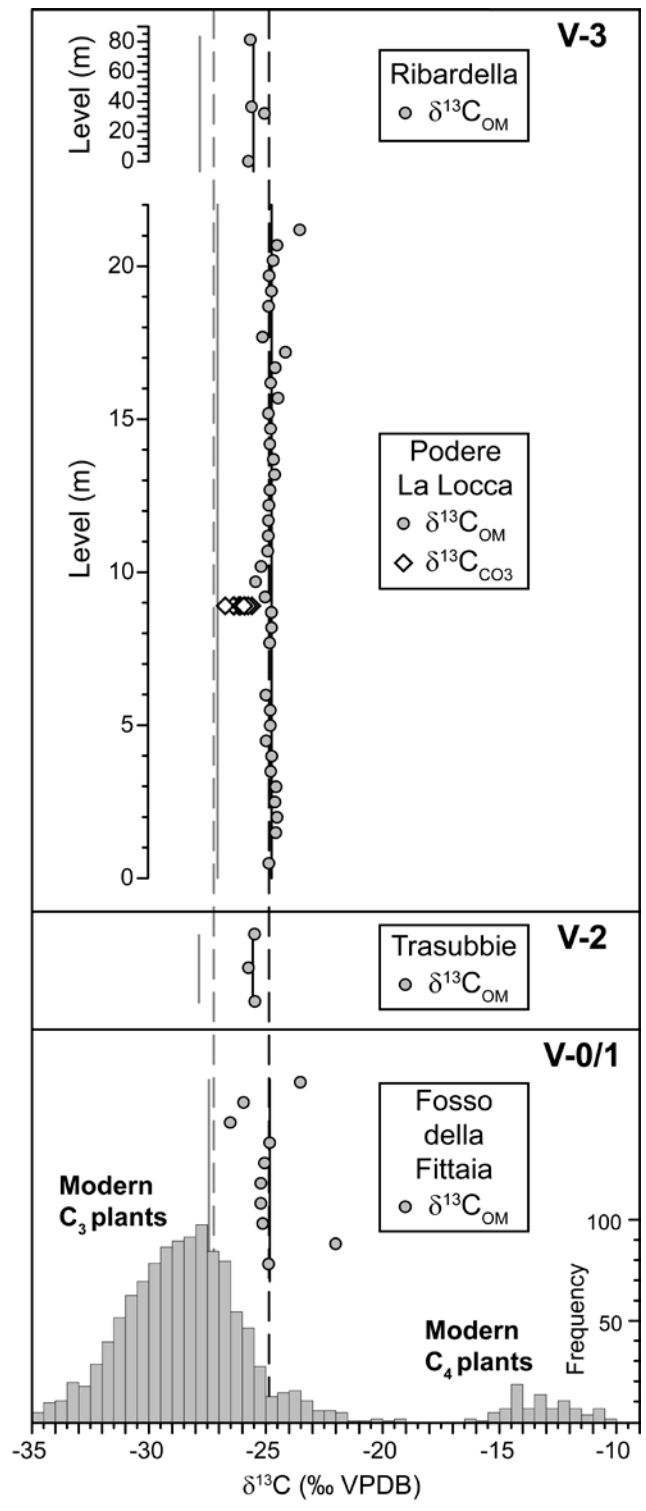


Figure 4.3. Comparison of Baccinello paleosol $\delta^{13}\text{C}_{\text{OM}}$ and $\delta^{13}\text{C}_{\text{CO}_3}$ with $\delta^{13}\text{C}$ of modern representatives of Baccinello palynoflora.

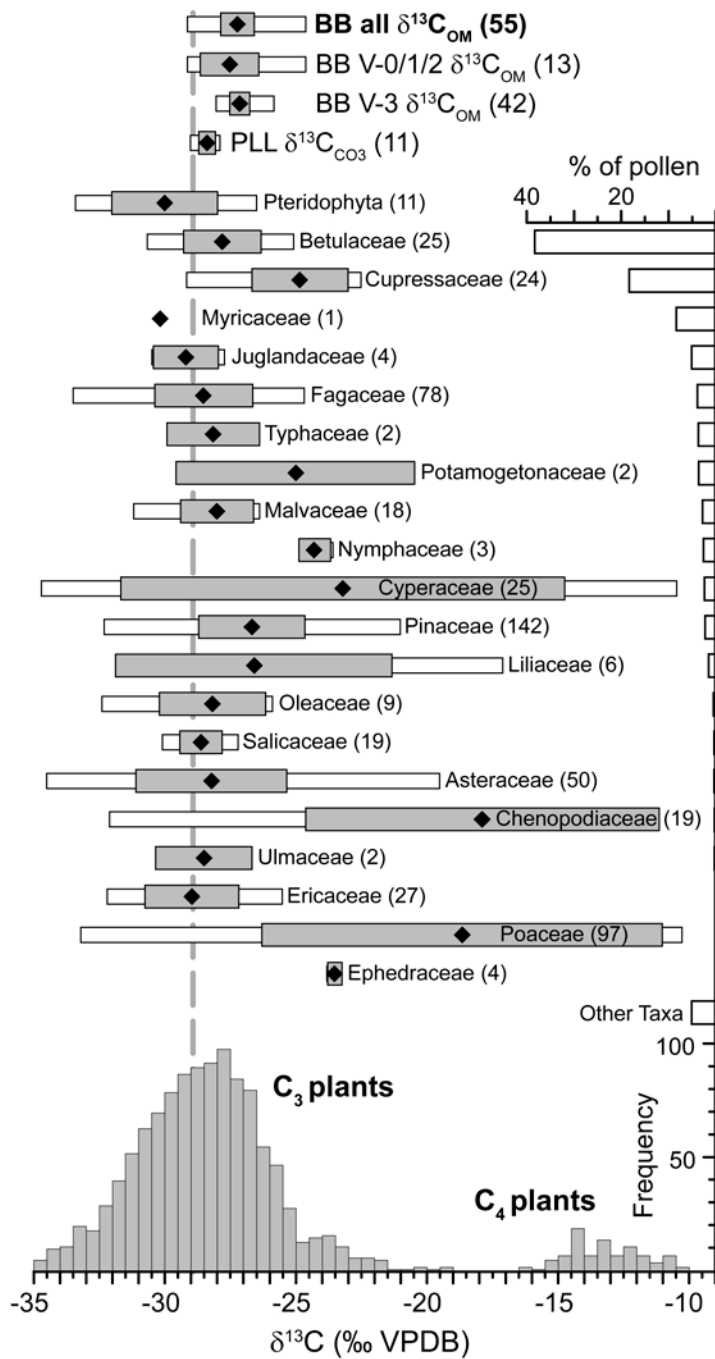


Figure 4.4. Comparison of Baccinello paleosol $\delta^{13}\text{C}_{\text{OM}}$ and $\delta^{13}\text{C}_{\text{CO}_3}$ with $\delta^{13}\text{C}$ of plants from modern biomes and ecosystems florally comparable to Baccinello.

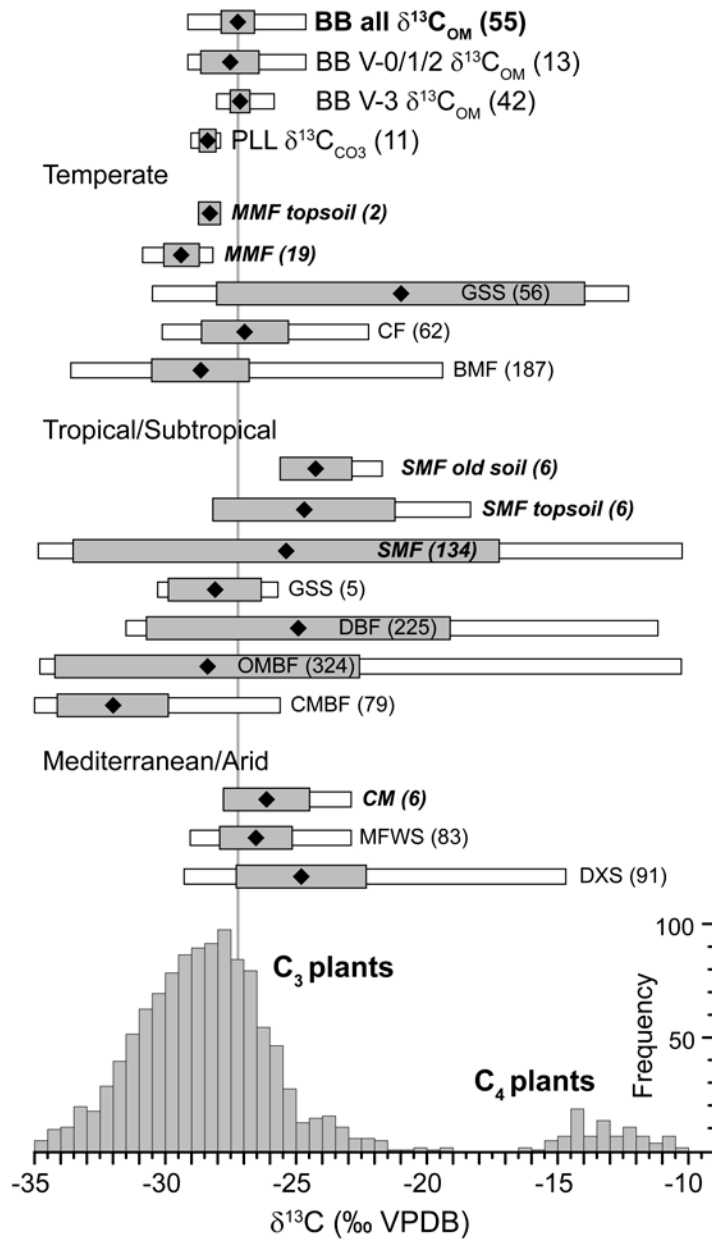


Table 4.1. Stable carbon and oxygen isotopic ratios of Baccinello paleosols.

Locality	Biozone	Material	Stratigraphic Level	$\delta^{13}\text{C}$ (‰ VPDB)	$\delta^{18}\text{O}$ (‰ VPDB)
RB	V-3	OM	0.0 m	-25.7	—
RB	V-3	OM	32.0 m	-25.1	—
RB	V-3	OM	36.4 m	-25.6	—
RB	V-3	OM	81.3 m	-25.7	—
PLL	V-3	OM	0.5 m	-24.9	—
PLL	V-3	OM	1.5 m	-24.6	—
PLL	V-3	OM	2.0 m	-24.5	—
PLL	V-3	OM	2.5 m	-24.6	—
PLL	V-3	OM	3.0 m	-24.6	—
PLL	V-3	OM	3.5 m	-24.8	—
PLL	V-3	OM	4.0 m	-24.7	—
PLL	V-3	OM	4.5 m	-25.0	—
PLL	V-3	OM	5.0 m	-24.8	—
PLL	V-3	OM	5.5 m	-24.8	—
PLL	V-3	OM	6.0 m	-25.0	—
PLL	V-3	OM	7.7 m	-24.8	—
PLL	V-3	OM	8.2 m	-24.8	—
PLL	V-3	OM	8.7 m	-24.8	—
PLL	V-3	OM	9.2 m	-25.0	—
PLL	V-3	OM	9.7 m	-25.4	—
PLL	V-3	OM	10.2 m	-25.2	—
PLL	V-3	OM	10.7 m	-24.9	—
PLL	V-3	OM	11.2 m	-24.9	—
PLL	V-3	OM	11.7 m	-24.9	—
PLL	V-3	OM	12.2 m	-24.9	—
PLL	V-3	OM	12.7 m	-24.8	—
PLL	V-3	OM	13.2 m	-24.6	—
PLL	V-3	OM	13.7 m	-24.7	—
PLL	V-3	OM	14.2 m	-24.8	—
PLL	V-3	OM	14.7 m	-24.8	—
PLL	V-3	OM	15.2 m	-24.9	—
PLL	V-3	OM	15.7 m	-24.5	—
PLL	V-3	OM	16.2 m	-24.8	—
PLL	V-3	OM	16.7 m	-24.6	—
PLL	V-3	OM	17.2 m	-24.2	—
PLL	V-3	OM	17.7 m	-25.1	—
PLL	V-3	OM	18.7 m	-24.9	—
PLL	V-3	OM	19.2 m	-24.8	—
PLL	V-3	OM	19.7 m	-24.9	—
PLL	V-3	OM	20.2 m	-24.7	—
PLL	V-3	OM	20.7 m	-24.5	—
PLL	V-3	OM	21.2 m	-23.5	—
TB	V-2	OM	1*	-25.5	—
TB	V-2	OM	2*	-25.5	—
TB	V-2	OM	3*	-25.7	—
FF	V-0/1	OM	1*	-24.9	—
FF	V-0/1	OM	2*	-22.0	—

Table 4.1 (continued)

Locality	Biozone	Material	Stratigraphic Level	$\delta^{13}\text{C}$ (‰ VPDB)	$\delta^{18}\text{O}$ (‰ VPDB)
FF	V-0/1	OM	3*	-25.1	–
FF	V-0/1	OM	4*	-25.2	–
FF	V-0/1	OM	5*	-25.2	–
FF	V-0/1	OM	6*	-25.1	–
FF	V-0/1	OM	7*	-24.8	–
FF	V-0/1	OM	8*	-26.5	–
FF	V-0/1	OM	9*	-25.9	–
FF	V-0/1	OM	10*	-23.5	–
PLL	V-3	CO ₃	8.9 m	-10.7	-3.8
PLL	V-3	CO ₃	8.9 m	-11.0	-3.6
PLL	V-3	CO ₃	8.9 m	-10.9	-3.8
PLL	V-3	CO ₃	8.9 m	-11.3	-3.6
PLL	V-3	CO ₃	8.9 m	-11.2	-3.6
PLL	V-3	CO ₃	8.9 m	-11.4	-3.8
PLL	V-3	CO ₃	8.9 m	-11.2	-3.5
PLL	V-3	CO ₃	8.9 m	-11.5	-3.5
PLL	V-3	CO ₃	8.9 m	-11.8	-3.3
PLL	V-3	CO ₃	8.9 m	-11.2	-3.6
PLL	V-3	CO ₃	8.9 m	-11.0	-3.6

*Relative stratigraphic position

Table 4.2. Results of MW comparisons of mean $\delta^{13}\text{C}_{\text{OM}}$ between localities and biozones *

	FF (V-0/1)	TB (V-2)	PLL (V3)	RB (V-3)	all V-0/1/2	all V-3
FF (V-0/1)	1 <i>-0.845</i>	0.128 <i>-1.523</i>	0.042 <i>-2.031</i>	0.203 <i>-1.274</i>	–	0.099 <i>-1.649</i>
TB (V-2)	0.398 <i>-0.845</i>	1	0.004 <i>-2.854</i>	0.858 <i>-0.178</i>	–	0.010 <i>-2.571</i>
PLL (V3)	0.006 <i>-2.742</i>	0.004 <i>-2.854</i>	1	0.002 <i>-3.128</i>	0.003 <i>-2.961</i>	–
RB (V-3)	0.396 <i>-0.849</i>	0.724 <i>-0.354</i>	0.002 <i>-3.128</i>	1	0.281 <i>-1.077</i>	–
all V-0/1/2	–	–	0.000 <i>-3.566</i>	0.428 <i>-0.793</i>	1	0.012 <i>-2.526</i>
all V-3	0.018 <i>-2.368</i>	0.011 <i>-2.548</i>	–	–	0.002 <i>-3.130</i>	1

*Values in upper right part of table are for measured $\delta^{13}\text{C}_{\text{OM}}$; values in lower left part are for $\delta^{13}\text{C}_{\text{OM}}$ corrected for past atmospheric $\delta^{13}\text{C}_{\text{CO}_2}$ (see text). Upper number in each cell is MW p value; lower, italicized number is MW Z -statistic. Means that are indistinguishable with 95% confidence are highlighted in bold.

Table 4.3. Results of MW comparisons of means between Baccinello $\delta^{13}\text{C}_{\text{OM}}$ (all samples) and $\delta^{13}\text{C}$ of modern members of plant families represented in Baccinello palynoflora*

	<i>N</i>	\bar{x} (‰)	<i>s.d.</i> (‰)	$\delta^{13}\text{C}_{\text{OM}}$ ($\bar{x} = -24.9\text{‰}$)		$\delta^{13}\text{C}_{\text{OM}}$ corrected for past atmospheric $\delta^{13}\text{C}_{\text{CO}_2}$ ($\bar{x} = -27.2\text{‰}$)		$\delta^{13}\text{C}_{\text{OM}}$ corrected for past atmospheric $\delta^{13}\text{C}_{\text{CO}_2}$ and assuming $\Delta^{13}\text{C}_{\text{OM-plant}} = 2\text{‰}$ ($\bar{x} = -29.2\text{‰}$)	
				MW <i>p</i>	MW <i>Z</i>	MW <i>p</i>	MW <i>Z</i>	MW <i>p</i>	MW <i>Z</i>
				Pteridophyta	11	-30.0	2.02	< 0.001	-5.188
Betulaceae	25	-27.8	1.47	< 0.001	-6.877	0.036	-2.092	0.000	-4.463
Cupressaceae	24	-24.9	1.83	0.709	-0.373	0.000	-5.234	0.000	-6.695
Myricaceae	1	-30.2	–	–	–	–	–	–	–
Juglandaceae	4	-29.2	1.25	0.001	-3.317	0.003	-2.985	0.928	-0.090
Fagaceae	78	-28.5	1.86	< 0.001	-9.572	0.000	-4.331	0.000	-3.651
Typhaceae	2	-28.2	1.77	0.004	-2.897	0.188	-1.317	0.712	-0.369
Potamogetonaceae	2	-25.0	4.55	1.000	0.000	0.931	-0.087	0.024	-2.255
Malvaceae	18	-28.0	1.39	< 0.001	-6.323	0.028	-2.201	0.000	-3.571
Nymphaeaceae	1	-24.3	0.60	0.056	-1.914	0.004	-2.861	0.004	-2.897
Cyperaceae	25	-23.2	8.47	0.046	-1.998	0.565	-0.576	0.000	-4.375
Pinaceae	142	-26.7	2.02	< 0.001	-7.155	0.151	-1.435	0.000	-9.057
Liliaceae	6	-26.6	5.27	0.146	-1.453	0.611	-0.509	0.545	-0.605
Oleaceae	9	-28.2	2.03	< 0.001	-3.923	0.513	-0.654	0.000	-3.899
Salicaceae	19	-28.6	0.80	< 0.001	-6.335	0.000	-5.593	0.006	-2.739
Asteraceae	50	-28.2	2.88	< 0.001	-7.353	0.099	-1.649	0.008	-2.650
Chenopodiaceae	19	-17.9	6.74	< 0.001	-3.743	0.000	-3.780	0.000	-4.956
Ulmaceae	2	-28.5	1.84	0.017	-2.385	0.152	-1.431	0.761	-0.304
Ericaceae	27	-29.0	1.80	< 0.001	-7.218	0.000	-4.544	0.372	-0.893
Poaceae	97	-18.6	7.65	0.001	-3.207	0.000	-4.741	0.000	-7.579
Ephedraceae	4	-23.5	0.27	0.002	-3.076	0.001	-3.317	0.001	-3.317

*MW *p*-values for indistinguishable means (95% confidence) highlighted in bold.

Table 4.4. Results of MW comparisons of means between Baccinello $\delta^{13}\text{C}_{\text{OM}}$ (all samples) and $\delta^{13}\text{C}$ of modern plants in various biomes*

	<i>N</i>	\bar{x} (‰)	<i>s.d.</i> (‰)	$\delta^{13}\text{C}_{\text{OM}}$ ($\bar{x} = -24.9\text{‰}$)		$\delta^{13}\text{C}_{\text{OM}}$ corrected for past atmospheric $\delta^{13}\text{C}_{\text{CO}_2}$ ($\bar{x} = -27.2\text{‰}$)		$\delta^{13}\text{C}_{\text{OM}}$ corrected for past atmospheric $\delta^{13}\text{C}_{\text{CO}_2}$ and assuming $\Delta^{13}\text{C}_{\text{OM-plant}} = 2\text{‰}$ ($\bar{x} = -29.2\text{‰}$)	
				MW <i>p</i>	MW <i>Z</i>	MW <i>p</i>	MW <i>Z</i>	MW <i>p</i>	MW <i>Z</i>
TROPICAL/SUBTROPICAL									
Moist Broadleaf Forest (closed)	79	-32.0	2.12	0.000	-9.827	0.000	-9.655	0.000	-8.081
Moist Broadleaf Forest (open)	324	-28.4	5.83	0.000	-9.346	0.000	-8.468	0.000	-3.654
Dry Broadleaf Forest	225	-24.9	5.80	0.000	-5.986	0.347	-0.941	0.000	-7.805
Grassland, Savanna, & Shrubland	5	-28.1	1.78	0.000	-3.571	0.118	-1.565	0.214	-1.244
Subtropical Monsoon Forest	134	-25.4	8.15	0.000	-5.146	0.000	-3.876	0.686	-0.404
Subtropical Monsoon Forest (topsoil)	6	-24.7	3.48	0.865	-0.170	0.042	-2.034	0.000	-3.923
Subtropical Monsoon Forest (old soil)	6	-24.2	1.38	0.537	-0.618	0.000	-3.923	0.000	-3.996
TEMPERATE									
Broadleaf and Mixed Forest	187	-28.7	1.86	0.000	-10.769	0.000	-6.806	0.002	-3.116
Coniferous Forest	62	-27.0	1.66	0.000	-7.001	0.639	-0.470	0.000	-7.755
Grassland, Savanna, & Shrubland	56	-21.0	7.03	0.520	-0.643	0.050	-1.964	0.000	-7.491
Mixed Mesophytic Forest	19	-29.4	0.68	0.000	-6.465	0.000	-6.354	0.516	-0.650
Mixed Mesophytic Forest (topsoil)	2	-28.3	0.42	0.017	-2.385	0.030	-2.168	0.034	-2.125
ARID/MEDITERRANEAN									
Mediterranean Forest, Woodland, & Scrub	83	-26.5	1.39	0.000	-7.432	0.000	-3.514	0.000	-9.474
Desert and Xeric Shrubland	91	-24.8	2.49	0.323	-0.987	0.000	-7.268	0.000	-9.828
Coastal Macchia	6	-26.1	1.65	0.009	-2.616	0.040	-2.059	0.000	-3.948

*MW *p*-values for indistinguishable means (95% confidence) highlighted in bold.

Chapter 5: Conclusions and directions for future research

1. Summary and Perspectives

The late Neogene was an important phase in the evolution of terrestrial biomes that encompass a large and important component of the modern global biosphere. The research presented in this dissertation focused on the reconstruction of continental paleoclimate and paleoecology in the Mediterranean region, where a distinct climatic and paleogeographic history allows exploration of the interplay between tectonics, biology, and climate during this critical phase in the global evolution of terrestrial systems. The results of this research supply significant new information that contributes to a more complete understanding of the geologic history of the Mediterranean region in particular, and of the late Cenozoic history of terrestrial ecosystems more generally.

Several of the results reported here confirm existing ideas. For example, paleotemperature reconstructions for the Late Miocene Iberian Peninsula based on oxygen isotopes in fossil mammals reveal climates that were approximately 1–5°C warmer than today, which is consistent with independent approaches to terrestrial paleotemperature reconstruction in this area (van Dam and Weltje, 1999; Fauquette et al., 2006), and with more general global reconstructions based on the marine record (Zachos et al., 2001). Paleoecological reconstruction for the Late Miocene in Spain and Libya based on oxygen isotopes in fossil mammals reveals taxonomic patterns that are consistent with the physiology and habitats for modern representatives of these clades. Paleoecological reconstruction of Late Miocene vegetation in northern Italy based on

carbon isotopes in paleosols confirms previous assumptions about the importance of species interaction for the extinction of an important endemic fauna.

On the other hand, several of the results reported here are surprising and challenge existing perceptions. For example, reconstruction of Late Miocene paleotemperature in Spain based on oxygen isotopes in mammals reveals a latitudinal gradient in temperature and/or aridity that was considerably higher than today. Reconstruction of paleoclimate and paleohydrology for the latest Miocene in southern Spain based on integrated sedimentological and isotopic study of alluvial and lacustrine sediments reveals a climate that became substantially wetter during the Messinian Salinity Crisis. This result challenges existing interpretations that the Messinian event had little to no effect on terrestrial environments in southwest Europe (Bertini, 2006). Further, these reconstructions provide evidence for water derived from relatively high elevations during the latest Miocene, constraining local evolution of the Betic Cordillera during this time. Paleocological reconstruction of the Late Miocene in northern Italy based on carbon isotopes in paleosols suggests overall stability in vegetation, with decreasing ecosystem variability through time. This result stands in contrast to sedimentological and palynological data, which suggest a trend toward greater aridity and increasing environmental variability in this area throughout the Late Miocene (Benvenuti et al., 1994).

In summary, the research presented in this dissertation underscores the importance of the Mediterranean region for consideration of the interplay of climate, tectonics, and ecology during important global transitions occurring in the Late Miocene.

The results of this research validate the utility of stable isotopic approaches to paleoenvironmental reconstruction, and provide a powerful complement to independent means of reconstructing terrestrial systems that are complex and often poorly understood, but nevertheless an extremely important component of the Earth System.

2. Directions for Future Research

While this research focused primarily on the Late Miocene of the western Mediterranean, I am interested in expanding on these results to allow comparison with similar data from southeastern Europe (e.g., Greece, Turkey) and northeastern Africa (e.g., Egypt). These regions are climatically distinct from much of the western Mediterranean today, and both proxy and model results indicate they may have responded very differently to events such as the Messinian Salinity Crisis (Griffin, 2002; Murphy et al., 2009).

I am also interested in expanding upon my dissertation research to include continental records from the Plio-Pleistocene, since I have come to appreciate that the Mediterranean region may be critical for understanding the onset and intensification of Northern Hemisphere glaciation (NHG) in the mid-Pliocene. Despite decades of study, the exact mechanisms underlying the onset of NHG remain a topic of intense debate (Ruddiman and Raymo, 1988; Driscoll and Haug, 1998; Philander and Fedorov, 2003; Ravelo et al., 2004). Disagreement also exists about the apparently non-linear response of glacial-interglacial cycles to orbital changes in insolation, especially for the last ~1 million years (Imbrie and Imbrie, 1980; Ruddiman and McIntyre, 1981; Kortenkamp and

Dermott, 1998; Ehrlich, 2007; Meyers et al., 2008). Further, most studies of global climate response to orbital forcings have focused on the marine record, which is more complete and continuous than that of continental basins; terrestrial environments are thus an important, often underrepresented, component of the Earth system.

The Mediterranean region is an exceptional natural laboratory in which to explore the onset of NHG, and to examine the effects of orbital cycles on both marine and terrestrial systems. High-resolution astrochronological dating is possible for many sediments in this area because the nearly land-locked nature of the Mediterranean Basin makes it especially sensitive to orbital-scale climate forcing. This sensitivity is well-documented by a Mediterranean seafloor record of cyclic, organic-rich sapropels, which are widely interpreted as representing changes in Mediterranean water column stratification and primary productivity during wet-dry climate cycles that are driven by orbital precession (Hilgen, 1991; Nijenhuis et al., 1996; Vázquez et al., 2000; Capozzi et al., 2006). The marine sapropel record has served as the basis for the construction of an extremely high-resolution, astronomically-calibrated timescale from 13 Ma to recent (Imbrie et al., 1984; Shackleton et al., 1995; Krijgsman, 2002; Krijgsman et al., 1997). In recent years, this marine astronomical timescale has been extended to continental sections in the circum-Mediterranean region, allowing unprecedented precision (<10 Kyr) in dating these records (Hilgen, 1991; Krijgsman et al., 1997; van Vugt, 2000; van Vugt et al., 2001). Furthermore, uplift of the Alpine orogenic belt and its associated ranges throughout the Neogene created many continental basins throughout the circum-

Mediterranean region that preserve a detailed sedimentary record spanning the onset of NHG.

Several aspects of the Iberian Peninsula make it particularly interesting for understanding the implications of orbital dynamics for terrestrial climate and ecosystem change. First, latitudinal climate gradients during glacial intervals were likely amplified in this area due to its position at the interface between the polar front and a warm, arid Mediterranean climate (Ruddiman and McIntyre, 1981). Second, many of the intramontane basins in Spain contain thick sequences of terrestrial Pliocene sediments spanning the onset of NHG. Finally, the effects of precession cycles on climate in Spain have been documented in terrestrial sediments extending back to the Late Miocene.

To explore the effects of orbital forcings on terrestrial climate and ecosystems during the onset of NHG, I will use an integrated, multi-proxy stable isotopic approach to study the sedimentary record of the Júcar Basin in eastern Spain. This basin is filled with more than 150 m of lacustrine, palustrine and alluvial sediments arranged in 0.5 to 1.5 m-thick beds exhibiting a strong cyclicity (Figure 5.1) that likely reflects orbital precession. Preliminary biostratigraphic and paleomagnetic analyses (Mein et al., 1978; Opdyke et al., 1997) reveal that they range in age from ca. 6 to 2 Ma, spanning the onset of NHG. The fossil record of the Júcar Basin includes the semi-aquatic water mole *Desmana* (Talpidae, Insectivora), whose oxygen isotope composition is likely a good recorder of surface and meteoric water composition. This assumption can be validated through isotopic analysis of close modern relatives, since the Iberian Peninsula is one of only two places globally with extant representatives of the subfamily Desmaninae. I will

use these constraints on changes in the oxygen isotope composition of surface water in conjunction with oxygen isotopic analysis of the extensive lacustrine carbonates in the Júcar Basin to reconstruct a high-resolution terrestrial paleotemperature record spanning most of the Pliocene.

References Cited

- Benvenuti, M., Bertini, A., and Rook, L., 1994. Facies analysis, vertebrate paleontology and palynology in the Late Miocene Baccinello-Cinigiano Basin (southern Tuscany). *Memorie della Società Geologica Italiana*, v. 48, p. 415–423.
- Bertini, A., 2006. The Northern Apennines palynological record as a contribute for the reconstruction of the Messinian palaeoenvironments. *Sedimentary Geology*, v. 188–189, p. 235–259.
- Capozzi, R., Dinelli, E., Negri, A., and Picotti, V., 2006. Productivity-generated annual laminae in mid-Pliocene sapropels deposited during precessionally forced periods of warmer Mediterranean climate. *Palaeogeography, Palaeoclimatology, Palaeoecology*, v. 235, p. 208–222.
- Driscoll, N. W. and Haug, G. H., 1998. A short circuit in thermohaline circulation: A cause for Northern Hemisphere glaciation? *Science*, v. 282, p. 436–438.
- Ehrlich, R., 2007. Solar resonant diffusion waves as a driver of terrestrial climate change. *Journal of Atmospheric and Solar-Terrestrial Physics*, v. 69, p. 759–766.

- Fauquette, S., Suc, J.-P., Bertini, A., Popescu, S.-M., Warny, S., Taoufiq, N.B., Perez Villa, M.-J., Chikhi, H., Feddi, N., Subally, D., Clauzon, G., and Ferrier, J., 2006. How much did climate force the Messinian salinity crisis? Quantified climatic conditions from pollen records in the Mediterranean region. *Palaeogeography, Palaeoclimatology, Palaeoecology*, v. 238, p. 281–301.
- Griffin, D.L., 2002, Aridity and humidity: two aspects of the late Miocene climate of North Africa and the Mediterranean: *Palaeogeography, Palaeoclimatology, Palaeoecology*, v. 182, p. 65–91.
- Hilgen, 1991. Astronomical calibration of Gauss to Matuyama sapropels in the Mediterranean and implication for the Geomagnetic Polarity Time Scale. *Earth and Planetary Science Letters*, v. 107, p. 226–244.
- Imbrie, J. and Imbrie, J.Z., 1980. Modeling the climatic response to orbital variations. *Science*, v. 207, p. 943–953.
- Imbrie, J., Hays, J.D., Martinson, D.G., McIntyre, A., Mix, A.C., Morley, J.J., Pisias, N.G., Prell, W.L., and Shackleton, N.J., 1984. The orbital theory of Pleistocene climate: support from a revised chronology of the marine $\delta^{18}\text{O}$ record. *In*: Berger, A., Imbrie, J., Hays, J., Kukla, G., and Saltzman, B. (Eds.), *Milankovitch and Climate (Part 1)*, NATO ASI Series C., Mathematical and Physical Sciences, v. 126, p. 269–305.
- Kortenkamp, S.J. and Dermott, S.F., 1998. A 100,000-year periodicity in the accretion rate of interplanetary dust. *Science*, v. 280, p. 874–876.

- Krijgsman, W., 2002. The Mediterranean: *Mare Nostrum* of Earth sciences. *Earth and Planetary Science Letters*, v. 205, p. 1–12.
- Krijgsman, W., Delahaije, W., Langereis, C.G., and de Boer, P.L., 1997. Cyclicity and NRM acquisition in the Armantes section (Miocene, Spain): Potential for an astronomical polarity time scale for the continental record. *Geophysical Research Letters*, v. 24, p. 1027–1030.
- Mein, P., Moissenet, E., and Truc, G., 1978. Les formations continentales du Néogène Supérieur des vallées du Júcar et du Cabriel au NE d'Albacete (Espagne). *Biostratigraphie et environnement. Documents des Laboratoires de Géologie de la Faculté des Sciences de Lyon*, v. 72, p. 99–147.
- Meyers, S.R., Sageman, B.B., and Pagani, M., 2008. Resolving Milankovitch: Consideration of signal and noise. *American Journal of Science*, v. 308, p. 770–786.
- Murphy, L.N., Kirk-Davidoff, D.B., Mahowald, N., and Otto-Bliesner, B.L., 2009. A numerical study of the climate response to lowered Mediterranean Sea level during the Messinian Salinity Crisis: *Palaeogeography, Palaeoclimatology, Palaeoecology*, v. 279, p. 41–59.
- Nijenhuis, I.A., Schenau, S.J., van der Weijden, C.H., Hilgen, F.J., Lourens, L.J., and Zachariasse, W.J., 1996. On the origin of upper Miocene sapropelites: A case study from the Faneromeni section, Crete (Greece). *Paleoceanography*, v. 11, p. 633–645.
- Opdyke, N.D., Mein, P., Lindsay, E.H., Perez-Gonzales, A., Moissenet, E., and Norton, V.L., 1997. Continental deposits, magnetostratigraphy and vertebrate paleontology,

- late Neogene of Eastern Spain. *Palaeogeography, Palaeoclimatology, Palaeoecology*, v. 133, p. 129–148.
- Philander, S.G. and Fedorov, A.V., 2003, Role of tropics in changing the response to Milankovitch forcing some three million years ago. *Paleoceanography*, v. 18, p.11–23.
- Ravelo, A.C., Andreasen, D., Lyle, M., Olivarez Lyle, A., and Wara, M.W., 2004. Regional climate shifts caused by gradual global cooling in the Pliocene epoch. *Nature*, v. 429, p. 263–267.
- Ruddiman, W.F. and McIntyre, A., 1981. Oceanic mechanisms for amplification of the 23,000-year ice-volume cycle. *Science*, v. 212, p. 617–627.
- Ruddiman, W.F. and McIntyre, A., 1981. The North Atlantic Ocean during the last deglaciation. *Palaeogeography, Palaeoclimatology, Palaeoecology*, v. 35, p. 145–214.
- Ruddiman, W.F., and Raymo, M.E., 1988. Northern Hemisphere climate regimes during the past 3 Ma: possible tectonic connections. *Philosophical Transactions of the Royal Society of London, B*, v. 318, p. 411–430.
- Shackleton, N.J., Crowhurst, S., Hagelberg, T, Pisias, N.G., and Schneider, D.A., 1995. A new late Neogene time scale: Application to leg 138 sites. *In*: Pisias, N.G., Mayer, L.A., Janecek, T.R., Palmer-Julson, A., and van Andel, T.H. (Eds.), *Proceedings of the Ocean Drilling Program, Scientific Results*, v. 138, p. 73–101.
- van Dam, J.A. and Weltje, G.J., 1999. Reconstruction of Late Miocene climate of Spain using rodent palaeocommunity successions: an application of end-member modeling. *Palaeogeography, Palaeoclimatology, Palaeoecology*, v. 151, p. 267–305.

- van Vugt, N., 2000. Orbital forcing in late Neogene lacustrine basins from the Mediterranean: A magnetostratigraphic and cyclostratigraphic study. *Geologica Ultraiectina*, v. 189, p. 1–167.
- van Vugt, N., Langereis, C.G., and Hilgen, F.J., 2001. Orbital forcing in Pliocene-Pleistocene Mediterranean lacustrine deposits: dominant expression of eccentricity versus precession. *Palaeogeography, Palaeoclimatology, Palaeoecology*, v. 172, p. 193–205.
- Vázquez, A., Utrilla, R., Zamarreño, I., Sierro, F.J., Flores, J.A., Francés, G., and Bárcena, M.A., 2000. Precession-related sapropelites of the Messinian Sorbas Basin (South Spain): paleoenvironmental significance. *Palaeogeography, Palaeoclimatology, Palaeoecology*, v. 158, p. 353–370.
- Zachos, J., Pagani, M., Sloan, L., Thomas, E., and Billups, K., 2001. Trends, rhythms, and aberrations in global climate 65 Ma to present. *Science*, v. 292, p. 686–693.

Figure 5.1. Cyclic sediments exposed along the Júcar River north of Alcalá del Júcar.



Complete References Cited

- Agustí, J., 2007. The biotic environments of the Late Miocene hominids. In: Henke, W. and Tattersall, I. (Eds.), *Handbook of Paleoanthropology*. Springer, Berlin, pp. 979–1010.
- Agustí, J., Cabrera, Ll., Garcés, M., and Llenas, M., 1999. Mammal turnover and global climate change in the late Miocene terrestrial record of the Vallès-Penedès Basin (NE Spain). *In*: Agustí, J., Rook, L., and Andrews, P. (Eds.), *The Evolution of Neogene Terrestrial Ecosystems in Europe*. Cambridge University Press, Cambridge, p. 397–412.
- Agustí, J., Cabrera, L., Garcés, M., Krijgsman, W., Oms, O., and Parés, J.M., 2001. A calibrated mammal scale for the Neogene of Western Europe. *State of the art. Earth-Science Reviews* 52, 247–260.
- Agustí, J., Sanz de Siria, A., and Garcés, M., 2003. Explaining the end of the hominoid experiment in Europe. *Journal of Human Evolution* 45, 145–53.
- Agustí, J., Garcés, M., and Krijgsman, W., 2006. Evidence for African-Iberian exchanges during the Messinian in the Spanish mammalian record. *Palaeogeography, Palaeoclimatology, Palaeoecology*, v. 238, p. 5–14.
- Alcalá, L., 1994. *Macromamíferos neógenos de la fosa de Alframbra-Teruel*. Instituto de Estudios Turolenses-Museo Nacional de Ciencias Naturales, Teruel.
- Alfaro, P., Delgado, J., Sanz de Galdeano, C., Galindo-Zaldívar, J., García-Tortosa, F.J., López-Garrido, A.C., López-Casado, C., Marín-Lechado, C., Gil, A., and Borque, M.J., 2008. The Baza Fault: a major active extensional fault in the central Betic

- Cordillera (south Spain). *International Journal of Earth Sciences (Geologische Rundschau)*, v. 97, p. 1353–1365.
- Alonso-Zarza, A.M. and Calvo, J.P., 2000. Palustrine sedimentation in an episodically subsiding basin: the Miocene of the northern Teruel Graben (Spain). *Palaeogeography, Palaeoclimatology, Palaeoecology*, 160, 1–21.
- Anadón, P. and Moissenet, E., 1996. Neogene basins in the Eastern Iberian Range. *In*: Friend, P.F. and Dabrio, C.J. (Eds.), *Tertiary Basins of Spain: The Stratigraphic Record of Crustal Kinematics*. Cambridge University Press, Cambridge, 68–76.
- Anadón, P., De Deckker, P., and Julià, R., 1986, The Pleistocene lake deposits of the NE Baza Basin (Spain): salinity variations and ostracod succession: *Hydrobiologia*, v. 143, p. 199–208.
- Andersen, N., Paul, H.A., Bernasconi, S.M., McKenzie, J.A., Behrens, A., Schaeffer, P., and Albrecht, P., 2001, Large and rapid climate variability during the Messinian salinity crisis: Evidence from deuterium concentrations of individual biomarkers: *Geology*, v. 29, p. 799–802.
- Anderson, J.B. and Shipp, S.S., 2001. Evolution of the West Antarctic ice-sheet. *In*: Alley, R.B. and Bindshadler, R.A. (Eds.), *The West Antarctic Ice Sheet: Behavior and Environment*. American Geophysical Union Antarctic Research Series, v. 77, p. 45–58.
- Andrews, J.E., Pedley, M., and Dennis, P.F., 2000, Palaeoenvironmental records in Holocene Spanish tufas: a stable isotope approach in search of reliable climatic archives: *Sedimentology*, v. 47, p. 961–978.

- Azzaroli, A., Boccaletti, M., Delson, E., Moratti, G., and Torre, D., 1986. Chronological and paleogeographical background to the study of *Oreopithecus bambolii*. *Journal of Human Evolution*, v. 15, p. 533–540.
- Badgley, C., Barry, J.C., Morgan, M.E., Nelson, S.V., Behrensmeyer, A.K., Cerling, T.E., and Pilbeam, D., 2008. Ecological changes in Miocene mammalian record show impact of prolonged climatic forcing. *Proceedings of the National Academy of Sciences, USA*, v. 105, p. 12145–12149.
- Bai, E., Boutton, T.W., Liu, F., Wu, X.B., Archer, S.R., and Hallmark, C.T., 2008. Spatial variation of the stable nitrogen isotope ratio of woody plants along a topographic gradient in a subtropical. *Oecologia* 159, 493–503.
- Baldocchi, D.D. and Bowling, D.R., 1999. Modelling the discrimination of $^{13}\text{CO}_2$ above and within a temperate broad-leaved forest canopy on hourly to seasonal time scales. *Plant, Cell, and Environment* 26, 231–244.
- Balesdent, J., Girardin, C., and Mariotti, A., 1993. Site-related $\delta^{13}\text{C}$ of tree leaves and soil organic matter in a temperate forest. *Ecology*, 74, 1713–1721.
- Barber, P.M., 1981, Messinian subaerial erosion of the Proto-Nile delta: *Marine Geology*, v. 44, p. 253–272.
- Bassett, D., MacLeod, K.G., Miller, J.F., Ethington, R.L., 2007. Oxygen isotopic composition of biogenic phosphate and the temperature of Early Ordovician seawater. *Palaios*, 22, 98–103.
- Begun, D.R., 2007. Fossil record of Miocene Hominoids. In: Henke, W. and Tattersall, I. (Eds.), *Handbook of Paleoanthropology*. Springer, Berlin, pp. 921–977.

- Bender, M.M., 1971. Variations in the $^{13}\text{C}/^{12}\text{C}$ ratios of plants in relation to the pathway of photosynthetic carbon dioxide fixation. *Phytochemistry* 10, 1239–1244.
- Benvenuti, M., Bertini, A., and Rook, L., 1994. Facies analysis, vertebrate paleontology and palynology in the Late Miocene Baccinello-Cinigiano Basin (southern Tuscany). *Memorie della Società Geologica Italiana* 48, 415–423.
- Benvenuti, M., Papini, M., and Rook, L., 2001. Mammal biochronology, UBSU and paleoenvironment evolution in a post-collisional basin: evidence from the Late Miocene Baccinello-Cinigiano basin in southern Tuscany, Italy. *Bollettino della Società Paleontologica Italiana* 120, 97–118.
- Bernor, R.L. and Scott, R.S., 2003. New interpretations of the systematics, biogeography and paleoecology of the Sahabi hipparions (latest Miocene) (Libya). *Geodiversitas*, 25, 297–319.
- Bertini, A., Londeix, L., Maniscalco, R., di Stefano, A., Suc, J.-P., Clauzon, G., Gautier, F., and Grasso, M., 1998. Paleobiological evidence of depositional conditions in the Salt Member, Gessoso-Solfifera Formation (Messinian, Upper Miocene) of Sicily. *Micropaleontology*, 44, 413–433.
- Bertini, A., 2006. The Northern Apennines palynological record as a contribute for the reconstruction of the Messinian palaeoenvironments. *Sedimentary Geology*, 188–189, 235–259.
- Berzi, A., 1973. The *Oreopithecus bambolii*. *Journal of Human Evolution* 2, 25–27.
- Beyer, C., 2008. Establishment of a chronostratigraphical framework for the As Sahabi sequence in northeast Libya. *In* N.T. Boaz, A. El-Arnauti, P. Pavlakis, and M.J.

- Salem (eds.) Circum-Mediterranean Geology and Biotic Evolution During the Neogene Period: The Perspective from Libya. *Garyounis Scientific Bulletin Special Issue 5*, University of Garyounis, Benghazi, Libya, p. 59–69.
- Blanc, P.-L., 2006. Improved modeling of the Messinian Salinity Crisis and conceptual implications. *Palaeogeography, Palaeoclimatology, Palaeoecology*, 238, 349–372.
- Boaz, N.T., El-Arnauti, A., Gaziry, A.W., de Heinzelin, J., and Boaz., D.D., 1987. *Neogene Paleontology and Geology of Sahabi.*, Alan R. Liss, Inc., New York.
- Bocherens, H., Koch, P.L., Mariotti, A., Geraads, D., and Jaeger, J.-J., 1996. Isotopic biogeochemistry (^{13}C , ^{18}O) of mammalian enamel from African Pleistocene hominid sites. *Palaios*, 11, 306–318.
- Bohanek, A.J., 2002. Software for reduced major axis regression. <http://www.bio.sdsu.edu/andy/rma.html>. 2009.
- Boisserie, J.-R., Lihoreau, F., and Brunet, M., 2005. The position of Hippopotamidae within Cetartiodactyla. *Proceedings of the National Academy of Sciences – USA*, 102, 1537–1541.
- Bonal, D., Sabatier, D., Motpied, P., Tremeaux, D., and Guehl, J.M., 2000. Interspecific variability of $\delta^{13}\text{C}$ among trees in rainforests of French Guiana: functional groups and canopy integration. *Oecologia* 124, 454–468.
- Boyle, E.A., 1997. Cool tropical temperatures shift the global $\square^{18}\text{O}$ -T relationship: An explanation for the ice core $\square^{18}\text{O}$ – borehole thermometry conflict? *Geophysical Research Letters*, 24, 273–276.

- Braga, J.C., Martín, J.M., and Quesada, C., 2003, Patterns and average rates of late Neogene-Recent uplift of the Betic Cordillera, SE Spain: *Geomorphology*, v. 50, p. 3–26.
- Brooks, J.R., Flanagan, L.B., Buchmann, N., and Ehleringer, J.R., 1997. Carbon isotope composition of boreal plants: Functional grouping of life forms. *Oecologia*, 110, 301–311.
- Brunet, C., Monié, P., Jolivet, L., and Cadet, J.-P., 2000. Migration of compression and extension in the Tyrrhenian Sea, insights from $^{40}\text{Ar}/^{39}\text{Ar}$ ages on micas along a transect from Corsica to Tuscany. *Tectonophysics*, v. 321, p. 127–155.
- Bryant, J.D., Luz, B., and Froelich, P.N., 1994. Oxygen isotopic composition of fossil horse tooth phosphate as a record of continental paleoclimate. *Palaeogeography, Palaeoclimatology, Palaeoecology*, 107, 303–316.
- Bryant, J.D., Koch, P.L., Froelich, P.N., Showers, W.J., and Genna, B.J., 1996. Oxygen isotope partitioning between phosphate and carbonate in mammalian apatite. *Geochimica et Cosmochimica Acta*, 60, 5145–5148.
- Buchmann, N., Guehl, J.-M., Barigah, T.S., and Ehleringer, J.R., 1997. Interseasonal comparison of CO_2 concentrations, isotopic composition, and carbon dynamics in an Amazonian rainforest (French Guiana). *Oecologia* 110, 120–131.
- Calvache, M.L. and Viseras, C., 1997, Long-term control mechanisms of stream piracy processes in southeast Spain: *Earth Surface Processes and Landforms*, v. 22, p. 93–105.

- Cande, S.C. and Kent, D.V., 1995, Revised calibration of the geomagnetic polarity timescale for the late Cretaceous and Cenozoic: *Journal of Geophysical Research*, v. 100, p. 6093–6095.
- Capozzi, R., Dinelli, E., Negri, A., and Picotti, V., 2006. Productivity-generated annual laminae in mid-Pliocene sapropels deposited during precessionally forced periods of warmer Mediterranean climate. *Palaeogeography, Palaeoclimatology, Palaeoecology*, v. 235, p. 208–222.
- Carnieri, E. and Mallegni, F., 2003. A new specimen and dental microwear in *Oreopithecus bambolii*. *HOMO* 54, 29–35.
- Casas, J.J., Gessner, M.O., Langton, P.H., Calle, D., Descals, E., and Salinas, M.J., 2006, Diversity of patterns and processes in rivers of eastern Andalusia: *Limnetica*, v. 25, p. 155–170.
- Cerling, T.E., 1984. The stable isotopic composition of modern soil carbonate and its relationship to climate. *Earth and Planetary Science Letters* 71, 229–240.
- Cerling, T.E. and Quade J., 1993, Stable carbon and oxygen isotopes in soil carbonates. *In* P.K. Swart, K.C. Lohmann, J.A. McKenzie, and S.M. Savin (eds.) *Climate Change in Continental Isotopic Records*. Geophysical Monograph 78, American Geophysical Union, Washington, D.C., p. 217–231.
- Cerling, T.E., Quade, J., Wang, Y., and Bowman, J.R., 1989. Carbon isotopes in soils and palaeosols as ecology and palaeoecology indicators. *Nature* 341, 138–139.

- Cerling, T.E., Solomon, D.K., Quade, J., and Bowman, J.R., 1991. On the isotopic composition of carbon in soil carbon dioxide. *Geochimica et Cosmochimica Acta* 55, 3403–3405.
- Cerling, T.E., Wang, Y., and Quade, J., 1993. Expansion of C₄ ecosystems as an indicator of global ecological change in the late Miocene.
- Cerling, T.E., Harris, J.M., MacFadden, B.J., Leakey, M.G., Quade, J., Eisenmann, V., and Ehleringer, J.R., 1997. Global vegetation change through the Miocene/Pliocene boundary. *Nature*, 389, 153–158.
- Cerling, T.E., Hart, J.A., Hart, T.B., 2004. Stable isotope ecology in the Ituri Forest. *Oecologia* 138, 5–12.
- Cerling, T.E., Harris, J.M., Hart, J.A., Kaleme, P., Klingel, H., Leakey, M.G., Levin, N.E., Lewison, R.L., and Passey, B.H., 2008. Stable isotope ecology of the common hippopotamus. *Journal of Zoology*, 276, 204–212.
- Chen, Q., Shen, C., Sun, Y., Peng, S., Yi, W., Li, Z., and Jiang, M., 2005. Spatial and temporal distribution of carbon isotopes in soil organic matter at the Dinghushan Biosphere Reserve, South China. *Plant and Soil* 273, 115–128.
- Chevillat, V.S., Siegwolf, R.T.W., Pepin, S., and Körner, C., 2005. Tissue-specific variation of $\delta^{13}\text{C}$ in mature canopy trees in a temperate forest in central Europe. *Basic and Applied Ecology* 6, 519–534.
- Cita, M.B., 1976, Biodynamic effects of the Messinian salinity crisis on the evolution of planktonic foraminifera in the Mediterranean: *Palaeogeography, Palaeoclimatology, Palaeoceanography*, v. 20, p. 23–42.

- Cita, M.B., 2006, Exhumation of Messinian evaporites in the deep-sea and creation of deep anoxic brine-filled collapsed basins: *Sedimentary Geology*, v. 188–189, p. 357–378.
- Clauzon, G., Suc, J.-P., Gautier, F., Berger, A., and Loutre, M.-F., 1996. Alternate interpretation of the Messinian salinity crisis: Controversy resolved? *Geology*, 24, 363–366.
- Clementz, M.T., Holroyd, P.A., and Koch, P.L., 2008. Identifying aquatic habits of herbivorous mammals through stable isotope analysis. *Palaios*, 23, 574–585.
- Collins, R.P. and Jones, M.B., 1986. The influence of climatic factors on the distribution of C4 species in Europe. *Plant Ecology* 64, 121–129.
- Collister, J.W., Rieley, G., Stern, B., Eglinton, G., and Fry, B., 1994. Compound-specific $\delta^{13}\text{C}$ analyses of leaf lipids from plants with differing carbon dioxide metabolisms. *Organic Geochemistry* 21, 619–627.
- Cormie, A.B., Luz, B., and Schwarz, H.P., 1994. Relationship between the hydrogen and oxygen isotopes of deer bone and their use in the estimation of relative humidity. *Geochimica et Cosmochimica Acta*, 58, 3439–3449.
- Costeur, L., Montuire, S., Legendre, S., and Maridet, O., 2007. The Messinian event: What happened to the peri-Mediterranean mammalian communities and local climate? *Geobios*, 40, 423–431.
- Cruz-San Julian, J., Araguas, L., Rozanski, K., Cardenal, J., Hidalgo, M.C., García-Lopez, S., Martínez-Garrido, J.C., Moral, F., and Olias, M., 1992, Sources of

- precipitation over South-Eastern Spain and groundwater recharge. An isotopic study: *Tellus*, v. 44B, p. 226–236.
- Dansgaard, W., 1964. Stable isotopes in precipitation. *Tellus*, 16, 436–438.
- de Heinzelin, J. and El-Arnauti, A., 1987. The Sahabi Formation and related deposits. *In* N.T. Boaz, A. El-Arnauti, A.W. Gaziry, J. de Heinzelin, and D.D. Boaz., 1987. *Neogene Paleontology and Geology of Sahabi.*, Alan R. Liss, Inc., New York., p. 1–21.
- Deines, P., Langmuir, D., and Harmon, R.S., 1974. Stable carbon isotope ratios and the existence of a gas phase in the evolution of carbonate ground waters. *Geochimica et Cosmochimica Acta* 38, 1147–1164.
- Delgado-Huertas, A., Iacumin, P., Stenni, B., Sánchez-Chillón, B., and Longinelli, A., 1995. Oxygen isotope variations of phosphate in mammalian bone and tooth enamel. *Geochimica et Cosmochimica Acta*, 59, 4299–4305.
- Delson, E., 1986. An anthropoid enigma: Historical introduction the study of *Oreopithecus bambolii*. *Journal of Human Evolution* 15, 523–531.
- DeLucia, E.H. and Schlesinger, W.H., 1991. Resource-use efficiency and drought tolerance in adjacent Great Basin and Sierran plants. *Ecology* 72, 51–58.
- Diefendorf, A.F., Mueller, K.E., Wing, S.L., Koch, P.L., and Freeman, K.H., 2010. Global patterns in leaf ^{13}C discrimination and implications for studies of past and future climate. *Proceedings of the National Academy of Sciences USA* 107, 5738–5743.

- Dodd, M.B., Lauenroth, W.K., and Welker, J.M., 1998. Differential water resource use by herbaceous and woody plant life-forms in a shortgrass steppe community. *Oecologia* 117, 504–512.
- Domingo, L., Grimes, S.T., Domingo, M.S., and Alberdi, M.T., 2009. Paleoenvironmental conditions in the Spanish Miocene-Pliocene boundary: isotopic analyses of Hipparion dental enamel. *Naturwissenschaften*, v. 96, p. 503–511.
- Domingo, L., Cuevas-González, J., Grimes, S.T., Hernández Fernández, M., and López-Martínez, N., 2009. Multiproxy reconstruction of the palaeoclimate and palaeoenvironment of the Middle Miocene Somosaguas site (Madrid, Spain) using herbivore dental enamel. *Palaeogeography, Palaeoclimatology, Palaeoecology*, 272, 53–68.
- Driscoll, N. W. and Haug, G. H., 1998. A short circuit in thermohaline circulation: A cause for Northern Hemisphere glaciation? *Science*, v. 282, p. 436–438.
- Dungait, J.A.J., Docherty, G., Straker, V., and Evershed, R.P., 2008. Interspecific variation in bulk tissue, fatty acid and monosaccharide $\delta^{13}\text{C}$ values of leaves from a mesotrophic grassland plant community. *Phytochemistry* 69, 2041–2051.
- Edwards, E.J., Osborne, C.P., Strömberg, C.A.E., Smith, S.A., and C₄ Grasses Consortium, 2010. The origins of C₄ grasslands: Integrating evolutionary and ecosystem science. *Science*, v. 328, p. 587–591.
- Ehleringer, J.R. and Cooper, T.A., 1988. Correlations between carbon isotope ratio and microhabitat in desert plants. *Oecologia* 76, 562–566.

- Ehleringer, J.R., Lin, Z.F., Field, C.B., Sun, G.C., and Kuo, C.Y., 1987. Leaf carbon isotope ratios of plants from a subtropical monsoon forest. *Oecologia* 72, 109–114.
- Ehrlich, R., 2007. Solar resonant diffusion waves as a driver of terrestrial climate change. *Journal of Atmospheric and Solar-Terrestrial Physics*, v. 69, p. 759–766.
- Engesser, B., 1989. The Late Tertiary small mammals of the Maremma region (Tuscany, Italy). II Part: Muridae and Cricetidae (Rodentia, Mammalia). *Bollettino della Società Paleontologica Italiana* 29, 227–252.
- Escuerdo, A., Mediavilla, S., and Heilmeyer, H., 2008. Leaf longevity and drought: avoidance of the costs and risks of early leaf abscission as inferred from the leaf carbon isotopic composition. *Functional Plant Biology* 35, 705–713.
- Farris, F. and Strain B.R., 1978. The effects of water-stress on leaf H₂¹⁸O enrichment. *Radiation and Environmental Biophysics*, 15, 167–202.
- Fauquette, S., Suc, J.-P., Guiot, J., Diniz, F., Feddi, N., Zheng, Z., Bessais, E., and Drivaliari, A., 1999. Climate and biomes in the West Mediterranean area during the Pliocene. *Palaeogeography, Palaeoclimatology, Palaeoecology*, 152, 15–36.
- Fauquette, S., Suc, J.-P., Bertini, A., Popescu, S.-M., Warny, S., Taoufiq, N.B., Perez Villa, M.-J., Chikhi, H., Feddi, N., Subally, D., Clauzon, G., and Ferrier, J., 2006. How much did climate force the Messinian salinity crisis? Quantified climatic conditions from pollen records in the Mediterranean region. *Palaeogeography, Palaeoclimatology, Palaeoecology*, 238, 281–301.
- Fernández, J., Soria, J., and Viseras, C., 1996, Stratigraphic architecture of the Neogene basins in the central sector of the Betic Cordillera (Spain): tectonic control and base-

- level changes, *in* Friend, P.F. and Dabrio, C., eds., *Tertiary Basins of Spain: The stratigraphic record of crustal kinematics*: Cambridge, Cambridge University Press, p. 353–365.
- Fluteau, F., Suc, J.P., and Fauquette, S., 2003. Modelling the climatic consequences of the Messinian Salinity Crisis. *Geophysical Research Abstracts*, 5, 11387.
- Fox, D.L. and Koch, P.L., 2003. Tertiary history of C₄ biomass in the Great Plains, USA. *Geology*, v. 31, p. 809–812.
- Fox, D.L. and Koch, P.L., 2004. Carbon and oxygen isotopic variability in Neogene paleosol carbonates: constraints on the evolution of the C₄-grasslands of the Great Plains, USA. *Palaeogeography, Palaeoclimatology, Palaeoecology* 207, 305–329.
- Fricke, H.C., Clyde, W.C., and O’Neil, J.R., 1998. Intra-tooth variations in $\delta^{18}\text{O}$ (PO₄) of mammalian tooth enamel as a record of seasonal variations in continental climate variables. *Geochimica et Cosmochimica Acta*, 62, 1839–1850.
- Fricke, H.C. and O’Neil, J.R., 1999. The correlation between ¹⁸O/¹⁶O ratios of meteoric water and surface temperature: Its use in investigating terrestrial climate change over geologic time. *Earth and Planetary Science Letters*, 170, 181–196.
- Garcés, M., Agustí, J., and Parés, J.M., 1997a. Late Pliocene continental magnetochronology in the Guadix-Baza Basin (Betic Ranges, Spain). *Earth and Planetary Science Letters*, 146, 677–687.
- Garcés, M., Krijgsman, W., van Dam, J., Calvo, J.P., Alcalá, L., and Alonso-Zarza, A.M., 1997b. Late Miocene alluvial sediments from the Teruel area:

- Magnetostratigraphy, magnetic susceptibility, and facies organization. *Acta Geologica Hispanica*, 32, 171–184.
- Garcés, M., Krijgsman, W., and Agustí, J., 1998. Chronology of the late Turolian deposits of the Fortuna basin (SE Spain): implications for the Messinian evolution of the eastern Betics. *Earth and Planetary Science Letters*, 163, 69–81.
- Garcés, M., Krijgsman, W., and Agustí, J., 2001. Chronostratigraphic framework and evolution of the Fortuna basin (Eastern Betics) since the Late Miocene. *Basin Research*, 13, 199–216.
- García, C.M. and Niell, F.X., 1993, Seasonal change in a saline temporary lake (Fuente de Piedra, southern Spain): *Hydrobiologia*, v. 267, p. 211–223.
- García Aguilar, J.M. and Martín, J.M., 2000, Late Neogene to recent continental history and evolution of the Guadix-Baza Basin (SE Spain): *Revista de la Sociedad Geologica de España*, v. 13, p. 65–77.
- García-Alix, A., Minwer-Barakat, R., Martín-Suárez, E., and Freudenthal, M., 2007. The southernmost record of fossil Castoridae (Mammalia, Rodentia) in Europe. *Geodiversitas*, 29, 435–440.
- García-Alix, A., Minwer-Barakat, R., Martín Suárez, E., Freudenthal, M., and Martín, J.M., 2008, Late Miocene-Early Pliocene climatic evolution of the Granada Basin (southern Spain) deduced from the paleoecology of the micromammal associations: *Palaeogeography, Palaeoclimatology, Palaeoceanography*, v. 265, p. 214–225.

- García-Alix, A., Minwer-Barakat, R., Martín, J.M., Martín Suárez, E., and Freudenthal, M., 2008, Biostratigraphy and sedimentary evolution of Late Miocene and Pliocene continental deposits of the Granada Basin: *Lethaia*, v. 41, p. 431–446.
- Garten, C.T. and Taylor, G.E., Jr., 1992. Foliar $\delta^{13}\text{C}$ within a temperate deciduous forest: spatial, temporal, and species sources of variation. *Oecologia* 90, 1–7.
- Garten, C.T., Jr., Cooper, L.W., Post, W.M., III, and Hanson, P.J., 2000. Climate controls on forest soil C isotope ratios in the southern Appalachian Mountains. *Ecology* 81, 1108–1119.
- Gat, J.R., 1995, Stable isotopes of fresh and saline lakes, *in* Lerman, A., Imboden, D., and Gat, J., eds., *Physics and chemistry of lakes*: New York, Springer-Verlag, p. 139–165.
- Gaziry, A.W., 1987. *Merycopotamus petrocchii* (Artiodactyla, Mammalia) from Sahabi, Libya. *In* N.T. Boaz, A. El-Arnauti, A.W. Gaziry, J. de Heinzelin, and D.D. Boaz., 1987. *Neogene Paleontology and Geology of Sahabi.*, Alan R. Liss, Inc., New York., p. 287–302.
- Gerdol, R., Iacumin, P., Marchesini, R., and Bragazza, L., 2000. Water- and nutrient-use efficiency of a deciduous species, *Vaccinium myrtillus*, and an evergreen species, *V. vitis-idaea*, in a subalpine dwarf shrub heath in the Southern Alps, Italy. *Oikos* 88, 19–32.
- Gervais, P., 1972. Sur un singe fossile, d'espèce non encore décrite, qui a été découvert au Monte-Bamboli (Italie). *Comptes Rendus de l'Académie des Sciences de Paris* 74, 1217–1223.

- Gibert, L., Scott, G., and Ferrández-Cañadel, C., 2006. Evaluation of the Olduvai subchron in the Orce ravine (SE Spain). Implications for Plio-Pleistocene mammal biostratigraphy and the age of the Orce archaeological sites. *Quaternary Science Reviews*, 25, 507–525.
- Gibert, L., Scott, G., Martin, R., Gibert, J., 2007. The Early to Middle Pleistocene boundary in the Baza Basin (Spain). *Quaternary Science Reviews*, 26, 2067–2089.
- González-Sampériz, P., Valero-Garcées, B.L., Moreno, A., Morellon, M., Navas, A., Machín, J., and Delgado-Huertas, A., 2008, Vegetation changes and hydrological fluctuations in the Central Ebro Basin (NE Spain) since the Late Glacial period: Saline lake records: *Palaeogeography, Palaeoclimatology, Palaeoecology*, v. 259, p. 157–181.
- Griffin, D.L., 2002. Aridity and humidity: two aspects of late Miocene climate of North Africa and the Mediterranean. *Palaeogeography, Palaeoclimatology, Palaeoecology*, 182, 65–91.
- Griffin, D.L., 2006. The late Neogene Sahabi rivers of the Sahara and their climatic and environmental implications for the Chad Basin. *Journal of the Geological Society*, London, 163, 905–921.
- Hanba, Y.T., Mori, S., Lei, T.T., Koike, T., and Wada, E., 1997. Variations in leaf $\delta^{13}\text{C}$ along a vertical profile of irradiance in a temperate Japanese forest. *Oecologia* 110, 253–261.
- Harrison, T., 1986. A reassessment of the phylogenetic relationships of *Oreopithecus bambolii* Gervais. *Journal of Human Evolution* 15, 541–583.

- Harrison, T., 2010. Apes among the tangled branches of human origins. *Science* 327, 532–534.
- Harrison, T.S. and Harrison, T., 1989. Palynology of the late Miocene Oreopithecus-bearing lignite from Baccinello, Italy. *Palaeogeography, Palaeoclimatology, Palaeoecology* 76, 45–65.
- He, C.-X., Li, J.-Y., Zhou, P., Guo, M., and Zheng, Q.-S., 2008. Changes of leaf morphological, anatomical structure and carbon isotope ratio with the height of the Wangtian Tree (*Parashorea chinensis*) in Xishuangbanna, China.
- Hedges, R.E.M., 2002. Bone diagenesis: An overview of processes. *Archaeometry*, 44, 319–328.
- Hemming, D., Yakir, D., Ambus, P., Aurela, M., Bessons, C., Black, K., Buchmann, N., Burlett, R., Cescatti, A., Clement, R., Gross, P., Granier, A., Grünwald, T., Havrankova, K., Janous, D., Janssens, I.A., Knohl, A., Östner, B., Kowalski, A., Laurila, T., Mata, C., Marcolla, B., Matteucci, G., Moncrieff, J., Moors, E.J., Osborne, B., Santos Pereira, J., Pihlatie, M., Pilegaard, K., Ponti, F., Rosova, Z., Rossi, F., Scartazza, A., and Vesala, T., 2005. Pan-European $\delta^{13}\text{C}$ values of air and organic matter from forest ecosystems. *Global Change Biology* 11, 1065–1093.
- Henderson, A.K. and Shuman, B.N., 2009, Hydrogen and oxygen isotopic compositions of lake water in the western United States: *Geological Society of America Bulletin*, v. 121, p. 1179–1189.

- Hilgen, 1991. Astronomical calibration of Gauss to Matuyama sapropels in the Mediterranean and implication for the Geomagnetic Polarity Time Scale. *Earth and Planetary Science Letters*, v. 107, p. 226–244.
- Hobbie, E.A., Johnson, M.G., Rygielwicz, P.T., Tingey, D.T., and Olszyk, D.M., 2004. Isotopic estimates of new carbon inputs into litter and soils in a four-year climate change experiment with Douglas-fir. *Plant and Soil* 259, 331–343.
- Hodell, D.A., Benson, R.H., Kent, D.V., Boersma, A., and Rakic-El Bied, K., 1994. Magnetostratigraphic, biostratigraphic, and stable isotope stratigraphy of an upper Miocene drill core from the Sale Briqueterie (northwestern Morocco): A high-resolution chronology for the Messinian stage. *Paleoceanography*, 9, 835–856.
- Hollander, D.J. and Smith, M.A., 2001, Microbially mediated carbon cycling as a control on the $\delta^{13}\text{C}$ of sedimentary carbon in eutrophic Lake Mendota (USA): New models for interpreting isotopic excursions in the sedimentary record: *Geochimica et Cosmochimica Acta*, v. 65, p. 4321–4337.
- Holtum, J.A.M. and Winter, K., 2005. Carbon isotope composition of canopy leaves in a tropical forest in Panama throughout a seasonal cycle. *Trees* 19, 545–551.
- Hoppe, K.A., Amundson, R., Vavra, M., McClaran, P., and Anderson, D.L., 2004a. Isotopic analysis of tooth enamel carbonate from modern North American feral horses: implications for paleoenvironmental reconstructions. *Palaeogeography, Palaeoclimatology, Palaeoecology*, 203, 299–311.

- Hoppe, K.A., Stover, S.M., Pascoe, J.R., and Amundson, R., 2004b. Tooth enamel biomineralization in extant horses: implications for isotopic microsampling. *Palaeogeography, Palaeoclimatology, Palaeoecology*, 206, 355–365.
- Hostetler, S.W., Giorgi, F., Bates, G.T., and Bartlein, P.J., 1994. Lake-atmosphere feedbacks associated with Paleolakes Bonneville and Lahontan. *Science*, 263, 665–668.
- Hsü, K.J., Ryan, W.B.F., and Cita, M.B., 1973. Late Miocene desiccation of the Mediterranean. *Nature*, 242, 240–244.
- Hsü, K.J., Montadert, L., Beroulli, D., Cita, M.B., Erickson, A., Garrison, R.E., Kidd, R.B., Mèlierés, F., Müller, C., and Wright, R., 1977. History of the Mediterranean salinity crisis. *Nature*, 267, 399–403.
- Hugueney, M. and Esuillie, F., 1996. Fossil evidence for the origin of behavioral strategies in Early Miocene Castoridae, and their role in the evolution of the family. *Paleobiology*, 22, 507–513.
- Hultine, K.R. and Marshall, J.D., 2000. Altitude trends in conifer leaf morphology and stable carbon isotope composition. *Oecologia* 123, 32–40.
- Hürzeler, J., 1958. *Oreopithecus bambolii* Gervais. A preliminary report. *Verhandlungen der Naturforschenden Gesellschaft in Basel* 69, 1–48.
- Iacumin, P., Bocherens, H., Mariotti, A., and Longinelli, A., 1996. Oxygen isotope analyses of co-existing carbonate and phosphate in biogenic apatite: a way to monitor diagenetic alteration of bone phosphate? *Earth and Planetary Science Letters*, 142, 1–6.

- IAEA, 2009. Global Network of Isotopes in Precipitation (GNIP) data: 2000–2004.
<http://isohis.iaea.org>. 2009.
- IAEA, 2010, Global Network of Isotopes in Precipitation (GNIP) data: 1961–2004:
<http://isohis.iaea.org> (May 2010).
- Imbrie, J. and Imbrie, J.Z., 1980. Modeling the climatic response to orbital variations.
Science, v. 207, p. 943–953.
- Imbrie, J., Hays, J.D., Martinson, D.G., McIntyre, A., Mix, A.C., Morley, J.J., Pisias, N.G., Prell, W.L., and Shackleton, N.J., 1984. The orbital theory of Pleistocene climate: support from a revised chronology of the marine $\delta^{18}\text{O}$ record. *In*: Berger, A., Imbrie, J., Hays, J., Kukla, G., and Saltzman, B. (Eds.), *Milankovitch and Climate (Part 1)*, NATO ASI Series C., Mathematical and Physical Sciences, v. 126, p. 269–305.
- Inagaki, Y., Miura, S., and Kohzu, A., 2004. Effects of forest type and stand age on litterfall quality and soil N dynamics in Shikoku district, southern Japan. *Forest Ecology and Management* 202, 107–117.
- Jacobs, B.F., Kingston, J.D., and Jacobs, L.L., 1999. The origin of grass-dominated ecosystems. *Annals of the Missouri Botanical Gardens*, v. 68, p. 590–643.
- Janis, C.M., Damuth, J., and Theodor, J.M., 2000. Miocene ungulates and terrestrial primary productivity: Where have all the browsers gone? *Proceedings of the National Academy of Sciences, USA*, v. 97, p. 7899–7904.

- Janis, C.M., Damuth, J., and Theodor, J.M., 2002. The origins and evolution of the North American grassland biome: the story from the hoofed mammals. *Palaeogeography, Palaeoclimatology, Palaeoecology*, v. 177, p. 183–198.
- Janis, C.M., Damuth, J., and Theodor, J.M., 2004. The species richness of Miocene browsers, and implications for habitat type and primary productivity in the North American grassland biome. *Palaeogeography, Palaeoclimatology, Palaeoecology*, v. 207, p. 371–398.
- Jessup, K.E., Barnes, P.W., and Boutton, T.W., 2003. Vegetation dynamics in a *Quercus-Juniperus* savanna: An isotopic assessment. *Journal of Vegetation Science* 14, 841–852.
- Johnson, C., Harbury, N., and Hurford, A.J., 1997. The role of extension in the Miocene denudation of the Nevado-Filábride Complex, Betic Cordillera (SE Spain): Tectonics, v. 16, p. 189–204.
- Jones, T.J., Luton, C.D., Santiago, L.S., and Goldstein, G., 2010. Hydraulic constraints on photosynthesis in subtropical evergreen broad leaf forest and pine woodland trees of the Florida Everglades. *Trees* 24, 471–478.
- Jungers, W.L., 1988. Body size and morphometric affinities of the appendicular skeleton in *Oreopithecus bambolii* (IGF 11778). *Journal of Human Evolution* 16, 445–456.
- Keogh, S.M. and Butler, R.W.H., 1999. The Mediterranean water body in the late Messinian: interpreting the record from marginal basins on Sicily. *Journal of the Geological Society, London*, 156, 837–846.

- Keough, J.R., Sierszen, M.E., and Hagley, C.A., 1996. Analysis of a Lake Superior coastal food web with stable isotope techniques. *Limnology and Oceanography* 41, 136–146.
- Kim, S.-T and O'Neil, J.R., 1997, Equilibrium and nonequilibrium oxygen isotope effects in synthetic carbonates: *Geochimica et Cosmochimica Acta*, v. 61, p. 3461–3475.
- Kloepfel, B.D., Gower, S.T., Treichel, I.W., and Kharuk, S., 1998. Foliar carbon isotope discrimination in *Larix* species and sympatric evergreen conifers: a global comparison. *Oecologia* 114, 153–159.
- Koch, P.L., 1998. Isotopic reconstruction of past continental environments. *Annual Review of Earth and Planetary Sciences*, 27, 573–613.
- Kohfahl, C., Rodriguez, M., Fenk, C., Menz, C., Benavente, J., Hubberten, H., Meyer, H., Paul, L., Knappe, A., López-Geta, J.A., and Pekdeger, A., 2008, Characterising flow regime and interrelation between surface-water and ground-water in the Fuente de Piedra salt lake basin by means of stable isotopes, hydrogeochemical and hydraulic data: *Journal of Hydrology*, v. 351, p. 170–187.
- Kohfahl, C., Sprenger, C., Benavente Herrera, J., Meyer, H., Fernández Chacón, F., and Pekdeger, A., 2008, Recharge sources and hydrogeochemical evolution of groundwater in semiarid and karstic environments: A field study in the Granada Basin (Southern Spain): *Applied Geochemistry*, v. 23, p. 846–862.
- Köhler, M. and Moyà-Sola, S., 1997. Ape-like or hominid-like? The positional behavior of *Oreopithecus bambolii* reconsidered. *Proceedings of the National Academy of Sciences USA* 94, 11747–11750.

- Köhler, M., Moyà-Sola, S., and Agustí, J., 1998. Miocene/Pliocene shift: one step or several? *Nature*, v. 393, p. 126.
- Köhler, M., Moyà-Solà, S., and Alba, D.M., 2000. *Macaca* (Primates, Cercopithecoidea) from the Late Miocene of Spain. *Journal of Human Evolution*, 38, 447–452.
- Kohn, M.J., 1996. Predicting animal $\delta^{18}\text{O}$: Accounting for diet and physiological adaptation. *Geochimica et Cosmochimica Acta*, 60, 4811–4829.
- Kohn, M.J., Schoeninger, M.J., and Barker, William W., 1999. Altered states: Effects of diagenesis on fossil tooth chemistry. *Geochimica et Cosmochimica Acta*, 63, 2737–2747.
- Kohn, M.J. and Cerling, T.E., 2002. Stable isotope compositions of biological apatite. In: Kohn, M.J., Rakovan, J., and Hughes, J.M. (Eds.), *Phosphates: Geochemical, Geobiological, and Materials Importance*. *Reviews in Mineralogy and Geochemistry*, 48, 455–488.
- Kohn, M.J., Schoeninger, M.J., and Valley, J.W., 1996. Herbivore tooth oxygen isotope compositions: Effects of diet and physiology. *Geochimica et Cosmochimica Acta*, 60, 3889–3896.
- Kohorn, L.U., Goldstein, G., and Rundel, P.W., 1994. Morphological and isotopic indicators of growth environment: variability in $\delta^{13}\text{C}$ in *Simmondsia chinensis*, a dioecious desert shrub. *Journal of Experimental Botany* 45, 1817–1822.
- Kortenkamp, S.J. and Dermott, S.F., 1998. A 100,000-year periodicity in the accretion rate of interplanetary dust. *Science*, v. 280, p. 874–876.

- Kouwenhoven, T.J., Seidenkrantz, M.-S., and van der Zwaan, G.J., 1999, Deep-water changes: the near-synchronous disappearance of a group of benthic foraminifera from the Late Miocene Mediterranean: *Palaeogeography, Palaeoclimatology, Palaeoecology*, v. 152, p. 259–281.
- Krijgsman, W., 2002. The Mediterranean: *Mare Nostrum* of Earth sciences. *Earth and Planetary Science Letters*, 205, 1–12.
- Krijgsman, W., Hilgen, F.J., Raffi, I., Sierro, F.J., and Wilson, D.S., 1999. Chronology, causes and progression of the Messinian Salinity Crisis. *Nature*, v. 400, p. 652–655.
- Krijgsman, W., Garcés, M., Agustí, J., Raffi, I., Taberner, C., and Zachariasse, W.J., 2000. The ‘Tortonian salinity crisis’ of the eastern Betics (Spain). *Earth and Planetary Science Letters*, 181, 497–511.
- Kruvier, P.P., Krijgsman, W., Langereis, C.G., and Dekkers, M.J., 2002. Cyclostratigraphy and rock-magnetic investigation of the NRM signal in late Miocene palustrine-alluvial deposits of the Librilla section (SE Spain). *Journal of Geophysical Research*, 107, 1–18.
- Ku, H., 1966. Notes on the use of propagation of error formulas. *Journal of Research of the National Bureau of Standards*, 70C, 263–273.
- Kuiper, K.F., Krijgsman, W., Garcés, M., and Wijbrans, J.R., 2006. Revised isotopic ($^{40}\text{Ar}/^{39}\text{Ar}$) age for the lamproite volcano of Cabezos Negros, Fortuna Basin (Eastern Betics, SE Spain). *Palaeogeography, Palaeoclimatology, Palaeoecology*, 238, 53–63.

- Land, L.S., Lundelius, E.L., and Valastro, S., 1980. Isotopic ecology of deer bones. *Palaeogeography, Palaeoclimatology, Palaeoecology*, 32, 143–151.
- Le Roux, X., Bariac, T., Sinoquet, H., Genty, B., Piel, C., Mariotti, A., Girardin, C., and Richard, P., 2001. Spatial distribution of leaf water-use efficiency and carbon isotope discrimination within an isolated tree crown. *Plant, Cell and Environment* 24, 1021–1032.
- Lear, C.H., Elderfield, H., and Wilson, P.A., 2000, Cenozoic deep-sea temperatures and global ice volumes from Mg/Ca in benthic foraminiferal calcite: *Science*, v. 287, p. 269–272.
- Levin, N.E., Cerling, T.E., Passey, B.H., Harris, J.M., and Ehleringer, J.R., 2006. A stable isotope aridity index for terrestrial environments. *Proceedings of the National Academy of Sciences – USA*, 103, 11201–11205.
- Lawver, L.A. Gahagan, L.M., 2003. Evolution of Cenozoic seaways in the circum-Antarctic region. *Palaeogeography, Palaeoclimatology, Palaeoecology*, v. 198, p. 11–37.
- Leffler, A.J. and Enquist, B.J., 2002. Carbon isotope composition of tree leaves from Guanacaste, Costa Rica: comparison across tropical forests and tree life history. *Journal of Tropical Ecology* 18, 151–159.
- Li, Z.-H., Leavitt, S.W., Mora, C.I., and Liu, R.-M., 2005. Influence of earlywood-latewood size and isotope differences on long-term tree-ring $\delta^{13}\text{C}$ trends. *Chemical Geology* 216, 191–201.

- Li, Hong-Chun, Xiao-Mei Xu, Teh-Lung Ku, Chen-Feng You, Buchenheim, H.P., and Peters, R., 2008, Isotopic and geochemical evidence of palaeoclimate changes in Salton Basin, California, during the past 20 kyr: 1. $\delta^{18}\text{O}$ and $\delta^{13}\text{C}$ records in lake tufa deposits: *Palaeogeography, Palaeoclimatology, Palaeoecology*, v. 259, p. 182–197.
- Liu, Z., Pagani, M., Zinniker, D., DeConto, R., Huber, M., Brinkhuis, H., Shah, S.R., Leckie, R.M., and Pearson, A., 2009. Global cooling during the Eocene-Oligocene climate transition. *Science*, v. 323, p. 1187–1190.
- Lockheart, M.J., Van Bergen, P.F., and Evershed, R.P., 1997. Variations in the stable carbon isotope compositions of individual lipids from the leaves of modern angiosperms: implications for the study of higher land plant-derived sedimentary organic matter. *Organic Geochemistry* 26, 137–153.
- Lofi, J., Gorini, C., Berné, S., Clauzon, G., Dos Reis, A.T., Ryan, W.B.F., and Steckler, M., 2005, Erosional processes and paleo-environmental changes in the western Gulf of Lions (SW France) during the Messinian Salinity Crisis: *Marine Geology*, v. 217, p. 1–30.
- Lonergan, L. and White, N., 1997. Origin of the Betic-Rif mountain belt. *Tectonics*, v. 16, p. 504–522.
- Longinelli, A., 1984. Oxygen isotopes in mammal bone phosphate: A new tool for paleohydrological and paleoclimatological research. *Geochimica et Cosmochimica Acta*, 48, 385–390.
- Longinelli, A. and Nuti, S., 1973. Revised phosphate-water isotopic temperature scale. *Earth and Planetary Science Letters*, 19, 373–376.

- Lorenz, H.G., 1968. Stratigraphisches und micropaläontologisches Untersuchungen des Braunkohlengebietes von Baccinello (Grosseto, Italien). *Rivista Italiana di Paleontologia e Stratigrafia* 74, 147–270.
- Luz, B. and Kolodny, Y., 1985. Oxygen isotope variations in phosphate of biogenic apatites, IV. Mammal teeth and bones. *Earth and Planetary Science Letters*, 75, 29–36.
- Luz, B. and Koldny, Y., 1989. Oxygen isotope variation in bone phosphate. *Applied Geochemistry*, 4, 317–323.
- Luz, B., Kolodny, Y., and Horowitz, M., 1984. Fractionation of oxygen isotopes between mammalian bone-phosphate and environmental drinking water. *Geochimica et Cosmochimica Acta*, 48, 1689–1693.
- Luz, B., Cormie, A.B., and Schwarz, H.P., 1990. Oxygen isotope variations in phosphate of deer bones. *Geochimica et Cosmochimica Acta*, 54, 1723–1728.
- Luzón, A., Mayayo, M.J., and Pérez, A., 2009, Stable isotope characterization of co-existing carbonates from the Holocene Gallocanta lake (NE Spain): Palaeolimnological implications: *International Journal of Earth Sciences (Geologische Rundschau)*, v. 98, p. 1129–1150.
- MacFadden, B.J., 1998. Equidae. *In*: Janis, C.M., Scott, K.M., and Jacobs, L.L. (Eds.), *Evolution of Tertiary Mammals of North America*. Cambridge University Press, Cambridge, p. 537–559.
- Majoube, M., 1971, Fractionnement en oxygen-18 et en deuterium entre l'eau et sa vapor: *Journal de Chimie et de Physique*, v. 68, p. 1423–1426.

- Martín-Puertas, C., Valero-Garcés, B.L., Mata, M.P., González-Sampériz, P., Bao, R., Moreno, A., and Stefanova, V., 2008, Arid and humid phases in southern Spain during the last 4000 years: the Zoñar Lake record, *Córdoba: The Holocene*, v. 18, p. 907–921.
- Martín-Puertas, C., Valero-Garcés, B.L., Brauer, A., Mata, M.P., Delgado-Huertas, A., and Dulski, P., 2009, The Iberian-Roman Humid Period (2600–1600 cal yr BP) in the Zoñar Lake varve record (Andalucía, southern Spain): *Quaternary Research*, v. 71, p. 108–120.
- Martín-Suárez, E., 1988, Sucesiones de micromamíferos en la depresión de Guadix-Baza (España) [Ph.D. thesis]: Universidad de Granada, 241 p.
- Martín-Suárez, E., Oms, O., Freudenthal, M., Agustí, J., and Parés, J.M., 1998, Continental Mio-Pliocene transition in the Granada Basin: *Lethaia*, v. 31, p. 161–166.
- Martini, I.P. and Sagri, M., 1993. Tectono-sedimentary characteristics of the late Miocene-Quaternary extensional basins of northern Appenines, Italy. *Earth-Sciences Review* 34, 197–233.
- Marzke, M.W. and Shrewsbury, M.M., 2006. The *Oreopithecus* thumb: Pitfalls in reconstructing muscle and ligament attachments from fossil bones. *Journal of Human Evolution* 51, 213–215.
- Matson, S.D. and Fox, D.L., 2010. Stable isotopic evidence for terrestrial latitudinal climate gradients in the Late Miocene of the Iberian Peninsula. *Palaeogeography, Palaeoclimatology, Palaeoecology* 287, 28–44.

- Maslin, M.A., Li, X.S., Loutre, M.-F., and Berger, A., 1998. The contribution of orbital forcing to the progressive intensification of northern hemisphere glaciation. *Quaternary Science Reviews*, v. 17, p. 411–426.
- Matson, S.D. and Fox, D.L., 2010. Stable isotopic evidence for terrestrial latitudinal climate gradients in the Late Miocene of the Iberian Peninsula. *Palaeogeography, Palaeoclimatology, Palaeoecology*, v. 287, p. 28–44.
- McArthur, J.V. and Moorhead, K.K., 1996. Characterization of riparian species and stream detritus using multiple stable isotopes. *Oecologia* 107, 232–238.
- McNab, B.K., 2002. *The Physiological Ecology of Vertebrates: A View from Energetics*. Cornell University Press, Ithaca, New York, 624 p.
- Meijer, P.Th. and Krijgsman, W., 2005. A quantitative analysis of the desiccation and re-filling of the Mediterranean during the Messinian Salinity Crisis: *Earth and Planetary Science Letters*, v. 240, p. 510–520.
- Mein, P., Bizon, G., Bizon, J.J., and Montenat, C., 1973. Le gisement de Mammifères de La Alberca (Murcia, Espagne méridionale). Corrélation avec les formations marines du Miocène terminal. *Comptes Rendus de l'Académie des Sciences de Paris, Série D*, 276, 3077–3080.
- Melillo, J.M., Aber, J.D., Linkins, A.E., Ricca, A., Fry, B., and Nadelhoffer, K.J., 1989. Carbon and nitrogen dynamics along the decay continuum: Plant litter to soil organic matter. *Plant and Soil* 115, 189–198.

- Merlivat, L. and Jouzel, J., 1979, Global climatic interpretation of the deuterium-oxygen 18 relationship for precipitation: *Journal of Geophysical Research*, v. 84, p. 5029–5033.
- Meyers, S.R., Sageman, B.B., and Pagani, M., 2008. Resolving Milankovitch: Consideration of signal and noise. *American Journal of Science*, v. 308, p. 770–786.
- Minwer-Barakat, R., García-Alix, A., Agustí, J., Martín Suarez, E., and Freudenthal, M., 2009, The micromammal fauna from Negratín-1 (Guadix Basin, southern Spain): New evidence of African-Iberian mammal exchanges during the Late Miocene: *Journal of Paleontology*, v. 83, p. 854–879.
- Moral, F., Cruz-Sanjulián, J.J., and Olías, M., 2008, Geochemical evolution of groundwater in the carbonate aquifers of Sierra de Segura (Betic Cordillera, southern Spain): *Journal of Hydrology*, v. 360, p. 281–296.
- Montigny, R., Edel, J.B., and Thuizat, R., 1981. Oligo-Miocene rotation of Sardinia: K-Ar ages and paleomagnetic data of Tertiary volcanics. *Earth and Planetary Science Letters*, v. 54, p. 261–271.
- Montoya, P., Morales, J., Robles, F., Abella, J., Benavent, J.V., Marín, M.D., and Ruiz Sánchez, F.J., 2006. Las nuevas excavaciones (1995-2006) en el yacimiento del Mioceno final de Venta del Moro, Valencia. *Estudios Geológicos*, 62, 313–326.
- Mooney, H.A., Bullock, S.H., and Ehleringer, J.R., 1989. Carbon isotope ratios of plants of a tropical dry forest in Mexico. *Functional Ecology* 3, 137–142.

- Moyà-Sola, S., Köhler, M., and Rook, L., 1999. Evidence of hominid-like precision grip capability in the hand of the Miocene ape *Oreopithecus*. *Proceedings of the National Academy of Sciences USA* 96, 313–317.
- Moyà-Sola, S., Köhler, M., and Rook, L., 2005. The *Oreopithecus* thumb: a strange case in hominoid evolution. *Journal of Human Evolution* 49, 395–404.
- Murphy, L.N., Kirk-Davidoff, D.B., Mahowald, N., and Otto-Bliesner, B.L., 2009. A numerical study of the climate response to lowered Mediterranean Sea level during the Messinian Salinity Crisis: *Palaeogeography, Palaeoclimatology, Palaeoecology*, v. 279, p. 41–59.
- Nagy, L. and Proctor, J., 2000. Leaf $\delta^{13}\text{C}$ signatures in heath and lowland evergreen rain forest species from Borneo. *Journal of Tropical Ecology* 16, 757–761.
- NCDC, 2009. Surface Data – Global Summary of the Day: 1957–2009.
<http://www.ncdc.noaa.gov/>. 2009.
- NCDC, 2010, Surface Data – Global Summary of the Day: 1974–2010:
<http://www.ncdc.noaa.gov> (May 2010).
- Nelson, S.V., 2005. Paleoseasonality inferred from equid teeth and intra-tooth isotopic variability. *Palaeogeography, Palaeoclimatology, Palaeoecology*, 222, 122–144.
- Nelson, S.V., 2007. Isotopic reconstructions of habitat change surrounding the extinction of *Sivapithecus*, a Miocene hominoid, in the Siwalik Group of Pakistan.
Palaeogeography, Palaeoclimatology, Palaeoecology 243, 204–222.
- Newesely, H., 1989. Fossil bone apatite. *Applied Geochemistry*, 4, 233–245.

- Nijenhuis, I.A., Schenau, S.J., van der Weijden, C.H., Hilgen, F.J., Lourens, L.J., and Zachariasse, W.J., 1996. On the origin of upper Miocene sapropelites: A case study from the Faneromeni section, Crete (Greece). *Paleoceanography*, v. 11, p. 633–645.
- O’Neil, J.R., Roe, L.J., Reinhard, E., and Blake, R.E., 1994. A rapid and precise method of oxygen isotope analysis of biogenic phosphate. *Israel Journal of Earth Sciences*, 43, 203–212.
- Opdyke, N., Mein, P., Moissenet, E., Pérez-González, A., Lindsay, E., and Petko, M., 1990. The magnetic stratigraphy of the Late Miocene sediments of the Cabriel Basin, Spain. *In*: Lindsay, E.H., Fahlbusch, V., and Mein, P. (Eds.), *European Neogene Mammal Chronology*. Plenum Press, New York, pp. 507–514.
- Opdyke, N., Mein, P., Lindsay, E., Perez-Gonzales, A., Moissenet, E., and Norton, V.L., 1997. Continental deposits, magnetostratigraphy and vertebrate paleontology, late Neogene of Eastern Spain. *Palaeogeography, Palaeoclimatology, Palaeoecology*, 133, 129–148.
- Ortiz, J.E., Torres, T., Delgado, A., Reyes, E., Llamas, J.F., Soler, V., and Raya, J., 2006. Pleistocene paleoenvironmental evolution at continental middle latitude inferred from carbon and oxygen stable isotope analysis of ostracodes from the Guadix-Baza Basin (Granada, SE Spain). *Palaeogeography, Palaeoclimatology, Palaeoecology*, 240, 536–561.
- Pagani, M., Freeman, K.H., and Arthur, M.A., 1999. Late Miocene atmospheric CO₂ concentrations and the expansion of C₄ grasses. *Science*, v. 285, p. 876–879.

- Passey, B.H. and Cerling, T.E., 2002. Tooth enamel mineralization in ungulates: Implications for recovering a primary isotopic time-series. *Geochimica et Cosmochimica Acta*, 66, 3225–3234.
- Passey, B.H., Cerling, T.E., Perkins, M.E., Voorhies, M.R., Harris, J.M., and Tucker, S.T., 2002. Environmental change in the Great Plains: An isotopic record from fossil horses. *The Journal of Geology* 110, 123–140.
- Peñuelas and Azcón-Bieto, 1992. Changes in leaf $\Delta^{13}\text{C}$ of herbarium plant species during the past 3 centuries of CO_2 increase. *Plant, Cell and Environment* 15 485–489.
- Philander, S.G. and Fedorov, A.V., 2003, Role of tropics in changing the response to Milankovitch forcing some three million years ago. *Paleoceanography*, v. 18, p.11–23.
- Pierre, C., Rouchy, J.-M., and Blanc-Valleron, M.-M., 2002, Gas hydrate dissociation in the Lorca Basin (SE Spain) during the Mediterranean Messinian salinity crisis: *Sedimentary Geology*, v. 147, p. 247–252.
- Potts, R. and Behrensmeyer, A.K., 1992. Late Cenozoic terrestrial ecosystems. *In*: Behrensmeyer, A.K., Damuth, J., DiMichele, W., Potts, R., Sues, H.D., and Wing, S. (Eds.), *Terrestrial Ecosystems Through Time*. University of Chicago Press, Chicago, p. 419–519.
- Quade, J. and Cerling, T.E., 1995. Expansion of C4 grasses in the Late Miocene of northern Pakistan: evidence from stable isotopes in paleosols. *Palaeogeography, Palaeoclimatology, Palaeoecology*, 115, 91–116.

- Quade, J., Solounias, N., and Cerling, T.E., 1994. Stable isotopic evidence from paleosol carbonates and fossil teeth in Greece for forest or woodlands over the past 11 Ma. *Palaeogeography, Palaeoclimatology, Palaeoecology*, v. 108, p. 41–53.
- Ravelo, A.C., Andreasen, D., Lyle, M., Olivarez Lyle, A., and Wara, M.W., 2004. Regional climate shifts caused by gradual global cooling in the Pliocene epoch. *Nature*, v. 429, p. 263–267.
- Rook, L., Harrison, T., and Engesser, B., 1996. The taxonomic status and biochronological implications of new finds of *Oreopithecus* from Baccinello (Tuscany, Italy). *Journal of Human Evolution* 30, 3–27.
- Rook, L., Abbazzi, L., and Engesser, B., 1999. An overview on the Italian Miocene land mammal faunas. In: Agustí, J., Rook, L., Andrews, P. (Eds.), *The Evolution of Neogene Terrestrial Ecosystems in Europe*. Cambridge University Press, Cambridge, pp. 191–204.
- Rook, L., Bondioli, L., Köhler, M., Moyà-Sola, S., and Macchiarelli, R., 1999. *Oreopithecus* was a bipedal ape after all: Evidence from the iliac cancellous architecture. *Proceedings of the National Academy of Sciences USA* 96, 8795–8799.
- Rook, L., Gallai, G., and Torre, D., 2000. Lands and endemic mammals in the Late Miocene of Italy: Constraints for paleogeographic outlines of Tyrrhenian area. *Palaeogeography, Palaeoclimatology, Palaeoecology*, v. 238, p. 263–269.
- Rook, L., Renne, P., Benvenuti, M., and Papini, M., 2000. Geochronology of *Oreopithecus*-bearing succession at Baccinello (Italy) and the extinction pattern of European Miocene hominoids. *Journal of Human Evolution* 39, 577–582.

- Rook, L., Bondioli, L., Casali, F., Rossi, M., Köhler, M., Moyà-Sola, S., and Macchiarelli, R., 2004. The bony labyrinth of *Oreopithecus bambolii*. *Journal of Human Evolution* 46, 349–356.
- Rosenbaum, G. and Lister, G.S., 2004. Formation of arcuate orogenic belts in the western Mediterranean region. *Special Paper – Geological Society of America*, v. 393, p. 41–56.
- Rosenbaum, G., Lister, G.S., and Duboz, C., 2002. Reconstruction of the tectonic evolution of the western Mediterranean since the Oligocene. *Journal of the Virtual Explorer*, v. 8, p. 107–126.
- Rouchy, J.M. and Caruso, A., 2006, The Messinian salinity crisis in the Mediterranean basin: A reassessment of the data and an integrated scenario: *Sedimentary Geology*, v. 188–189, p. 35–67.
- Rozanski, K., Araguás-Araguás, L., and Gonfiantini, R., 1993. Isotopic patterns in modern global precipitation. *In* P.K. Swart, K.C. Lohmann, J.A. McKenzie, and S.M. Savin (eds.) *Climate Change in Continental Isotopic Records*. *Geophysical Monograph 78*, American Geophysical Union, Washington, D.C., p. 1–36.
- Ruddiman, W.F. and McIntyre, A., 1981. Oceanic mechanisms for amplification of the 23,000-year ice-volume cycle. *Science*, v. 212, p. 617–627.
- Ruddiman, W.F. and McIntyre, A., 1981. The North Atlantic Ocean during the last deglaciation. *Palaeogeography, Palaeoclimatology, Palaeoecology*, v. 35, p. 145–214.

- Ruddiman, W.F., and Raymo, M.E., 1988. Northern Hemisphere climate regimes during the past 3 Ma: possible tectonic connections. *Philosophical Transactions of the Royal Society of London, B*, v. 318, p. 411–430.
- Ruiz-Bustos, A., 1999, Biostratigraphy of the continental deposits in the Granada, Guadix, and Baza Basins (Betic Cordillera), *in* Proceedings, Congreso Internacional de Paleontología Humana, Orce, Spain, 1995: Museo de Prehistoria y Paleontología “J. Gibert”, p. 153–174.
- Ruiz Bustos, A., 2007, Aportaciones de las faunas de mamíferos a la bioestratigrafía y paleoecología de la Cuenca de Guadix y Baza, *in* Sanz de Galdeano, C. and Peláez, J.A., eds., Estructura, tectónica activa, sismicidad, geomorfología y dataciones existentes: Granada, Universidad de Granada, p. 11–27.
- Sacks, L.A., Herman, J.S., Konikow, L.F., and Vela, A.L., 1992, Seasonal dynamics of groundwater-lake interactions at Doñana National Park, Spain: *Journal of Hydrology*, v. 136, p. 123–154.
- Sánchez-Chillón, B., Alberdi, M.T., Leone, G., Bonadonna, F.P., Stenni, B., and Longinelli, A., 1994. Oxygen isotopic composition of fossil equid tooth and bone phosphate: an archive of difficult interpretation. *Palaeogeography, Palaeoclimatology, Palaeoecology*, 107, 317–328.
- Sandquist, D.R. and Cordell, S., 2007. Functional diversity of carbon-gain, water-use, and leaf-allocation traits in trees of a threatened lowland dry forest in Hawaii. *American Journal of Botany* 94, 1459–1469.

- Sanz de Galdeano, C. and Alfaro, P., 2004, Tectonic significance of the present relief of the Betic Cordillera: *Geomorphology*, v. 63, p. 175–190.
- Sanz de Galdeano, C. and López-Garrido, A.C., 1999, Nature and impact of the Neotectonic deformation in the western Sierra Nevada (Spain): *Geomorphology*, v. 30, p. 259–272.
- Sanz de Galdeano, C. and Vera, J.A., 1992, Stratigraphic record and palaeogeographical context of the Neogene basins in the Betic Cordillera, Spain: *Basin Research*, v. 4, p. 21–36.
- Sarmiento, E.E. and Marcus, L.F., 2000. The Os navicular of humans, great apes, OH 8, Hadar, and *Oreopithecus*: Function, phylogeny, and multivariate analyses. *American Museum Novitates* 3288, 1–38.
- Scott, G.R., Gibert, L., and Gibert, J., 2007. Magnetostratigraphy of the Orce region (Baza Basin), SE Spain: New chronologies for Early Pleistocene faunas and hominid occupation sites. *Quaternary Science Reviews*, 26, 415–435.
- Shackleton, N.J., Imbrie, J., Pisias, N.G., and Rose, J., 1988. The evolution of oceanic oxygen-isotope variability in the North Atlantic over the past three million years. *Philosophical Transactions of the Royal Society of London, Series B*, v. 318, p. 679–688.
- Shackleton, N.J., Crowthurst, S., Hagelberg, T, Pisias, N.G., and Schneider, D.A., 1995. A new late Neogene time scale: Application to leg 138 sites. *In*: Pisias, N.G., Mayer, L.A., Janecek, T.R., Palmer-Julson, A., and van Andel, T.H. (Eds.), *Proceedings of the Ocean Drilling Program, Scientific Results*, v. 138, p. 73–101.

- Simón, M., Sánchez, S., and García, I., 2000, Soil-landscape evolution on a Mediterranean high mountain: *Catena*, v. 39, p. 211–231.
- Small, E.E., Giorgi, F., Sloan, L.C., and Hostetler, S., 2001a. The effects of desiccation and climatic change on the hydrology of the Aral Sea. *Journal of Climate*, 14, 300–322.
- Small, E.E., Sloan, L.C., and Nychka, D., 2001b. Changes in surface air temperature caused by desiccation of the Aral Sea. *Journal of Climate*, 14, 284–299.
- Sokal, R.R. and Rohlf, F.J., 1995. *Biometry: The Principles and Practice of Statistics in Biological Research*. W.H. Freeman and Co., New York, 887 pp.
- Solounias, N., Plavcan, J.M., Quade, J., and Witmer, L., 1999. The paleoecology of the Pikermian Biome and the savanna myth. *In*: Agustí, J., Rook, L., and Andrews, P. (Eds.), *The Evolution of Neogene Terrestrial Ecosystems in Europe*. Cambridge University Press, Cambridge, UK, p. 436–453.
- Soria, J.M., Viseras, C., and Fernández, J., 1998, Late Miocene-Pleistocene tectono-sedimentary evolution and subsidence history of the central Betic Cordillera (Spain): a case study in the Guadix intramontane basin: *Geological Magazine*, v. 135, p. 565–574.
- Stampfli, G.M., Borel, G.D., Cavazza, W., Mosar, J., and Ziegler, P.A., 2001. Palaeotectonic and palaeogeographic evolution of the western Tethys and PeriTethyan domain (IGCP Project 369). *Episodes*, v. 24, p. 222–228.
- Steininger, F.F., Berggren, W.A., Kent, D.V., Bernor, R.L., Sen. S., and Agustí, J., 1996. Circum-Mediterranean Neogene (Miocene and Pliocene) marine-continental

- chronologic correlations of European mammal units. *In*: Bernor, R.L., Fahlbusch, V., and Mittmann, H.-W. (Eds.), *The Evolution of Western Eurasian Neogene Mammal Faunas*. Columbia University Press, New York, pp. 7–46.
- Stickley, C.E., Brinkhuis, H., Schellenberg, S.A., Sluijs, A., Röhl, U., Fuller, M., Grauert, M., Huber, M., Warnaar, J., and Williams, G.L., 2004. Timing and nature of the deepening of the Tasmanian Gateway. *Paleoceanography*, v. 19, p. 1–18.
- Straus, W.L., Jr., and Schon, M.A., 1960. Cranial capacity of *Oreopithecus bambolii*. *Science* 132, 670–672.
- Strömberg, C., 2005. Decoupled taxonomic radiation and ecological expansion of open-habitat grasses in the Cenozoic of North America. *Proceedings of the National Academy of Sciences, USA*, 102, 11980–11984.
- Suc, J.-P. and Popescu, S.-M., 2005. Pollen records and climatic cycles in the North Mediterranean region since 2.7 Ma. *In*: Head, M.J. and Gibbard, P.L. (Eds.), *Early-Middle Pleistocene Transitions: The Land-Ocean Evidence*. Geological Society Special Publication, London, pp. 147–158.
- Suc, J.-P., Diniz, F., Leroy, S., Poumont, C., Bertini, A., Dupont, L., Clet, M., Bessais, E., Zheng, Z., Fauquette, S., and Ferrier, J., 1995. Zanclean (Brunssumian) to early Piacenzian (early-middle Reuverian) climate from 4° to 54° north latitude (West Africa, West Europe and West Mediterranean areas). *Mededelingen Rijks Geologische Dienst* 52, 43–56.
- Susman, R.L., 2004. *Oreopithecus bambolii*: and unlikely case of hominidlike grip capability in a Miocene ape. *Journal of Human Evolution* 46, 105–117.

- Susman, R.L., 2005. *Oreopithecus*: still apelike after all these years. *Journal of Human Evolution* 49, 405–411.
- Szalay, F.S. and Berzi, A., 1973. Cranial anatomy of *Oreopithecus*. *Science* 180, 183–185.
- Szalay, F.S. and Langdon, J.H., 1986. The foot of *Oreopithecus*: an evolutionary assessment. *Journal of Human Evolution* 15, 585–621.
- Talbot, M.R., 1990. A review of the palaeohydrological interpretation of carbon and oxygen isotopic ratios in primary lacustrine carbonates: *Chemical Geology*, v. 80, p. 261–279.
- Tedford, R.H., Albright, L.B., III, Barnosky, A.D., Ferrusquia-Villafranca, I., Hunt, R.M., Jr., Storer, J.E., Swisher, C.C., III, Voorhies, M.R., Webb, S.D., and Whistler, D.P., 2004. Mammalian biochronology of the Arikareean through Hemphillian interval (Late Oligocene through early Pliocene epochs). *In*: Woodburne, M.O. (Ed.), *Late Cretaceous and Cenozoic Mammals of North America: Biostratigraphy and Geochronology*. Columbia University Press, New York, p. 169–231.
- Terwilliger, V.J., Changes in the $\delta^{13}\text{C}$ values of trees during a tropical rainy season: some effects in addition to diffusion and carboxylation by Rubisco. *American Journal of Botany* 84, 1693–1700.
- Toft, N.L., Anderson, J.E., and Nowak, R.S., 1989. Water use efficiency and carbon isotope composition of plants in a cold desert environment. *Oecologia* 80, 11–18.

- Tudge, A.P., 1960. A method of analysis of oxygen isotopes in orthophosphate – its use in the measurement of paleotemperatures. *Geochimica et Cosmochimica Acta*, 18, 81–93.
- Uemura, A., Harayama, H., Koike, N., and Ishida, A., 2006. Coordination of crown structure, leaf plasticity and carbon gain within the crowns of three winter-deciduous mature trees. *Tree Physiology* 26, 633–641.
- Valentini, R., Scarascia Mugnozz, G.E., and Ehleringer, J.R., 1992. Hydrogen and carbon isotope ratios of selected species of a Mediterranean macchia ecosystem. *Functional Ecology* 6, 627–631.
- Valentini, R., Anfodillo, T., and Ehleringer, J.R., 1994. Water sources and carbon isotope composition ($\delta^{13}\text{C}$) of selected tree species of the Italian Alps. *Canadian Journal of Forest Research* 24, 1575–1578.
- Valero-Garcés, B.L., Delgado-Huertas, A., Navas, A., Machín, J., González-Sampériz, P., and Kelts, K., 2000, Quaternary palaeohydrological evolution of a playa lake: Salada Mediana, central Ebro Basin, Spain: *Sedimentology*, v. 47, p. 1135–1156.
- Valero-Garcés, B.L., Navas, A., Mata, P., Delgado-Huertas, A., Machín, J., González-Sampériz, P., Moreno Caballud, A., Schwalb, A., Ariztegui, D., Schnellmann, M., Bao, R., and González-Barrios, A., 2003, Sedimentary facies analyses in lacustrine cores: From initial core descriptions to detailed paleoenvironmental reconstructions. A case study from Zoñar Lake (Córdoba province, Spain), *in* Valero-Garcés, B.L., ed., *Limnogeology in Spain: A tribute to Kerry Kelts*: Madrid, Consejo Superior de Investigaciones Científicas, p. 385–414.

- Valero-Garcés, B.L., Moreno, A., Navas, A., Mata, P., Machín, J., Delgado Huertas, A., González Sampériz, P., Schwalb, A., Morellón, M., Hai Cheng, and Edwards, R.L., 2008, The Taravilla lake and tufa deposits (Central Iberian Range, Spain) as palaeohydrological and palaeoclimatic indicators: *Palaeogeography, Palaeoclimatology, Palaeoecology*, v. 259, p. 136–156.
- van Dam, J.A., 2006. Geographic and temporal patterns in the late Neogene (12–3 Ma) aridification of Europe: The use of small mammals as paleoprecipitation proxies. *Palaeogeography, Palaeoclimatology, Palaeoecology*, 238, 190–218.
- van Dam, J.A. and Weltje, G.J., 1999. Reconstruction of Late Miocene climate of Spain using rodent palaeocommunity successions: an application of end-member modeling. *Palaeogeography, Palaeoclimatology, Palaeoecology*, 151, 267–305.
- van Dam, J.A. and Reichart, G.J., 2009. Oxygen and carbon isotope signatures in late Neogene horse teeth from Spain and application as temperature and seasonality proxies. *Palaeogeography, Palaeoclimatology, Palaeoecology*, v. 274, p. 64–81.
- van Dam, J.A., Alcalá, L., Alonso-Zarza, A., Calvo, J.P., Garcés, M., and Krijgsman, W., 2001. The Upper Miocene mammal record from the Teruel-Alfambra region (Spain): the MN system and continental stage/age concepts discussed. *Journal of Vertebrate Paleontology*, 21, 367–385.
- Van Dam, J.A., Abdul Aziz, H., Álvarez Sierra, M.A., Hilgen, F.J., van den Hoek Ostende, L.W., Lourens, L., Mein, P., van der Meulen, A.J., and Pelaez-Campomanes, P., 2006. Long-period astronomical forcing of mammal turnover. *Nature*, 443, 687–691.

- Van de Water, P.K., Leavitt, S.W., and Betancourt, J.L., 2002. Leaf $\delta^{13}\text{C}$ variability with elevation, slope aspect, and precipitation in the southwest United States. *Oecologia* 132, 332–343.
- Van der Made, J., Morales, J., and Montoya, P., 2006. Late Miocene turnover in the Spanish mammal record in relation to palaeoclimate and the Messinian Salinity Crisis. *Palaeogeography, Palaeoclimatology, Palaeoecology*, 238, 228–246.
- Van der Merwe, N.J. and Medina, E., 1989. Photosynthesis and $^{13}\text{C}/^{12}\text{C}$ ratios in Amazonian rain forests. *Geochimica et Cosmochimica Acta* 53, 1091–1094.
- van Vugt, N., 2000. Orbital forcing in late Neogene lacustrine basins from the Mediterranean: A magnetostratigraphic and cyclostratigraphic study. *Geologica Ultraiectina*, v. 189, p. 1–167.
- van Vugt, N., Langereis, C.G., and Hilgen, F.J., 2001. Orbital forcing in Pliocene-Pleistocene Mediterranean lacustrine deposits: dominant expression of eccentricity versus precession. *Palaeogeography, Palaeoclimatology, Palaeoecology*, v. 172, p. 193–205.
- Vandenschrick, G., van Wesemael, B., Frot, E., Pulido-Bosch, A., Molina, L., Stiévenard, M., and Souchez, R., 2002, Using stable isotope analysis ($\delta\text{D}-\delta^{18}\text{O}$) to characterize the regional hydrology of the Sierra de Gador, south east Spain: *Journal of Hydrology*, v. 265, p. 43–55.
- Vázquez, A., Utrilla, R., Zamarreño, I., Sierro, F.J., Flores, J.A., Francés, G., and Bárcena, M.A., 2000. Precession-related sapropelites of the Messinian Sorbas Basin

- (South Spain): paleoenvironmental significance. *Palaeogeography, Palaeoclimatology, Palaeoecology*, v. 158, p. 353–370.
- Wedin, D.A., Tieszen, L.L., Dewey, B., and Pastor, J., 1995. Carbon isotope dynamics during grass decomposition and soil organic matter formation. *Ecology* 76, 1383–1392.
- Weiner, S., Traub, W., Elster, H., and DeNiro, M.J., 1989. The molecular structure of bone and its relation to diagenesis. *Applied Geochemistry*, 4, 231–232.
- Whitman, J.M. and Berger, W.H., 1993. Pliocene-Pleistocene carbon isotope record, site 586, Ontong Java Plateau. In: Maddox, E.M. (Ed.), *Proceedings of the Ocean Drilling Program, Scientific Results* 130, 333–348.
- Willett, S.D., Schlunegger, F., and Picotti, V., 2006. Messinian climate change and erosional destruction of the central European Alps: *Geology*, v. 34, p. 613–616.
- Williams, D.G. and Ehleringer, J.R., 1996. Carbon isotope discrimination in three semi-arid woodland species along a monsoon gradient. *Oecologia* 106, 455–460.
- Zachos, J., Pagani, M., Sloan, L., Thomas, E., and Billups, K., 2001. Trends, rhythms, and aberrations in global climate 65 Ma to present. *Science*, v. 292, p. 686–693.
- Zachos, J.C., Shackleton, N.J., Revenaugh, J.S., Pälike, H., and Flower, B.P., 2001. Climate response to orbital forcing across the Oligocene-Miocene boundary. *Science*, v. 292, p. 274–278.
- Zazzo, A., Lecuyer, C., Mariotti, A., 2004. Experimentally-controlled carbon and oxygen isotope exchange between bioapatites and water under inorganic and microbially-mediated conditions. *Geochimica et Cosmochimica Acta*, 68, 1–12.

Appendix I. Published $\delta^{13}\text{C}$ values of modern plants

	Family	Genus	species	$\delta^{13}\text{C}$	pathway	N	Biome	Reference
dicot	Acanthaceae	<i>Jacobinia</i>	<i>cornea</i>	-29.6	C ₃	1	domestic	Collister et al. (1994)
dicot	Acanthaceae	<i>Rostellularia</i>	<i>procumbens</i>	-29.1	C ₃	1	TrSOMBF	Ehleringer et al. (1987)
dicot	Adoxaceae	<i>Sambucus</i>	<i>nigra</i>	-29.3	C ₃	1	TmBMF	Dungait et al. (2008)
dicot	Adoxaceae	<i>Sambucus</i>	<i>nigra</i>	-27.6	C ₃	4	MFWS	Escuerdo et al. (2008)
dicot	Adoxaceae	<i>Viburnum</i>	<i>édule</i>	-27.6	C ₃	5	BFT	Brooks et al. (1997)
dicot	Altingiaceae	<i>Liquidambar</i>	<i>styraciflua</i>	-30.5	C ₃	5	TmBMF	McArthur and Moorhead (1996)
dicot	Amaranthaceae	<i>Aerva</i>	<i>javanica</i>	-13.3	C ₄	1	unknown	Bender (1971)
dicot	Amaranthaceae	<i>Aerva</i>	<i>pseudotomentosa</i>	-14.5	C ₄	1	unknown	Bender (1971)
dicot	Amaranthaceae	<i>Alternanthera</i>	<i>philoxeroides</i>	-29.3	C ₃	1	TrSOMBF	Ehleringer et al. (1987)
dicot	Amaranthaceae	<i>Amaranthus</i>	<i>ascendens</i>	-13.2	C ₄	1	TrSOMBF	Ehleringer et al. (1987)
dicot	Amaranthaceae	<i>Amaranthus</i>	<i>blitoides</i>	-14.1	C ₄	1	unknown	Bender (1971)
dicot	Amaranthaceae	<i>Amaranthus</i>	<i>retroflexus</i>	-13.3	C ₄	1	unknown	Bender (1971)
dicot	Amaranthaceae	<i>Pupalia</i>	<i>lappacea</i>	-24.4	C ₃	1	unknown	Bender (1971)
dicot	Anacardiaceae	<i>Anacardium</i>	<i>excelsum</i>	-23.8	C ₃	8	TrSDBF	Holtum and Winter (2005)
dicot	Anacardiaceae	<i>Anacardium</i>	<i>excelsum</i>	-25.4	C ₃	6	TrSDBF	Holtum and Winter (2005)
dicot	Anacardiaceae	<i>Anacardium</i>	<i>excelsum</i>	-25.5	C ₃	9	TrSDBF	Holtum and Winter (2005)
dicot	Anacardiaceae	<i>Anacardium</i>	<i>excelsum</i>	-25.7	C ₃	6	TrSDBF	Holtum and Winter (2005)
dicot	Anacardiaceae	<i>Anacardium</i>	<i>excelsum</i>	-25.8	C ₃	6	TrSDBF	Holtum and Winter (2005)
dicot	Anacardiaceae	<i>Anacardium</i>	<i>excelsum</i>	-26.1	C ₃	10	TrSDBF	Holtum and Winter (2005)
dicot	Anacardiaceae	<i>Anacardium</i>	<i>excelsum</i>	-26.1	C ₃	10	TrSDBF	Holtum and Winter (2005)
dicot	Anacardiaceae	<i>Anacardium</i>	<i>excelsum</i>	-26.4	C ₃	10	TrSDBF	Holtum and Winter (2005)
dicot	Anacardiaceae	<i>Anacardium</i>	<i>excelsum</i>	-26.4	C ₃	10	TrSDBF	Holtum and Winter (2005)
dicot	Anacardiaceae	<i>Anacardium</i>	<i>excelsum</i>	-26.4	C ₃	6	TrSDBF	Holtum and Winter (2005)
dicot	Anacardiaceae	<i>Anacardium</i>	<i>excelsum</i>	-26.7	C ₃	6	TrSDBF	Holtum and Winter (2005)
dicot	Anacardiaceae	<i>Anacardium</i>	<i>excelsum</i>	-27.6	C ₃	6	TrSDBF	Holtum and Winter (2005)
dicot	Anacardiaceae	<i>Anacardium</i>	<i>excelsum</i>	-29.0	C ₃	6	TrSDBF	Holtum and Winter (2005)
dicot	Anacardiaceae	<i>Anacardium</i>	<i>excelsum</i>	-29.0	C ₃	6	TrSDBF	Holtum and Winter (2005)
dicot	Anacardiaceae	<i>Anacardium</i>	<i>excelsum</i>	-29.3	C ₃	6	TrSDBF	Holtum and Winter (2005)
dicot	Anacardiaceae	<i>Anacardium</i>	<i>excelsum</i>	-29.7	C ₃	6	TrSDBF	Holtum and Winter (2005)
dicot	Anacardiaceae	<i>Astronium</i>	<i>graveolens</i>	-27.1	C ₃	6	TrSDBF	Holtum and Winter (2005)
dicot	Anacardiaceae	<i>Astronium</i>	<i>graveolens</i>	-27.3	C ₃	6	TrSDBF	Holtum and Winter (2005)
dicot	Anacardiaceae	<i>Astronium</i>	<i>graveolens</i>	-28.0	C ₃	6	TrSDBF	Holtum and Winter (2005)
dicot	Anacardiaceae	<i>Astronium</i>	<i>graveolens</i>	-28.5	C ₃	6	TrSDBF	Holtum and Winter (2005)

Appendix I. (continued)

	Family	Genus	species	$\delta^{13}\text{C}$	pathway	N	Biome	Reference
dicot	Anacardiaceae	<i>Astronium</i>	<i>graveolens</i>	-30.3	C ₃	5	TrSDBF	Leffler and Enquist (2002)
dicot	Anacardiaceae	<i>Pistacia</i>	<i>lentiscus</i>	-26.6	C ₃	1	MFWS	Peñuelas and Azcón-Bieto (1992)
dicot	Anacardiaceae	<i>Pistacia</i>	<i>lentiscus</i>	-27.0	C ₃	1	MFWS	Peñuelas and Azcón-Bieto (1992)
dicot	Anacardiaceae	<i>Pistacia</i>	<i>lentiscus</i>	-27.1	C ₃	1	MFWS	Peñuelas and Azcón-Bieto (1992)
dicot	Anacardiaceae	<i>Pistacia</i>	<i>lentiscus</i>	-27.6	C ₃	1	MFWS	Peñuelas and Azcón-Bieto (1992)
dicot	Anacardiaceae	<i>Pistacia</i>	<i>lentiscus</i>	-26.2	C ₃	1	MFWS	Valentini et al. (1992)
dicot	Anacardiaceae	<i>Rhus</i>	<i>copallina</i>	-29.7	C ₃	1	TrSOMBF	Jones et al. (2010)
dicot	Anacardiaceae	<i>Schinus</i>	<i>terebinthefolius</i>	-30.7	C ₃	1	TrSOMBF	Jones et al. (2010)
dicot	Anacardiaceae	<i>Spondias</i>	<i>mombin</i>	-25.1	C ₃	6	TrSDBF	Holtum and Winter (2005)
dicot	Anacardiaceae	<i>Spondias</i>	<i>mombin</i>	-27.4	C ₃	6	TrSDBF	Holtum and Winter (2005)
dicot	Anacardiaceae	<i>Spondias</i>	<i>mombin</i>	-28.1	C ₃	6	TrSDBF	Holtum and Winter (2005)
dicot	Anacardiaceae	<i>Spondias</i>	<i>mombin</i>	-28.7	C ₃	6	TrSDBF	Holtum and Winter (2005)
dicot	Anacardiaceae	<i>Swintonia</i>	<i>glauca</i>	-30.3	C ₃	5	TrSOMBF	Nagy and Proctor (2000)
dicot	Anacardiaceae	<i>Swintonia</i>	<i>glauca</i>	-30.4	C ₃	2	TrSOMBF	Nagy and Proctor (2000)
dicot	Anacardiaceae	<i>Thyrsodium</i>	<i>guianense</i>	-30.2	C ₃	1	TrSOMBF	Bonal et al. (2000)
dicot	Annonaceae	<i>Annona</i>	<i>spraguei</i>	-26.7	C ₃	6	TrSDBF	Holtum and Winter (2005)
dicot	Annonaceae	<i>Annona</i>	<i>spraguei</i>	-27.8	C ₃	6	TrSDBF	Holtum and Winter (2005)
dicot	Annonaceae	<i>Annona</i>	<i>spraguei</i>	-28.3	C ₃	6	TrSDBF	Holtum and Winter (2005)
dicot	Annonaceae	<i>Fissistigma</i>	<i>glaucescens</i>	-29.6	C ₃	1	TrSCMBF	Ehleringer et al. (1987)
dicot	Annonaceae	<i>Oxandra</i>	<i>asbeckii</i>	-31.9	C ₃	1	TrSOMBF	Buchmann et al. (1997)
dicot	Annonaceae	<i>Oxandra</i>	<i>asbeckii</i>	-32.6	C ₃	1	TrSOMBF	Buchmann et al. (1997)
dicot	Annonaceae	<i>Oxandra</i>	<i>asbeckii</i>	-33.2	C ₃	1	TrSCMBF	Buchmann et al. (1997)
dicot	Annonaceae	<i>Oxandra</i>	<i>asbeckii</i>	-33.2	C ₃	1	TrSCMBF	Buchmann et al. (1997)
dicot	Annonaceae	<i>Xylopia</i>	<i>frutescens</i>	-29.9	C ₃	6	TrSDBF	Holtum and Winter (2005)
dicot	Annonaceae	<i>Xylopia</i>	<i>frutescens</i>	-30.0	C ₃	6	TrSDBF	Holtum and Winter (2005)
dicot	Annonaceae	<i>Xylopia</i>	<i>frutescens</i>	-31.0	C ₃	6	TrSDBF	Holtum and Winter (2005)
dicot	Annonaceae	<i>Xylopia</i>	<i>sp.</i>	-32.5	C ₃	1	TrSOMBF	Bonal et al. (2000)
dicot	Apocynaceae	<i>Alstonia</i>	<i>boonei</i>	-29.4	C ₃	1	TrSOMBF	Cerling et al. (2004)
dicot	Apocynaceae	<i>Apocynum</i>	<i>androsaemifolium</i>	-29.5	C ₃	5	BFT	Brooks et al. (1997)
dicot	Apocynaceae	<i>Couma</i>	<i>guianensis</i>	-28.9	C ₃	1	TrSOMBF	Bonal et al. (2000)
dicot	Apocynaceae	<i>Stemmadenia</i>	<i>sp.</i>	-28.8	C ₃	1	TrSDBF	Mooney et al. (1989)
dicot	Apocynaceae	<i>Thevetia</i>	<i>ovata</i>	-27.6	C ₃	1	TrSDBF	Mooney et al. (1989)

Appendix I. (continued)

	Family	Genus	species	$\delta^{13}\text{C}$	pathway	N	Biome	Reference
dicot	Aquifoliaceae	<i>Ilex</i>	<i>aquifolium</i>	-26.2	C ₃	4	MFWS	Escuerdo et al. (2008)
dicot	Aquifoliaceae	<i>Ilex</i>	<i>krugiana</i>	-29.1	C ₃	1	TrSOMBF	Jones et al. (2010)
dicot	Aquifoliaceae	<i>Ilex</i>	<i>opaca</i>	-29.2	C ₃	5	TmBMF	McArthur and Moorhead (1996)
dicot	Aquifoliaceae	<i>Ilex</i>	<i>opaca</i>	-29.5	C ₃	5	TmBMF	McArthur and Moorhead (1996)
dicot	Araliaceae	<i>Aralia</i>	<i>nudicaulis</i>	-31.7	C ₃	5	BFT	Brooks et al. (1997)
dicot	Araliaceae	<i>Didymopanax</i>	<i>morototoni</i>	-25.5	C ₃	6	TrSDBF	Holtum and Winter (2005)
dicot	Araliaceae	<i>Didymopanax</i>	<i>morototoni</i>	-26.6	C ₃	6	TrSDBF	Holtum and Winter (2005)
dicot	Araliaceae	<i>Didymopanax</i>	<i>morototoni</i>	-26.9	C ₃	6	TrSDBF	Holtum and Winter (2005)
dicot	Araliaceae	<i>Didymopanax</i>	<i>morototoni</i>	-27.1	C ₃	6	TrSDBF	Holtum and Winter (2005)
dicot	Araliaceae	<i>Didymopanax</i>	<i>morototoni</i>	-27.9	C ₃	6	TrSDBF	Holtum and Winter (2005)
dicot	Araliaceae	<i>Didymopanax</i>	<i>morototoni</i>	-28.4	C ₃	6	TrSDBF	Holtum and Winter (2005)
dicot	Araliaceae	<i>Didymopanax</i>	<i>morototoni</i>	-28.5	C ₃	6	TrSDBF	Holtum and Winter (2005)
dicot	Araliaceae	<i>Schefflera</i>	<i>decaphylla</i>	-30.2	C ₃	1	TrSOMBF	Bonal et al. (2000)
dicot	Araliaceae	<i>Schefflera</i>	<i>octophylla</i>	-32.0	C ₃	1	TrSOMBF	Ehleringer et al. (1987)
dicot	Asclepiadaceae	<i>Asclepias</i>	<i>syriaca</i>	-28.6	C ₃	1	unknown	Bender (1971)
dicot	Asclepiadaceae	<i>Dischidia</i>	<i>chinensis</i>	-15.2	CAM	1	TrSOMBF	Ehleringer et al. (1987)
dicot	Asclepiadaceae	<i>Hoya</i>	<i>carinosa</i>	-16.7	CAM	1	unknown	Bender (1971)
dicot	Asclepiadaceae	<i>Stapelia</i>	<i>semota</i>	-17.6	CAM	1	unknown	Bender (1971)
dicot	Asparagales	<i>Maianthemum</i>	<i>canadense</i>	-27.9	C ₃	5	BFT	Brooks et al. (1997)
dicot	Asteraceae	<i>Achillea</i>	<i>millefolium</i>	-31.2	C ₃	1	TmBMF	Dungait et al. (2008)
dicot	Asteraceae	<i>Ageratum</i>	<i>conyzoides</i>	-30.9	C ₃	1	TrSOMBF	Ehleringer et al. (1987)
dicot	Asteraceae	<i>Ambrosia</i>	<i>dumosa</i>	-25.4	C ₃	1	DXS	Ehleringer and Cooper (1988)
dicot	Asteraceae	<i>Ambrosia</i>	<i>dumosa</i>	-26.0	C ₃	1	DXS	Ehleringer and Cooper (1988)
dicot	Asteraceae	<i>Ambrosia</i>	<i>dumosa</i>	-27.4	C ₃	1	DXS	Ehleringer and Cooper (1988)
dicot	Asteraceae	<i>Ambrosia</i>	<i>eriocentra</i>	-29.3	C ₃	1	DXS	Ehleringer and Cooper (1988)
dicot	Asteraceae	<i>Ambrosia</i>	<i>psilostachya</i>	-29.4	C ₃	2	TmGSS	Jessup et al. (2003)
dicot	Asteraceae	<i>Artemisia</i>	<i>abrotanum</i>	-29.7	C ₃	1	unknown	Bender (1971)
dicot	Asteraceae	<i>Artemisia</i>	<i>tridentata</i>	-28.8	C ₃	1	unknown	Bender (1971)
dicot	Asteraceae	<i>Artemisia</i>	<i>tridentata</i>	-25.9	C ₃	1	TmCF	DeLucia and Schlesinger (1991)
dicot	Asteraceae	<i>Artemisia</i>	<i>tridentata</i>	-24.1	C ₃	1	DXS	DeLucia and Schlesinger (1991)
dicot	Asteraceae	<i>Artemisia</i>	<i>tridentata</i>	-24.8	C ₃	1	DXS	DeLucia and Schlesinger (1991)
dicot	Asteraceae	<i>Artemisia</i>	<i>tridentata</i>	-25.4	C ₃	1	DXS	DeLucia and Schlesinger (1991)

Appendix I. (continued)

	Family	Genus	species	$\delta^{13}\text{C}$	pathway	N	Biome	Reference
dicot	Asteraceae	<i>Artemisia</i>	<i>tridentata</i>	-25.8	C ₃	4	DXS	Toft et al. (1989)
dicot	Asteraceae	<i>Bebbia</i>	<i>juncea</i>	-25.8	C ₃	1	DXS	Ehleringer and Cooper (1988)
dicot	Asteraceae	<i>Bebbia</i>	<i>juncea</i>	-26.7	C ₃	1	DXS	Ehleringer and Cooper (1988)
dicot	Asteraceae	<i>Bebbia</i>	<i>juncea</i>	-28.3	C ₃	1	DXS	Ehleringer and Cooper (1988)
dicot	Asteraceae	<i>Bellis</i>	<i>perennis</i>	-32.0	C ₃	1	TmBMF	Dungait et al. (2008)
dicot	Asteraceae	<i>Centaurea</i>	<i>nigra</i>	-30.7	C ₃	1	TmBMF	Dungait et al. (2008)
dicot	Asteraceae	<i>Chrysothamnus</i>	<i>paniculatus</i>	-26.7	C ₃	1	DXS	Ehleringer and Cooper (1988)
dicot	Asteraceae	<i>Cirsium</i>	<i>arvense</i>	-28.2	C ₃	1	TmBMF	Dungait et al. (2008)
dicot	Asteraceae	<i>Cirsium</i>	<i>vulgare</i>	-28.7	C ₃	1	TmBMF	Dungait et al. (2008)
dicot	Asteraceae	<i>Crepis</i>	<i>sp.</i>	-30.2	C ₃	1	TmBMF	Dungait et al. (2008)
dicot	Asteraceae	<i>Encelia</i>	<i>farinosa</i>	-25.5	C ₃	1	DXS	Ehleringer and Cooper (1988)
dicot	Asteraceae	<i>Encelia</i>	<i>farinosa</i>	-26.1	C ₃	1	DXS	Ehleringer and Cooper (1988)
dicot	Asteraceae	<i>Encelia</i>	<i>frutescens</i>	-27.5	C ₃	1	DXS	Ehleringer and Cooper (1988)
dicot	Asteraceae	<i>Gutierrezia</i>	<i>texana</i>	-29.3	C ₃	2	TmGSS	Jessup et al. (2003)
dicot	Asteraceae	<i>Hymenoclea</i>	<i>salsola</i>	-23.5	C ₃	1	DXS	Ehleringer and Cooper (1988)
dicot	Asteraceae	<i>Hymenoclea</i>	<i>salsola</i>	-26.5	C ₃	1	DXS	Ehleringer and Cooper (1988)
dicot	Asteraceae	<i>Leucanthemum</i>	<i>vulgare</i>	-29.5	C ₃	1	TmBMF	Dungait et al. (2008)
dicot	Asteraceae	<i>Petasites</i>	<i>palmatius</i>	-32.4	C ₃	5	BFT	Brooks et al. (1997)
dicot	Asteraceae	<i>Petasites</i>	<i>palmatius</i>	-32.7	C ₃	5	BFT	Brooks et al. (1997)
dicot	Asteraceae	<i>Petasites</i>	<i>palmatius</i>	-33.2	C ₃	5	BFT	Brooks et al. (1997)
dicot	Asteraceae	<i>Petasites</i>	<i>palmatius</i>	-33.7	C ₃	5	BFT	Brooks et al. (1997)
dicot	Asteraceae	<i>Porophyllum</i>	<i>gracile</i>	-26.6	C ₃	1	DXS	Ehleringer and Cooper (1988)
dicot	Asteraceae	<i>Porophyllum</i>	<i>gracile</i>	-26.8	C ₃	1	DXS	Ehleringer and Cooper (1988)
dicot	Asteraceae	<i>Porophyllum</i>	<i>gracile</i>	-27.5	C ₃	1	DXS	Ehleringer and Cooper (1988)
dicot	Asteraceae	<i>Psilostrophe</i>	<i>cooperi</i>	-27.0	C ₃	1	DXS	Ehleringer and Cooper (1988)
dicot	Asteraceae	<i>Psilostrophe</i>	<i>cooperi</i>	-27.7	C ₃	1	DXS	Ehleringer and Cooper (1988)
dicot	Asteraceae	<i>Ratibida</i>	<i>columnifera</i>	-28.5	C ₃	2	TmGSS	Jessup et al. (2003)
dicot	Asteraceae	<i>Senecio</i>	<i>gregori</i>	-19.5	CAM	1	unknown	Bender (1971)
dicot	Asteraceae	<i>Senecio</i>	<i>hoi</i>	-34.5	C ₃	1	TrSCMBF	Ehleringer et al. (1987)
dicot	Asteraceae	<i>Senecio</i>	<i>scandens</i>	-31.9	C ₃	1	TrSOMBF	Ehleringer et al. (1987)
dicot	Asteraceae	<i>Solidago</i>	<i>canadensis</i>	-30.4	C ₃	5	BFT	Brooks et al. (1997)
dicot	Asteraceae	<i>Tagetes</i>	<i>sp.</i>	-28.9	C ₃	1	unknown	Bender (1971)

Appendix I. (continued)

	Family	Genus	species	$\delta^{13}\text{C}$	pathway	N	Biome	Reference
dicot	Asteraceae	<i>Taraxacum</i>	<i>officinale</i>	-30.4	C ₃	1	TmBMF	Dungait et al. (2008)
dicot	Asteraceae	<i>Tragopogon</i>	<i>pratensis</i>	-29.1	C ₃	1	unknown	Bender (1971)
dicot	Asteraceae	<i>Viguiera</i>	<i>laciniata</i>	-26.1	C ₃	1	DXS	Ehleringer and Cooper (1988)
dicot	Asteraceae	<i>Viguiera</i>	<i>laciniata</i>	-26.4	C ₃	1	DXS	Ehleringer and Cooper (1988)
dicot	Asteraceae	<i>Wedelia</i>	<i>texana</i>	-28.6	C ₃	2	TmGSS	Jessup et al. (2003)
dicot	Begoniaceae	<i>Begonia</i>	<i>fimbristipula</i>	-33.1	C ₃	1	TrSCMBF	Ehleringer et al. (1987)
dicot	Berberidaceae	<i>Berberis</i>	<i>trifoliolata</i>	-27.6	C ₃	2	TmGSS	Jessup et al. (2003)
dicot	Betulaceae	<i>Alnus</i>	<i>crispa</i>	-27.3	C ₃	10	BFT	Brooks et al. (1997)
dicot	Betulaceae	<i>Alnus</i>	<i>crispa</i>	-27.8	C ₃	10	BFT	Brooks et al. (1997)
dicot	Betulaceae	<i>Alnus</i>	<i>crispa</i>	-28.4	C ₃	10	BFT	Brooks et al. (1997)
dicot	Betulaceae	<i>Alnus</i>	<i>crispa</i>	-29.8	C ₃	10	BFT	Brooks et al. (1997)
dicot	Betulaceae	<i>Alnus</i>	<i>glutinosa</i>	-26.1	C ₃	1	MFWS	Peñuelas and Azcón-Bieto (1992)
dicot	Betulaceae	<i>Alnus</i>	<i>glutinosa</i>	-26.6	C ₃	1	MFWS	Peñuelas and Azcón-Bieto (1992)
dicot	Betulaceae	<i>Alnus</i>	<i>glutinosa</i>	-27.2	C ₃	1	MFWS	Peñuelas and Azcón-Bieto (1992)
dicot	Betulaceae	<i>Alnus</i>	<i>glutinosa</i>	-28.8	C ₃	1	MFWS	Peñuelas and Azcón-Bieto (1992)
dicot	Betulaceae	<i>Alnus</i>	<i>rugosa</i>	-27.0	C ₃	5	TmBMF	Keough et al. (1996)
dicot	Betulaceae	<i>Betula</i>	<i>grossa</i>	-27.2	C ₃	1	TmBMF	Uemura et al. (2006)
dicot	Betulaceae	<i>Betula</i>	<i>pendula</i>	-28.1	C ₃	1	TmBMF	Balesdent et al. (1993)
dicot	Betulaceae	<i>Betula</i>	<i>pendula</i>	-29.1	C ₃	1	TmBMF	Balesdent et al. (1993)
dicot	Betulaceae	<i>Betula</i>	<i>pendula</i>	-29.5	C ₃	1	TmBMF	Balesdent et al. (1993)
dicot	Betulaceae	<i>Betula</i>	<i>pendula</i>	-25.1	C ₃	1	MFWS	Peñuelas and Azcón-Bieto (1992)
dicot	Betulaceae	<i>Betula</i>	<i>pendula</i>	-25.2	C ₃	1	MFWS	Peñuelas and Azcón-Bieto (1992)
dicot	Betulaceae	<i>Betula</i>	<i>pendula</i>	-26.0	C ₃	1	MFWS	Peñuelas and Azcón-Bieto (1992)
dicot	Betulaceae	<i>Betula</i>	<i>pendula</i>	-27.0	C ₃	1	MFWS	Peñuelas and Azcón-Bieto (1992)
dicot	Betulaceae	<i>Betula</i>	<i>pubescens</i>	-28.9	C ₃	4	MFWS	Escuerdo et al. (2008)
dicot	Betulaceae	<i>Carpinus</i>	<i>betulus</i>	-28.0	C ₃	1	TmBMF	Balesdent et al. (1993)
dicot	Betulaceae	<i>Carpinus</i>	<i>betulus</i>	-28.1	C ₃	1	TmBMF	Balesdent et al. (1993)
dicot	Betulaceae	<i>Carpinus</i>	<i>betulus</i>	-28.2	C ₃	1	TmBMF	Balesdent et al. (1993)
dicot	Betulaceae	<i>Carpinus</i>	<i>betulus</i>	-26.7	C ₃	7	TmBMF	Chevillat et al. (2005)
dicot	Betulaceae	<i>Carpinus</i>	<i>caroliniana</i>	-30.1	C ₃	5	TmBMF	McArthur and Moorhead (1996)
dicot	Betulaceae	<i>Carpinus</i>	<i>caroliniana</i>	-30.7	C ₃	5	TmBMF	McArthur and Moorhead (1996)
dicot	Betulaceae	<i>Corylus</i>	<i>cornuta</i>	-28.8	C ₃	5	BFT	Brooks et al. (1997)

Appendix I. (continued)

	Family	Genus	species	$\delta^{13}\text{C}$	pathway	N	Biome	Reference
dicot	Bignoniaceae	<i>Chilopsis</i>	<i>linearis</i>	-25.4	C ₃	1	DXS	Ehleringer and Cooper (1988)
dicot	Bignoniaceae	<i>Jacaranda</i>	<i>copaia</i>	-31.6	C ₃	1	TrSOMBF	Bonal et al. (2000)
dicot	Bignoniaceae	<i>Tabebuia</i>	<i>ochracea</i>	-31.4	C ₃	3	TrSDBF	Leffler and Enquist (2002)
dicot	Bombacaceae	<i>Catostemma</i>	<i>fragrans</i>	-30.4	C ₃	1	TrSOMBF	Bonal et al. (2000)
dicot	Bombacaceae	<i>Catostemma</i>	<i>fragrans</i>	-31.4	C ₃	1	TrSOMBF	Bonal et al. (2000)
dicot	Boraginaceae	<i>Cordia</i>	<i>alliodora</i>	-27.7	C ₃	6	TrSDBF	Holtum and Winter (2005)
dicot	Boraginaceae	<i>Cordia</i>	<i>alliodora</i>	-28.5	C ₃	6	TrSDBF	Holtum and Winter (2005)
dicot	Boraginaceae	<i>Cordia</i>	<i>alliodora</i>	-28.9	C ₃	6	TrSDBF	Holtum and Winter (2005)
dicot	Boraginaceae	<i>Cordia</i>	<i>alliodora</i>	-28.6	C ₃	5	TrSDBF	Leffler and Enquist (2002)
dicot	Boraginaceae	<i>Cordia</i>	<i>alliodora</i>	-27.0	C ₃	6	TrSDBF	Mooney et al. (1989)
dicot	Boraginaceae	<i>Cordia</i>	<i>sp.</i>	-33.1	C ₃	1	TrSOMBF	Bonal et al. (2000)
dicot	Boraginaceae	<i>Myosotis</i>	<i>scorpiodes</i>	-29.5	C ₃	1	TmBMF	Dungait et al. (2008)
dicot	Burseraceae	<i>Bursera</i>	<i>instabilis</i>	-26.8	C ₃	1	TrSDBF	Mooney et al. (1989)
dicot	Burseraceae	<i>Bursera</i>	<i>simaruba</i>	-29.9	C ₃	1	TrSCMBF	Jones et al. (2010)
dicot	Burseraceae	<i>Canarium</i>	<i>album</i>	-28.3	C ₃	1	TrSOMBF	Ehleringer et al. (1987)
dicot	Burseraceae	<i>Dacryodes</i>	<i>nitens</i>	-31.7	C ₃	1	TrSOMBF	Bonal et al. (2000)
dicot	Burseraceae	<i>Protium</i>	<i>sp.</i>	-31.7	C ₃	1	TrSOMBF	Bonal et al. (2000)
dicot	Burseraceae	<i>Protium</i>	<i>subserratum</i>	-31.1	C ₃	1	TrSOMBF	Bonal et al. (2000)
dicot	Burseraceae	<i>Tetragastris</i>	<i>panamensis</i>	-28.7	C ₃	1	TrSOMBF	Bonal et al. (2000)
dicot	Buxaceae	<i>Buxus</i>	<i>sempervirens</i>	-23.3	C ₃	1	MFWS	Peñuelas and Azcón-Bieto (1992)
dicot	Buxaceae	<i>Buxus</i>	<i>sempervirens</i>	-23.7	C ₃	1	MFWS	Peñuelas and Azcón-Bieto (1992)
dicot	Buxaceae	<i>Buxus</i>	<i>sempervirens</i>	-24.3	C ₃	1	MFWS	Peñuelas and Azcón-Bieto (1992)
dicot	Buxaceae	<i>Buxus</i>	<i>sempervirens</i>	-25.9	C ₃	1	MFWS	Peñuelas and Azcón-Bieto (1992)
dicot	Cactaceae	<i>Acanthocereus</i>	<i>occidentalis</i>	-13.2	CAM	3	TrSDBF	Mooney et al. (1989)
dicot	Cactaceae	<i>Cephalocereus</i>	<i>purpusii</i>	-12.7	CAM	3	TrSDBF	Mooney et al. (1989)
dicot	Cactaceae	<i>Cereus</i>	<i>peruvianus</i>	-15.2	CAM	1	unknown	Bender (1971)
dicot	Cactaceae	<i>Epiphyllum</i>	<i>phyllanthus</i>	-12.9	CAM	6	TrSDBF	Holtum and Winter (2005)
dicot	Cactaceae	<i>Epiphyllum</i>	<i>phyllanthus</i>	-13.2	CAM	6	TrSDBF	Holtum and Winter (2005)
dicot	Cactaceae	<i>Epiphyllum</i>	<i>phyllanthus</i>	-13.5	CAM	3	TrSDBF	Holtum and Winter (2005)
dicot	Cactaceae	<i>Epiphyllum</i>	<i>phyllanthus</i>	-13.6	CAM	3	TrSDBF	Holtum and Winter (2005)
dicot	Cactaceae	<i>Epiphyllum</i>	<i>phyllanthus</i>	-14.2	CAM	6	TrSDBF	Holtum and Winter (2005)
dicot	Cactaceae	<i>Epiphyllum</i>	<i>phyllanthus</i>	-14.6	CAM	3	TrSDBF	Holtum and Winter (2005)

Appendix I. (continued)

	Family	Genus	species	δ¹³C	pathway	N	Biome	Reference
dicot	Cactaceae	<i>Epiphyllum</i>	<i>phyllanthus</i>	-14.7	CAM	3	TrSDBF	Holtum and Winter (2005)
dicot	Cactaceae	<i>Mammillaria</i>	<i>sp.</i>	-12.2	CAM	1	TrSDBF	Mooney et al. (1989)
dicot	Cactaceae	<i>Nopalea</i>	<i>karwinksiana</i>	-13.0	CAM	2	TrSDBF	Mooney et al. (1989)
dicot	Cactaceae	<i>Opuntia</i>	<i>engelmannii</i>	-13.5	CAM	2	TmGSS	Jessup et al. (2003)
dicot	Cactaceae	<i>Opuntia</i>	<i>excelsa</i>	-13.1	CAM	8	TrSDBF	Mooney et al. (1989)
dicot	Cactaceae	<i>Opuntia</i>	<i>humifusa</i>	-13.8	CAM	1	unknown	Bender (1971)
dicot	Cactaceae	<i>Opuntia</i>	<i>puberula</i>	-12.4	CAM	8	TrSDBF	Mooney et al. (1989)
dicot	Cactaceae	<i>Opuntia</i>	<i>strobiliformis</i>	-15.7	CAM	1	unknown	Bender (1971)
dicot	Cactaceae	<i>Pachycereus</i>	<i>pecten-aboriginum</i>	-12.3	CAM	3	TrSDBF	Mooney et al. (1989)
dicot	Cactaceae	<i>Peniocereus</i>	<i>cuixmalensis</i>	-14.1	CAM	4	TrSDBF	Mooney et al. (1989)
dicot	Cactaceae	<i>Peniocereus</i>	<i>rosei</i>	-12.3	CAM	1	TrSDBF	Mooney et al. (1989)
dicot	Cactaceae	<i>Selenicereus</i>	<i>grandiflorus</i>	-13.0	CAM	1	domestic	Collister et al. (1994)
dicot	Cactaceae	<i>Selenicereus</i>	<i>vagens</i>	-13.0	CAM	1	TrSDBF	Mooney et al. (1989)
dicot	Cactaceae	<i>Stenocereus</i>	<i>chrysocarpus</i>	-14.4	CAM	3	TrSDBF	Mooney et al. (1989)
dicot	Caesalpinaceae	<i>Anthothena</i>	<i>macrophylla</i>	-31.0	C ₃	1	TrSCMBF	Cerling et al. (2004)
dicot	Caesalpinaceae	<i>Bocoa</i>	<i>prouacensis</i>	-29.7	C ₃	1	TrSOMBF	Bonal et al. (2000)
dicot	Caesalpinaceae	<i>Bocoa</i>	<i>prouacensis</i>	-30.7	C ₃	1	TrSOMBF	Bonal et al. (2000)
dicot	Caesalpinaceae	<i>Bocoa</i>	<i>prouacensis</i>	-31.8	C ₃	1	TrSOMBF	Bonal et al. (2000)
dicot	Caesalpinaceae	<i>Cynometra</i>	<i>alexandri</i>	-33.7	C ₃	1	TrSCMBF	Cerling et al. (2004)
dicot	Caesalpinaceae	<i>Dicorynia</i>	<i>guianensis</i>	-28.0	C ₃	1	TrSOMBF	Bonal et al. (2000)
dicot	Caesalpinaceae	<i>Dicorynia</i>	<i>guianensis</i>	-28.6	C ₃	1	TrSOMBF	Bonal et al. (2000)
dicot	Caesalpinaceae	<i>Dicorynia</i>	<i>guianensis</i>	-29.0	C ₃	1	TrSOMBF	Bonal et al. (2000)
dicot	Caesalpinaceae	<i>Eperua</i>	<i>falcata</i>	-28.3	C ₃	1	TrSOMBF	Bonal et al. (2000)
dicot	Caesalpinaceae	<i>Eperua</i>	<i>falcata</i>	-28.5	C ₃	1	TrSOMBF	Bonal et al. (2000)
dicot	Caesalpinaceae	<i>Eperua</i>	<i>falcata</i>	-28.6	C ₃	1	TrSOMBF	Bonal et al. (2000)
dicot	Caesalpinaceae	<i>Eperua</i>	<i>grandiflora</i>	-28.9	C ₃	1	TrSOMBF	Bonal et al. (2000)
dicot	Caesalpinaceae	<i>Eperua</i>	<i>grandiflora</i>	-28.9	C ₃	1	TrSOMBF	Bonal et al. (2000)
dicot	Caesalpinaceae	<i>Eperua</i>	<i>grandiflora</i>	-29.5	C ₃	1	TrSOMBF	Bonal et al. (2000)
dicot	Caesalpinaceae	<i>Eperua</i>	<i>grandiflora</i>	-28.4	C ₃	1	TrSOMBF	Buchmann et al. (1997)
dicot	Caesalpinaceae	<i>Eperua</i>	<i>grandiflora</i>	-31.9	C ₃	1	TrSOMBF	Buchmann et al. (1997)
dicot	Caesalpinaceae	<i>Gilbertiodendron</i>	<i>dewevrei</i>	-29.5	C ₃	1	TrSOMBF	Cerling et al. (2004)
dicot	Caesalpinaceae	<i>Julbernardia</i>	<i>seretii</i>	-30.2	C ₃	1	TrSOMBF	Cerling et al. (2004)

Appendix I. (continued)

	Family	Genus	species	$\delta^{13}\text{C}$	pathway	N	Biome	Reference
dicot	Caesalpiniaceae	<i>Peltogyne</i>	<i>venosa</i>	-27.9	C ₃	1	TrSOMBF	Bonal et al. (2000)
dicot	Caesalpiniaceae	<i>Peltogyne</i>	<i>venosa</i>	-29.7	C ₃	1	TrSOMBF	Bonal et al. (2000)
dicot	Caesalpiniaceae	<i>Recordoxylon</i>	<i>speciosum</i>	-26.6	C ₃	1	TrSOMBF	Buchmann et al. (1997)
dicot	Caesalpiniaceae	<i>Recordoxylon</i>	<i>speciosum</i>	-27.6	C ₃	1	TrSOMBF	Buchmann et al. (1997)
dicot	Caesalpiniaceae	<i>Recordoxylon</i>	<i>venosa</i>	-28.0	C ₃	1	TrSOMBF	Bonal et al. (2000)
dicot	Caesalpiniaceae	<i>Sclerolobium</i>	<i>albiflorum</i>	-30.0	C ₃	1	TrSOMBF	Bonal et al. (2000)
dicot	Caesalpiniaceae	<i>Sclerolobium</i>	<i>melinonii</i>	-28.6	C ₃	1	TrSOMBF	Bonal et al. (2000)
dicot	Caesalpiniaceae	<i>Sclerolobium</i>	<i>melinonii</i>	-30.0	C ₃	1	TrSOMBF	Bonal et al. (2000)
dicot	Caesalpiniaceae	<i>Sclerolobium</i>	<i>melinonii</i>	-30.1	C ₃	1	TrSOMBF	Bonal et al. (2000)
dicot	Caesalpiniaceae	<i>Swartzia</i>	<i>polyphylla</i>	-28.4	C ₃	1	TrSOMBF	Bonal et al. (2000)
dicot	Caesalpiniaceae	<i>Swartzia</i>	<i>polyphylla</i>	-29.2	C ₃	1	TrSOMBF	Bonal et al. (2000)
dicot	Caesalpiniaceae	<i>Vouacapoua</i>	<i>americana</i>	-30.7	C ₃	1	TrSOMBF	Bonal et al. (2000)
dicot	Caesalpiniaceae	<i>Vouacapoua</i>	<i>americana</i>	-31.1	C ₃	1	TrSOMBF	Bonal et al. (2000)
dicot	Caesalpiniaceae	<i>Vouacapoua</i>	<i>americana</i>	-32.4	C ₃	1	TrSOMBF	Bonal et al. (2000)
dicot	Caesalpiniaceae	<i>Vouacapoua</i>	<i>americana</i>	-29.7	C ₃	1	TrSOMBF	Buchmann et al. (1997)
dicot	Caesalpiniaceae	<i>Vouacapoua</i>	<i>americana</i>	-30.3	C ₃	1	TrSOMBF	Buchmann et al. (1997)
dicot	Cannabaceae	<i>Celtis</i>	<i>laevigata</i>	-28.1	C ₃	2	TmGSS	Jessup et al. (2003)
dicot	Capparaceae	<i>Capparis</i>	<i>indica</i>	-29.3	C ₃	6	TrSDBF	Leffler and Enquist (2002)
dicot	Capparaceae	<i>Capparis</i>	<i>indica</i>	-27.5	C ₃	7	TrSDBF	Mooney et al. (1989)
dicot	Capparaceae	<i>Forchhammeria</i>	<i>pallida</i>	-24.1	C ₃	3	TrSDBF	Mooney et al. (1989)
dicot	Caricaceae	<i>Carica</i>	<i>papaya</i>	-25.9	C ₃	6	TrSDBF	Holtum and Winter (2005)
dicot	Caricaceae	<i>Carica</i>	<i>papaya</i>	-26.2	C ₃	6	TrSDBF	Holtum and Winter (2005)
dicot	Caricaceae	<i>Carica</i>	<i>papaya</i>	-26.2	C ₃	6	TrSDBF	Holtum and Winter (2005)
dicot	Caricaceae	<i>Carica</i>	<i>papaya</i>	-27.5	C ₃	6	TrSDBF	Holtum and Winter (2005)
dicot	Caryocaraceae	<i>Caryocar</i>	<i>glabrum</i>	-29.4	C ₃	1	TrSOMBF	Bonal et al. (2000)
dicot	Caryocaraceae	<i>Caryocar</i>	<i>glabrum</i>	-29.4	C ₃	1	TrSOMBF	Bonal et al. (2000)
dicot	Caryophyllaceae	<i>Cerastium</i>	<i>holosteoides</i>	-28.2	C ₃	1	TmBMF	Dungait et al. (2008)
dicot	Caryophyllaceae	<i>Stellaria</i>	<i>graminea</i>	-27.7	C ₃	1	TmBMF	Dungait et al. (2008)
dicot	Celastraceae	<i>Goupia</i>	<i>glabra</i>	-29.9	C ₃	1	TrSOMBF	Bonal et al. (2000)
dicot	Celastraceae	<i>Goupia</i>	<i>glabra</i>	-30.0	C ₃	1	TrSOMBF	Bonal et al. (2000)
dicot	Celastraceae	<i>Semialarium</i>	<i>mexicanum</i>	-28.2	C ₃	5	TrSDBF	Leffler and Enquist (2002)
dicot	Chenopodiaceae	<i>Atriplex</i>	<i>canescens</i>	-13.7	C ₄	1	TmGSS	Dodd et al. (1998)

Appendix I. (continued)

	Family	Genus	species	$\delta^{13}\text{C}$	pathway	N	Biome	Reference
dicot	Chenopodiaceae	<i>Atriplex</i>	<i>canescens</i>	-14.0	C ₄	1	TmGSS	Dodd et al. (1998)
dicot	Chenopodiaceae	<i>Atriplex</i>	<i>canescens</i>	-14.1	C ₄	1	TmGSS	Dodd et al. (1998)
dicot	Chenopodiaceae	<i>Atriplex</i>	<i>canescens</i>	-14.1	C ₄	1	TmGSS	Dodd et al. (1998)
dicot	Chenopodiaceae	<i>Atriplex</i>	<i>canescens</i>	-14.3	C ₄	1	TmGSS	Dodd et al. (1998)
dicot	Chenopodiaceae	<i>Atriplex</i>	<i>canescens</i>	-14.3	C ₄	1	TmGSS	Dodd et al. (1998)
dicot	Chenopodiaceae	<i>Atriplex</i>	<i>canescens</i>	-14.4	C ₄	1	TmGSS	Dodd et al. (1998)
dicot	Chenopodiaceae	<i>Atriplex</i>	<i>canescens</i>	-14.5	C ₄	1	TmGSS	Dodd et al. (1998)
dicot	Chenopodiaceae	<i>Atriplex</i>	<i>canescens</i>	-14.7	C ₄	20	DXS	Van de Water et al. (2002)
dicot	Chenopodiaceae	<i>Atriplex</i>	<i>canescens</i>	-16.3	C ₄	34	DXS	Van de Water et al. (2002)
dicot	Chenopodiaceae	<i>Atriplex</i>	<i>confertifolia</i>	-16.4	C ₄	57	DXS	Van de Water et al. (2002)
dicot	Chenopodiaceae	<i>Atriplex</i>	<i>hastata</i>	-32.1	C ₃	1	unknown	Bender (1971)
dicot	Chenopodiaceae	<i>Atriplex</i>	<i>patula</i>	-31.6	C ₃	1	unknown	Bender (1971)
dicot	Chenopodiaceae	<i>Atriplex</i>	<i>rosea</i>	-19.4	C ₄	1	unknown	Bender (1971)
dicot	Chenopodiaceae	<i>Ceratoides</i>	<i>lanata</i>	-28.9	C ₃	4	DXS	Toft et al. (1989)
dicot	Chenopodiaceae	<i>Chenopodium</i>	<i>album</i>	-28.1	C ₃	1	unknown	Bender (1971)
dicot	Chenopodiaceae	<i>Haloxylon</i>	<i>salicornicum</i>	-14.5	C ₄	1	unknown	Bender (1971)
dicot	Chenopodiaceae	<i>Salsola</i>	<i>foetida</i>	-12.4	C ₄	1	unknown	Bender (1971)
dicot	Chenopodiaceae	<i>Suaeda</i>	<i>fruticosa</i>	-12.2	C ₄	1	unknown	Bender (1971)
dicot	Chrysobalanaceae	<i>Couepia</i>	<i>caryophylloides</i>	-29.6	C ₃	1	TrSOMBF	Bonal et al. (2000)
dicot	Chrysobalanaceae	<i>Couepia</i>	<i>caryophylloides</i>	-30.7	C ₃	1	TrSOMBF	Bonal et al. (2000)
dicot	Chrysobalanaceae	<i>Couepia</i>	<i>guianensis</i>	-31.7	C ₃	1	TrSOMBF	Bonal et al. (2000)
dicot	Chrysobalanaceae	<i>indet.</i>	<i>indet.</i>	-31.8	C ₃	1	TrSOMBF	Bonal et al. (2000)
dicot	Chrysobalanaceae	<i>Licania</i>	<i>alba</i>	-31.5	C ₃	1	TrSOMBF	Bonal et al. (2000)
dicot	Chrysobalanaceae	<i>Licania</i>	<i>alba</i>	-31.6	C ₃	1	TrSOMBF	Bonal et al. (2000)
dicot	Chrysobalanaceae	<i>Licania</i>	<i>alba</i>	-32.1	C ₃	1	TrSOMBF	Bonal et al. (2000)
dicot	Chrysobalanaceae	<i>Licania</i>	<i>glabriflora</i>	-32.1	C ₃	1	TrSOMBF	Bonal et al. (2000)
dicot	Chrysobalanaceae	<i>Licania</i>	<i>granvillei</i>	-31.0	C ₃	1	TrSOMBF	Bonal et al. (2000)
dicot	Chrysobalanaceae	<i>Licania</i>	<i>membranacea</i>	-32.0	C ₃	1	TrSOMBF	Bonal et al. (2000)
dicot	Chrysobalanaceae	<i>Licania</i>	<i>membranacea</i>	-32.0	C ₃	1	TrSOMBF	Bonal et al. (2000)
dicot	Chrysobalanaceae	<i>Licania</i>	<i>membranacea</i>	-33.4	C ₃	1	TrSOMBF	Bonal et al. (2000)
dicot	Chrysobalanaceae	<i>Licania</i>	<i>ovalifolia</i>	-31.8	C ₃	1	TrSOMBF	Bonal et al. (2000)
dicot	Chrysobalanaceae	<i>Licania</i>	<i>sp. 1</i>	-30.6	C ₃	1	TrSOMBF	Bonal et al. (2000)

Appendix I. (continued)

	Family	Genus	species	$\delta^{13}\text{C}$	pathway	N	Biome	Reference
dicot	Chrysobalanaceae	<i>Licania</i>	<i>sp. 2</i>	-32.5	C ₃	1	TrSOMBF	Bonal et al. (2000)
dicot	Chrysobalanaceae	<i>Parinari</i>	<i>excelsa</i>	-30.8	C ₃	1	TrSOMBF	Bonal et al. (2000)
dicot	Chrysobalanaceae	<i>Parinari</i>	<i>montana</i>	-29.8	C ₃	1	TrSOMBF	Bonal et al. (2000)
dicot	Chrysobalanaceae	<i>Parinari</i>	<i>sp.</i>	-31.5	C ₃	1	TrSOMBF	Bonal et al. (2000)
dicot	Chrysobalanaceae	<i>Marantese</i>	<i>glabra</i>	-28.6	C ₃	1	TrSOMBF	Cerling et al. (2004)
dicot	Chrysobalanaceae	<i>Licania</i>	<i>alba</i>	-33.5	C ₃	1	TrSOMBF	Buchmann et al. (1997)
dicot	Chrysobalanaceae	<i>Licania</i>	<i>alba</i>	-33.5	C ₃	1	TrSOMBF	Buchmann et al. (1997)
dicot	Chrysobalanaceae	<i>Licania</i>	<i>alba</i>	-34.2	C ₃	1	TrSCMBF	Buchmann et al. (1997)
dicot	Chrysobalanaceae	<i>Licania</i>	<i>alba</i>	-34.4	C ₃	1	TrSCMBF	Buchmann et al. (1997)
dicot	Cistaceae	<i>Hudsonia</i>	<i>tomentosa</i>	-28.4	C ₃	1	unknown	Bender (1971)
dicot	Clusiaceae	<i>Cratoxylum</i>	<i>glaucum</i>	-31.3	C ₃	4	TrSOMBF	Nagy and Proctor (2000)
dicot	Clusiaceae	<i>Moronobea</i>	<i>coccinea</i>	-30.3	C ₃	1	TrSOMBF	Bonal et al. (2000)
dicot	Clusiaceae	<i>Moronobea</i>	<i>coccinea</i>	-30.8	C ₃	1	TrSOMBF	Bonal et al. (2000)
dicot	Clusiaceae	<i>Platonia</i>	<i>insignis</i>	-28.0	C ₃	1	TrSOMBF	Bonal et al. (2000)
dicot	Clusiaceae	<i>Symphonia</i>	<i>sp.</i>	-30.1	C ₃	1	TrSOMBF	Bonal et al. (2000)
dicot	Clusiaceae	<i>Symphonia</i>	<i>sp.</i>	-30.2	C ₃	1	TrSOMBF	Bonal et al. (2000)
dicot	Clusiaceae	<i>Symphonia</i>	<i>sp.</i>	-30.4	C ₃	1	TrSOMBF	Bonal et al. (2000)
dicot	Clusiaceae	<i>Tovomita</i>	<i>sp.</i>	-32.5	C ₃	1	TrSOMBF	Bonal et al. (2000)
dicot	Connaraceae	<i>Agelaea</i>	<i>paradoxa</i>	-34.5	C ₃	1	TrSCMBF	Cerling et al. (2004)
dicot	Connaraceae	<i>Cnestis</i>	<i>urens</i>	-28.7	C ₃	1	TrSOMBF	Cerling et al. (2004)
dicot	Connaraceae	<i>Rourea</i>	<i>thomsonii</i>	-31.6	C ₃	1	TrSOMBF	Cerling et al. (2004)
dicot	Convolvulaceae	<i>Convolvulus</i>	<i>sepium</i>	-25.7	C ₃	1	unknown	Bender (1971)
dicot	Cornaceae	<i>Nyssa</i>	<i>sylvatica</i>	-32.0	C ₃	5	TmBMF	McArthur and Moorhead (1996)
dicot	Crassulaceae	<i>Crassula</i>	<i>tomentosa</i>	-18.9	CAM	1	unknown	Bender (1971)
dicot	Crassulaceae	<i>Echeveria</i>	<i>cilva</i>	-18.1	CAM	1	unknown	Bender (1971)
dicot	Crassulaceae	<i>Kalanchoe</i>	<i>tubiflora</i>	-14.2	CAM	1	unknown	Bender (1971)
dicot	Crassulaceae	<i>Sedum</i>	<i>rubrotinctum</i>	-13.8	CAM	1	unknown	Bender (1971)
dicot	Crassulaceae	<i>Sedum</i>	<i>spectabile</i>	-26.6	CAM	1	unknown	Bender (1971)
dicot	Crassulaceae	<i>Sedum</i>	<i>spurius</i>	-27.6	CAM	1	unknown	Bender (1971)
dicot	Crassulaceae	<i>Sempervivum</i>	<i>calcareum</i>	-16.8	CAM	1	unknown	Bender (1971)
dicot	Dipterocarpaceae	<i>Cotylelobium</i>	<i>burckii</i>	-31.3	C ₃	6	TrSOMBF	Nagy and Proctor (2000)
dicot	Dipterocarpaceae	<i>Cotylelobium</i>	<i>melanoxyton</i>	-30.3	C ₃	3	TrSOMBF	Nagy and Proctor (2000)

Appendix I. (continued)

	Family	Genus	species	$\delta^{13}\text{C}$	pathway	N	Biome	Reference
dicot	Dipterocarpaceae	<i>Cotylelobium</i>	<i>melanoxydon</i>	-30.8	C ₃	5	TrSOMBF	Nagy and Proctor (2000)
dicot	Dipterocarpaceae	<i>Dipterocarpus</i>	<i>eurynchus</i>	-30.4	C ₃	3	TrSOMBF	Nagy and Proctor (2000)
dicot	Dipterocarpaceae	<i>Parashorea</i>	<i>chinensis</i>	-27.8		1		He et al. (2008)
dicot	Dipterocarpaceae	<i>Shorea</i>	<i>amplexicaulis</i>	-31.2	C ₃	3	TrSOMBF	Nagy and Proctor (2000)
dicot	Dipterocarpaceae	<i>Shorea</i>	<i>leprosula</i>	-31.6	C ₃	3	TrSOMBF	Nagy and Proctor (2000)
dicot	Dipterocarpaceae	<i>Shorea</i>	<i>pinanga</i>	-29.5	C ₃	2	TrSOMBF	Nagy and Proctor (2000)
dicot	Dipterocarpaceae	<i>Shorea</i>	<i>rugosa</i>	-32.3	C ₃	3	TrSOMBF	Nagy and Proctor (2000)
dicot	Dipterocarpaceae	<i>Shorea</i>	<i>scabrida</i>	-29.9	C ₃	6	TrSOMBF	Nagy and Proctor (2000)
dicot	Dipterocarpaceae	<i>Vatica</i>	<i>brunigii</i>	-31.0	C ₃	6	TrSOMBF	Nagy and Proctor (2000)
dicot	Ebenaceae	<i>Diospyros</i>	<i>bipendensis</i>	-32.1	C ₃	1	TrSCMBF	Cerling et al. (2004)
dicot	Ebenaceae	<i>Diospyros</i>	<i>nicaraguensis</i>	-30.4	C ₃	5	TrSDBF	Leffler and Enquist (2002)
dicot	Ebenaceae	<i>Diospyros</i>	<i>sandwicensis</i>	-27.1	C ₃	8	TrSDBF	Sandquist and Cordell (2007)
dicot	Ebenaceae	<i>Diospyros</i>	<i>texana</i>	-28.6	C ₃	2	TmGSS	Jessup et al. (2003)
dicot	Elaeocarpaceae	<i>Sloanea</i>	<i>sp.</i>	-27.9	C ₃	1	TrSOMBF	Bonal et al. (2000)
dicot	Ericaceae	<i>Arbutus</i>	<i>menziesii</i>	-27.1	C ₃	3	MFWS	Diefendorf et al. (2010)
dicot	Ericaceae	<i>Arctostaphylos</i>	<i>patula</i>	-26.5	C ₃	1	TmCF	DeLucia and Schlesinger (1991)
dicot	Ericaceae	<i>Arctostaphylos</i>	<i>uva-ursi</i>	-28.6	C ₃	5	BFT	Brooks et al. (1997)
dicot	Ericaceae	<i>Arctostaphylos</i>	<i>uva-ursi</i>	-29.0	C ₃	5	BFT	Brooks et al. (1997)
dicot	Ericaceae	<i>Arctostaphylos</i>	<i>uva-ursi</i>	-32.2	C ₃	5	BFT	Brooks et al. (1997)
dicot	Ericaceae	<i>Cassiope</i>	<i>tetragona</i>	-27.9	C ₃	1	unknown	Bender (1971)
dicot	Ericaceae	<i>Gaultheria</i>	<i>procumbens</i>	-29.4	C ₃	5	BFT	Brooks et al. (1997)
dicot	Ericaceae	<i>Ledum</i>	<i>groenlandicum</i>	-28.5	C ₃	5	BFT	Brooks et al. (1997)
dicot	Ericaceae	<i>Oxydendrum</i>	<i>arboreum</i>	-29.4	C ₃	6	TmBMF	Garten and Taylor (1992)
dicot	Ericaceae	<i>Oxydendrum</i>	<i>arboreum</i>	-29.7	C ₃	6	TmBMF	Garten and Taylor (1992)
dicot	Ericaceae	<i>Oxydendrum</i>	<i>arboreum</i>	-30.9	C ₃	2	TmBMF	Garten and Taylor (1992)
dicot	Ericaceae	<i>Pyrola</i>	<i>secunda</i>	-31.3	C ₃	5	BFT	Brooks et al. (1997)
dicot	Ericaceae	<i>Rhododendron</i>	<i>ferrugineum</i>	-25.5	C ₃	1	MFWS	Peñuelas and Azcón-Bieto (1992)
dicot	Ericaceae	<i>Rhododendron</i>	<i>ferrugineum</i>	-25.9	C ₃	1	MFWS	Peñuelas and Azcón-Bieto (1992)
dicot	Ericaceae	<i>Rhododendron</i>	<i>ferrugineum</i>	-25.9	C ₃	1	MFWS	Peñuelas and Azcón-Bieto (1992)
dicot	Ericaceae	<i>Rhododendron</i>	<i>ferrugineum</i>	-28.7	C ₃	1	MFWS	Peñuelas and Azcón-Bieto (1992)
dicot	Ericaceae	<i>Vaccinium</i>	<i>myrtilloides</i>	-29.1	C ₃	5	BFT	Brooks et al. (1997)
dicot	Ericaceae	<i>Vaccinium</i>	<i>myrtilloides</i>	-29.4	C ₃	5	BFT	Brooks et al. (1997)

Appendix I. (continued)

	Family	Genus	species	δ¹³C	pathway	N	Biome	Reference
dicot	Ericaceae	<i>Vaccinium</i>	<i>myrtilloides</i>	-31.1	C ₃	5	BFT	Brooks et al. (1997)
dicot	Ericaceae	<i>Vaccinium</i>	<i>myrtilloides</i>	-31.6	C ₃	5	BFT	Brooks et al. (1997)
dicot	Ericaceae	<i>Vaccinium</i>	<i>myrtillus</i>	-30.1	C ₃	10	TmCF	Gerdol et al. (2000)
dicot	Ericaceae	<i>Vaccinium</i>	<i>ovatum</i>	-28.2	C ₃	1	MFWS	Diefendorf et al. (2010)
dicot	Ericaceae	<i>Vaccinium</i>	<i>vitis-idaea</i>	-27.6	C ₃	5	BFT	Brooks et al. (1997)
dicot	Ericaceae	<i>Vaccinium</i>	<i>vitis-idaea</i>	-28.5	C ₃	5	BFT	Brooks et al. (1997)
dicot	Ericaceae	<i>Vaccinium</i>	<i>vitis-idaea</i>	-30.5	C ₃	5	BFT	Brooks et al. (1997)
dicot	Ericaceae	<i>Vaccinium</i>	<i>vitis-idaea</i>	-30.8	C ₃	5	BFT	Brooks et al. (1997)
dicot	Ericaceae	<i>Vaccinium</i>	<i>vitis-idaea</i>	-28.5	C ₃	10	TmCF	Gerdol et al. (2000)
dicot	Erythroxylaceae	<i>Erythroxylum</i>	<i>havanense</i>	-27.0	C ₃	1	TrSDBF	Mooney et al. (1989)
dicot	Euphorbiaceae	<i>Alchornea</i>	<i>floribunda</i>	-33.4	C ₃	1	TrSCMBF	Cerling et al. (2004)
dicot	Euphorbiaceae	<i>Alchornea</i>	<i>trewioides</i>	-29.7	C ₃	1	TrSOMBF	Ehleringer et al. (1987)
dicot	Euphorbiaceae	<i>Amanoa</i>	<i>congesta</i>	-28.4	C ₃	1	TrSOMBF	Bonal et al. (2000)
dicot	Euphorbiaceae	<i>Aporosa</i>	<i>yunnanensis</i>	-30.8	C ₃	1	TrSCMBF	Ehleringer et al. (1987)
dicot	Euphorbiaceae	<i>Chaetocarpus</i>	<i>schomburg</i>	-31.3	C ₃	1	TrSOMBF	Bonal et al. (2000)
dicot	Euphorbiaceae	<i>Chaetocarpus</i>	<i>schomburg</i>	-31.9	C ₃	1	TrSOMBF	Bonal et al. (2000)
dicot	Euphorbiaceae	<i>Chaetocarpus</i>	<i>schomburg</i>	-33.8	C ₃	1	TrSOMBF	Bonal et al. (2000)
dicot	Euphorbiaceae	<i>Cleistanthus</i>	<i>michelsonii</i>	-25.0	C ₃	1	TrSOMBF	Cerling et al. (2004)
dicot	Euphorbiaceae	<i>Croton</i>	<i>fruticosus</i>	-28.7	C ₃	2	TmGSS	Jessup et al. (2003)
dicot	Euphorbiaceae	<i>Croton</i>	<i>lachnocarpus</i>	-34.4	C ₃	1	TrSOMBF	Ehleringer et al. (1987)
dicot	Euphorbiaceae	<i>Croton</i>	<i>monanthogynus</i>	-28.7	C ₃	2	TmGSS	Jessup et al. (2003)
dicot	Euphorbiaceae	<i>Croton</i>	<i>pseudoniveus</i>	-28.1	C ₃	6	TrSDBF	Mooney et al. (1989)
dicot	Euphorbiaceae	<i>Croton</i>	<i>tiglium</i>	-29.5	C ₃	1	TrSCMBF	Ehleringer et al. (1987)
dicot	Euphorbiaceae	<i>Drypetes</i>	<i>variabilis</i>	-31.0	C ₃	1	TrSOMBF	Bonal et al. (2000)
dicot	Euphorbiaceae	<i>Euphorbia</i>	<i>antiquorum</i>	-28.8	C ₃	1	TrSOMBF	Ehleringer et al. (1987)
dicot	Euphorbiaceae	<i>Euphorbia</i>	<i>corollata</i>	-26.1	C ₃	1	unknown	Bender (1971)
dicot	Euphorbiaceae	<i>Euphorbia</i>	<i>pulcherrima</i>	-29.4	C ₃	1	unknown	Bender (1971)
dicot	Euphorbiaceae	<i>Euphorbia</i>	<i>tirucalli</i>	-15.3	CAM	1	unknown	Bender (1971)
dicot	Euphorbiaceae	<i>Glycydendron</i>	<i>amazoni</i>	-30.8	C ₃	1	TrSOMBF	Bonal et al. (2000)
dicot	Euphorbiaceae	<i>Hevea</i>	<i>amazonensis</i>	-29.2	C ₃	1	TrSOMBF	Bonal et al. (2000)
dicot	Euphorbiaceae	<i>Macaranga</i>	<i>spinosa</i>	-31.1	C ₃	1	TrSOMBF	Cerling et al. (2004)
dicot	Euphorbiaceae	<i>Mallotus</i>	<i>apelta</i>	-26.7	C ₃	1	TrSOMBF	Ehleringer et al. (1987)

Appendix I. (continued)

	Family	Genus	species	$\delta^{13}\text{C}$	pathway	N	Biome	Reference
dicot	Euphorbiaceae	<i>Manniophyton</i>	<i>fulvum</i>	-31.8	C ₃	1	TrSOMBF	Cerling et al. (2004)
dicot	Euphorbiaceae	<i>Margaritaria</i>	<i>pynnertii</i>	-28.4	C ₃	1	TrSOMBF	Cerling et al. (2004)
dicot	Euphorbiaceae	<i>Margaritaria</i>	<i>pynnertii</i>	-29.3	C ₃	1	TrSOMBF	Cerling et al. (2004)
dicot	Euphorbiaceae	<i>Pedilanthus</i>	<i>thithymaloides</i>	-15.9	CAM	1	unknown	Bender (1971)
dicot	Euphorbiaceae	<i>Phyllanthus</i>	<i>urinaria</i>	-30.6	C ₃	1	TrSOMBF	Ehleringer et al. (1987)
dicot	Euphorbiaceae	<i>Ricinodendron</i>	<i>heudelotii</i>	-30.2	C ₃	1	TrSOMBF	Cerling et al. (2004)
dicot	Euphorbiaceae	<i>Ricinus</i>	<i>communis</i>	-30.2	C ₃	1	unknown	Bender (1971)
dicot	Euphorbiaceae	<i>Sapium</i>	<i>discolor</i>	-31.3	C ₃	1	TrSCMBF	Ehleringer et al. (1987)
dicot	Fabaceae	<i>Acacia</i>	<i>angustissima</i>	-26.9	C ₃	1	TrSDBF	Mooney et al. (1989)
dicot	Fabaceae	<i>Acacia</i>	<i>greggii</i>	-25.8	C ₃	1	DXS	Ehleringer and Cooper (1988)
dicot	Fabaceae	<i>Acacia</i>	<i>greggii</i>	-27.4	C ₃	1	DXS	Ehleringer and Cooper (1988)
dicot	Fabaceae	<i>Albizia</i>	<i>adinocephala</i>	-27.1	C ₃	6	TrSDBF	Holtum and Winter (2005)
dicot	Fabaceae	<i>Albizia</i>	<i>adinocephala</i>	-28.6	C ₃	6	TrSDBF	Holtum and Winter (2005)
dicot	Fabaceae	<i>Albizia</i>	<i>adinocephala</i>	-29.5	C ₃	6	TrSDBF	Holtum and Winter (2005)
dicot	Fabaceae	<i>Amorpha</i>	<i>canescens</i>	-27.9	C ₃	1	unknown	Bender (1971)
dicot	Fabaceae	<i>Andira</i>	<i>coriacea</i>	-30.8	C ₃	1	TrSOMBF	Bonal et al. (2000)
dicot	Fabaceae	<i>Apoplanesia</i>	<i>paniculata</i>	-27.3	C ₃	1	TrSDBF	Mooney et al. (1989)
dicot	Fabaceae	<i>Ateleia</i>	<i>herbert-smithii</i>	-31.1	C ₃	5	TrSDBF	Leffler and Enquist (2002)
dicot	Fabaceae	<i>Caesalpinia</i>	<i>coriaria</i>	-26.9	C ₃	1	TrSDBF	Mooney et al. (1989)
dicot	Fabaceae	<i>Caesalpinia</i>	<i>sclerocarpa</i>	-26.5	C ₃	1	TrSDBF	Mooney et al. (1989)
dicot	Fabaceae	<i>Cassia</i>	<i>covesii</i>	-26.0	C ₃	1	DXS	Ehleringer and Cooper (1988)
dicot	Fabaceae	<i>Cassia</i>	<i>covesii</i>	-26.7	C ₃	1	DXS	Ehleringer and Cooper (1988)
dicot	Fabaceae	<i>Cassia</i>	<i>covesii</i>	-26.8	C ₃	1	DXS	Ehleringer and Cooper (1988)
dicot	Fabaceae	<i>Ceratonia</i>	<i>siliqua</i>	-24.4	C ₃	1	MFWS	Peñuelas and Azcón-Bieto (1992)
dicot	Fabaceae	<i>Ceratonia</i>	<i>siliqua</i>	-26.1	C ₃	1	MFWS	Peñuelas and Azcón-Bieto (1992)
dicot	Fabaceae	<i>Ceratonia</i>	<i>siliqua</i>	-26.2	C ₃	1	MFWS	Peñuelas and Azcón-Bieto (1992)
dicot	Fabaceae	<i>Ceratonia</i>	<i>siliqua</i>	-26.8	C ₃	1	MFWS	Peñuelas and Azcón-Bieto (1992)
dicot	Fabaceae	<i>Cercidium</i>	<i>floridum</i>	-24.1	C ₃	1	DXS	Ehleringer and Cooper (1988)
dicot	Fabaceae	<i>Diploptropis</i>	<i>purpurea</i>	-30.7	C ₃	1	TrSOMBF	Bonal et al. (2000)
dicot	Fabaceae	<i>Diploptropis</i>	<i>purpurea</i>	-31.2	C ₃	1	TrSOMBF	Bonal et al. (2000)
dicot	Fabaceae	<i>Enterolobium</i>	<i>cyclocarpum</i>	-27.1	C ₃	6	TrSDBF	Holtum and Winter (2005)
dicot	Fabaceae	<i>Enterolobium</i>	<i>cyclocarpum</i>	-28.3	C ₃	6	TrSDBF	Holtum and Winter (2005)

Appendix I. (continued)

	Family	Genus	species	$\delta^{13}\text{C}$	pathway	N	Biome	Reference
dicot	Fabaceae	<i>Enterolobium</i>	<i>cyclocarpum</i>	-28.8	C ₃	6	TrSDBF	Holtum and Winter (2005)
dicot	Fabaceae	<i>Glycine</i>	<i>soja</i>	-28.9	C ₃	1	unknown	Bender (1971)
dicot	Fabaceae	<i>Hymenaea</i>	<i>courbaril</i>	-29.0	C ₃	5	TrSDBF	Leffler and Enquist (2002)
dicot	Fabaceae	<i>Lotus</i>	<i>tenuis</i>	-30.5	C ₃	1	TmBMF	Dungait et al. (2008)
dicot	Fabaceae	<i>Lupinus</i>	<i>perennis</i>	-28.5	C ₃	1	unknown	Bender (1971)
dicot	Fabaceae	<i>Lysiloma</i>	<i>latisiquum</i>	-29.4	C ₃	1	TrSCMBF	Jones et al. (2010)
dicot	Fabaceae	<i>Medicago</i>	<i>lupulina</i>	-29.0	C ₃	1	TmBMF	Dungait et al. (2008)
dicot	Fabaceae	<i>Prosopis</i>	<i>glandulosa</i>	-25.7	C ₃	1	TrSGSS	Bai et al. (2008)
dicot	Fabaceae	<i>Trifolium</i>	<i>pratense</i>	-30.1	C ₃	1	TmBMF	Dungait et al. (2008)
dicot	Fabaceae	<i>Trifolium</i>	<i>repens</i>	-28.7	C ₃	1	TmBMF	Dungait et al. (2008)
dicot	Fagaceae	<i>Castanea</i>	<i>sativa</i>	-28.5	C ₃	1	TmBMF	Balesdent et al. (1993)
dicot	Fagaceae	<i>Castanea</i>	<i>sativa</i>	-28.8	C ₃	1	TmBMF	Balesdent et al. (1993)
dicot	Fagaceae	<i>Castanea</i>	<i>sativa</i>	-28.9	C ₃	1	TmBMF	Balesdent et al. (1993)
dicot	Fagaceae	<i>Castanopsis</i>	<i>chinensis</i>	-29.8	C ₃	1	TrSOMBF	Ehleringer et al. (1987)
dicot	Fagaceae	<i>Fagus</i>	<i>crenata</i>	-27.8	C ₃	1	TmBMF	Uemura et al. (2006)
dicot	Fagaceae	<i>Fagus</i>	<i>japonica</i>	-27.3	C ₃	1	TmBMF	Uemura et al. (2006)
dicot	Fagaceae	<i>Fagus</i>	<i>silvatica</i>	-27.1	C ₃	1	TmBMF	Balesdent et al. (1993)
dicot	Fagaceae	<i>Fagus</i>	<i>silvatica</i>	-28.4	C ₃	1	TmBMF	Balesdent et al. (1993)
dicot	Fagaceae	<i>Fagus</i>	<i>silvatica</i>	-28.5	C ₃	1	TmBMF	Balesdent et al. (1993)
dicot	Fagaceae	<i>Fagus</i>	<i>silvatica</i>	-28.8	C ₃	1	TmBMF	Balesdent et al. (1993)
dicot	Fagaceae	<i>Fagus</i>	<i>silvatica</i>	-29.2	C ₃	1	TmBMF	Balesdent et al. (1993)
dicot	Fagaceae	<i>Fagus</i>	<i>silvatica</i>	-29.6	C ₃	1	TmBMF	Balesdent et al. (1993)
dicot	Fagaceae	<i>Fagus</i>	<i>sylvatica</i>	-27.9	C ₃	8	TmBMF	Chevillat et al. (2005)
dicot	Fagaceae	<i>Fagus</i>	<i>sylvatica</i>	-29.8	C ₃	1	domestic	Collister et al. (1994)
dicot	Fagaceae	<i>Fagus</i>	<i>sylvatica</i>	-24.7	C ₃	1	TmBMF	Hemming et al. (2005)
dicot	Fagaceae	<i>Fagus</i>	<i>sylvatica</i>	-27.5	C ₃	1	TmBMF	Hemming et al. (2005)
dicot	Fagaceae	<i>Fagus</i>	<i>sylvatica</i>	-27.7	C ₃	1	TmBMF	Hemming et al. (2005)
dicot	Fagaceae	<i>Fagus</i>	<i>sylvatica</i>	-27.8	C ₃	1	TmBMF	Hemming et al. (2005)
dicot	Fagaceae	<i>Fagus</i>	<i>sylvatica</i>	-27.8	C ₃	1	TmBMF	Hemming et al. (2005)
dicot	Fagaceae	<i>Fagus</i>	<i>sylvatica</i>	-28.1	C ₃	1	TmBMF	Hemming et al. (2005)
dicot	Fagaceae	<i>Fagus</i>	<i>sylvatica</i>	-28.4	C ₃	1	TmBMF	Hemming et al. (2005)
dicot	Fagaceae	<i>Fagus</i>	<i>sylvatica</i>	-28.5	C ₃	1	TmBMF	Hemming et al. (2005)

Appendix I. (continued)

	Family	Genus	species	$\delta^{13}\text{C}$	pathway	N	Biome	Reference
dicot	Fagaceae	<i>Fagus</i>	<i>sylvatica</i>	-28.7	C ₃	1	TmBMF	Hemming et al. (2005)
dicot	Fagaceae	<i>Fagus</i>	<i>sylvatica</i>	-29.6	C ₃	1	TmBMF	Hemming et al. (2005)
dicot	Fagaceae	<i>Fagus</i>	<i>sylvatica</i>	-29.7	C ₃	1	TmBMF	Hemming et al. (2005)
dicot	Fagaceae	<i>Fagus</i>	<i>sylvatica</i>	-30.0	C ₃	1	TmBMF	Hemming et al. (2005)
dicot	Fagaceae	<i>Fagus</i>	<i>sylvatica</i>	-30.2	C ₃	1	TmBMF	Hemming et al. (2005)
dicot	Fagaceae	<i>Fagus</i>	<i>sylvatica</i>	-30.3	C ₃	1	TmBMF	Hemming et al. (2005)
dicot	Fagaceae	<i>Fagus</i>	<i>sylvatica</i>	-30.6	C ₃	1	TmBMF	Hemming et al. (2005)
dicot	Fagaceae	<i>Fagus</i>	<i>sylvatica</i>	-31.3	C ₃	1	TmBMF	Hemming et al. (2005)
dicot	Fagaceae	<i>Fagus</i>	<i>sylvatica</i>	-31.6	C ₃	1	TmBMF	Hemming et al. (2005)
dicot	Fagaceae	<i>Fagus</i>	<i>sylvatica</i>	-31.6	C ₃	1	TmBMF	Hemming et al. (2005)
dicot	Fagaceae	<i>Fagus</i>	<i>sylvatica</i>	-32.1	C ₃	1	TmBMF	Hemming et al. (2005)
dicot	Fagaceae	<i>Fagus</i>	<i>sylvatica</i>	-32.2	C ₃	1	TmBMF	Hemming et al. (2005)
dicot	Fagaceae	<i>Fagus</i>	<i>sylvatica</i>	-32.4	C ₃	1	TmBMF	Hemming et al. (2005)
dicot	Fagaceae	<i>Fagus</i>	<i>sylvatica</i>	-32.9	C ₃	1	TmBMF	Hemming et al. (2005)
dicot	Fagaceae	<i>Fagus</i>	<i>sylvatica</i>	-32.9	C ₃	1	TmBMF	Hemming et al. (2005)
dicot	Fagaceae	<i>Fagus</i>	<i>sylvatica</i>	-33.5	C ₃	1	TmBMF	Hemming et al. (2005)
dicot	Fagaceae	<i>Fagus</i>	<i>sylvatica</i>	-26.4	C ₃	1	TmBMF	Lockheart et al. (1997)
dicot	Fagaceae	<i>Quercus</i>	<i>agrifolia</i>	-27.5	C ₃	3	MFWS	Diefendorf et al. (2010)
dicot	Fagaceae	<i>Quercus</i>	<i>alba</i>	-28.8	C ₃	1	TmBMF	Baldocchi and Bowling (1999)
dicot	Fagaceae	<i>Quercus</i>	<i>alba</i>	-30.0	C ₃	1	TmBMF	Baldocchi and Bowling (1999)
dicot	Fagaceae	<i>Quercus</i>	<i>alba</i>	-30.1	C ₃	1	TmBMF	Baldocchi and Bowling (1999)
dicot	Fagaceae	<i>Quercus</i>	<i>cerris</i>	-27.5	C ₃	1	MFWS	Valentini et al. (1992)
dicot	Fagaceae	<i>Quercus</i>	<i>coccifera</i>	-25.9	C ₃	4	MFWS	Escuerdo et al. (2008)
dicot	Fagaceae	<i>Quercus</i>	<i>ilex</i>	-26.4	C ₃	1	MFWS	Valentini et al. (1992)
dicot	Fagaceae	<i>Quercus</i>	<i>laurifolia</i>	-29.8	C ₃	5	TmBMF	McArthur and Moorhead (1996)
dicot	Fagaceae	<i>Quercus</i>	<i>nigra</i>	-29.8	C ₃	5	TmBMF	McArthur and Moorhead (1996)
dicot	Fagaceae	<i>Quercus</i>	<i>petraea</i>	-26.0	C ₃	1	TmBMF	Balesdent et al. (1993)
dicot	Fagaceae	<i>Quercus</i>	<i>petraea</i>	-26.1	C ₃	1	TmBMF	Balesdent et al. (1993)
dicot	Fagaceae	<i>Quercus</i>	<i>petraea</i>	-26.3	C ₃	1	TmBMF	Balesdent et al. (1993)
dicot	Fagaceae	<i>Quercus</i>	<i>petraea</i>	-26.8	C ₃	8	TmBMF	Chevillat et al. (2005)
dicot	Fagaceae	<i>Quercus</i>	<i>prinus</i>	-28.9	C ₃	1	TmBMF	Baldocchi and Bowling (1999)
dicot	Fagaceae	<i>Quercus</i>	<i>pubescens</i>	-27.2	C ₃	1	MFWS	Valentini et al. (1992)

Appendix I. (continued)

	Family	Genus	species	$\delta^{13}\text{C}$	pathway	N	Biome	Reference
dicot	Fagaceae	<i>Quercus</i>	<i>pyrenaica</i>	-26.4	C ₃	4	MFWS	Escuerdo et al. (2008)
dicot	Fagaceae	<i>Quercus</i>	<i>pyrenaica</i>	-27.0	C ₃	4	MFWS	Escuerdo et al. (2008)
dicot	Fagaceae	<i>Quercus</i>	<i>pyrenaica</i>	-27.1	C ₃	4	MFWS	Escuerdo et al. (2008)
dicot	Fagaceae	<i>Quercus</i>	<i>pyrenaica</i>	-27.5	C ₃	4	MFWS	Escuerdo et al. (2008)
dicot	Fagaceae	<i>Quercus</i>	<i>rober</i>	-30.5	C ₃	1	domestic	Collister et al. (1994)
dicot	Fagaceae	<i>Quercus</i>	<i>rober</i>	-28.7	C ₃	1	TmBMF	Lockheart et al. (1997)
dicot	Fagaceae	<i>Quercus</i>	<i>robur</i>	-27.7	C ₃	1	TmBMF	Balesdent et al. (1993)
dicot	Fagaceae	<i>Quercus</i>	<i>robur</i>	-28.1	C ₃	1	TmBMF	Balesdent et al. (1993)
dicot	Fagaceae	<i>Quercus</i>	<i>rotundifolia</i>	-26.6	C ₃	4	MFWS	Escuerdo et al. (2008)
dicot	Fagaceae	<i>Quercus</i>	<i>rotundifolia</i>	-26.8	C ₃	4	MFWS	Escuerdo et al. (2008)
dicot	Fagaceae	<i>Quercus</i>	<i>rotundifolia</i>	-27.4	C ₃	4	MFWS	Escuerdo et al. (2008)
dicot	Fagaceae	<i>Quercus</i>	<i>rotundifolia</i>	-27.6	C ₃	4	MFWS	Escuerdo et al. (2008)
dicot	Fagaceae	<i>Quercus</i>	<i>rotundifolia</i>	-27.8	C ₃	4	MFWS	Escuerdo et al. (2008)
dicot	Fagaceae	<i>Quercus</i>	<i>suber</i>	-26.5	C ₃	4	MFWS	Escuerdo et al. (2008)
dicot	Fagaceae	<i>Quercus</i>	<i>suber</i>	-27.2	C ₃	4	MFWS	Escuerdo et al. (2008)
dicot	Fagaceae	<i>Quercus</i>	<i>turneri</i>	-28.8	C ₃	1	domestic	Collister et al. (1994)
dicot	Fagaceae	<i>Quercus</i>	<i>virginiana</i>	-27.1	C ₃	3	TmGSS	Jessup et al. (2003)
dicot	Fagaceae	<i>Quercus</i>	<i>virginiana</i>	-29.7	C ₃	1	TrSCMBF	Jones et al. (2010)
dicot	Fagaceae	<i>Quercus</i>	<i>gambelii</i>	-26.9	C ₃	6	TmCF	Williams and Ehleringer (1996)
dicot	Fagaceae	<i>Quercus</i>	<i>gambelii</i>	-27.0	C ₃	5	TmCF	Williams and Ehleringer (1996)
dicot	Fagaceae	<i>Quercus</i>	<i>gambelii</i>	-27.3	C ₃	5	TmCF	Williams and Ehleringer (1996)
dicot	Fagaceae	<i>Quercus</i>	<i>gambelii</i>	-26.9	C ₃	5	DXS	Williams and Ehleringer (1996)
dicot	Fagaceae	<i>Quercus</i>	<i>gambelii</i>	-27.2	C ₃	6	DXS	Williams and Ehleringer (1996)
dicot	Fagaceae	<i>Quercus</i>	<i>gambelii</i>	-27.5	C ₃	4	DXS	Williams and Ehleringer (1996)
dicot	Flacourtiaceae	<i>Casearia</i>	<i>corymbosa</i>	-28.1	C ₃	1	TrSDBF	Mooney et al. (1989)
dicot	Flacourtiaceae	<i>Casearia</i>	<i>sylvestris</i>	-30.0	C ₃	5	TrSDBF	Leffler and Enquist (2002)
dicot	Flacourtiaceae	<i>Homalium</i>	<i>africana</i>	-34.3	C ₃	1	TrSCMBF	Cerling et al. (2004)
dicot	Flacourtiaceae	<i>Homalium</i>	<i>africana</i>	-35.4	C ₃	1	TrSCMBF	Cerling et al. (2004)
dicot	Flacourtiaceae	<i>Laetia</i>	<i>procera</i>	-31.3	C ₃	1	TrSOMBF	Bonal et al. (2000)
dicot	Gesneriaceae	<i>Codonanthe</i>	<i>uleana</i>	-19.9	C ₃	6	TrSDBF	Holtum and Winter (2005)
dicot	Gesneriaceae	<i>Codonanthe</i>	<i>uleana</i>	-20.1	C ₃	6	TrSDBF	Holtum and Winter (2005)
dicot	Gesneriaceae	<i>Codonanthe</i>	<i>uleana</i>	-22.1	C ₃	6	TrSDBF	Holtum and Winter (2005)

Appendix I. (continued)

	Family	Genus	species	$\delta^{13}\text{C}$	pathway	N	Biome	Reference
dicot	Guttiferae	<i>Garcinia</i>	<i>oblongifolia</i>	-30.0	C ₃	1	TrSCMBF	Ehleringer et al. (1987)
dicot	Haloragidaceae	<i>Myriophyllum</i>	<i>sibiricum</i>	-19.4	C ₃	5	TmBMF	Keough et al. (1996)
dicot	Hippocrateaceae	<i>Salicia</i>	<i>cerasifera</i>	-31.4	C ₃	1	TrSOMBF	Cerling et al. (2004)
dicot	Hippocratiaceae	<i>Salacia</i>	<i>pyriformis</i>	-29.7	C ₃	1	TrSOMBF	Cerling et al. (2004)
dicot	Hippocratiaceae	<i>Salacia</i>	<i>pyriformis</i>	-29.7	C ₃	1	TrSOMBF	Cerling et al. (2004)
dicot	Hugoniaceae	<i>Hebepetalum</i>	<i>humiriifoli</i>	-31.8	C ₃	1	TrSOMBF	Bonal et al. (2000)
dicot	Humiriaceae	<i>Humiriastrum</i>	<i>subcrenat</i>	-32.7	C ₃	1	TrSOMBF	Bonal et al. (2000)
dicot	Humiriaceae	<i>Humiriastrum</i>	<i>subcrenat</i>	-34.8	C ₃	1	TrSOMBF	Bonal et al. (2000)
dicot	Humiriaceae	<i>Vantanea</i>	<i>parviflora</i>	-30.1	C ₃	1	TrSOMBF	Bonal et al. (2000)
dicot	Humiriaceae	<i>Vantanea</i>	<i>parviflora</i>	-31.3	C ₃	1	TrSOMBF	Bonal et al. (2000)
dicot	Icacinaceae	<i>Dendrobangia</i>	<i>boliviana</i>	-31.1	C ₃	1	TrSOMBF	Bonal et al. (2000)
dicot	Icacinaceae	<i>Dendrobangia</i>	<i>boliviana</i>	-31.3	C ₃	1	TrSOMBF	Bonal et al. (2000)
dicot	Icacinaceae	<i>Dendrobangia</i>	<i>boliviana</i>	-31.5	C ₃	1	TrSOMBF	Bonal et al. (2000)
dicot	Icacinaceae	<i>Poraqueiba</i>	<i>guianensis</i>	-32.9	C ₃	1	TrSOMBF	Bonal et al. (2000)
dicot	Irvingiaceae	<i>Irvingia</i>	<i>robur</i>	-28.0	C ₃	1	TrSOMBF	Cerling et al. (2004)
dicot	Irvingiaceae	<i>Klainedoxa</i>	<i>trillesii</i>	-29.4	C ₃	1	TrSOMBF	Cerling et al. (2004)
dicot	Irvingiaceae	<i>Klainedoxa</i>	<i>trillesii</i>	-30.8	C ₃	1	TrSOMBF	Cerling et al. (2004)
dicot	Juglandaceae	<i>Juglans</i>	<i>ailanthifolia</i>	-28.6	C ₃	6	TmBMF	Hanba et al. (1997)
dicot	Juglandaceae	<i>Juglans</i>	<i>ailanthifolia</i>	-29.9	C ₃	6	TmBMF	Hanba et al. (1997)
dicot	Juglandaceae	<i>Juglans</i>	<i>ailanthifolia</i>	-30.5	C ₃	4	TmBMF	Hanba et al. (1997)
dicot	Juglandaceae	<i>Juglans</i>	<i>regia</i>	-27.7	C ₃	1	TmBMF	Le Roux et al. (2001)
dicot	Krameriaceae	<i>Krameria</i>	<i>parvifolia</i>	-23.9	C ₃	1	DXS	Ehleringer and Cooper (1988)
dicot	Krameriaceae	<i>Krameria</i>	<i>parvifolia</i>	-24.6	C ₃	1	DXS	Ehleringer and Cooper (1988)
dicot	Lamiaceae	<i>Perilla</i>	<i>frutescens</i>	-29.4	C ₃	1	TrSOMBF	Ehleringer et al. (1987)
dicot	Lamiaceae	<i>Prunella</i>	<i>vulgaris</i>	-30.2	C ₃	1	TmBMF	Dungait et al. (2008)
dicot	Lauraceae	<i>Cryptocarya</i>	<i>chinensis</i>	-33.6	C ₃	1	TrSCMBF	Ehleringer et al. (1987)
dicot	Lauraceae	<i>Cryptocarya</i>	<i>concinna</i>	-34.9	C ₃	1	TrSCMBF	Ehleringer et al. (1987)
dicot	Lauraceae	<i>Cryptomeria</i>	<i>japonica</i>	-27.8	C ₃	1	TmBMF	Inagaki et al. (2004)
dicot	Lauraceae	<i>Cryptomeria</i>	<i>japonica</i>	-28.7	C ₃	1	TmBMF	Inagaki et al. (2004)
dicot	Lauraceae	<i>Evodia</i>	<i>lepta</i>	-31.3	C ₃	1	TrSCMBF	Ehleringer et al. (1987)
dicot	Lauraceae	<i>Lindera</i>	<i>chunii</i>	-31.4	C ₃	1	TrSCMBF	Ehleringer et al. (1987)
dicot	Lauraceae	<i>Lindera</i>	<i>communis</i>	-29.1	C ₃	1	TrSOMBF	Ehleringer et al. (1987)

Appendix I. (continued)

	Family	Genus	species	$\delta^{13}\text{C}$	pathway	N	Biome	Reference
dicot	Lauraceae	<i>Machilus</i>	<i>velutina</i>	-32.3	C ₃	1	TrSCMBF	Ehleringer et al. (1987)
dicot	Lauraceae	<i>Nectandra</i>	<i>gentlei</i>	-29.2	C ₃	6	TrSDBF	Holtum and Winter (2005)
dicot	Lauraceae	<i>Nectandra</i>	<i>gentlei</i>	-30.4	C ₃	6	TrSDBF	Holtum and Winter (2005)
dicot	Lauraceae	<i>Nectandra</i>	<i>gentlei</i>	-30.8	C ₃	6	TrSDBF	Holtum and Winter (2005)
dicot	Lauraceae	<i>Nectandra</i>	<i>grandis</i>	-33.6	C ₃	1	TrSCMBF	Buchmann et al. (1997)
dicot	Lauraceae	<i>Nectandra</i>	<i>grandis</i>	-35.1	C ₃	1	TrSCMBF	Buchmann et al. (1997)
dicot	Lauraceae	<i>Ocotea</i>	<i>glomerata</i>	-33.3	C ₃	1	TrSOMBF	Buchmann et al. (1997)
dicot	Lauraceae	<i>Ocotea</i>	<i>glomerata</i>	-34.4	C ₃	1	TrSOMBF	Buchmann et al. (1997)
dicot	Lauraceae	<i>Ocotea</i>	<i>rubra</i>	-29.1	C ₃	1	TrSOMBF	Bonal et al. (2000)
dicot	Lauraceae	<i>Ocotea</i>	<i>rubra</i>	-31.9	C ₃	1	TrSOMBF	Bonal et al. (2000)
dicot	Lauraceae	<i>Ocotea</i>	<i>veraguensis</i>	-30.7	C ₃	5	TrSDBF	Leffler and Enquist (2002)
dicot	Lauraceae	<i>Phoebe</i>	<i>cinnamomifolia</i>	-30.3	C ₃	6	TrSDBF	Holtum and Winter (2005)
dicot	Lauraceae	<i>Phoebe</i>	<i>cinnamomifolia</i>	-30.9	C ₃	6	TrSDBF	Holtum and Winter (2005)
dicot	Lauraceae	<i>Phoebe</i>	<i>cinnamomifolia</i>	-31.0	C ₃	6	TrSDBF	Holtum and Winter (2005)
dicot	Lauraceae	<i>Umbellularia</i>	<i>californica</i>	-27.2	C ₃	2	MFWS	Diefendorf et al. (2010)
dicot	Lecythidaceae	<i>Couratari</i>	<i>guianensis</i>	-30.9	C ₃	1	TrSOMBF	Bonal et al. (2000)
dicot	Lecythidaceae	<i>Eschweilera</i>	<i>amara</i>	-33.4	C ₃	1	TrSOMBF	Buchmann et al. (1997)
dicot	Lecythidaceae	<i>Eschweilera</i>	<i>amara</i>	-34.0	C ₃	1	TrSOMBF	Buchmann et al. (1997)
dicot	Lecythidaceae	<i>Eschweilera</i>	<i>amara</i>	-33.1	C ₃	1	TrSCMBF	Buchmann et al. (1997)
dicot	Lecythidaceae	<i>Eschweilera</i>	<i>amara</i>	-34.0	C ₃	1	TrSCMBF	Buchmann et al. (1997)
dicot	Lecythidaceae	<i>Eschweilera</i>	<i>coriacea</i>	-31.1	C ₃	1	TrSOMBF	Bonal et al. (2000)
dicot	Lecythidaceae	<i>Eschweilera</i>	<i>decolorans</i>	-29.8	C ₃	1	TrSOMBF	Bonal et al. (2000)
dicot	Lecythidaceae	<i>Eschweilera</i>	<i>decolorans</i>	-31.1	C ₃	1	TrSOMBF	Bonal et al. (2000)
dicot	Lecythidaceae	<i>Eschweilera</i>	<i>micrantha</i>	-31.3	C ₃	1	TrSOMBF	Bonal et al. (2000)
dicot	Lecythidaceae	<i>Eschweilera</i>	<i>micrantha</i>	-31.8	C ₃	1	TrSOMBF	Bonal et al. (2000)
dicot	Lecythidaceae	<i>Eschweilera</i>	<i>odora</i>	-30.3	C ₃	1	TrSOMBF	Buchmann et al. (1997)
dicot	Lecythidaceae	<i>Eschweilera</i>	<i>odora</i>	-31.7	C ₃	1	TrSOMBF	Buchmann et al. (1997)
dicot	Lecythidaceae	<i>Eschweilera</i>	<i>odora</i>	-32.8	C ₃	1	TrSOMBF	Buchmann et al. (1997)
dicot	Lecythidaceae	<i>Eschweilera</i>	<i>odora</i>	-32.8	C ₃	1	TrSOMBF	Buchmann et al. (1997)
dicot	Lecythidaceae	<i>Eschweilera</i>	<i>odora</i>	-34.0	C ₃	1	TrSCMBF	Buchmann et al. (1997)
dicot	Lecythidaceae	<i>Eschweilera</i>	<i>odora</i>	-34.4	C ₃	1	TrSCMBF	Buchmann et al. (1997)
dicot	Lecythidaceae	<i>Eschweilera</i>	<i>parviflora</i>	-30.7	C ₃	1	TrSOMBF	Bonal et al. (2000)

Appendix I. (continued)

	Family	Genus	species	$\delta^{13}\text{C}$	pathway	N	Biome	Reference
dicot	Lecythidaceae	<i>Eschweilera</i>	<i>parviflora</i>	-33.2	C ₃	1	TrSOMBF	Bonal et al. (2000)
dicot	Lecythidaceae	<i>Eschweilera</i>	<i>sagotiana</i>	-31.3	C ₃	1	TrSOMBF	Bonal et al. (2000)
dicot	Lecythidaceae	<i>Eschweilera</i>	<i>sagotiana</i>	-32.2	C ₃	1	TrSOMBF	Bonal et al. (2000)
dicot	Lecythidaceae	<i>Eschweilera</i>	<i>sp.</i>	-31.0	C ₃	1	TrSOMBF	Bonal et al. (2000)
dicot	Lecythidaceae	<i>Gustavia</i>	<i>hexapetala</i>	-32.0	C ₃	1	TrSOMBF	Bonal et al. (2000)
dicot	Lecythidaceae	<i>Lecythis</i>	<i>hartacea</i>	-30.8	C ₃	1	TrSOMBF	Bonal et al. (2000)
dicot	Lecythidaceae	<i>Lecythis</i>	<i>idatimon</i>	-31.4	C ₃	1	TrSOMBF	Bonal et al. (2000)
dicot	Lecythidaceae	<i>Lecythis</i>	<i>idatimon</i>	-31.5	C ₃	1	TrSOMBF	Bonal et al. (2000)
dicot	Lecythidaceae	<i>Lecythis</i>	<i>idatimon</i>	-32.0	C ₃	1	TrSOMBF	Bonal et al. (2000)
dicot	Lecythidaceae	<i>Lecythis</i>	<i>persistens</i>	-30.7	C ₃	1	TrSOMBF	Bonal et al. (2000)
dicot	Lecythidaceae	<i>Lecythis</i>	<i>persistens</i>	-32.1	C ₃	1	TrSOMBF	Bonal et al. (2000)
dicot	Lecythidaceae	<i>Lecythis</i>	<i>zabucajo</i>	-27.7	C ₃	1	TrSOMBF	Bonal et al. (2000)
dicot	Lobeliaceae	<i>Lobelia</i>	<i>chinensis</i>	-30.8	C ₃	1	TrSOMBF	Ehleringer et al. (1987)
dicot	Loganiaceae	<i>Strychnos</i>	<i>sp.</i>	-27.9	C ₃	1	TrSOMBF	Cerling et al. (2004)
dicot	Loranthaceae	<i>Elytranthe</i>	<i>cochinchinensis</i>	-29.8	C ₃	1	TrSOMBF	Ehleringer et al. (1987)
dicot	Loranthaceae	<i>Loranthus</i>	<i>pentapetalus</i>	-30.8	C ₃	1	TrSOMBF	Ehleringer et al. (1987)
dicot	Loranthaceae	<i>Taxillus</i>	<i>chinensis</i>	-30.8	C ₃	1	TrSOMBF	Ehleringer et al. (1987)
dicot	Lythraceae	<i>Lythrum</i>	<i>salicaria</i>	-28.0	C ₃	4	TmBMF	Keough et al. (1996)
dicot	Magnoliaceae	<i>Liriodendron</i>	<i>tulipifera</i>	-28.4	C ₃	1	TmBMF	Baldocchi and Bowling (1999)
dicot	Magnoliaceae	<i>Magnolia</i>	<i>delabayi</i>	-28.7	C ₃	1	domestic	Collister et al. (1994)
dicot	Magnoliaceae	<i>Tsoongiodendron</i>	<i>odorum</i>	-31.2	C ₃	1	TrSCMBF	Ehleringer et al. (1987)
dicot	Malpighiaceae	<i>Bunchosia</i>	<i>biocellata</i>	-30.0	C ₃	5	TrSDBF	Leffler and Enquist (2002)
dicot	Malvaceae	<i>Apeiba</i>	<i>membranacea</i>	-30.3	C ₃	3	TrSOMBF	Terwilliger (1997)
dicot	Malvaceae	<i>Apeiba</i>	<i>membranacea</i>	-31.2	C ₃	3	TrSCMBF	Terwilliger (1997)
dicot	Malvaceae	<i>Apeiba</i>	<i>tibourbou</i>	-29.5	C ₃	3	TrSOMBF	Terwilliger (1997)
dicot	Malvaceae	<i>Apeiba</i>	<i>tibourbou</i>	-30.5	C ₃	3	TrSCMBF	Terwilliger (1997)
dicot	Malvaceae	<i>Luehea</i>	<i>seemannii</i>	-27.1	C ₃	6	TrSDBF	Holtum and Winter (2005)
dicot	Malvaceae	<i>Luehea</i>	<i>seemannii</i>	-27.3	C ₃	6	TrSDBF	Holtum and Winter (2005)
dicot	Malvaceae	<i>Luehea</i>	<i>seemannii</i>	-27.3	C ₃	6	TrSDBF	Holtum and Winter (2005)
dicot	Malvaceae	<i>Luehea</i>	<i>seemannii</i>	-27.4	C ₃	6	TrSDBF	Holtum and Winter (2005)
dicot	Malvaceae	<i>Luehea</i>	<i>seemannii</i>	-27.5	C ₃	6	TrSDBF	Holtum and Winter (2005)
dicot	Malvaceae	<i>Luehea</i>	<i>seemannii</i>	-27.6	C ₃	12	TrSDBF	Holtum and Winter (2005)

Appendix I. (continued)

	Family	Genus	species	$\delta^{13}\text{C}$	pathway	N	Biome	Reference
dicot	Malvaceae	<i>Luehea</i>	<i>seemannii</i>	-27.7	C ₃	6	TrSDBF	Holtum and Winter (2005)
dicot	Malvaceae	<i>Luehea</i>	<i>seemannii</i>	-28.1	C ₃	6	TrSDBF	Holtum and Winter (2005)
dicot	Malvaceae	<i>Pseudobombax</i>	<i>septenatum</i>	-26.4	C ₃	8	TrSDBF	Holtum and Winter (2005)
dicot	Malvaceae	<i>Pseudobombax</i>	<i>septenatum</i>	-26.7	C ₃	8	TrSDBF	Holtum and Winter (2005)
dicot	Malvaceae	<i>Pseudobombax</i>	<i>septenatum</i>	-27.5	C ₃	8	TrSDBF	Holtum and Winter (2005)
dicot	Malvaceae	<i>Sphaeralcea</i>	<i>ambigua</i>	-27.4	C ₃	1	DXS	Ehleringer and Cooper (1988)
dicot	Malvaceae	<i>Sphaeralcea</i>	<i>ambigua</i>	-27.6	C ₃	1	DXS	Ehleringer and Cooper (1988)
dicot	Malvaceae	<i>Tilia</i>	<i>platyphyllos</i>	-26.9	C ₃	3	TmBMF	Chevillat et al. (2005)
dicot	Maranthaceae	<i>Ataenidia</i>	<i>conferta</i>	-36.5	C ₃	1	TrSCMBF	Cerling et al. (2004)
dicot	Maranthaceae	<i>Megaphrynium</i>	<i>macrostachyum</i>	-36.2	C ₃	1	TrSCMBF	Cerling et al. (2004)
dicot	Melastomataceae	<i>Memecylon</i>	<i>ligustrifolium</i>	-29.6	C ₃	1	TrSCMBF	Ehleringer et al. (1987)
dicot	Melastomataceae	<i>Mouriri</i>	<i>crassifolia</i>	-29.4	C ₃	1	TrSOMBF	Bonal et al. (2000)
dicot	Melastomataceae	<i>Mouriri</i>	<i>crassifolia</i>	-30.9	C ₃	1	TrSOMBF	Bonal et al. (2000)
dicot	Melastomataceae	<i>Mouriri</i>	<i>crassifolia</i>	-30.9	C ₃	1	TrSOMBF	Bonal et al. (2000)
dicot	Melastomataceae	<i>Tetrazygia</i>	<i>bicolor</i>	-29.9	C ₃	1	TrSCMBF	Jones et al. (2010)
dicot	Meliaceae	<i>Carapa</i>	<i>procera</i>	-29.2	C ₃	1	TrSOMBF	Bonal et al. (2000)
dicot	Meliaceae	<i>Carapa</i>	<i>procera</i>	-29.3	C ₃	1	TrSOMBF	Bonal et al. (2000)
dicot	Meliaceae	<i>Carapa</i>	<i>procera</i>	-31.1	C ₃	1	TrSOMBF	Bonal et al. (2000)
dicot	Meliaceae	<i>Guarea</i>	<i>glabra</i>	-29.5	C ₃	5	TrSDBF	Leffler and Enquist (2002)
dicot	Meliaceae	<i>Trichilia</i>	<i>sp.</i>	-30.8	C ₃	1	TrSOMBF	Bonal et al. (2000)
dicot	Menispermaceae	<i>indet.</i>	<i>indet.</i>	-26.0	C ₃	1	TrSOMBF	Cerling et al. (2004)
dicot	Menispermaceae	<i>Tricilisia</i>	<i>gilessi</i>	-30.2	C ₃	1	TrSOMBF	Cerling et al. (2004)
dicot	Mimosaceae	<i>Abarema</i>	<i>curvicarpa</i>	-29.2	C ₃	1	TrSOMBF	Bonal et al. (2000)
dicot	Mimosaceae	<i>Abarema</i>	<i>jupunba</i>	-29.1	C ₃	1	TrSOMBF	Bonal et al. (2000)
dicot	Mimosaceae	<i>Abarema</i>	<i>jupunba</i>	-29.4	C ₃	1	TrSOMBF	Bonal et al. (2000)
dicot	Mimosaceae	<i>Abarema</i>	<i>jupunba</i>	-29.4	C ₃	1	TrSOMBF	Bonal et al. (2000)
dicot	Mimosaceae	<i>Balizia</i>	<i>pedicellaris</i>	-27.5	C ₃	1	TrSOMBF	Bonal et al. (2000)
dicot	Mimosaceae	<i>Balizia</i>	<i>pedicellaris</i>	-28.3	C ₃	1	TrSOMBF	Bonal et al. (2000)
dicot	Mimosaceae	<i>Balizia</i>	<i>pedicellaris</i>	-29.5	C ₃	1	TrSOMBF	Bonal et al. (2000)
dicot	Mimosaceae	<i>Entada</i>	<i>sp.</i>	-27.3	C ₃	1	TrSOMBF	Cerling et al. (2004)
dicot	Mimosaceae	<i>Inga</i>	<i>alba</i>	-32.4	C ₃	1	TrSOMBF	Bonal et al. (2000)
dicot	Mimosaceae	<i>Inga</i>	<i>paraensis</i>	-28.3	C ₃	1	TrSOMBF	Bonal et al. (2000)

Appendix I. (continued)

	Family	Genus	species	$\delta^{13}\text{C}$	pathway	N	Biome	Reference
dicot	Mimosaceae	<i>Inga</i>	<i>thibaudiana</i>	-29.7	C ₃	1	TrSOMBF	Bonal et al. (2000)
dicot	Mimosaceae	<i>Parkia</i>	<i>nitida</i>	-31.3	C ₃	1	TrSOMBF	Bonal et al. (2000)
dicot	Mimosaceae	<i>Parkia</i>	<i>nitida</i>	-31.5	C ₃	1	TrSOMBF	Bonal et al. (2000)
dicot	Mimosaceae	<i>Pithecellobium</i>	<i>clypearia</i>	-30.3	C ₃	1	TrSCMBF	Ehleringer et al. (1987)
dicot	Mimosaceae	<i>Pseudopiptadenia</i>	<i>suaveolens</i>	-29.0	C ₃	1	TrSOMBF	Bonal et al. (2000)
dicot	Molluginaceae	<i>Mollugo</i>	<i>pentaphylla</i>	-26.9	C ₃	1	TrSOMBF	Ehleringer et al. (1987)
dicot	Moraceae	<i>Brosimum</i>	<i>acutifolium</i>	-31.6	C ₃	1	TrSOMBF	Bonal et al. (2000)
dicot	Moraceae	<i>Brosimum</i>	<i>alicastrum</i>	-30.5	C ₃	4	TrSDBF	Leffler and Enquist (2002)
dicot	Moraceae	<i>Brosimum</i>	<i>guianense</i>	-29.6	C ₃	1	TrSOMBF	Bonal et al. (2000)
dicot	Moraceae	<i>Brosimum</i>	<i>rubescens</i>	-31.1	C ₃	1	TrSOMBF	Bonal et al. (2000)
dicot	Moraceae	<i>Castilla</i>	<i>elastica</i>	-26.0	C ₃	6	TrSDBF	Holtum and Winter (2005)
dicot	Moraceae	<i>Castilla</i>	<i>elastica</i>	-27.3	C ₃	6	TrSDBF	Holtum and Winter (2005)
dicot	Moraceae	<i>Castilla</i>	<i>elastica</i>	-27.4	C ₃	6	TrSDBF	Holtum and Winter (2005)
dicot	Moraceae	<i>Castilla</i>	<i>elastica</i>	-27.6	C ₃	6	TrSDBF	Holtum and Winter (2005)
dicot	Moraceae	<i>Castilla</i>	<i>elastica</i>	-28.1	C ₃	6	TrSDBF	Holtum and Winter (2005)
dicot	Moraceae	<i>Castilla</i>	<i>elastica</i>	-28.2	C ₃	6	TrSDBF	Holtum and Winter (2005)
dicot	Moraceae	<i>Castilla</i>	<i>elastica</i>	-29.1	C ₃	6	TrSDBF	Holtum and Winter (2005)
dicot	Moraceae	<i>Castilla</i>	<i>elastica</i>	-29.3	C ₃	6	TrSDBF	Holtum and Winter (2005)
dicot	Moraceae	<i>Castilla</i>	<i>elastica</i>	-29.8	C ₃	6	TrSDBF	Holtum and Winter (2005)
dicot	Moraceae	<i>Chlorophora</i>	<i>tinctoria</i>	-26.7	C ₃	1	TrSDBF	Mooney et al. (1989)
dicot	Moraceae	<i>Ficus</i>	<i>insipida</i>	-23.8	C ₃	6	TrSDBF	Holtum and Winter (2005)
dicot	Moraceae	<i>Ficus</i>	<i>insipida</i>	-24.3	C ₃	6	TrSDBF	Holtum and Winter (2005)
dicot	Moraceae	<i>Ficus</i>	<i>insipida</i>	-25.0	C ₃	6	TrSDBF	Holtum and Winter (2005)
dicot	Moraceae	<i>Ficus</i>	<i>insipida</i>	-25.5	C ₃	6	TrSDBF	Holtum and Winter (2005)
dicot	Moraceae	<i>Ficus</i>	<i>insipida</i>	-25.8	C ₃	6	TrSDBF	Holtum and Winter (2005)
dicot	Moraceae	<i>Ficus</i>	<i>insipida</i>	-26.1	C ₃	6	TrSDBF	Holtum and Winter (2005)
dicot	Moraceae	<i>Ficus</i>	<i>insipida</i>	-26.3	C ₃	6	TrSDBF	Holtum and Winter (2005)
dicot	Moraceae	<i>Ficus</i>	<i>insipida</i>	-26.5	C ₃	6	TrSDBF	Holtum and Winter (2005)
dicot	Moraceae	<i>Ficus</i>	<i>insipida</i>	-26.8	C ₃	6	TrSDBF	Holtum and Winter (2005)
dicot	Moraceae	<i>Ficus</i>	<i>insipida</i>	-26.8	C ₃	6	TrSDBF	Holtum and Winter (2005)
dicot	Moraceae	<i>Ficus</i>	<i>insipida</i>	-26.9	C ₃	6	TrSDBF	Holtum and Winter (2005)
dicot	Moraceae	<i>Ficus</i>	<i>insipida</i>	-26.9	C ₃	6	TrSDBF	Holtum and Winter (2005)

Appendix I. (continued)

	Family	Genus	species	$\delta^{13}\text{C}$	pathway	N	Biome	Reference
dicot	Moraceae	<i>Ficus</i>	<i>insipida</i>	-27.1	C ₃	6	TrSDBF	Holtum and Winter (2005)
dicot	Moraceae	<i>Ficus</i>	<i>insipida</i>	-27.3	C ₃	6	TrSDBF	Holtum and Winter (2005)
dicot	Moraceae	<i>Ficus</i>	<i>insipida</i>	-27.3	C ₃	6	TrSDBF	Holtum and Winter (2005)
dicot	Moraceae	<i>Ficus</i>	<i>insipida</i>	-27.6	C ₃	6	TrSDBF	Holtum and Winter (2005)
dicot	Moraceae	<i>Ficus</i>	<i>insipida</i>	-28.1	C ₃	6	TrSDBF	Holtum and Winter (2005)
dicot	Moraceae	<i>Ficus</i>	<i>insipida</i>	-28.3	C ₃	6	TrSDBF	Holtum and Winter (2005)
dicot	Moraceae	<i>Ficus</i>	<i>maxima</i>	-26.6	C ₃	6	TrSDBF	Holtum and Winter (2005)
dicot	Moraceae	<i>Ficus</i>	<i>maxima</i>	-26.7	C ₃	6	TrSDBF	Holtum and Winter (2005)
dicot	Moraceae	<i>Ficus</i>	<i>maxima</i>	-26.7	C ₃	6	TrSDBF	Holtum and Winter (2005)
dicot	Moraceae	<i>Ficus</i>	<i>maxima</i>	-27.1	C ₃	6	TrSDBF	Holtum and Winter (2005)
dicot	Moraceae	<i>Helicostylis</i>	<i>pedunculata</i>	-30.3	C ₃	1	TrSOMBF	Bonal et al. (2000)
dicot	Moraceae	<i>Musanga</i>	<i>cecropioides</i>	-31.4	C ₃	1	TrSOMBF	Cerling et al. (2004)
dicot	Moraceae	<i>Trophis</i>	<i>racemosa</i>	-31.5	C ₃	5	TrSDBF	Leffler and Enquist (2002)
dicot	Myricaceae	<i>Myrica</i>	<i>cerifera</i>	-30.2	C ₃	1	TrSOMBF	Jones et al. (2010)
dicot	Myristicaceae	<i>Iryanthera</i>	<i>hostmanii</i>	-32.0	C ₃	1	TrSOMBF	Bonal et al. (2000)
dicot	Myristicaceae	<i>Iryanthera</i>	<i>hostmanii</i>	-32.4	C ₃	1	TrSOMBF	Bonal et al. (2000)
dicot	Myristicaceae	<i>Iryanthera</i>	<i>sagotiana</i>	-32.2	C ₃	1	TrSOMBF	Bonal et al. (2000)
dicot	Myristicaceae	<i>Iryanthera</i>	<i>sagotiana</i>	-32.6	C ₃	1	TrSOMBF	Bonal et al. (2000)
dicot	Myristicaceae	<i>Iryanthera</i>	<i>sagotiana</i>	-33.2	C ₃	1	TrSOMBF	Bonal et al. (2000)
dicot	Myristicaceae	<i>Virola</i>	<i>michelii</i>	-31.2	C ₃	1	TrSOMBF	Bonal et al. (2000)
dicot	Myristicaceae	<i>Virola</i>	<i>michelii</i>	-31.7	C ₃	1	TrSOMBF	Bonal et al. (2000)
dicot	Myrsinaceae	<i>Ardisia</i>	<i>elliptica</i>	-30.9	C ₃	1	TrSCMBF	Jones et al. (2010)
dicot	Myrsinaceae	<i>Ardisia</i>	<i>escallonoides</i>	-30.1	C ₃	1	TrSCMBF	Jones et al. (2010)
dicot	Myrsinaceae	<i>Ardisia</i>	<i>quinquegona</i>	-31.4	C ₃	1	TrSCMBF	Ehleringer et al. (1987)
dicot	Myrtaceae	<i>Baeckea</i>	<i>frutescens</i>	-29.4	C ₃	1	TrSOMBF	Ehleringer et al. (1987)
dicot	Myrtaceae	<i>Eucalyptus</i>	<i>robusta</i>	-27.4	C ₃	1	TrSOMBF	Ehleringer et al. (1987)
dicot	Myrtaceae	<i>Eugenia</i>	<i>axillaris</i>	-27.1	C ₃	1	TrSCMBF	Jones et al. (2010)
dicot	Myrtaceae	<i>Eugenia</i>	<i>ecostulata</i>	-31.1	C ₃	6	TrSOMBF	Nagy and Proctor (2000)
dicot	Myrtaceae	<i>Metrosideros</i>	<i>polymorpha</i>	-28.1	C ₃	3	TrSDBF	Sandquist and Cordell (2007)
dicot	Myrtaceae	<i>Psidium</i>	<i>cattleionum</i>	-29.7	C ₃	1	domestic	Collister et al. (1994)
dicot	Myrtaceae	<i>Rhodomyrtus</i>	<i>tomentosa</i>	-30.4	C ₃	1	TrSOMBF	Ehleringer et al. (1987)
dicot	Myrtaceae	<i>Syzygium</i>	<i>rehderianum</i>	-30.0	C ₃	1	TrSOMBF	Ehleringer et al. (1987)

Appendix I. (continued)

	Family	Genus	species	$\delta^{13}\text{C}$	pathway	N	Biome	Reference
dicot	Myrtaceae	<i>Tristaniopsis</i>	<i>obovata</i>	-30.2	C ₃	4	TrSOMBF	Nagy and Proctor (2000)
dicot	Nymphaeaceae	<i>Nuphar</i>	<i>advena</i>	-24.3	C ₃	4	TmBMF	Keough et al. (1996)
dicot	Olacaceae	<i>Minuartia</i>	<i>guianensis</i>	-29.2	C ₃	1	TrSOMBF	Bonal et al. (2000)
dicot	Olacaceae	<i>Minuartia</i>	<i>guianensis</i>	-32.4	C ₃	1	TrSOMBF	Bonal et al. (2000)
dicot	Olacaceae	<i>Strombosiopsis</i>	<i>tetrandra</i>	-29.9	C ₃	1	TrSOMBF	Cerling et al. (2004)
dicot	Oleaceae	<i>Forestiera</i>	<i>pubescens</i>	-26.7	C ₃	2	TmGSS	Jessup et al. (2003)
dicot	Oleaceae	<i>Fraxinus</i>	<i>angustifolia</i>	-25.9	C ₃	4	MFWS	Escuerdo et al. (2008)
dicot	Oleaceae	<i>Fraxinus</i>	<i>angustifolia</i>	-27.7	C ₃	4	MFWS	Escuerdo et al. (2008)
dicot	Oleaceae	<i>Minuartia</i>	<i>guianensis</i>	-27.6	C ₃	1	TrSOMBF	Buchmann et al. (1997)
dicot	Oleaceae	<i>Minuartia</i>	<i>guianensis</i>	-27.7	C ₃	1	TrSOMBF	Buchmann et al. (1997)
dicot	Oleaceae	<i>Phillyrea</i>	<i>angustifolia</i>	-26.5	C ₃	1	MFWS	Valentini et al. (1992)
dicot	Oxalidaceae	<i>Oxalis</i>	<i>corniculata</i>	-30.2	C ₃	1	TrSOMBF	Ehleringer et al. (1987)
dicot	Oxalidaceae	<i>Oxalis</i>	<i>corymbosa</i>	-30.8	C ₃	1	TrSOMBF	Ehleringer et al. (1987)
dicot	Piperaceae	<i>Peperomia</i>	<i>macrostachya</i>	-20.5	C ₃	3	TrSDBF	Holtum and Winter (2005)
dicot	Piperaceae	<i>Peperomia</i>	<i>macrostachya</i>	-22.0	C ₃	3	TrSDBF	Holtum and Winter (2005)
dicot	Piperaceae	<i>Peperomia</i>	<i>macrostachya</i>	-14.5	CAM	6	TrSDBF	Holtum and Winter (2005)
dicot	Piperaceae	<i>Peperomia</i>	<i>macrostachya</i>	-18.6	CAM	3	TrSDBF	Holtum and Winter (2005)
dicot	Piperaceae	<i>Peperomia</i>	<i>pellucida</i>	-26.9	C ₃	1	TrSOMBF	Ehleringer et al. (1987)
dicot	Piperaceae	<i>Piper</i>	<i>sp.</i>	-27.3	C ₃	6	TrSDBF	Holtum and Winter (2005)
dicot	Piperaceae	<i>Piper</i>	<i>sp.</i>	-27.7	C ₃	6	TrSDBF	Holtum and Winter (2005)
dicot	Piperaceae	<i>Piper</i>	<i>sp.</i>	-28.2	C ₃	6	TrSDBF	Holtum and Winter (2005)
dicot	Piperaceae	<i>Piper</i>	<i>sp.</i>	-28.5	C ₃	6	TrSDBF	Holtum and Winter (2005)
dicot	Piperaceae	<i>Piper</i>	<i>amalago</i>	-31.2	C ₃	5	TrSDBF	Leffler and Enquist (2002)
dicot	Plantaginaceae	<i>Plantago</i>	<i>lanceolata</i>	-28.8	C ₃	1	TmBMF	Dungait et al. (2008)
dicot	Plantaginaceae	<i>Plantago</i>	<i>major</i>	-30.8	C ₃	1	TmBMF	Dungait et al. (2008)
dicot	Plantaginaceae	<i>Plantago</i>	<i>major</i>	-28.2	C ₃	1	TrSOMBF	Ehleringer et al. (1987)
dicot	Plantaginaceae	<i>Plantago</i>	<i>media</i>	-27.4	C ₃	1	TmBMF	Dungait et al. (2008)
dicot	Plantaginaceae	<i>Veronica</i>	<i>serpyllifolia</i>	-31.0	C ₃	1	TmBMF	Dungait et al. (2008)
dicot	Polygalaceae	<i>Salomonina</i>	<i>cantonensis</i>	-30.7	C ₃	1	TrSOMBF	Ehleringer et al. (1987)
dicot	Polygonaceae	<i>Coccoloba</i>	<i>diversifolia</i>	-33.1	C ₃	1	TrSCMBF	Jones et al. (2010)
dicot	Polygonaceae	<i>Coccoloba</i>	<i>liebmannii</i>	-26.8	C ₃	5	TrSDBF	Mooney et al. (1989)
dicot	Polygonaceae	<i>Eriogonum</i>	<i>fasciculatum</i>	-26.4	C ₃	1	DXS	Ehleringer and Cooper (1988)

Appendix I. (continued)

	Family	Genus	species	δ¹³C	pathway	N	Biome	Reference
dicot	Polygonaceae	<i>Eriogonum</i>	<i>fasciculatum</i>	-26.5	C ₃	1	DXS	Ehleringer and Cooper (1988)
dicot	Polygonaceae	<i>Eriogonum</i>	<i>inflatum</i>	-25.7	C ₃	1	DXS	Ehleringer and Cooper (1988)
dicot	Polygonaceae	<i>Eriogonum</i>	<i>inflatum</i>	-25.8	C ₃	1	DXS	Ehleringer and Cooper (1988)
dicot	Polygonaceae	<i>Eriogonum</i>	<i>inflatum</i>	-28.2	C ₃	1	DXS	Ehleringer and Cooper (1988)
dicot	Polygonaceae	<i>Oxyria</i>	<i>digyna</i>	-27.2	C ₃	1	unknown	Bender (1971)
dicot	Polygonaceae	<i>Polygonum</i>	<i>hydropiper</i>	-29.8	C ₃	1	TrSOMBF	Ehleringer et al. (1987)
dicot	Polygonaceae	<i>Rumex</i>	<i>acetosa</i>	-28.5	C ₃	1	TmBMF	Dungait et al. (2008)
dicot	Polygonaceae	<i>Rumex</i>	<i>conglomeratus</i>	-28.4	C ₃	1	TmBMF	Dungait et al. (2008)
dicot	Portulacaceae	<i>Portulaca</i>	<i>grandiflora</i>	-11.4	C ₄	1	unknown	Bender (1971)
dicot	Portulacaceae	<i>Portulaca</i>	<i>oleracea</i>	-12.1	C ₄	1	unknown	Bender (1971)
dicot	Primulaceae	<i>Lysimachia</i>	<i>fortunei</i>	-30.9	C ₃	1	TrSCMBF	Ehleringer et al. (1987)
dicot	Proteaceae	<i>Helicia</i>	<i>reticulata</i>	-28.4	C ₃	1	TrSOMBF	Ehleringer et al. (1987)
dicot	Ranunculaceae	<i>Ranunculus</i>	<i>acris</i>	-30.7	C ₃	1	TmBMF	Dungait et al. (2008)
dicot	Ranunculaceae	<i>Ranunculus</i>	<i>repens</i>	-28.4	C ₃	1	TmBMF	Dungait et al. (2008)
dicot	Rhamnaceae	<i>Colubrina</i>	<i>oppositifolia</i>	-25.1	C ₃	5	TrSDBF	Sandquist and Cordell (2007)
dicot	Rhamnaceae	<i>Colubrina</i>	<i>triflora</i>	-27.6	C ₃	1	TrSDBF	Mooney et al. (1989)
dicot	Rhamnaceae	<i>Condalia</i>	<i>hookeri</i>	-27.8	C ₃	1	TrSGSS	Bai et al. (2008)
dicot	Rhamnaceae	<i>Frangula</i>	<i>alnus</i>	-29.0	C ₃	4	MFWS	Escuerdo et al. (2008)
dicot	Rosaceae	<i>Amelanchier</i>	<i>alnifolia</i>	-25.7	C ₃	1	DXS	DeLucia and Schlesinger (1991)
dicot	Rosaceae	<i>Amelanchier</i>	<i>utahensis</i>	-25.0	C ₃	88	DXS	Van de Water et al. (2002)
dicot	Rosaceae	<i>Cercocarpus</i>	<i>montanus</i>	-24.9	C ₃	55	DXS	Van de Water et al. (2002)
dicot	Rosaceae	<i>Cercocarpus</i>	<i>montanus</i>	-25.3	C ₃	64	DXS	Van de Water et al. (2002)
dicot	Rosaceae	<i>Cowania</i>	<i>mexicana</i>	-25.1	C ₃	48	DXS	Van de Water et al. (2002)
dicot	Rosaceae	<i>Crataegus</i>	<i>monogyna</i>	-29.7	C ₃	1	TmBMF	Dungait et al. (2008)
dicot	Rosaceae	<i>Crataegus</i>	<i>monogyna</i>	-28.1	C ₃	4	MFWS	Escuerdo et al. (2008)
dicot	Rosaceae	<i>Crataegus</i>	<i>monogyna</i>	-28.2	C ₃	4	MFWS	Escuerdo et al. (2008)
dicot	Rosaceae	<i>Crataegus</i>	<i>monogyna</i>	-28.9	C ₃	4	MFWS	Escuerdo et al. (2008)
dicot	Rosaceae	<i>Fragaria</i>	<i>virginiana</i>	-31.0	C ₃	5	BFT	Brooks et al. (1997)
dicot	Rosaceae	<i>Fragaria</i>	<i>virginiana</i>	-31.7	C ₃	5	BFT	Brooks et al. (1997)
dicot	Rosaceae	<i>Malus</i>	<i>sylvestris</i>	-27.3	C ₃	1	TmBMF	Dungait et al. (2008)
dicot	Rosaceae	<i>Potentilla</i>	<i>anserine</i>	-29.2	C ₃	1	TmBMF	Dungait et al. (2008)
dicot	Rosaceae	<i>Potentilla</i>	<i>palustris</i>	-29.6	C ₃	5	BFT	Brooks et al. (1997)

Appendix I. (continued)

	Family	Genus	species	$\delta^{13}\text{C}$	pathway	N	Biome	Reference
dicot	Rosaceae	<i>Potentilla</i>	<i>reptans</i>	-29.2	C ₃	1	TmBMF	Dungait et al. (2008)
dicot	Rosaceae	<i>Prunus</i>	<i>avium</i>	-26.8	C ₃	3	TmBMF	Chevillat et al. (2005)
dicot	Rosaceae	<i>Prunus</i>	<i>spinosa</i>	-27.7	C ₃	4	MFWS	Escuerdo et al. (2008)
dicot	Rosaceae	<i>Prunus</i>	<i>spinosa</i>	-28.6	C ₃	4	MFWS	Escuerdo et al. (2008)
dicot	Rosaceae	<i>Purshia</i>	<i>tridentata</i>	-24.2	C ₃	1	DXS	DeLucia and Schlesinger (1991)
dicot	Rosaceae	<i>Pygeum</i>	<i>topengii</i>	-30.2	C ₃	1	TrSCMBF	Ehleringer et al. (1987)
dicot	Rosaceae	<i>Pyrus</i>	<i>bourgaeana</i>	-26.1	C ₃	4	MFWS	Escuerdo et al. (2008)
dicot	Rosaceae	<i>Pyrus</i>	<i>bourgaeana</i>	-27.6	C ₃	4	MFWS	Escuerdo et al. (2008)
dicot	Rosaceae	<i>Pyrus</i>	<i>bourgaeana</i>	-27.7	C ₃	4	MFWS	Escuerdo et al. (2008)
dicot	Rosaceae	<i>Rhapiolepis</i>	<i>indica</i>	-27.1	C ₃	1	TrSOMBF	Ehleringer et al. (1987)
dicot	Rosaceae	<i>Rosa</i>	<i>acicularis</i>	-27.9	C ₃	5	BFT	Brooks et al. (1997)
dicot	Rosaceae	<i>Rosa</i>	<i>acicularis</i>	-28.8	C ₃	5	BFT	Brooks et al. (1997)
dicot	Rosaceae	<i>Rosa</i>	<i>acicularis</i>	-29.6	C ₃	5	BFT	Brooks et al. (1997)
dicot	Rosaceae	<i>Rosa</i>	<i>acicularis</i>	-30.5	C ₃	5	BFT	Brooks et al. (1997)
dicot	Rubiaceae	<i>Aidia</i>	<i>micrantha</i>	-33.0	C ₃	1	TrSCMBF	Cerling et al. (2004)
dicot	Rubiaceae	<i>Antirrhoea</i>	<i>trichantha</i>	-26.0	C ₃	6	TrSDBF	Holtum and Winter (2005)
dicot	Rubiaceae	<i>Antirrhoea</i>	<i>trichantha</i>	-28.5	C ₃	6	TrSDBF	Holtum and Winter (2005)
dicot	Rubiaceae	<i>Antirrhoea</i>	<i>trichantha</i>	-28.7	C ₃	6	TrSDBF	Holtum and Winter (2005)
dicot	Rubiaceae	<i>Antirrhoea</i>	<i>trichantha</i>	-29.6	C ₃	6	TrSDBF	Holtum and Winter (2005)
dicot	Rubiaceae	<i>Calycophyllum</i>	<i>candidissimum</i>	-30.7	C ₃	5	TrSDBF	Leffler and Enquist (2002)
dicot	Rubiaceae	<i>Galium</i>	<i>verum</i>	-29.7	C ₃	1	TmBMF	Dungait et al. (2008)
dicot	Rubiaceae	<i>Genipa</i>	<i>americana</i>	-29.5	C ₃	5	TrSDBF	Leffler and Enquist (2002)
dicot	Rubiaceae	<i>Guettarda</i>	<i>macrosperma</i>	-30.5	C ₃	5	TrSDBF	Leffler and Enquist (2002)
dicot	Rubiaceae	<i>Guettarda</i>	<i>scabra</i>	-30.2	C ₃	1	TrSOMBF	Jones et al. (2010)
dicot	Rubiaceae	<i>Hamelia</i>	<i>versicolor</i>	-27.4	C ₃	1	TrSDBF	Mooney et al. (1989)
dicot	Rubiaceae	<i>Hedyotis</i>	<i>diffusa</i>	-28.6	C ₃	1	TrSOMBF	Ehleringer et al. (1987)
dicot	Rubiaceae	<i>Posoqueria</i>	<i>latifolia</i>	-28.9	C ₃	1	TrSOMBF	Bonal et al. (2000)
dicot	Rubiaceae	<i>Posoqueria</i>	<i>latifolia</i>	-32.7	C ₃	1	TrSOMBF	Bonal et al. (2000)
dicot	Rubiaceae	<i>Posoqueria</i>	<i>latifolia</i>	-32.7	C ₃	1	TrSOMBF	Bonal et al. (2000)
dicot	Rubiaceae	<i>Psychotria</i>	<i>rubra</i>	-33.8	C ₃	1	TrSCMBF	Ehleringer et al. (1987)
dicot	Rubiaceae	<i>Psydrax</i>	<i>odorata</i>	-25.8	C ₃	5	TrSDBF	Sandquist and Cordell (2007)
dicot	Rubiaceae	<i>Sherbournia</i>	<i>batesii</i>	-33.7	C ₃	1	TrSCMBF	Cerling et al. (2004)

Appendix I. (continued)

	Family	Genus	species	$\delta^{13}\text{C}$	pathway	N	Biome	Reference
dicot	Rutaceae	<i>Zanthoxylum</i>	<i>fagara</i>	-27.4	C ₃	1	TrSGSS	Bai et al. (2008)
dicot	Rutaceae	<i>Zanthoxylum</i>	<i>setulosum</i>	-27.7	C ₃	5	TrSDBF	Leffler and Enquist (2002)
dicot	Salicaceae	<i>Populus</i>	<i>sargentii</i>	-27.4	C ₃	1	TmGSS	Dodd et al. (1998)
dicot	Salicaceae	<i>Populus</i>	<i>sargentii</i>	-27.9	C ₃	1	TmGSS	Dodd et al. (1998)
dicot	Salicaceae	<i>Populus</i>	<i>sargentii</i>	-28.1	C ₃	1	TmGSS	Dodd et al. (1998)
dicot	Salicaceae	<i>Populus</i>	<i>sargentii</i>	-28.4	C ₃	1	TmGSS	Dodd et al. (1998)
dicot	Salicaceae	<i>Populus</i>	<i>sargentii</i>	-28.8	C ₃	1	TmGSS	Dodd et al. (1998)
dicot	Salicaceae	<i>Populus</i>	<i>sargentii</i>	-28.8	C ₃	1	TmGSS	Dodd et al. (1998)
dicot	Salicaceae	<i>Populus</i>	<i>sargentii</i>	-29.1	C ₃	1	TmGSS	Dodd et al. (1998)
dicot	Salicaceae	<i>Populus</i>	<i>sargentii</i>	-29.2	C ₃	1	TmGSS	Dodd et al. (1998)
dicot	Salicaceae	<i>Populus</i>	<i>tremula</i>	-28.9	C ₃	1	TmBMF	Balesdent et al. (1993)
dicot	Salicaceae	<i>Populus</i>	<i>tremuloides</i>	-27.2	C ₃	10	BFT	Brooks et al. (1997)
dicot	Salicaceae	<i>Populus</i>	<i>tremuloides</i>	-28.0	C ₃	10	BFT	Brooks et al. (1997)
dicot	Salicaceae	<i>Populus</i>	<i>tremuloides</i>	-29.3	C ₃	10	BFT	Brooks et al. (1997)
dicot	Salicaceae	<i>Salix</i>	<i>fragilis</i>	-28.7	C ₃	1	TmBMF	Dungait et al. (2008)
dicot	Salicaceae	<i>Salix</i>	<i>nigra</i>	-28.0	C ₃	5	TmBMF	Keough et al. (1996)
dicot	Salicaceae	<i>Salix</i>	<i>salvifolia</i>	-29.0	C ₃	4	MFWS	Escuerdo et al. (2008)
dicot	Salicaceae	<i>Salix</i>	<i>spp.</i>	-29.8	C ₃	10	BFT	Brooks et al. (1997)
dicot	Salicaceae	<i>Zuelania</i>	<i>guidonia</i>	-27.7	C ₃	6	TrSDBF	Holtum and Winter (2005)
dicot	Salicaceae	<i>Zuelania</i>	<i>guidonia</i>	-29.5	C ₃	6	TrSDBF	Holtum and Winter (2005)
dicot	Salicaceae	<i>Zuelania</i>	<i>guidonia</i>	-30.1	C ₃	6	TrSDBF	Holtum and Winter (2005)
dicot	Santalaceae	<i>Phoradendron</i>	<i>californicum</i>	-27.0	C ₃	1	DXS	Ehleringer and Cooper (1988)
dicot	Santalaceae	<i>Phoradendron</i>	<i>californicum</i>	-27.1	C ₃	1	DXS	Ehleringer and Cooper (1988)
dicot	Santalaceae	<i>Santalum</i>	<i>paniculatum</i>	-26.1	C ₃	5	TrSDBF	Sandquist and Cordell (2007)
dicot	Sapindaceae	<i>Acer</i>	<i>campestre</i>	-27.8	C ₃	1	TmBMF	Balesdent et al. (1993)
dicot	Sapindaceae	<i>Acer</i>	<i>campestre</i>	-27.8	C ₃	4	TmBMF	Chevillat et al. (2005)
dicot	Sapindaceae	<i>Acer</i>	<i>campestre</i>	-30.4	C ₃	1	domestic	Collister et al. (1994)
dicot	Sapindaceae	<i>Acer</i>	<i>campestre</i>	-27.5	C ₃	1	TmBMF	Dungait et al. (2008)
dicot	Sapindaceae	<i>Acer</i>	<i>glutinosa</i>	-28.7	C ₃	1	TmBMF	Balesdent et al. (1993)
dicot	Sapindaceae	<i>Acer</i>	<i>monspessulanum</i>	-26.7	C ₃	4	MFWS	Escuerdo et al. (2008)
dicot	Sapindaceae	<i>Acer</i>	<i>monspessulanum</i>	-26.7	C ₃	4	MFWS	Escuerdo et al. (2008)
dicot	Sapindaceae	<i>Acer</i>	<i>pseudoplatanus</i>	-28.2	C ₃	1	TmBMF	Balesdent et al. (1993)

Appendix I. (continued)

	Family	Genus	species	$\delta^{13}\text{C}$	pathway	N	Biome	Reference
dicot	Sapindaceae	<i>Acer</i>	<i>rubrum</i>	-28.2	C ₃	1	TmBMF	Baldocchi and Bowling (1999)
dicot	Sapindaceae	<i>Acer</i>	<i>rubrum</i>	-29.6	C ₃	1	TmBMF	Baldocchi and Bowling (1999)
dicot	Sapindaceae	<i>Acer</i>	<i>rubrum</i>	-30.2	C ₃	1	TmBMF	Baldocchi and Bowling (1999)
dicot	Sapindaceae	<i>Acer</i>	<i>rubrum</i>	-28.8	C ₃	6	TmBMF	Garten and Taylor (1992)
dicot	Sapindaceae	<i>Acer</i>	<i>rubrum</i>	-29.8	C ₃	4	TmBMF	Garten and Taylor (1992)
dicot	Sapindaceae	<i>Acer</i>	<i>rubrum</i>	-30.0	C ₃	6	TmBMF	Garten and Taylor (1992)
dicot	Sapindaceae	<i>Acer</i>	<i>rubrum</i>	-29.6	C ₃	5	TmBMF	McArthur and Moorhead (1996)
dicot	Sapindaceae	<i>Acer</i>	<i>rubrum</i>	-30.8	C ₃	5	TmBMF	McArthur and Moorhead (1996)
dicot	Sapindaceae	<i>Acer</i>	<i>rubrum</i>	-31.0	C ₃	5	TmBMF	McArthur and Moorhead (1996)
dicot	Sapindaceae	<i>Cupania</i>	<i>guatemalensis</i>	-30.3	C ₃	5	TrSDBF	Leffler and Enquist (2002)
dicot	Sapotaceae	<i>Chrysophyllum</i>	<i>brenessii</i>	-31.1	C ₃	6	TrSDBF	Leffler and Enquist (2002)
dicot	Sapotaceae	<i>Chrysophyllum</i>	<i>cainito</i>	-28.6	C ₃	6	TrSDBF	Holtum and Winter (2005)
dicot	Sapotaceae	<i>Chrysophyllum</i>	<i>cainito</i>	-29.6	C ₃	6	TrSDBF	Holtum and Winter (2005)
dicot	Sapotaceae	<i>Chrysophyllum</i>	<i>cainito</i>	-29.7	C ₃	6	TrSDBF	Holtum and Winter (2005)
dicot	Sapotaceae	<i>Chrysophyllum</i>	<i>prieurii</i>	-29.7	C ₃	1	TrSOMBF	Bonal et al. (2000)
dicot	Sapotaceae	<i>Chrysophyllum</i>	<i>prieurii</i>	-30.0	C ₃	1	TrSOMBF	Bonal et al. (2000)
dicot	Sapotaceae	<i>Chrysophyllum</i>	<i>sanguinolentum</i>	-29.4	C ₃	1	TrSOMBF	Bonal et al. (2000)
dicot	Sapotaceae	<i>Chrysophyllum</i>	<i>sanguinolentum</i>	-30.3	C ₃	1	TrSOMBF	Bonal et al. (2000)
dicot	Sapotaceae	<i>Ecclinusa</i>	<i>guianensis</i>	-29.9	C ₃	1	TrSOMBF	Bonal et al. (2000)
dicot	Sapotaceae	<i>Manilkara</i>	<i>chicle</i>	-28.6	C ₃	3	TrSDBF	Leffler and Enquist (2002)
dicot	Sapotaceae	<i>Micropholis</i>	<i>guianensis a</i>	-29.4	C ₃	1	TrSOMBF	Bonal et al. (2000)
dicot	Sapotaceae	<i>Micropholis</i>	<i>guianensis a</i>	-31.4	C ₃	1	TrSOMBF	Bonal et al. (2000)
dicot	Sapotaceae	<i>Micropholis</i>	<i>guianensis b</i>	-32.4	C ₃	1	TrSOMBF	Bonal et al. (2000)
dicot	Sapotaceae	<i>Micropholis</i>	<i>obscura</i>	-30.8	C ₃	1	TrSOMBF	Bonal et al. (2000)
dicot	Sapotaceae	<i>Micropholis</i>	<i>obscura</i>	-31.0	C ₃	1	TrSOMBF	Bonal et al. (2000)
dicot	Sapotaceae	<i>Micropholis</i>	<i>venulosa</i>	-30.6	C ₃	1	TrSOMBF	Bonal et al. (2000)
dicot	Sapotaceae	<i>Pouteria</i>	<i>eugeniifolia</i>	-28.8	C ₃	1	TrSOMBF	Bonal et al. (2000)
dicot	Sapotaceae	<i>Pouteria</i>	<i>grandis</i>	-30.4	C ₃	1	TrSOMBF	Bonal et al. (2000)
dicot	Sapotaceae	<i>Pouteria</i>	<i>guianensis</i>	-32.8	C ₃	1	TrSOMBF	Bonal et al. (2000)
dicot	Sapotaceae	<i>Pouteria</i>	<i>melanopoda</i>	-29.1	C ₃	1	TrSOMBF	Bonal et al. (2000)
dicot	Sapotaceae	<i>Pouteria</i>	<i>sandwicensis</i>	-27.1	C ₃	5	TrSDBF	Sandquist and Cordell (2007)
dicot	Sapotaceae	<i>Pradosia</i>	<i>cochlearia</i>	-30.6	C ₃	1	TrSOMBF	Bonal et al. (2000)

Appendix I. (continued)

	Family	Genus	species	$\delta^{13}\text{C}$	pathway	N	Biome	Reference
dicot	Sapotaceae	<i>Sideroxylon</i>	<i>capiri</i>	-28.5	C ₃	5	TrSDBF	Leffler and Enquist (2002)
dicot	Sarcospermataceae	<i>Sarcosperma</i>	<i>laurinum</i>	-29.6	C ₃	1	TrSCMBF	Ehleringer et al. (1987)
dicot	Scrophulariaceae	<i>Adenosma</i>	<i>gluthosum</i>	-30.3	C ₃	1	TrSOMBF	Ehleringer et al. (1987)
dicot	Simaroubaceae	<i>Simaba</i>	<i>cedron</i>	-31.6	C ₃	1	TrSOMBF	Bonal et al. (2000)
dicot	Simmondsiaceae	<i>Simmondsia</i>	<i>chinensis</i>	-24.8	C ₃	36	DXS	Kohorn et al. (1994)
dicot	Solanaceae	<i>Capsicum</i>	<i>annuum</i>	-28.7	C ₃	1	TrSDBF	Mooney et al. (1989)
dicot	Solanaceae	<i>Lycium</i>	<i>andersonii</i>	-25.1	C ₃	1	DXS	Ehleringer and Cooper (1988)
dicot	Solanaceae	<i>Lycium</i>	<i>andersonii</i>	-25.3	C ₃	1	DXS	Ehleringer and Cooper (1988)
dicot	Solanaceae	<i>Physalis</i>	<i>heterophylla</i>	-27.2	C ₃	1	unknown	Bender (1971)
dicot	Sterculiaceae	<i>Scaphopetalum</i>	<i>dewevrei</i>	-36.0	C ₃	1	TrSCMBF	Cerling et al. (2004)
dicot	Sterculiaceae	<i>Sterculia</i>	<i>lanceolata</i>	-29.7	C ₃	1	TrSCMBF	Ehleringer et al. (1987)
dicot	Sterculiaceae	<i>Sterculia</i>	<i>sp.</i>	-30.8	C ₃	1	TrSOMBF	Bonal et al. (2000)
dicot	Theaceae	<i>Eurya</i>	<i>chinensis</i>	-29.0	C ₃	1	TrSOMBF	Ehleringer et al. (1987)
dicot	Theaceae	<i>Schima</i>	<i>superba</i>	-31.6	C ₃	1	TrSCMBF	Ehleringer et al. (1987)
dicot	Theaceae	<i>Schima</i>	<i>superba</i>	-29.7	C ₃	13	TmBMF	Li et al. (2005)
dicot	Theophrastaceae	<i>Jacquinia</i>	<i>pungens</i>	-25.7	C ₃	8	TrSDBF	Mooney et al. (1989)
dicot	Tiliaceae	<i>Lueheopsis</i>	<i>rugosa</i>	-32.7	C ₃	1	TrSOMBF	Bonal et al. (2000)
dicot	Ulmaceae	<i>Trema</i>	<i>guineensis</i>	-29.8	C ₃	1	TrSOMBF	Cerling et al. (2004)
dicot	Ulmaceae	<i>Ulmus</i>	<i>crassifolia</i>	-27.2	C ₃	2	TmGSS	Jessup et al. (2003)
dicot	Umbelliferae	<i>Eryngium</i>	<i>yaccifolium</i>	-27.5	C ₃	1	unknown	Bender (1971)
dicot	Urticaceae	<i>Cecropia</i>	<i>insignis</i>	-31.5	C ₃	3	TrSOMBF	Terwilliger (1997)
dicot	Urticaceae	<i>Cecropia</i>	<i>insignis</i>	-29.9	C ₃	3	TrSCMBF	Terwilliger (1997)
dicot	Urticaceae	<i>Cecropia</i>	<i>longipes</i>	-25.3	C ₃	6	TrSDBF	Holtum and Winter (2005)
dicot	Urticaceae	<i>Cecropia</i>	<i>longipes</i>	-25.7	C ₃	6	TrSDBF	Holtum and Winter (2005)
dicot	Urticaceae	<i>Cecropia</i>	<i>longipes</i>	-26.1	C ₃	6	TrSDBF	Holtum and Winter (2005)
dicot	Urticaceae	<i>Cecropia</i>	<i>longipes</i>	-26.6	C ₃	6	TrSDBF	Holtum and Winter (2005)
dicot	Urticaceae	<i>Cecropia</i>	<i>peltata</i>	-25.4	C ₃	6	TrSDBF	Holtum and Winter (2005)
dicot	Urticaceae	<i>Cecropia</i>	<i>peltata</i>	-25.5	C ₃	6	TrSDBF	Holtum and Winter (2005)
dicot	Urticaceae	<i>Cecropia</i>	<i>peltata</i>	-26.8	C ₃	6	TrSDBF	Holtum and Winter (2005)
dicot	Urticaceae	<i>Cecropia</i>	<i>peltata</i>	-27.7	C ₃	6	TrSDBF	Holtum and Winter (2005)
dicot	Urticaceae	<i>Cecropia</i>	<i>peltata</i>	-29.2	C ₃	3	TrSOMBF	Terwilliger (1997)
dicot	Urticaceae	<i>Cecropia</i>	<i>peltata</i>	-29.7	C ₃	1	TrSCMBF	Terwilliger (1997)

Appendix I. (continued)

	Family	Genus	species	$\delta^{13}\text{C}$	pathway	N	Biome	Reference
dicot	Urticaceae	<i>Urea</i>	<i>cameroonensis</i>	-34.9	C ₃	1	TrSCMBF	Cerling et al. (2004)
dicot	Urticaceae	<i>Urtica</i>	<i>dioica</i>	-27.2	C ₃	1	TmBMF	Dungait et al. (2008)
dicot	Verbenaceae	<i>Citharexylum</i>	<i>fruticosum</i>	-29.1	C ₃	1	TrSOMBF	Jones et al. (2010)
dicot	Verbenaceae	<i>Citharexylum</i>	<i>sp.</i>	-24.8	C ₃	1	TrSDBF	Mooney et al. (1989)
dicot	Violaceae	<i>Rinorea</i>	<i>sp.</i>	-32.7	C ₃	1	TrSCMBF	Cerling et al. (2004)
dicot	Violaceae	<i>Rinorea</i>	<i>sp.</i>	-34.4	C ₃	1	TrSCMBF	Cerling et al. (2004)
dicot	Vitaceae	<i>Cissus</i>	<i>sicyoides</i>	-25.6	C ₃	2	TrSDBF	Mooney et al. (1989)
dicot	Vochysiaceae	<i>Ruizterania</i>	<i>albiflora</i>	-28.2	C ₃	1	TrSOMBF	Bonal et al. (2000)
dicot	Vochysiaceae	<i>Ruizterania</i>	<i>albiflora</i>	-28.9	C ₃	1	TrSOMBF	Bonal et al. (2000)
dicot	Zygophyllaceae	<i>Larrea</i>	<i>divaricata</i>	-22.7	C ₃	1	DXS	Ehleringer and Cooper (1988)
dicot	Zygophyllaceae	<i>Larrea</i>	<i>divaricata</i>	-23.6	C ₃	1	DXS	Ehleringer and Cooper (1988)
dicot	Zygophyllaceae	<i>Larrea</i>	<i>divaricata</i>	-24.1	C ₃	1	DXS	Ehleringer and Cooper (1988)
monocot	Agavaceae	<i>Agave</i>	<i>angustifolia</i>	-12.7	CAM	3	TrSDBF	Mooney et al. (1989)
monocot	Agavaceae	<i>Agave</i>	<i>colimana</i>	-13.6	CAM	2	TrSDBF	Mooney et al. (1989)
monocot	Alismataceae	<i>Alisma</i>	<i>plantago-aquatica</i>	-27.8	C ₃	1	TmBMF	Dungait et al. (2008)
monocot	Araceae	<i>Alocasia</i>	<i>macrorrhiza</i>	-27.7	C ₃	1	TrSOMBF	Ehleringer et al. (1987)
monocot	Araceae	<i>Philodendron</i>	<i>warscewiczii</i>	-26.0	C ₃	6	TrSDBF	Mooney et al. (1989)
monocot	Arecaceae	<i>Acrocomia</i>	<i>aculeata</i>	-26.3	C ₃	6	TrSDBF	Holtum and Winter (2005)
monocot	Arecaceae	<i>Acrocomia</i>	<i>aculeata</i>	-26.5	C ₃	6	TrSDBF	Holtum and Winter (2005)
monocot	Arecaceae	<i>Acrocomia</i>	<i>aculeata</i>	-27.0	C ₃	6	TrSDBF	Holtum and Winter (2005)
monocot	Arecaceae	<i>Acrocomia</i>	<i>aculeata</i>	-27.8	C ₃	6	TrSDBF	Holtum and Winter (2005)
monocot	Arecaceae	<i>Acrocomia</i>	<i>aculeata</i>	-28.0	C ₃	6	TrSDBF	Holtum and Winter (2005)
monocot	Arecaceae	<i>Acrocomia</i>	<i>aculeata</i>	-28.3	C ₃	6	TrSDBF	Holtum and Winter (2005)
monocot	Arecaceae	<i>Acrocomia</i>	<i>aculeata</i>	-28.7	C ₃	6	TrSDBF	Holtum and Winter (2005)
monocot	Bromeliaceae	<i>Aechmea</i>	<i>bracteata</i>	-15.4	CAM	1	TrSDBF	Mooney et al. (1989)
monocot	Bromeliaceae	<i>Aechmea</i>	<i>tillandsioides</i>	-12.3	CAM	3	TrSDBF	Holtum and Winter (2005)
monocot	Bromeliaceae	<i>Aechmeade</i>	<i>albata</i>	-16.2	CAM	1	domestic	Collister et al. (1994)
monocot	Bromeliaceae	<i>Billbergia</i>	<i>mexicana</i>	-14.7	CAM	3	TrSDBF	Mooney et al. (1989)
monocot	Bromeliaceae	<i>Bromelia</i>	<i>palmeri</i>	-13.0	CAM	2	TrSDBF	Mooney et al. (1989)
monocot	Bromeliaceae	<i>Bromelia</i>	<i>plumieri</i>	-14.0	CAM	3	TrSDBF	Mooney et al. (1989)
monocot	Bromeliaceae	<i>Hechtia</i>	<i>sp.</i>	-14.1	CAM	2	TrSDBF	Mooney et al. (1989)
monocot	Bromeliaceae	<i>Tillandsia</i>	<i>circinnata</i>	-12.3	CAM	4	TrSDBF	Mooney et al. (1989)

Appendix I. (continued)

	Family	Genus	species	δ¹³C	pathway	N	Biome	Reference
monocot	Bromeliaceae	<i>Tillandsia</i>	<i>diguetii</i>	-14.2	CAM	1	TrSDBF	Mooney et al. (1989)
monocot	Bromeliaceae	<i>Tillandsia</i>	<i>fasciculata</i>	-13.1	CAM	4	TrSDBF	Mooney et al. (1989)
monocot	Bromeliaceae	<i>Tillandsia</i>	<i>ionantha</i>	-13.1	CAM	6	TrSDBF	Mooney et al. (1989)
monocot	Bromeliaceae	<i>Tillandsia</i>	<i>makoyana</i>	-12.9	CAM	11	TrSDBF	Mooney et al. (1989)
monocot	Bromeliaceae	<i>Tillandsia</i>	<i>setacea</i>	-11.2	CAM	2	TrSDBF	Mooney et al. (1989)
monocot	Bromeliaceae	<i>Tillandsia</i>	<i>sp.</i>	-16.1	CAM	2	TmGSS	Jessup et al. (2003)
monocot	Bromeliaceae	<i>Tillandsia</i>	<i>usneoides</i>	-14.9	CAM	1	domestic	Collister et al. (1994)
monocot	Bromeliaceae	<i>Tillandsia</i>	<i>usneoides</i>	-13.9	CAM	1	TrSDBF	Mooney et al. (1989)
monocot	Commelinaceae	<i>Tradescantia</i>	<i>ohiensis</i>	-26.1	C ₃	1	unknown	Bender (1971)
monocot	Cyperaceae	<i>Carex</i>	<i>lacustris</i>	-27.8	C ₃	1	unknown	Bender (1971)
monocot	Cyperaceae	<i>Carex</i>	<i>planostachys</i>	-28.0	C ₃	2	TmGSS	Jessup et al. (2003)
monocot	Cyperaceae	<i>Carex</i>	<i>stricta</i>	-27.0	C ₃	1	unknown	Bender (1971)
monocot	Cyperaceae	<i>Cladium</i>	<i>jamaicensis</i>	-28.6	C ₃	1	unknown	Bender (1971)
monocot	Cyperaceae	<i>Cyperus</i>	<i>alternifolius</i>	-30.4	C ₃	1	TrSOMBF	Ehleringer et al. (1987)
monocot	Cyperaceae	<i>Cyperus</i>	<i>diffusus</i>	-28.9	C ₃	1	domestic	Collister et al. (1994)
monocot	Cyperaceae	<i>Cyperus</i>	<i>filiculmis</i>	-13.3	C ₄	1	unknown	Bender (1971)
monocot	Cyperaceae	<i>Cyperus</i>	<i>odoratus</i>	-13.2	C ₄	1	unknown	Bender (1971)
monocot	Cyperaceae	<i>Cyperus</i>	<i>pilosus</i>	-10.8	C ₄	1	TrSOMBF	Ehleringer et al. (1987)
monocot	Cyperaceae	<i>Cyprus</i>	<i>alternifolius</i>	-27.6	C ₃	1	domestic	Collister et al. (1994)
monocot	Cyperaceae	<i>Eleocharis</i>	<i>parvula</i>	-21.6	C ₃	1	unknown	Bender (1971)
monocot	Cyperaceae	<i>Eleocharis</i>	<i>smallii</i>	-28.0	C ₃	5	TmBMF	Keough et al. (1996)
monocot	Cyperaceae	<i>Eriophorum</i>	<i>angustifolium</i>	-27.6	C ₃	1	unknown	Bender (1971)
monocot	Cyperaceae	<i>Fimbristylis</i>	<i>aestivalis</i>	-12.7	C ₄	1	TrSOMBF	Ehleringer et al. (1987)
monocot	Cyperaceae	<i>Fimbristylis</i>	<i>annua</i>	-11.0	C ₄	1	TrSOMBF	Ehleringer et al. (1987)
monocot	Cyperaceae	<i>Fimbristylis</i>	<i>complanata</i>	-10.6	C ₄	1	TrSOMBF	Ehleringer et al. (1987)
monocot	Cyperaceae	<i>Fimbristylis</i>	<i>schoenoides</i>	-10.8	C ₄	1	TrSOMBF	Ehleringer et al. (1987)
monocot	Cyperaceae	<i>Hypolytrum</i>	<i>nemorum</i>	-34.7	C ₃	1	TrSOMBF	Ehleringer et al. (1987)
monocot	Cyperaceae	<i>Lipocarpa</i>	<i>microcephala</i>	-10.5	C ₄	1	TrSOMBF	Ehleringer et al. (1987)
monocot	Cyperaceae	<i>Scirpus</i>	<i>cespitosus</i>	-28.1	C ₃	1	unknown	Bender (1971)
monocot	Cyperaceae	<i>Scirpus</i>	<i>olneyi</i>	-29.1	C ₃	1	unknown	Bender (1971)
monocot	Cyperaceae	<i>Scirpus</i>	<i>robustus</i>	-26.9	C ₃	1	unknown	Bender (1971)
monocot	Cyperaceae	<i>Scirpus</i>	<i>validus</i>	-28.0	C ₃	1	unknown	Bender (1971)

Appendix I. (continued)

	Family	Genus	species	δ¹³C	pathway	N	Biome	Reference
monocot	Cyperaceae	<i>Scleria</i>	<i>levis</i>	-33.0	C ₃	1	TrSOMBF	Ehleringer et al. (1987)
monocot	Cyperaceae	<i>Scleria</i>	<i>terrestris</i>	-32.0	C ₃	1	TrSOMBF	Ehleringer et al. (1987)
monocot	Eriocaulaceae	<i>Eriocaulon</i>	<i>wallichianum</i>	-28.6	C ₃	1	TrSCMBF	Ehleringer et al. (1987)
monocot	Juncaceae	<i>Juncus</i>	<i>effusus</i>	-30.1	C ₃	1	unknown	Bender (1971)
monocot	Juncaceae	<i>Juncus</i>	<i>roemerianus</i>	-28.6	C ₃	1	unknown	Bender (1971)
monocot	Liliaceae	<i>Aloe</i>	<i>arborescens</i>	-24.5	CAM	1	unknown	Bender (1971)
monocot	Liliaceae	<i>Dianella</i>	<i>ensifolia</i>	-29.7	C ₃	1	TrSOMBF	Ehleringer et al. (1987)
monocot	Liliaceae	<i>Hemerocallis</i>	<i>fulva</i>	-29.5	C ₃	1	TrSOMBF	Ehleringer et al. (1987)
monocot	Liliaceae	<i>Ophiopogon</i>	<i>japonicus</i>	-31.7	C ₃	1	TrSCMBF	Ehleringer et al. (1987)
monocot	Liliaceae	<i>Sanseveria</i>	<i>fasciata</i>	-17.1	CAM	1	unknown	Bender (1971)
monocot	Liliaceae	<i>Yucca</i>	<i>filamentosa</i>	-27.1	CAM	1	unknown	Bender (1971)
monocot	Orchidaceae	<i>Arundina</i>	<i>chinensis</i>	-29.9	C ₃	1	TrSOMBF	Ehleringer et al. (1987)
monocot	Orchidaceae	<i>Campylocentrum</i>	<i>sp.</i>	-12.9	CAM	3	TrSDBF	Mooney et al. (1989)
monocot	Orchidaceae	<i>Epidendrum</i>	<i>imatophyllum</i>	-13.3	CAM	6	TrSDBF	Holtum and Winter (2005)
monocot	Orchidaceae	<i>Epidendrum</i>	<i>imatophyllum</i>	-13.7	CAM	6	TrSDBF	Holtum and Winter (2005)
monocot	Orchidaceae	<i>Epidendrum</i>	<i>imatophyllum</i>	-14.5	CAM	6	TrSDBF	Holtum and Winter (2005)
monocot	Orchidaceae	<i>Erycina</i>	<i>echinata</i>	-11.9	CAM	1	TrSDBF	Mooney et al. (1989)
monocot	Orchidaceae	<i>Myrmecophila</i>	<i>chinodora</i>	-11.7	CAM	2	TrSDBF	Mooney et al. (1989)
monocot	Orchidaceae	<i>Oncidium</i>	<i>sp.</i>	-14.8	CAM	1	TrSDBF	Mooney et al. (1989)
monocot	Palmae	<i>Daemonorops</i>	<i>margaritae</i>	-29.6	C ₃	1	TrSCMBF	Ehleringer et al. (1987)
monocot	Pandanaceae	<i>Pandanus</i>	<i>austrosinensis</i>	-31.3	C ₃	1	TrSCMBF	Ehleringer et al. (1987)
monocot	Poaceae	<i>Agropyron</i>	<i>intermedium</i>	-28.3	C ₃	1	unknown	Bender (1971)
monocot	Poaceae	<i>Agrostis</i>	<i>perennans</i>	-30.0	C ₃	1	unknown	Bender (1971)
monocot	Poaceae	<i>Agrostis</i>	<i>scabra</i>	-28.7	C ₃	1	unknown	Bender (1971)
monocot	Poaceae	<i>Ammophila</i>	<i>brevigulata</i>	-27.7	C ₃	1	unknown	Bender (1971)
monocot	Poaceae	<i>Andropogon</i>	<i>gerardii*</i>	-12.3	C ₄	3	TmGSS	Jessup et al. (2003)
monocot	Poaceae	<i>Andropogon</i>	<i>glomeratus</i>	-14.2	C ₄	1	unknown	Bender (1971)
monocot	Poaceae	<i>Aristida</i>	<i>sp.</i>	-14.6	C ₄	2	TmGSS	Jessup et al. (2003)
monocot	Poaceae	<i>Arundinaria</i>	<i>sp.</i>	-29.2	C ₃	1	unknown	Bender (1971)
monocot	Poaceae	<i>Arundinella</i>	<i>setosa</i>	-11.9	C ₄	1	TrSOMBF	Ehleringer et al. (1987)
monocot	Poaceae	<i>Bothriochloa</i>	<i>ischaemum</i>	-14.9	C ₄	2	TmGSS	Jessup et al. (2003)
monocot	Poaceae	<i>Bothriochloa</i>	<i>laguroides</i>	-12.8	C ₄	2	TmGSS	Jessup et al. (2003)

Appendix I. (continued)

	Family	Genus	species	$\delta^{13}\text{C}$	pathway	N	Biome	Reference
monocot	Poaceae	<i>Bouteloua</i>	<i>curtipendula</i>	-14.2	C ₄	1	unknown	Bender (1971)
monocot	Poaceae	<i>Bouteloua</i>	<i>curtipendula</i>	-14.4	C ₄	2	TmGSS	Jessup et al. (2003)
monocot	Poaceae	<i>Bouteloua</i>	<i>gracilis</i>	-12.7	C ₄	1	unknown	Bender (1971)
monocot	Poaceae	<i>Bouteloua</i>	<i>gracilis</i>	-14.4	C ₄	1	TmGSS	Dodd et al. (1998)
monocot	Poaceae	<i>Bouteloua</i>	<i>gracilis</i>	-14.5	C ₄	1	TmGSS	Dodd et al. (1998)
monocot	Poaceae	<i>Bouteloua</i>	<i>gracilis</i>	-14.8	C ₄	1	TmGSS	Dodd et al. (1998)
monocot	Poaceae	<i>Bouteloua</i>	<i>gracilis</i>	-14.9	C ₄	1	TmGSS	Dodd et al. (1998)
monocot	Poaceae	<i>Bouteloua</i>	<i>gracilis</i>	-15.0	C ₄	1	TmGSS	Dodd et al. (1998)
monocot	Poaceae	<i>Bouteloua</i>	<i>gracilis</i>	-15.1	C ₄	1	TmGSS	Dodd et al. (1998)
monocot	Poaceae	<i>Bouteloua</i>	<i>gracilis</i>	-15.3	C ₄	1	TmGSS	Dodd et al. (1998)
monocot	Poaceae	<i>Bouteloua</i>	<i>gracilis</i>	-15.5	C ₄	1	TmGSS	Dodd et al. (1998)
monocot	Poaceae	<i>Bouteloua</i>	<i>hirsuta</i>	-14.1	C ₄	2	TmGSS	Jessup et al. (2003)
monocot	Poaceae	<i>Bouteloua</i>	<i>rigidiseta</i>	-15.1	C ₄	2	TmGSS	Jessup et al. (2003)
monocot	Poaceae	<i>Bromus</i>	<i>catharticus</i>	-30.7	C ₃	1	unknown	Bender (1971)
monocot	Poaceae	<i>Bromus</i>	<i>kalmii</i>	-30.3	C ₃	1	unknown	Bender (1971)
monocot	Poaceae	<i>Bromus</i>	<i>sp.</i>	-30.5	C ₃	2	TmGSS	Jessup et al. (2003)
monocot	Poaceae	<i>Buchloe</i>	<i>dactyloides</i>	-14.2	C ₄	1	unknown	Bender (1971)
monocot	Poaceae	<i>Buchloe</i>	<i>dactyloides</i>	-15.7	C ₄	2	TmGSS	Jessup et al. (2003)
monocot	Poaceae	<i>Capillipedium</i>	<i>parviflorum</i>	-13.6	C ₄	1	TrSOMBF	Ehleringer et al. (1987)
monocot	Poaceae	<i>Cenchrus</i>	<i>calyculatus</i>	-10.3	C ₄	1	TrSOMBF	Ehleringer et al. (1987)
monocot	Poaceae	<i>Cymbopogon</i>	<i>caesius</i>	-12.9	C ₄	1	TrSOMBF	Ehleringer et al. (1987)
monocot	Poaceae	<i>Cynodon</i>	<i>dactylon</i>	-15.3	C ₄	1	unknown	Bender (1971)
monocot	Poaceae	<i>Dactylis</i>	<i>glomerata</i>	-28.4	C ₃	1	TmBMF	Dungait et al. (2008)
monocot	Poaceae	<i>Dendrocalamus</i>	<i>stricus</i>	-28.5	C ₃	1	domestic	Collister et al. (1994)
monocot	Poaceae	<i>Digitaria</i>	<i>longiflora</i>	-12.2	C ₄	1	TrSOMBF	Ehleringer et al. (1987)
monocot	Poaceae	<i>Digitaria</i>	<i>microbachne</i>	-10.9	C ₄	1	TrSOMBF	Ehleringer et al. (1987)
monocot	Poaceae	<i>Digitaria</i>	<i>violascens</i>	-11.5	C ₄	1	TrSOMBF	Ehleringer et al. (1987)
monocot	Poaceae	<i>Distichlis</i>	<i>spicata</i>	-15.0	C ₄	1	unknown	Bender (1971)
monocot	Poaceae	<i>Echinochloa</i>	<i>crus-galli</i>	-13.1	C ₄	1	unknown	Bender (1971)
monocot	Poaceae	<i>Elymus</i>	<i>canadensis</i>	-27.1	C ₃	1	unknown	Bender (1971)
monocot	Poaceae	<i>Elymus</i>	<i>elymoides</i>	-25.8	C ₃	4	DXS	Toft et al. (1989)
monocot	Poaceae	<i>Elymus</i>	<i>lanceolatus</i>	-26.0	C ₃	4	DXS	Toft et al. (1989)

Appendix I. (continued)

	Family	Genus	species	$\delta^{13}\text{C}$	pathway	N	Biome	Reference
monocot	Poaceae	<i>Elymus</i>	<i>mollis</i>	-27.6	C ₃	1	unknown	Bender (1971)
monocot	Poaceae	<i>Elymus</i>	<i>sp.</i>	-29.4	C ₃	2	TmGSS	Jessup et al. (2003)
monocot	Poaceae	<i>Eragrostis</i>	<i>amabilia</i>	-11.7	C ₄	1	TrSOMBF	Ehleringer et al. (1987)
monocot	Poaceae	<i>Eragrostis</i>	<i>cilianensis</i>	-13.3	C ₄	1	unknown	Bender (1971)
monocot	Poaceae	<i>Eragrostis</i>	<i>perennans</i>	-13.1	C ₄	1	TrSOMBF	Ehleringer et al. (1987)
monocot	Poaceae	<i>Eragrostis</i>	<i>perlaxa</i>	-12.5	C ₄	1	TrSOMBF	Ehleringer et al. (1987)
monocot	Poaceae	<i>Eragrostis</i>	<i>pilosissima</i>	-13.5	C ₄	1	TrSOMBF	Ehleringer et al. (1987)
monocot	Poaceae	<i>Eragrostis</i>	<i>reflexa</i>	-12.5	C ₄	1	TrSOMBF	Ehleringer et al. (1987)
monocot	Poaceae	<i>Eragrostis</i>	<i>sp.</i>	-13.6	C ₄	2	TmGSS	Jessup et al. (2003)
monocot	Poaceae	<i>Eragrostis</i>	<i>tenella</i>	-13.7	C ₄	1	TrSOMBF	Ehleringer et al. (1987)
monocot	Poaceae	<i>Eragrostis</i>	<i>tephrosanthos</i>	-12.3	C ₄	1	TrSOMBF	Ehleringer et al. (1987)
monocot	Poaceae	<i>Eragrostis</i>	<i>zeylanica</i>	-11.6	C ₄	1	TrSOMBF	Ehleringer et al. (1987)
monocot	Poaceae	<i>Eriachne</i>	<i>pallescens</i>	-11.7	C ₄	1	TrSOMBF	Ehleringer et al. (1987)
monocot	Poaceae	<i>Eulalia</i>	<i>quadrinervis</i>	-12.1	C ₄	1	TrSOMBF	Ehleringer et al. (1987)
monocot	Poaceae	<i>Festuca</i>	<i>rubra</i>	-27.3	C ₃	1	unknown	Bender (1971)
monocot	Poaceae	<i>Garnotia</i>	<i>patula</i>	-12.6	C ₄	1	TrSOMBF	Ehleringer et al. (1987)
monocot	Poaceae	<i>Holcus</i>	<i>lanatus</i>	-30.4	C ₃	1	TmBMF	Dungait et al. (2008)
monocot	Poaceae	<i>Indocalamus</i>	<i>longiauritus</i>	-32.9	C ₃	1	TrSCMBF	Ehleringer et al. (1987)
monocot	Poaceae	<i>Isachne</i>	<i>globosa</i>	-28.7	C ₃	1	TrSOMBF	Ehleringer et al. (1987)
monocot	Poaceae	<i>Ischaemum</i>	<i>aristatum</i>	-11.4	C ₄	1	TrSOMBF	Ehleringer et al. (1987)
monocot	Poaceae	<i>Ischaemum</i>	<i>ciliare</i>	-10.9	C ₄	1	TrSOMBF	Ehleringer et al. (1987)
monocot	Poaceae	<i>Leersia</i>	<i>hexandra</i>	-29.9	C ₃	1	TrSCMBF	Ehleringer et al. (1987)
monocot	Poaceae	<i>Leptaspis</i>	<i>zeylanica</i>	-32.2	C ₃	1	TrSCMBF	Cerling et al. (2004)
monocot	Poaceae	<i>Leptochloa</i>	<i>chinensis</i>	-12.4	C ₄	1	TrSOMBF	Ehleringer et al. (1987)
monocot	Poaceae	<i>Miscanthus</i>	<i>floridulus</i>	-12.4	C ₄	1	TrSOMBF	Ehleringer et al. (1987)
monocot	Poaceae	<i>Miscanthuys</i>	<i>sacchariflorum</i>	-11.9	C ₄	1	domestic	Collister et al. (1994)
monocot	Poaceae	<i>Muhlenbergia</i>	<i>schreberi</i>	-13.0	C ₄	1	unknown	Bender (1971)
monocot	Poaceae	<i>Nassella</i>	<i>leucotricha</i>	-28.4	C ₃	3	TmGSS	Jessup et al. (2003)
monocot	Poaceae	<i>Oplismenus</i>	<i>compositus</i>	-27.6	C ₃	1	TrSOMBF	Ehleringer et al. (1987)
monocot	Poaceae	<i>Oryzopsis</i>	<i>hyemoides</i>	-28.0	C ₃	1	unknown	Bender (1971)
monocot	Poaceae	<i>Panicum</i>	<i>amarulum</i>	-13.4	C ₄	1	unknown	Bender (1971)
monocot	Poaceae	<i>Panicum</i>	<i>dichotomiflorum</i>	-13.2	C ₄	1	unknown	Bender (1971)

Appendix I. (continued)

	Family	Genus	species	$\delta^{13}\text{C}$	pathway	N	Biome	Reference
monocot	Poaceae	<i>Panicum</i>	<i>leibergii</i>	-26.4	C ₃	1	unknown	Bender (1971)
monocot	Poaceae	<i>Panicum</i>	<i>oligosanthes</i>	-27.8	C ₃	2	TmGSS	Jessup et al. (2003)
monocot	Poaceae	<i>Panicum</i>	<i>pacificum</i>	-33.2	C ₃	1	unknown	Bender (1971)
monocot	Poaceae	<i>Panicum</i>	<i>scribnerianum</i>	-32.1	C ₃	1	unknown	Bender (1971)
monocot	Poaceae	<i>Panicum</i>	<i>virgatum</i>	-14.3	C ₄	1	unknown	Bender (1971)
monocot	Poaceae	<i>Paspalum</i>	<i>orbiculare</i>	-13.4	C ₄	1	TrSOMBF	Ehleringer et al. (1987)
monocot	Poaceae	<i>Phragmites</i>	<i>communis</i>	-26.6	C ₃	1	unknown	Bender (1971)
monocot	Poaceae	<i>Pogonatherum</i>	<i>crinitum</i>	-12.2	C ₄	1	TrSOMBF	Ehleringer et al. (1987)
monocot	Poaceae	<i>Saccharum</i>	<i>officinarum</i>	-10.7	C ₄	1	domestic	Collister et al. (1994)
monocot	Poaceae	<i>Sacciolepis</i>	<i>indica</i>	-10.9	C ₄	1	TrSOMBF	Ehleringer et al. (1987)
monocot	Poaceae	<i>Schizachyrium</i>	<i>scoparium</i>	-13.1	C ₄	2	TmGSS	Jessup et al. (2003)
monocot	Poaceae	<i>Setaria</i>	<i>pallide-fusca</i>	-11.6	C ₄	1	TrSOMBF	Ehleringer et al. (1987)
monocot	Poaceae	<i>Sorghastrum</i>	<i>nutans</i>	-13.6	C ₄	2	TmGSS	Jessup et al. (2003)
monocot	Poaceae	<i>Spartina</i>	<i>cynosuroides</i>	-14.4	C ₄	1	unknown	Bender (1971)
monocot	Poaceae	<i>Spartina</i>	<i>pectinata</i>	-13.4	C ₄	1	unknown	Bender (1971)
monocot	Poaceae	<i>Sporobolus</i>	<i>poiretti</i>	-13.7	C ₄	1	unknown	Bender (1971)
monocot	Poaceae	<i>Stipa</i>	<i>comata</i>	-24.8	C ₃	1	unknown	Bender (1971)
monocot	Poaceae	<i>Stipa</i>	<i>spartea</i>	-27.8	C ₃	1	unknown	Bender (1971)
monocot	Poaceae	<i>Thysanolaena</i>	<i>maxima</i>	-28.4	C ₃	1	TrSOMBF	Ehleringer et al. (1987)
monocot	Poaceae	<i>Zea</i>	<i>mays</i>	-11.2	C ₄	1	domestic	Collister et al. (1994)
monocot	Poaceae	<i>Zizania</i>	<i>aquatica</i>	-30.9	C ₃	1	unknown	Bender (1971)
monocot	Poaceae	<i>Zizaniopsis</i>	<i>miliacea</i>	-26.3	C ₃	1	unknown	Bender (1971)
monocot	Potamogetonaceae	<i>Potamogeton</i>	<i>sp.</i>	-28.2	C ₃	5	TmBMF	McArthur and Moorhead (1996)
monocot	Potamogetonaceae	<i>Potamogeton</i>	<i>foliosus</i>	-21.8	C ₃	5	TmBMF	Keough et al. (1996)
monocot	Typhaceae	<i>Sparganium</i>	<i>americanum</i>	-29.4	C ₃	5	TmBMF	McArthur and Moorhead (1996)
monocot	Typhaceae	<i>Sparganium</i>	<i>eurycarpum</i>	-26.9	C ₃	5	TmBMF	Keough et al. (1996)
monocot	Typhaceae	<i>Typha</i>	<i>angustifolia</i>	-31.0	C ₃	1	unknown	Bender (1971)
monocot	Zingiberaceae	<i>Afromomum</i>	<i>sp.</i>	-34.5	C ₃	1	TrSCMBF	Cerling et al. (2004)
monocot	Zingiberaceae	<i>Alpinia</i>	<i>chinensis</i>	-33.2	C ₃	1	TrSCMBF	Ehleringer et al. (1987)
monocot	Zingiberaceae	<i>Alpinia</i>	<i>pumila</i>	-28.2	C ₃	1	TrSOMBF	Ehleringer et al. (1987)
monocot	Zingiberaceae	<i>Alpinia</i>	<i>zerumbet</i>	-34.6	C ₃	1	TrSCMBF	Ehleringer et al. (1987)
monocot	Zingiberaceae	<i>Costus</i>	<i>speciosus</i>	-29.6	C ₃	1	TrSOMBF	Ehleringer et al. (1987)

Appendix I. (continued)

	Family	Genus	species	$\delta^{13}\text{C}$	pathway	N	Biome	Reference
monocot	Zingiberaceae	<i>Costus</i>	<i>tonkinensis</i>	-27.4	C ₃	1	TrSOMBF	Ehleringer et al. (1987)
monocot	Zingiberaceae	<i>Zingiber</i>	<i>zerumbet</i>	-32.0	C ₃	1	TrSCMBF	Ehleringer et al. (1987)
gymnosperm	Araucariaceae	<i>Araucaria</i>	<i>angustifolia</i>	-29.3	C ₃	6	TrSGSS	Franco et al. (2005)
gymnosperm	Araucariaceae	<i>Araucaria</i>	<i>angustifolia</i>	-30.3	C ₃	6	TrSGSS	Franco et al. (2005)
gymnosperm	Cephalotaxaceae	<i>Cephalotaxus</i>	<i>harringtonia</i>	-29.0	C ₃	6	TmBMF	Hanba et al. (1997)
gymnosperm	Cornaceae	<i>Cornus</i>	<i>canadensis</i>	-26.8	C ₃	5	BFT	Brooks et al. (1997)
gymnosperm	Cornaceae	<i>Cornus</i>	<i>canadensis</i>	-27.9	C ₃	5	BFT	Brooks et al. (1997)
gymnosperm	Cornaceae	<i>Cornus</i>	<i>canadensis</i>	-28.8	C ₃	5	BFT	Brooks et al. (1997)
gymnosperm	Cornaceae	<i>Cornus</i>	<i>canadensis</i>	-28.8	C ₃	5	BFT	Brooks et al. (1997)
gymnosperm	Cornaceae	<i>Cornus</i>	<i>canadensis</i>	-31.0	C ₃	5	BFT	Brooks et al. (1997)
gymnosperm	Cornaceae	<i>Cornus</i>	<i>florida</i>	-28.9	C ₃	6	TmBMF	Garten and Taylor (1992)
gymnosperm	Cornaceae	<i>Cornus</i>	<i>florida</i>	-29.2	C ₃	6	TmBMF	Garten and Taylor (1992)
gymnosperm	Cornaceae	<i>Cornus</i>	<i>florida</i>	-29.3	C ₃	4	TmBMF	Garten and Taylor (1992)
gymnosperm	Cupressaceae-Taxaceae	<i>Chamaecyparis</i>	<i>obtusa</i>	-25.7	C ₃	1	TmBMF	Inagaki et al. (2004)
gymnosperm	Cupressaceae-Taxaceae	<i>Chamaecyparis</i>	<i>obtusa</i>	-26.3	C ₃	1	TmBMF	Inagaki et al. (2004)
gymnosperm	Cupressaceae-Taxaceae	<i>Cunninghamia</i>	<i>lanceolata</i>	-29.2	C ₃	13	TmBMF	Li et al. (2005)
gymnosperm	Cupressaceae-Taxaceae	<i>Juniperus</i>	<i>ashei</i>	-26.7	C ₃	3	TmGSS	Jessup et al. (2003)
gymnosperm	Cupressaceae-Taxaceae	<i>Juniperus</i>	<i>coahuilensis</i>	-22.8	C ₃	9	DXS	Van de Water et al. (2002)
gymnosperm	Cupressaceae-Taxaceae	<i>Juniperus</i>	<i>communis</i>	-23.1	C ₃	1	MFWS	Peñuelas and Azcón-Bieto (1992)
gymnosperm	Cupressaceae-Taxaceae	<i>Juniperus</i>	<i>communis</i>	-23.3	C ₃	1	MFWS	Peñuelas and Azcón-Bieto (1992)
gymnosperm	Cupressaceae-Taxaceae	<i>Juniperus</i>	<i>communis</i>	-25.8	C ₃	1	MFWS	Peñuelas and Azcón-Bieto (1992)
gymnosperm	Cupressaceae-Taxaceae	<i>Juniperus</i>	<i>communis</i>	-26.1	C ₃	1	MFWS	Peñuelas and Azcón-Bieto (1992)
gymnosperm	Cupressaceae-Taxaceae	<i>Juniperus</i>	<i>depeana</i>	-25.0	C ₃	24	DXS	Van de Water et al. (2002)
gymnosperm	Cupressaceae-Taxaceae	<i>Juniperus</i>	<i>monosperma</i>	-23.9	C ₃	35	DXS	Van de Water et al. (2002)
gymnosperm	Cupressaceae-Taxaceae	<i>Juniperus</i>	<i>osteosperma</i>	-22.5	C ₃	1	DXS	DeLucia and Schlesinger (1991)
gymnosperm	Cupressaceae-Taxaceae	<i>Juniperus</i>	<i>osteosperma</i>	-23.1	C ₃	1	DXS	DeLucia and Schlesinger (1991)
gymnosperm	Cupressaceae-Taxaceae	<i>Juniperus</i>	<i>osteosperma</i>	-23.3	C ₃	121	DXS	Van de Water et al. (2002)
gymnosperm	Cupressaceae-Taxaceae	<i>Juniperus</i>	<i>oxycedrus</i>	-22.9	C ₃	1	MFWS	Valentini et al. (1992)
gymnosperm	Cupressaceae-Taxaceae	<i>Juniperus</i>	<i>osteosperma</i>	-23.8	C ₃	6	TmCF	Williams and Ehleringer (1996)
gymnosperm	Cupressaceae-Taxaceae	<i>Juniperus</i>	<i>osteosperma</i>	-24.1	C ₃	5	TmCF	Williams and Ehleringer (1996)
gymnosperm	Cupressaceae-Taxaceae	<i>Juniperus</i>	<i>osteosperma</i>	-25.2	C ₃	5	TmCF	Williams and Ehleringer (1996)
gymnosperm	Cupressaceae-Taxaceae	<i>Juniperus</i>	<i>osteosperma</i>	-23.5	C ₃	5	DXS	Williams and Ehleringer (1996)

Appendix I. (continued)

	Family	Genus	species	$\delta^{13}\text{C}$	pathway	N	Biome	Reference
gymnosperm	Cupressaceae-Taxaceae	<i>Juniperus</i>	<i>osteosperma</i>	-23.9	C ₃	4	DXS	Williams and Ehleringer (1996)
gymnosperm	Cupressaceae-Taxaceae	<i>Juniperus</i>	<i>osteosperma</i>	-25.2	C ₃	5	DXS	Williams and Ehleringer (1996)
gymnosperm	Cupressaceae-Taxaceae	<i>Platyclusus</i>	<i>orientalis</i>	-27.8	C ₃	1	TrSOMBF	Ehleringer et al. (1987)
gymnosperm	Cupressaceae-Taxaceae	<i>Taxodium</i>	<i>distichum</i>	-28.1	C ₃	5	TmBMF	McArthur and Moorhead (1996)
gymnosperm	Cupressaceae-Taxaceae	<i>Taxus</i>	<i>baccata</i>	-25.4	C ₃	4	MFWS	Escuerdo et al. (2008)
gymnosperm	Ephedraceae	<i>Ephedra</i>	<i>viridis</i>	-23.3	C ₃	1	DXS	Ehleringer and Cooper (1988)
gymnosperm	Ephedraceae	<i>Ephedra</i>	<i>viridis</i>	-23.8	C ₃	1	DXS	Ehleringer and Cooper (1988)
gymnosperm	Ephedraceae	<i>Ephedra</i>	<i>viridis</i>	-23.3	C ₃	15	DXS	Van de Water et al. (2002)
gymnosperm	Ephedraceae	<i>Ephedra</i>	<i>viridis</i>	-23.7	C ₃	82	DXS	Van de Water et al. (2002)
gymnosperm	Linnaceae	<i>Hougonia</i>	<i>platysepala</i>	-29.3	C ₃	1	TrSOMBF	Cerling et al. (2004)
gymnosperm	Linnaceae	<i>Linnaea</i>	<i>borealis</i>	-33.2	C ₃	5	BFT	Brooks et al. (1997)
gymnosperm	Pinaceae	<i>Abies</i>	<i>alba</i>	-27.7	C ₃	1	TmBMF	Chevillat et al. (2005)
gymnosperm	Pinaceae	<i>Abies</i>	<i>alba</i>	-25.7	C ₃	1	TmCF	Hemming et al. (2005)
gymnosperm	Pinaceae	<i>Abies</i>	<i>alba</i>	-28.7	C ₃	1	TmCF	Hemming et al. (2005)
gymnosperm	Pinaceae	<i>Abies</i>	<i>lasiocarpa</i>	-27.3	C ₃	30	TmCF	Hultine and Marshall (2000)
gymnosperm	Pinaceae	<i>Larix</i>	<i>decidua</i>	-28.2	C ₃	8	TmBMF	Chevillat et al. (2005)
gymnosperm	Pinaceae	<i>Larix</i>	<i>decidua</i>	-26.4	C ₃	3	TmBMF	Kloppel et al. (1998)
gymnosperm	Pinaceae	<i>Larix</i>	<i>decidua</i>	-26.7	C ₃	3	TmBMF	Kloppel et al. (1998)
gymnosperm	Pinaceae	<i>Larix</i>	<i>decidua</i>	-27.8	C ₃	2	TmBMF	Kloppel et al. (1998)
gymnosperm	Pinaceae	<i>Larix</i>	<i>decidua</i>	-26.2	C ₃	1	TmCF	Kloppel et al. (1998)
gymnosperm	Pinaceae	<i>Larix</i>	<i>decidua</i>	-26.4	C ₃	5	TmCF	Kloppel et al. (1998)
gymnosperm	Pinaceae	<i>Larix</i>	<i>decidua</i>	-27.5	C ₃	1	TmCF	Kloppel et al. (1998)
gymnosperm	Pinaceae	<i>Larix</i>	<i>decidua</i>	-28.0	C ₃	3	TmCF	Kloppel et al. (1998)
gymnosperm	Pinaceae	<i>Larix</i>	<i>decidua</i>	-28.2	C ₃	1	TmCF	Kloppel et al. (1998)
gymnosperm	Pinaceae	<i>Larix</i>	<i>decidua</i>	-28.6	C ₃	1	TmCF	Kloppel et al. (1998)
gymnosperm	Pinaceae	<i>Larix</i>	<i>decidua</i>	-28.3	C ₃	1	TmCF	Valentini et al. (1994)
gymnosperm	Pinaceae	<i>Larix</i>	<i>decidua</i>	-29.0	C ₃	1	TmCF	Valentini et al. (1994)
gymnosperm	Pinaceae	<i>Larix</i>	<i>gmelinii</i>	-27.6	C ₃	2	TmBMF	Kloppel et al. (1998)
gymnosperm	Pinaceae	<i>Larix</i>	<i>larcina</i>	-28.6	C ₃	5	TmBMF	Kloppel et al. (1998)
gymnosperm	Pinaceae	<i>Larix</i>	<i>larcina</i>	-28.8	C ₃	5	TmBMF	Kloppel et al. (1998)
gymnosperm	Pinaceae	<i>Larix</i>	<i>larcina</i>	-28.0	C ₃	5	BFT	Kloppel et al. (1998)
gymnosperm	Pinaceae	<i>Larix</i>	<i>larcina</i>	-28.5	C ₃	5	BFT	Kloppel et al. (1998)

Appendix I. (continued)

	Family	Genus	species	$\delta^{13}\text{C}$	pathway	N	Biome	Reference
gymnosperm	Pinaceae	<i>Larix</i>	<i>lyallii</i>	-26.9	C ₃	5	TmCF	Kloeppe et al. (1998)
gymnosperm	Pinaceae	<i>Larix</i>	<i>occidentalis</i>	-25.4	C ₃	5	TmCF	Kloeppe et al. (1998)
gymnosperm	Pinaceae	<i>Larix</i>	<i>occidentalis</i>	-26.7	C ₃	5	TmCF	Kloeppe et al. (1998)
gymnosperm	Pinaceae	<i>Larix</i>	<i>occidentalis</i>	-27.3	C ₃	5	TmCF	Kloeppe et al. (1998)
gymnosperm	Pinaceae	<i>Larix</i>	<i>occidentalis</i>	-27.3	C ₃	5	TmCF	Kloeppe et al. (1998)
gymnosperm	Pinaceae	<i>Larix</i>	<i>occidentalis</i>	-27.4	C ₃	5	TmCF	Kloeppe et al. (1998)
gymnosperm	Pinaceae	<i>Larix</i>	<i>occidentalis</i>	-28.0	C ₃	5	TmCF	Kloeppe et al. (1998)
gymnosperm	Pinaceae	<i>Larix</i>	<i>olgensis</i>	-27.8	C ₃	2	TmBMF	Kloeppe et al. (1998)
gymnosperm	Pinaceae	<i>Larix</i>	<i>siberica</i>	-27.1	C ₃	5	BFT	Kloeppe et al. (1998)
gymnosperm	Pinaceae	<i>Larix</i>	<i>siberica</i>	-27.8	C ₃	3	BFT	Kloeppe et al. (1998)
gymnosperm	Pinaceae	<i>Larix</i>	<i>siberica</i>	-29.5	C ₃	5	BFT	Kloeppe et al. (1998)
gymnosperm	Pinaceae	<i>Picea</i>	<i>abies</i>	-25.7	C ₃	8	TmBMF	Chevillat et al. (2005)
gymnosperm	Pinaceae	<i>Picea</i>	<i>abies</i>	-26.1	C ₃	1	TmBMF	Hemming et al. (2005)
gymnosperm	Pinaceae	<i>Picea</i>	<i>abies</i>	-26.6	C ₃	1	TmBMF	Hemming et al. (2005)
gymnosperm	Pinaceae	<i>Picea</i>	<i>abies</i>	-26.6	C ₃	1	TmBMF	Hemming et al. (2005)
gymnosperm	Pinaceae	<i>Picea</i>	<i>abies</i>	-26.6	C ₃	1	TmBMF	Hemming et al. (2005)
gymnosperm	Pinaceae	<i>Picea</i>	<i>abies</i>	-26.6	C ₃	1	TmBMF	Hemming et al. (2005)
gymnosperm	Pinaceae	<i>Picea</i>	<i>abies</i>	-26.7	C ₃	1	TmBMF	Hemming et al. (2005)
gymnosperm	Pinaceae	<i>Picea</i>	<i>abies</i>	-27.0	C ₃	1	TmBMF	Hemming et al. (2005)
gymnosperm	Pinaceae	<i>Picea</i>	<i>abies</i>	-27.9	C ₃	1	TmBMF	Hemming et al. (2005)
gymnosperm	Pinaceae	<i>Picea</i>	<i>abies</i>	-27.9	C ₃	1	TmBMF	Hemming et al. (2005)
gymnosperm	Pinaceae	<i>Picea</i>	<i>abies</i>	-27.3	C ₃	1	TmCF	Hemming et al. (2005)
gymnosperm	Pinaceae	<i>Picea</i>	<i>abies</i>	-27.5	C ₃	1	TmCF	Hemming et al. (2005)
gymnosperm	Pinaceae	<i>Picea</i>	<i>abies</i>	-28.4	C ₃	1	TmCF	Hemming et al. (2005)
gymnosperm	Pinaceae	<i>Picea</i>	<i>abies</i>	-28.6	C ₃	1	TmCF	Hemming et al. (2005)
gymnosperm	Pinaceae	<i>Picea</i>	<i>abies</i>	-29.0	C ₃	1	TmCF	Hemming et al. (2005)
gymnosperm	Pinaceae	<i>Picea</i>	<i>abies</i>	-29.1	C ₃	1	TmCF	Hemming et al. (2005)
gymnosperm	Pinaceae	<i>Picea</i>	<i>abies</i>	-25.8	C ₃	2	TmBMF	Kloeppe et al. (1998)
gymnosperm	Pinaceae	<i>Picea</i>	<i>abies</i>	-25.7	C ₃	1	TmCF	Kloeppe et al. (1998)
gymnosperm	Pinaceae	<i>Picea</i>	<i>abies</i>	-26.1	C ₃	2	TmCF	Kloeppe et al. (1998)
gymnosperm	Pinaceae	<i>Picea</i>	<i>abies</i>	-26.5	C ₃	1	TmCF	Kloeppe et al. (1998)
gymnosperm	Pinaceae	<i>Picea</i>	<i>abies</i>	-27.1	C ₃	1	TmCF	Kloeppe et al. (1998)

Appendix I. (continued)

	Family	Genus	species	$\delta^{13}\text{C}$	pathway	N	Biome	Reference
gymnosperm	Pinaceae	<i>Picea</i>	<i>abies</i>	-27.5	C ₃	1	TmCF	Kloeppe et al. (1998)
gymnosperm	Pinaceae	<i>Picea</i>	<i>abies</i>	-27.1	C ₃	1	TmCF	Valentini et al. (1994)
gymnosperm	Pinaceae	<i>Picea</i>	<i>abies</i>	-27.8	C ₃	1	TmCF	Valentini et al. (1994)
gymnosperm	Pinaceae	<i>Picea</i>	<i>engelmannii</i>	-26.1	C ₃	30	TmCF	Hultine and Marshall (2000)
gymnosperm	Pinaceae	<i>Picea</i>	<i>mariana</i>	-26.5	C ₃	10	BFT	Brooks et al. (1997)
gymnosperm	Pinaceae	<i>Picea</i>	<i>mariana</i>	-26.5	C ₃	10	BFT	Brooks et al. (1997)
gymnosperm	Pinaceae	<i>Picea</i>	<i>mariana</i>	-25.5	C ₃	5	TmBMF	Kloeppe et al. (1998)
gymnosperm	Pinaceae	<i>Picea</i>	<i>mariana</i>	-26.7	C ₃	5	TmBMF	Kloeppe et al. (1998)
gymnosperm	Pinaceae	<i>Picea</i>	<i>mariana</i>	-27.0	C ₃	5	BFT	Kloeppe et al. (1998)
gymnosperm	Pinaceae	<i>Picea</i>	<i>mariana</i>	-27.3	C ₃	5	BFT	Kloeppe et al. (1998)
gymnosperm	Pinaceae	<i>Picea</i>	<i>obavata</i>	-24.9	C ₃	3	BFT	Kloeppe et al. (1998)
gymnosperm	Pinaceae	<i>Picea</i>	<i>obavata</i>	-25.4	C ₃	5	BFT	Kloeppe et al. (1998)
gymnosperm	Pinaceae	<i>Picea</i>	<i>sitchensis</i>	-29.8	C ₃	1	TmBMF	Hemming et al. (2005)
gymnosperm	Pinaceae	<i>Picea</i>	<i>sitchensis</i>	-32.3	C ₃	1	TmBMF	Hemming et al. (2005)
gymnosperm	Pinaceae	<i>Picea</i>	<i>sitchensis</i>	-28.3	C ₃	1	TmCF	Hemming et al. (2005)
gymnosperm	Pinaceae	<i>Picea</i>	<i>sitchensis</i>	-29.2	C ₃	1	TmCF	Hemming et al. (2005)
gymnosperm	Pinaceae	<i>Picea</i>	<i>sitchensis</i>	-29.4	C ₃	1	TmCF	Hemming et al. (2005)
gymnosperm	Pinaceae	<i>Picea</i>	<i>sitchensis</i>	-30.1	C ₃	1	TmCF	Hemming et al. (2005)
gymnosperm	Pinaceae	<i>Picea</i>	<i>sitchensis</i>	-27.6	C ₃	5	BFT	Kloeppe et al. (1998)
gymnosperm	Pinaceae	<i>Picea</i>	<i>sp.</i>	-27.6	C ₃	3	TmBMF	Kloeppe et al. (1998)
gymnosperm	Pinaceae	<i>Pinus</i>	<i>albicaulis</i>	-25.6	C ₃	5	TmCF	Kloeppe et al. (1998)
gymnosperm	Pinaceae	<i>Pinus</i>	<i>banksiana</i>	-24.8	C ₃	10	BFT	Brooks et al. (1997)
gymnosperm	Pinaceae	<i>Pinus</i>	<i>banksiana</i>	-26.6	C ₃	10	BFT	Brooks et al. (1997)
gymnosperm	Pinaceae	<i>Pinus</i>	<i>cembra</i>	-24.5	C ₃	5	TmCF	Kloeppe et al. (1998)
gymnosperm	Pinaceae	<i>Pinus</i>	<i>cembra</i>	-28.3	C ₃	1	TmCF	Valentini et al. (1994)
gymnosperm	Pinaceae	<i>Pinus</i>	<i>contorta</i>	-27.4	C ₃	30	TmCF	Hultine and Marshall (2000)
gymnosperm	Pinaceae	<i>Pinus</i>	<i>contorta</i>	-28.1	C ₃	5	TmCF	Kloeppe et al. (1998)
gymnosperm	Pinaceae	<i>Pinus</i>	<i>contorta</i>	-28.3	C ₃	5	TmCF	Kloeppe et al. (1998)
gymnosperm	Pinaceae	<i>Pinus</i>	<i>densiflora</i>	-27.6	C ₃	1	TmBMF	Inagaki et al. (2004)
gymnosperm	Pinaceae	<i>Pinus</i>	<i>densiflora</i>	-27.9	C ₃	1	TmBMF	Inagaki et al. (2004)
gymnosperm	Pinaceae	<i>Pinus</i>	<i>edulis</i>	-21.0	C ₃	83	DXS	Van de Water et al. (2002)
gymnosperm	Pinaceae	<i>Pinus</i>	<i>edulis</i>	-21.8	C ₃	44	DXS	Van de Water et al. (2002)

Appendix I. (continued)

	Family	Genus	species	δ¹³C	pathway	N	Biome	Reference
gymnosperm	Pinaceae	<i>Pinus</i>	<i>elliottii</i>	-28.2	C ₃	1	TrSOMBF	Jones et al. (2010)
gymnosperm	Pinaceae	<i>Pinus</i>	<i>elliottii</i>	-29.9	C ₃	13	TmBMF	Li et al. (2005)
gymnosperm	Pinaceae	<i>Pinus</i>	<i>halepensis</i>	-24.0	C ₃	4	MFWS	Escuerdo et al. (2008)
gymnosperm	Pinaceae	<i>Pinus</i>	<i>halepensis</i>	-22.3	C ₃	1	DXS	Hemming et al. (2005)
gymnosperm	Pinaceae	<i>Pinus</i>	<i>halepensis</i>	-22.7	C ₃	1	DXS	Hemming et al. (2005)
gymnosperm	Pinaceae	<i>Pinus</i>	<i>halepensis</i>	-23.1	C ₃	1	DXS	Hemming et al. (2005)
gymnosperm	Pinaceae	<i>Pinus</i>	<i>halepensis</i>	-23.4	C ₃	1	DXS	Hemming et al. (2005)
gymnosperm	Pinaceae	<i>Pinus</i>	<i>halepensis</i>	-23.6	C ₃	1	DXS	Hemming et al. (2005)
gymnosperm	Pinaceae	<i>Pinus</i>	<i>halepensis</i>	-23.9	C ₃	1	DXS	Hemming et al. (2005)
gymnosperm	Pinaceae	<i>Pinus</i>	<i>jeffreyi</i>	-22.2	C ₃	1	TmCF	DeLucia and Schlesinger (1991)
gymnosperm	Pinaceae	<i>Pinus</i>	<i>jeffreyi</i>	-23.0	C ₃	1	DXS	DeLucia and Schlesinger (1991)
gymnosperm	Pinaceae	<i>Pinus</i>	<i>massoniana</i>	-26.4	C ₃	1	TrSOMBF	Ehleringer et al. (1987)
gymnosperm	Pinaceae	<i>Pinus</i>	<i>massoniana</i>	-29.2	C ₃	13	TmBMF	Li et al. (2005)
gymnosperm	Pinaceae	<i>Pinus</i>	<i>monophylla</i>	-21.4	C ₃	1	DXS	DeLucia and Schlesinger (1991)
gymnosperm	Pinaceae	<i>Pinus</i>	<i>pinaster</i>	-25.3	C ₃	4	MFWS	Escuerdo et al. (2008)
gymnosperm	Pinaceae	<i>Pinus</i>	<i>pinaster</i>	-26.6	C ₃	4	MFWS	Escuerdo et al. (2008)
gymnosperm	Pinaceae	<i>Pinus</i>	<i>pinaster</i>	-28.1	C ₃	1	TmBMF	Hemming et al. (2005)
gymnosperm	Pinaceae	<i>Pinus</i>	<i>pinaster</i>	-28.2	C ₃	1	TmBMF	Hemming et al. (2005)
gymnosperm	Pinaceae	<i>Pinus</i>	<i>pinaster</i>	-29.7	C ₃	1	TmBMF	Hemming et al. (2005)
gymnosperm	Pinaceae	<i>Pinus</i>	<i>pinea</i>	-25.2	C ₃	4	MFWS	Escuerdo et al. (2008)
gymnosperm	Pinaceae	<i>Pinus</i>	<i>pinea</i>	-25.6	C ₃	4	MFWS	Escuerdo et al. (2008)
gymnosperm	Pinaceae	<i>Pinus</i>	<i>pinea</i>	-25.7	C ₃	4	MFWS	Escuerdo et al. (2008)
gymnosperm	Pinaceae	<i>Pinus</i>	<i>pinea</i>	-26.8	C ₃	1	MFWS	Peñuelas and Azcón-Bieto (1992)
gymnosperm	Pinaceae	<i>Pinus</i>	<i>pinea</i>	-26.9	C ₃	1	MFWS	Peñuelas and Azcón-Bieto (1992)
gymnosperm	Pinaceae	<i>Pinus</i>	<i>pinea</i>	-26.9	C ₃	1	MFWS	Peñuelas and Azcón-Bieto (1992)
gymnosperm	Pinaceae	<i>Pinus</i>	<i>pinea</i>	-27.6	C ₃	1	MFWS	Peñuelas and Azcón-Bieto (1992)
gymnosperm	Pinaceae	<i>Pinus</i>	<i>ponderosa</i>	-21.6	C ₃	1	DXS	DeLucia and Schlesinger (1991)
gymnosperm	Pinaceae	<i>Pinus</i>	<i>ponderosa</i>	-22.2	C ₃	1	DXS	DeLucia and Schlesinger (1991)
gymnosperm	Pinaceae	<i>Pinus</i>	<i>ponderosa</i>	-22.3	C ₃	1	DXS	DeLucia and Schlesinger (1991)
gymnosperm	Pinaceae	<i>Pinus</i>	<i>strobus</i>	-28.0	C ₃	1	TmBMF	Balesdent et al. (1993)
gymnosperm	Pinaceae	<i>Pinus</i>	<i>strobus</i>	-28.1	C ₃	1	TmBMF	Balesdent et al. (1993)
gymnosperm	Pinaceae	<i>Pinus</i>	<i>sylvestris</i>	-25.9	C ₃	5	TmBMF	Chevillat et al. (2005)

Appendix I. (continued)

	Family	Genus	species	$\delta^{13}\text{C}$	pathway	N	Biome	Reference
gymnosperm	Pinaceae	<i>Pinus</i>	<i>sylvestris</i>	-27.5	C ₃	4	MFWS	Escuerdo et al. (2008)
gymnosperm	Pinaceae	<i>Pinus</i>	<i>sylvestris</i>	-27.9	C ₃	1	TmBMF	Hemming et al. (2005)
gymnosperm	Pinaceae	<i>Pinus</i>	<i>sylvestris</i>	-28.5	C ₃	1	TmBMF	Hemming et al. (2005)
gymnosperm	Pinaceae	<i>Pinus</i>	<i>sylvestris</i>	-29.2	C ₃	1	TmBMF	Hemming et al. (2005)
gymnosperm	Pinaceae	<i>Pinus</i>	<i>sylvestris</i>	-29.4	C ₃	1	TmBMF	Hemming et al. (2005)
gymnosperm	Pinaceae	<i>Pinus</i>	<i>sylvestris</i>	-26.3	C ₃	1	BFT	Hemming et al. (2005)
gymnosperm	Pinaceae	<i>Pinus</i>	<i>sylvestris</i>	-26.6	C ₃	1	BFT	Hemming et al. (2005)
gymnosperm	Pinaceae	<i>Pinus</i>	<i>sylvestris</i>	-27.1	C ₃	1	BFT	Hemming et al. (2005)
gymnosperm	Pinaceae	<i>Pinus</i>	<i>sylvestris</i>	-29.2	C ₃	1	BFT	Hemming et al. (2005)
gymnosperm	Pinaceae	<i>Pinus</i>	<i>sylvestris</i>	-26.9	C ₃	2	TmBMF	Kloeppe et al. (1998)
gymnosperm	Pinaceae	<i>Pinus</i>	<i>sylvestris</i>	-25.9	C ₃	1	TmCF	Valentini et al. (1994)
gymnosperm	Pinaceae	<i>Pinus</i>	<i>uncinata</i>	-24.0	C ₃	1	MFWS	Peñuelas and Azcón-Bieto (1992)
gymnosperm	Pinaceae	<i>Pinus</i>	<i>uncinata</i>	-25.4	C ₃	1	MFWS	Peñuelas and Azcón-Bieto (1992)
gymnosperm	Pinaceae	<i>Pinus</i>	<i>uncinata</i>	-26.9	C ₃	1	MFWS	Peñuelas and Azcón-Bieto (1992)
gymnosperm	Pinaceae	<i>Pinus</i>	<i>uncinata</i>	-26.9	C ₃	1	MFWS	Peñuelas and Azcón-Bieto (1992)
gymnosperm	Pinaceae	<i>Pinus</i>	<i>edulis</i>	-23.5	C ₃	5	TmCF	Williams and Ehleringer (1996)
gymnosperm	Pinaceae	<i>Pinus</i>	<i>edulis</i>	-23.8	C ₃	5	TmCF	Williams and Ehleringer (1996)
gymnosperm	Pinaceae	<i>Pinus</i>	<i>edulis</i>	-24.3	C ₃	5	TmCF	Williams and Ehleringer (1996)
gymnosperm	Pinaceae	<i>Pinus</i>	<i>edulis</i>	-23.3	C ₃	4	DXS	Williams and Ehleringer (1996)
gymnosperm	Pinaceae	<i>Pinus</i>	<i>edulis</i>	-23.7	C ₃	5	DXS	Williams and Ehleringer (1996)
gymnosperm	Pinaceae	<i>Pseudotsuga</i>	<i>menziesii</i>	-25.7	C ₃	30	TmCF	Hultine and Marshall (2000)
gymnosperm	Pinaceae	<i>Pseudotsuga</i>	<i>menziesii</i>	-25.3	C ₃	5	TmCF	Kloeppe et al. (1998)
gymnosperm	Pinaceae	<i>Pseudotsuga</i>	<i>menziesii</i>	-25.9	C ₃	5	TmCF	Kloeppe et al. (1998)
gymnosperm	Pinaceae	<i>Pseudotsuga</i>	<i>menziesii</i>	-26.7	C ₃	5	TmCF	Kloeppe et al. (1998)
gymnosperm	Pinaceae	<i>Pseudotsuga</i>	<i>menziesii</i>	-27.0	C ₃	5	TmCF	Kloeppe et al. (1998)
pteridophyte	Adiantaceae	<i>Adiantum</i>	<i>capillus</i>	-29.2	C ₃	1	TrSOMBF	Ehleringer et al. (1987)
pteridophyte	Adiantaceae	<i>Adiantum</i>	<i>flabellulatum</i>	-32.8	C ₃	1	TrSCMBF	Ehleringer et al. (1987)
pteridophyte	Angiopteridaceae	<i>Angiopteris</i>	<i>fokiensis</i>	-30.7	C ₃	1	TrSCMBF	Ehleringer et al. (1987)
pteridophyte	Aspidiaceae	<i>Hemigramma</i>	<i>decurrens</i>	-33.4	C ₃	1	TrSCMBF	Ehleringer et al. (1987)
pteridophyte	Cyatheaaceae	<i>Cyathea</i>	<i>podophylla</i>	-30.6	C ₃	1	TrSCMBF	Ehleringer et al. (1987)
pteridophyte	Dicksoniaceae	<i>Cibotium</i>	<i>barometz</i>	-29.7	C ₃	1	TrSCMBF	Ehleringer et al. (1987)
pteridophyte	Gleicheniaceae	<i>Dicranopteris</i>	<i>linearis</i>	-28.0	C ₃	1	TrSOMBF	Ehleringer et al. (1987)

Appendix I. (continued)

	Family	Genus	species	$\delta^{13}\text{C}$	pathway	N	Biome	Reference
pteridophyte	Lindsaeaceae	<i>Stenoloma</i>	<i>chusanum</i>	-28.3	C ₃	1	TrSCMBF	Ehleringer et al. (1987)
pteridophyte	Osmundaceae	<i>Osmunda</i>	<i>vachelli</i>	-31.0	C ₃	1	TrSCMBF	Ehleringer et al. (1987)
pteridophyte	Polypodiaceae	<i>Lemmaphyllum</i>	<i>microphyllum</i>	-26.5	C ₃	1	TrSOMBF	Ehleringer et al. (1987)
pteridophyte	Thelypteridaceae	<i>Abacopteris</i>	<i>multilineatum</i>	-29.9	C ₃	1	TrSCMBF	Ehleringer et al. (1987)
lycopod	Lygodiaceae	<i>Lygodium</i>	<i>japonicum</i>	-27.8	C ₃	1	TrSOMBF	Ehleringer et al. (1987)
lycopod	Selaginellaceae	<i>Selaginella</i>	<i>apoda</i>	-33.6	C ₃	5	TmBMF	McArthur and Moorhead (1996)
lycopod	Selaginellaceae	<i>Selaginella</i>	<i>uncinata</i>	-28.7	C ₃	1	TrSCMBF	Ehleringer et al. (1987)
bryophyte	Diacranaceae	<i>Dicranum</i>	<i>polysetum</i>	-30.3	C ₃	5	BFT	Brooks et al. (1997)
bryophyte	Hylocomiaceae	<i>Hylocomium</i>	<i>splendens</i>	-30.3	C ₃	5	BFT	Brooks et al. (1997)
bryophyte	Hylocomiaceae	<i>Hylocomium</i>	<i>splendens</i>	-31.0	C ₃	5	BFT	Brooks et al. (1997)
bryophyte	Hylocomiaceae	<i>Pleurozium</i>	<i>shreberi</i>	-30.6	C ₃	5	BFT	Brooks et al. (1997)
bryophyte	Hylocomiaceae	<i>Pleurozium</i>	<i>shreberi</i>	-31.3	C ₃	5	BFT	Brooks et al. (1997)
bryophyte	Hylocomiaceae	<i>Pleurozium</i>	<i>shreberi</i>	-31.7	C ₃	5	BFT	Brooks et al. (1997)
bryophyte	Hylocomiaceae	<i>Pleurozium</i>	<i>shreberi</i>	-32.3	C ₃	5	BFT	Brooks et al. (1997)
bryophyte	Hylocomiaceae	<i>Pleurozium</i>	<i>shreberi</i>	-32.5	C ₃	5	BFT	Brooks et al. (1997)
bryophyte	Hypnaceae	<i>Ptilium</i>	<i>crista-cretensis</i>	-32.5	C ₃	5	BFT	Brooks et al. (1997)
bryophyte	Sphagnaceae	<i>Sphagnum</i>	<i>sp.</i>	-29.5	C ₃	1	TmBMF	Balesdent et al. (1993)
bryophyte	Sphagnaceae	<i>Sphagnum</i>	<i>spp.</i>	-31.4	C ₃	5	BFT	Brooks et al. (1997)
lichen	Cladoniaceae	<i>Cladina</i>	<i>mitis</i>	-25.7	C ₃	5	BFT	Brooks et al. (1997)
lichen	Cladoniaceae	<i>Cladina</i>	<i>mitis</i>	-26.0	C ₃	5	BFT	Brooks et al. (1997)
lichen		<i>indet.</i>	<i>indet.</i>	-22.3	C ₃	2	TmGSS	Jessup et al. (2003)

Biome Codes:

DXS = Desert and Xeric Shrubland

MFWS = Mediterranean Forest, Woodland, and Scrub

TmBMF = Temperate Broadleaf and Mixed Forest

TmCF = Temperate Coniferous Forest

TmGSS = Temperate Grassland, Savanna, and Shrubland

TrSCMBF = Tropical and Subtropical Moist Broadleaf Forest - Closed (Subcanopy)

TrSGSS = Tropical and Subtropical Grassland, Savanna, & Shrubland

TrSOMBF = Tropical and Subtropical Moist Broadleaf Forest - Open (Canopy and Gap)